The Hong Kong Polytechnic University

Department of Health Technology and Informatics

DEVELOPMENT OF AN IN-VITRO DENDRITIC CELL MODEL FOR STUDYING DENGUE VIRUS AND HOST INTERACTION

ZHANG JINGSHU

A thesis submitted in partial fulfilment of the requirements for the degree of Doctor of Philosophy

May 2013

Certification of Originality

I hereby declare that this thesis is my own work and that, to the best of my knowledge and belief, except for my publications listed or those under preparation, it reproduces no material previously published or written, nor material that has been accepted for the award of any other degree or diploma, except where due acknowledgement has been made in the text.

ZHANG JINGSHU

Abstract

Dengue virus (DENV) infection is one of the most important arthropod-borne infections threatening populations in tropical and sub-tropical areas. The pathogen causes a mild flu-like illness, which may progress into life-threatening dengue haemorrhagic fever and dengue shock syndrome. So far, there is no specific treatment for dengue infections. Although dengue vaccines are undergoing different stages of clinical trials, the effectiveness remains to be assessed. Despite the immense research efforts on the pathogenesis of dengue virus, there are still a lot of virus-host interactions that remain unknown. The lack of suitable *in-vivo* animal models and *in-vitro* cell models is one of the obstacles to the understanding of dengue virus pathogenesis.

Dendritic cells (DCs) are among the major targets of the DENV virus and are initiator of innate immune responses against DENV. However, current *in-vitro* research on the interaction between DENV-DC is hampered by the low availability of *ex-vivo* DCs and by donor variation. This project aimed to develop a novel *in-vitro* immature DC model derived from a myeloid leukaemia cell line MUTZ-3 for studying the DENV-DC interaction during type 2 dengue virus (DENV2) infection. The DC model derived from MUTZ-3 cells was compared to DCs derived from primary human monocytes in terms of the morphology, phenotypes, virus entry mechanism, permissiveness to DENV replication and antiviral pathway responses.

In the current study, immature MUTZ-3-derived DCs (IMDCs) were shown to morphologically and phenotypically resemble immature human monocyte derived-DCs (IMMoDCs). However, RT-PCR arrays revealed that certain antiviral genes in IMDC, especially the interferon (IFN)-inducible genes such as IFIT1, IFITM1, and IFI27, had much higher expression levels than that of the IMMoDCs.

When challenged with DENV2, it was found that the replication level of DENV2 in IMDCs was significantly lower than that in IMMoDCs. To better understand the causal relationship between the activated IFN-inducible genes and the reduced permissiveness in IMDCs, post-infection RT-PCR arrays on antiviral genes were conducted. It was found that the IFN-inducible genes, such as IFIT1, IFITM1, and IFI27, were significantly up-regulated in the DENV2-infected IMMoDCs but not in DENV2-infected IMDCs. Further investigation showed that protein expression levels of IFIT1 and IFIT3 were also higher in the naïve IMDCs compared to that in the naïve IMMoDCs. Similarly, DENV2 infection significantly triggered the expression of these two proteins in the IMMoDCs. It was suggested that spontaneous activation of these genes and the protein products might be important factors in the reduced permissiveness of IMDCs to DENV2.

DENV2 entry mechanism was also investigated using the established IMDC model. In the current study, DENV2 was shown to enter the immature DCs via clathrin-dependent endocytosis, while an alternative internalisation

pathway was suggested because inhibiting the endocytosis pathway with inhibitors failed to completely block DENV2 entry. Two known DENV receptors, Dendritic cell-specific ICAM-3 grabbing nonintegrin (DC-SIGN) and mannose receptor (MR), were shown to co-express on approximately half of the populations of IMDCs and IMMoDCs. Blocking these two receptors at the same time efficiently inhibited DENV2 entry into IMDCs and IMMoDCs, even though the blockage was incomplete. These evidences together indicated that both DC-SIGN and MR were needed during DENV internalisation.

Due to the fact that blocking of DENV2 receptors and inhibition of endocytosis could not completely block entry of DENV2, this study also investigated the possible involvement of other molecules during DENV2 entry. Using immunoprecipitation, the inter-α-trypsin inhibitor protein heavy chain 2 (ITIH2) was pulled down by the DENV2 virion from the transmembrane protein mixture, indicating an interaction of DENV2 with this molecule. Blocking ITIH2 together with DC-SIGN and MR significantly inhibited DENV2 entry to DCs. Thus, ITIH2 might be involved in DENV2 entry into its target cells.

In summary, the IMDC model has been established and evaluated in this study. It was found that the IMDC model was similar with IMMoDCs in morphology and phenotype. The IMDC model was also found to express DC-

SIGN and MR, which made it a useful platform for studying entry mechanisms of DENV2. Although IMDC had lower permissiveness to DENV2, when being used in parallel with the standard IMMoDC model, this novel IMDC model may help to expand the knowledge of DENV2 life-cycle, and of cellular factors that modulate DENV2 infection in the human body.

Publications

Conference Papers

J.S. Zhang, D.M.Y. Sze, P.H.M Leung, B.Y.M Yung. Gene expression profiles between dendritic cells generated from primary human monocytes and MUTZ-3 cells. 12th International Symposium on Dendritic Cells (DC2012), 7-11 October, 2012, Daegu, Korea

J.S. Zhang, D.M.Y. Sze, P.H.M Leung. MUTZ-3-derived myeloid dendritic cell as a model to study Dengue virus and host interaction. DC2010: Forum on Vaccine Science, 11th International Symposium on Dendritic Cells in Fundamental and Clinical Immunology. 26-30 September, 2010, Lugano, Switzerland

Acknowledgements

I would like to express my sincere appreciation to my chief supervisor, Dr Polly Leung, for her patience, guidance, advice and encouragement throughout the whole PhD study. I also would like to thank my co-supervisor Dr Daniel Sze for his valuable comments and advice during my project.

I sincerely thank Prof Wei-June Chen from the Department of Public Health and Parasitology, Chang Gung University for the generous support and precious advice during my attachment in Chang Gung University. Special thanks are due to Prof Wei-Kung Wang of the University of Hawaii (previously from National Taiwan University) for providing the DENV2 sub-genomic replicon. I would like to thank Dr Kwok-hung Chan from the Department of Microbiology, Queen Mary Hospital for providing the native dengue virus samples.

I wish to acknowledge Dr Tien-Huang Chen of the Department of Public Health and Parasitology, Chang Gung University, for advice and assistance in the DENV culture and titration assay; Dr Chao-Fu Yang from the Department of Public Health and Parasitology, Chang Gung University, for guidance and advice in confocal microscope observation; Miss Hsi-Chien Su kof the transmission electron microscopy observation; the Proteomic Core

Lab of Chang Gung University for providing mass spectrometry analysis; and Dr Peigang Wang from the Pasteur Research Centre of The University of Hong Kong for sharing his experience and providing the anti-DENV antibody.

Great appreciation to Prof Shea-Ping Yip, Prof Benjamin Yung, Dr Tony To from the Department of Health Technology and Informatics for their support and suggestions. Thanks are also extended to my colleagues from the Department of Health Technology and Informatics, especially to Dr Constance Lo, Dr Edith Cheung, Dr Vincy Wong, and Ms Grace Au for their great friendship; and to Ms Sharon Ho, Mr Ka-Tik Cheung, Ms Carina Luk, Ms Donna Chiu, Ms Chun-Ting Chan, and Ms Michelle Ng for their technical support.

Special thanks are due to my mother, for her continuous patience, support and encouragement throughout my PhD study.

Finally I would like to thank my family and all of my friends for their love.

Table of Contents

List of Figures

List of Tables

List of Abbreviations

%	percent
11-MUA	11-Mercaptoundecanoic acid
ADE	antibody-dependent enhancement
$AgNO_3$	silver nitrate
AMBP	α1-microglobulin (a1m)/bikunin precursor (*AMBP*) gene
AML	acute myelomonocytic leukaemia
APC	antigen presenting cell
APLP2	amyloid precursor-like protein 2
Asn	asparagine
Asp	aspartic acid
ATCC	American Type Culture Collection
ATG	autophagy-related
BIK	BCL2-interacting killer (apoptosis-inducing)
bp	base pair
BSA	bovine serum albumin
BSL	biosafety level
CCR	C-C chemokine receptor
CD	cluster of differentiation
CDC42	cell division control protein 42 homologue
cDNA	complementary DNA
CIDEA	cell death-inducing DFFA-like effector a
CLEC	C-type lectin domain family
CLR	C-type lectin receptor

CLTC	clathrin heavy polypeptide
CM	confocal microscopy
CO	conjugation
CO2	carbon dioxide
CoIP	complex immunoprecipitation
CR	Cys-rich
CRD	carbohydrate recognition domain
CS	conserved sequence
Ct	threshold cycle
CTL	cytotoxic T cells
CXCL	chemokine (C-X-C motif) ligand
Cys	cysteine
DC-SIGN	dendritic cell-specific ICAM-3 grabbing nonintegrin
DCIR	dendritic cell immunoreceptor
ddH2O	double distilled water
DENV	dengue virus
DF	dengue fever
DHF	dengue haemorrhagic fever
DNA	deoxyribonucleic acid
DNJ	deoxynojirimycin
DNM2	dynamin 2
dNTPs	deoxyribonucleotide triphosphates [N= adenosine (A), guanosine (G), cytidine (C), thymine (T)]
DOMINE	Database of Protein domain interactions
DSP	dithiobis[succinimidylpropionate]

DSS	dengue shock syndrome
DTT	dithiothreitol
E	envelope protein
E. coli	*Escherichia coli*
ECM	extracellular matrix
EDC	Dimethylaminopropyl-N'Ethylcarbodiimide N-3-hydrochloride
EDTA	ethylene-diamine-tetra acetic acid
eEF1A	eukaryotic elongation factor-1A
EIF-3	eukaryotic initiation factor-3
eIF4E	eukaryotic translation initiation factor 4E
EMSA	electrophoretic mobility shift assay
ER	endoplasmic reticulum
F	forward
FBS	fetal bovine serum
FC	flow cytometry
FITC	fluorescein
FNII	fibronectin type-II
g	gram
GalNAc	N-Acetylgalactosamine
GADD45A	growth arrest and DNA-damage-inducible, alpha
GAPDH	glyceraldehyde 3-phosphate dehydrogenase
GBP1	guanylate binding protein 1, interferon-inducible, 67kDa
Gly	glycine
GM-CSF	granulocyte macrophage colony-stimulating factor

GPI	glycosylphosphatidyl inositol
GRP	glucose-regulated protein
h	hour
HA	hyaluronan
HAV	hepatitis A virus
HEPES	4-(2-hydroxyethyl)-1-piperazineethanesulfonic acid
HIV	human immunodeficiency virus
His	histidine
HLA	human leukocyte antigen
HLA-C	major histocompatibility complex, class I, C
HRP	horseradish peroxidase
HSP	heat shock protein
i.v.	intravenous
ICAM	intercellular adhesion molecule
IFN	interferon
IGF1R	insulin-like growth factor 1 receptor
IL	interleukin
Ile	isoleucine
ILT	immunoglobulin-like transcript
IM	immunostaining
IMHDC	immature HL-60-derived DCs
IMKDC	immature K562-drived DCs
IMTDC	immature THP-1-derived DCs
ITI	inter-α-trypsin inhibitor proteins
ITIH	inter-α-trypsin inhibitor proteins heavy chain

kb	kilo-base
kDa	kilo-Dalton
KO	knockout
L	litre
L-SIGN	liver/lymph node-specific ICAM-3 grabbing non-integrin
LARG	leukaemia-associated Rho guanine nucleotide exchange factor
LC	Langerhan cell
LC3	microtubule-associated protein light chain 3
Lin	lineage
log	logarithm
LOX	lectin-like oxidized low-density lipoprotein receptor
LSP1	lymphocyte-specific protein 1
M	molar
m°	millidegree
M-CSF	macrophage colony-stimulating factor
MALDI-TOF	matrix-assisted laser desorption/ionization time-of-flight
Mf	macrophage
MHC	major histocompatibility complex
min	minute
ml	millilitre
MLC	MUTZ-3-derived Langerhan cell
MLR	mixed leukocyte responses
mM	millimolar
MMP	matrix metalloproteinase

MR	mannose receptor
MS	mass spectrometry
MTase	methyltransferase
mTOR	mammalian target of rapamycin
MW	molecular weight
Na_2EDTA	disodium ethylenediamine tetraacetate
$Na_2S_2O_3$	sodium thiosulphate
NeuAc	N-acetylneuraminic acid
NF-κB	nuclear factor kappa-light-chain-enhancer of activated B cells
ng	nanogram
NH_4HCO_3	ammonium bicarbonate
NHS	N-Hydroxy Succinimide
NK cell	natural killer cell
NKT	natural killer T cell
NLRs	nucleotide oligomerisation domain-like receptors
nm	nanometre
NOD	non-obese diabetic
NS	non-structural protein
NTPase	RNA nucleoside triphosphatases
ORF	open reading frame
p	prevalence
PABP	poly(A)-binding protein
PAK	p21 protein (Cdc42/Rac)-activated kinase
PAMP	pathogen-associated molecular pattern

PBS	phosphate buffer saline
PBST	phosphate buffer saline with 0.2% Tween 20
PCR	polymerase chain reaction
PD-L2	programmed cell death 1 ligand 2
PE	phosphatidylethanolamine
PE-TR	Phycoerythrin Texas Red
PFU	plaque forming unit
PGP	protein-glycosaminoglycan-protein
PI3K	phosphoinositide 3-kinase
PIPS	pseudo-infectious particles
prM	membrane precursor
PRR	pathogen-recognition receptor
PVDF	polyvinylidene fluoride
R	reverse
R-PE	R-Phycoerythrin
RAF1	v-raf-1 murine leukaemia viral oncogene homolog 1
RdRp	RNA-dependant RNA polymerase
Rho	ras homolog gene family
RI	replicative intermediate complex
RIG-I	retinoic acid-inducible gene 1
RNA	ribonucleic acid
RoCK	Rho-associated protein kinase
RPL13A	ribosomal protein L13a
RT-PCR	reverse transcription-polymerase chain reaction
RTPase	RNA Triphosphatase

SAM	self assembled monolayer
s.c.	sub-cutaneous
SCID	severe combined immunodeficient
SDS-PAGE	sodium dodecyl sulphate polyacrylamide gel electrophoresis
sec	second
Ser	serine
SHAP	serum-derived hyaluronan-associated proteins
SL	stem loop
SLA	stem loop A
SLB	stem loop B
SNP	single nucleotide polymorphism
SPR	surface plasmon resonance
Src	sarcoma
SS	disulphide
TBS	Tris-buffered saline
TBST	Tris-buffered saline with Tween-20
TEM	transmission electron microscopy
TGF	transforming growth factor
TGN	trans-Golgi network
Th	T helper cell
Thr	threonine
TIMP	tissue inhibitor of metalloproteinase
TLR	toll-like receptor
Tm	melting temperature

TNF	tumour necrosis factor
TPR	tetratricopeptide repeat motifs
TSG-6	tumour necrosis-stimulated gene 6
Tyr	tyrosine
U	unit
UAR	upstream AUG region
UPR	unfolded protein response
UTR	untranslated region
V	voltage
VIT	adult protein inter-alpha-trypsin domain
VOPBA	virus overlay protein binding assay
VWFA	Von Willebrand factor type A domain
WB	western blot
WHO	World Health Organisation
WNV	West Nile virus
XCR	chemokine (C motif) ligand receptor
µg	microgram
µl	microliter
µM	micromole

1 Introduction

The Dengue virus (DENV) is an arbovirus transmitted by the female *Aedes* mosquito (Halstead, 2007). After a DENV infection, mild flu-like symptoms develop and may progress into more severe diseases such as dengue haemorrhagic fever (DHF) and dengue shock syndrome (DSS), both of which can be fatal (Martina *et al.*, 2009). According to the World Health Organisation (WHO), in comparison to the 1970s, not only is the number of cases increasing, but the affected regions are also expanding (World Health Organisation, 2012). Nowadays, two-fifths of the world's population are at risk of DENV infections, and the Asia Pacific Region has the highest incidence rate (World Health Organisation, 2012). Although some anti-DENV strategies are under development, there is no effective and safe anti-DENV agent currently available on the market (Sayce *et al.*, 2010). Thus, further investigation of the pathology of DENV infection is crucial for therapeutic strategy development.

In the following sections of this Chapter, the morphology and life-cycle (section 1.1), diagnosis and drug/vaccine development of DENV (section 1.2), DENV pathogenesis (section 1.3), the DENV infection initiating target cell dendritic cells (DCs) and the interaction between DENV and DCs (section 1.4) will all be introduced.

1.1 Background of dengue virus

Dengue-like disease was first recorded in Philadelphia in 1780. However, it may have been widely-distributed geographically even before that according to written records in China in the late 10th century and in the West Indies in the 1600s (Gubler, 1998). Since then, dengue outbreaks have been reported throughout the world. After World War II, new endemic patterns of DENV began to emerge (Henchal and Putnak, 1990). Particularly, in the last two decades of the 20th century, a global geographically expanded DF/DHF was observed. This may have been due to the modern globalisation and poorly-planned urbanisation in developing countries in tropical/subtropical areas. Currently, epidemic DF/DHF is still one of the most serious infectious diseases in the world in the 21st century (Gubler, 2006).

DENV is a single-strand and positive-sense RNA virus, which belongs to the *Flaviviridae* family (Malavige *et al.*, 2004). There are four serotypes of DENV (i.e., DENV 1-4), classified according to their immunogenicity in the human body, which are antigenically and genetically different from one another (Henchal and Putnak, 1990).

1.1.1 Morphology of DENV

The DENV particle is spherical in shape. The diameter of the DENV particle is approximately 50 nanometres (nm). In each DENV particle, the nucleocapsid is surrounded by a host-derived lipid membrane, in which two

transmembrane proteins are integrated: the major envelope (E) glycoprotein (53 kilo-daltons [kDa]) and the membrane (M) protein (8 kDa). There are two types of DENV morphology: mature type and immature type.

Unlike other enveloped viruses, such as human immunodeficiency virus (HIV) and influenza, mature DENVs have spikeless and smooth surfaces (Kuhn *et al.*, 2002). The envelope of a mature DENV particle is composed of 180 copies of the E glycoprotein, which are arranged as 90 head-to-tail homodimers of E protein that lie in 30 rafts. These homodimers form a herringbone pattern (Figure 1-1, B) (Kuhn *et al.*, 2002). However, the structure of the immature DENV envelope is dramatically different from that of the mature one (Figure 1-1, A), as the latter has 60 prominent spikes on its surface. Each spike is composed of three heterodimers of a precursor of the membrane protein (prM)-E proteins. In both the immature and mature virions, there are 3-nm gaps between the inner lipid leaflets and the nucleocapsids. The arrangements of the E monomers in both particles do not obey the conventional *T*=3 quasi-symmetry* (Zhang *et al.*, 2003a; Zhang *et al.*, 2003b). The structural details of the mature and immature particles are to be reviewed in section 1.1.3.3, and the process of DENV conformational change from immature to mature is to be introduced in section 1.1.4.5.

* In icosahedron particle, the size of the equilateral triangle is proportional to the T number. Each particle will contain 60T subunits (Johnson and Speir, 1997).

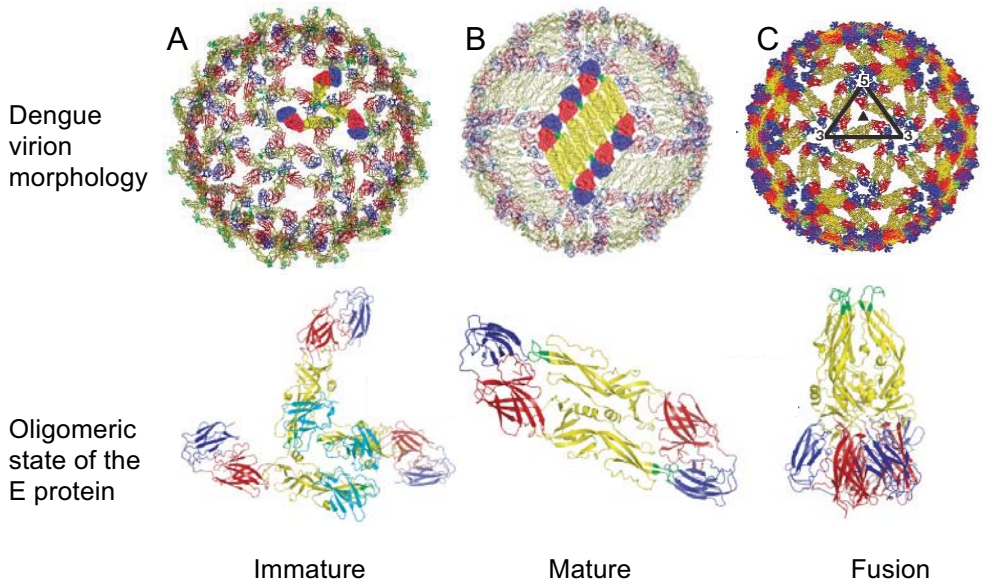

Figure 1-1 Structure of DENV particles and the arrangement of E proteins under different viral life stages.

E protein domains I, II, and III are shown in red, yellow, and blue, respectively. The fusion peptide is green. (A) An immature DENV has a spiky surface. The E protein forms a trimer with three copies of prM-E heterodimers. An immature particle is initially budded into the endoplasmic reticulum (ER) before maturation. (B) A mature DENV has a diameter of 50 nm and a smooth surface. Ninety copies of E protein head-to-tail homodimers lie on the surface of the virion. (C) During membrane fusion, the E protein dimers in the mature particle experience conformational changes. The E pre-fusion protein dimers form the putative *T*=3 fusogenic intermediate structure. Later, under low-pH conditions, the E proteins form more stable post-fusion homotrimers (Mukhopadhyay *et al.*, 2005; Perera *et al.*, 2008).

1.1.2 Genome organisation of DENV

DENV has a genome of ~10,700 nucleotides. There are three structural proteins in DENV: capsid (C), membrane (M), envelope (E); along with seven non-structural (NS) proteins (i.e., NS1, NS2a, NS2b, NS3, NS4a, NS4b, and NS5). The order of proteins encoded by the genome is 5′-C-prM-E-NS1-NS2a-NS2bNS3-NS4a-NS4b-NS5-3′ (Halstead, 2008).

The genome of DENV contains a 5′ type I cap[†] structure followed by a dinucleotide sequence AG (m^7GpppAmG), and by a single open reading frame (ORF) with 5′ and 3′ untranslated regions (UTRs) at both termini (Figure 1-2) (Dong *et al.*, 2012). N^7 methylation of the 5′ type I RNA cap is a significant factor for efficient translation (Edgil *et al.*, 2006). Another methylation site of the 5′ cap is on the 2′-*O* of internal adenosine, which is critical for viral escape from innate immune regulation (Daffis *et al.*, 2010). The 5′ UTR is about 100 nucleotides in length, while the 3′ UTR is approximately 400 nucleotides in length. There are two stem loops within the 5′ UTR: one is the large stem loop A (SLA) and the other is the short stem loop B (SLB), which ends at the start codon, AUG. SLB contains an upstream AUG region (5′ UAR), which is complementary to the 3′ UAR. The 3′ UAR is located at a conserved 3′ stem loop (3′ SL) of the 3′UTR of the viral genome. Upstream of the 3′ SL, there is a conserved sequence (CS), which

[†] Type 0 cap ($m^7G^{5'}ppp^{5'}X$), type I cap ($m^7G^{5'}ppp^{5'}XmY$), and type II cap ($m^7G^{5'}ppp^{5'}XmYmZ$) (Shatkin, 1976).

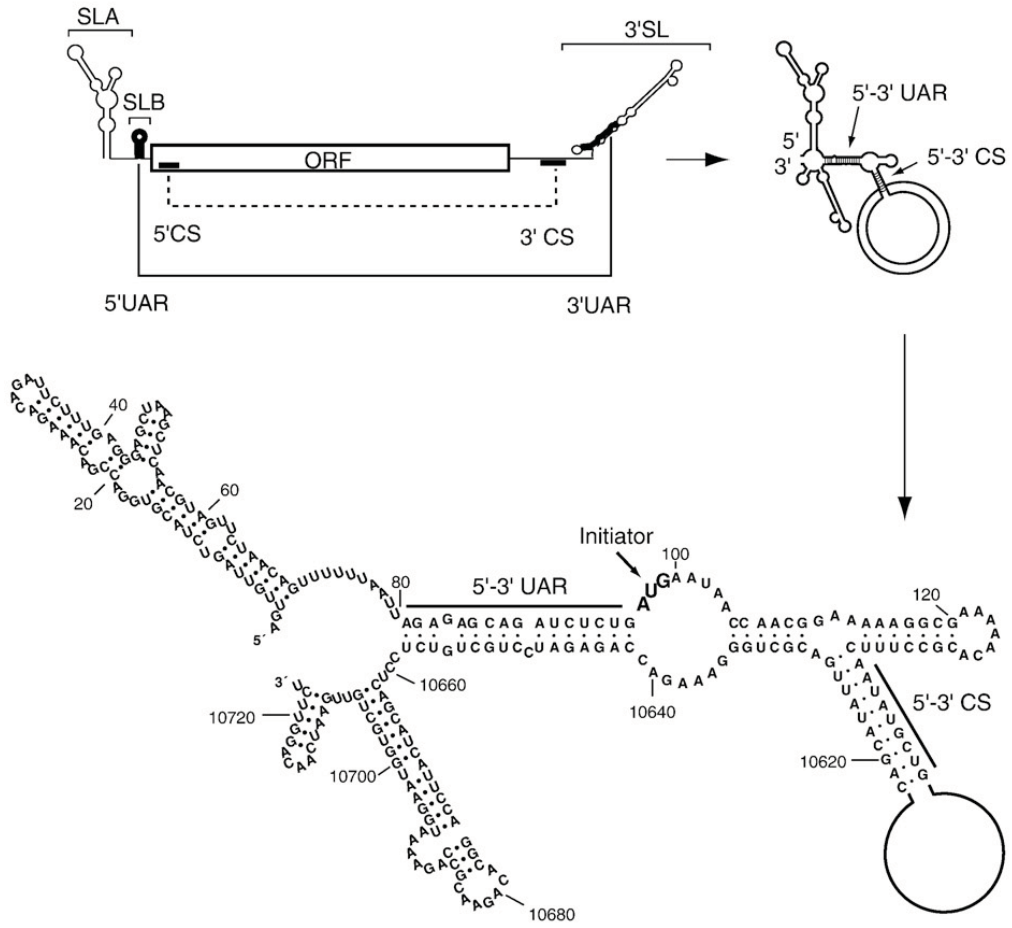

Figure 1-2 Schematic representation of DENV2 genome.

A DENV genome has complementary regions 5'-3' UAR and 5'-3' CS. SLA and SLB are located at the 5' termini. The DENV genome forms a circular conformation during replication, with hybridisation between the 5'-3' UAR and the 5'-3' CS. The sequences of the hybridised 5'-3' UAR and 5'-3' CS are displayed. The start-codon AUG is indicated by the arrow. (Adapted from Alzarez *et al.,* 2008, Figure 1A)

encloses the cyclisation sequence 3′CS. The latter is complementary to a region located at the CS region at the 5′ end of the ORF (Alvarez *et al.*, 2008) (Figure 1-2).

The genome of DENV is structured as a cellular mRNA, except for the absence of a 3' poly(A) tail. The DENV RNA has a relative maximisation of coding capacity as a result of its restricted size (Clyde *et al.*, 2006).

1.1.3 Proteins of DENV

1.1.3.1 Capsid protein

The DENV nucleocapsid core consists of multiple copies of C protein (~120 amino acids [aa]) surrounding a single copy of the positive-sense viral genomic RNA (Kuhn *et al.*, 2002).

The C protein is an alpha-helical protein, in which there are four alpha helixes (Ma *et al.*, 2004). The first 13 aa residues of the C protein are essential for protein folding (Li *et al.*, 2008). The C protein forms homodimers, and the homotypic interaction domain is located at residues 37-72. The internal hydrophobic domain within helix II plays a critical role during homodimer formation, as it forms an extensive apolar surface at the interface of the homodimer (Pichlmair *et al.*, 2011; Wang *et al.*, 2004). The asymmetric charge distribution of the C protein homodimer may contribute to the

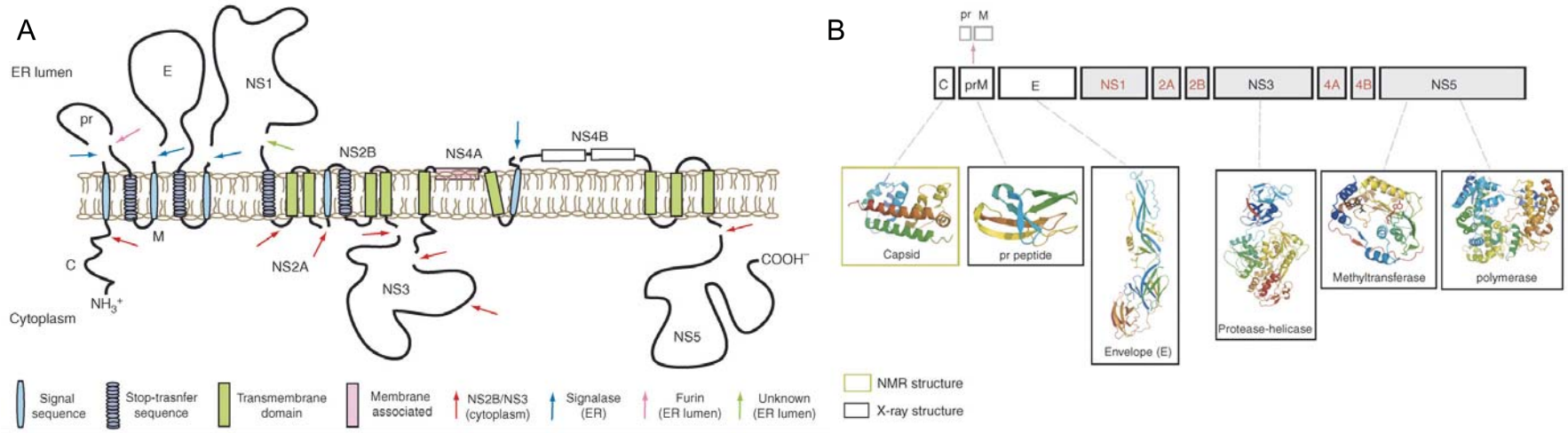

Figure 1-3 Membrane topology of the DENV polyprotein.

The figure is extracted from Perera and Kuhn, 2008; Figure 1. (A) DENV polyprotein is translated by cellular and viral proteases. In the ER, prM and E proteins are released by signalase cleavage. The cleaved prM and E proteins remain on the luminal side of the ER membrane. The C protein is anchored on the cytoplasmic side of the ER membrane by a conserved hydrophobic signal sequence in the C termini. The signal sequence is cut by viral protease NS2BNS3, which is also responsible for the processing of major NS proteins. During viral maturation, the pr peptide is released from M protein by furin in TGN. (B) The structural proteome of DENV is shown.

interaction between the C protein and the M protein, and between the C protein and viral RNA (Pichlmair *et al.*, 2011).

1.1.3.2 Membrane protein

The C-terminal hydrophobic domain of the C protein contributes to the translocation of the 26 kDa prM protein (~165 aa residues). The cleavage of prM leads to the generation of a mature C protein (Kuhn *et al.*, 2002). During viral maturation in the secretory pathway, the pr peptide (91 residues) is released from the M protein (~75 aa residues) by the Golgi-resident protease furin from the N terminus (Li *et al.*, 2008; Yu *et al.*, 2008). The remaining ectodomain (residues 92-130) and transmembrane region at the C terminus (residues 131-166) represent the mature M protein (Li *et al.*, 2008). The most important function of prM is to protect E from premature fusion during morphogenesis (Kuhn *et al.*, 2002).

1.1.3.3 Envelope protein

The E protein (~495 aa residues), which is the dominant glycoprotein on the surface of a DENV virion, is approximately 53 kDa in size (Modis *et al.*, 2004). The DENV E protein conformation is different between an immature virion and a mature virion.

1.1.3.3.1 E protein structure

There are three domains on the ectodomain of the E protein (residues 1-395). Domain I is the structurally-central domain, containing the N termini of the whole protein. Domain II (residues 98–110), located on one side of Domain I, contains the fusion loop and mediates dimerisation of the E protein. Domain III, which is located on the other side of domain I, has an immunoglobulin-like fold and participates in receptor binding and antibody neutralisation (Modis *et al.*, 2003; Zhang *et al.*, 2004). Domains I and II are linked by four polypeptide chains, while domains I and III are attached to each other by a single polypeptide linker. In the homodimer of the E protein, the fusion peptide from one monomer is buried in the junction between domain I and domain III of the other monomer (Zhang *et al.*, 2004). There is a hydrophobic pocket on the ectodomain of the E protein at the interface between domain I and domain II, which can accept a hydrophobic ligand: N-octyl-β-D-glucoside. The pocket opens and closes via the conformation shift on a β-hairpin, indicating the structural flexibility for a larger conformational change experienced by DENV during maturation and fusion (Modis *et al.*, 2003).

There are 12 conserved cysteine (Cys) residues in the ectodomain of DENV E protein. These Cys residues form six disulphide (SS) bonds. Each of these SS bonds has a specific function. For instance, SS1 is responsible for maintaining an amino-terminal loop. SS2, together with SS4, stabilises the amino-proximal part of protein domain II of the E protein. The carboxy-proximal loop in domain II is preserved by SS5. In addition, the bridge of E

protein domain III is made by SS6. The elimination of any SS bond can cause the impaired function of epitopes in the E protein (Roehrig *et al.*, 2004).

1.1.3.3.2 E protein of immature DENV virion

As described before, there are 60 spikes on the surface of an immature dengue virion. The three E monomers of each spike are raked towards the viral surface. The distal ends of the three monomers make contact with one another, forming a short superhelix in the process. The fusion peptide of each E monomer is located at the tip of the spike, covered by prM proteins. Therefore, the cleavage of the pr peptide may dissociate the trimeric spike, inducing the development of E protein dimers, as in a mature virus (Zhang *et al.*, 2003b).

1.1.3.3.3 E protein of mature DENV virion

On a mature DENV virion, the alpha helical regions of the E protein, together with the partial N terminus of the M protein, are hidden in the outer layer of the viral membrane. The transmembrane domains of the E protein (residues 452–467 and 473–491) and those of the M protein (residues 40–54 and 58–70) form the antiparallel coiled-coil helices. The anchor regions of the E protein and of the M protein assist the formation of the antiparallel homodimer, keeping the C terminus on the external surface of the viral membrane (Zhang *et al.*, 2003a).The first helix of the E protein stem region

(residues 398–420) forms an angle toward the exterior lipid leaflet. In contrast, the stem region (residues 426–448), which belongs to the second helix of the E protein, lies flat in the outer lipid leaflet connecting the E protein to the lipid (Zhang *et al.*, 2003a).

1.1.3.3.4 E protein N-linked glycosylation

The E protein of DENV has two N-linked glycosylation sites, one of which, at asparagine (Asn) 153, is conserved in *Flaviviridae*, while the other, at Asn67, is specific to DENV (Heinz and Allison, 2003). Although the glycosylation of E had no effect on viral replication in insect cells, Asn153 was indicated to influence viral infectivity (Roehrig *et al.*, 2007). Meanwhile, Asn67 glycan was essential for virion assembly, budding, as well as the DENV receptor-mediated entry (Bryant *et al.*, 2007; Mondotte *et al.*, 2007). Extensive studies have elucidated that dendritic cell-specific ICAM-grabbing non-integrin (DC-SIGN) is responsible for viral attachment (Alen *et al.*, 2009; Lozach *et al.*, 2005; Sakuntabhai *et al.*, 2005). This well-known C-type lectin preferentially binds to terminal mannose sugars on the Asn67 glycan of DENV's E protein (Mondotte *et al.*, 2007; Pokidysheva *et al.*, 2006). The interaction between the E protein of DENV and DC-SIGN is described in-depth in section 1.1.4.1.2.

The structure of DENV particle experiences conformational changes at different stages of the viral life cycles: internalisation (Nayak *et al.*, 2009),

fusion (Zhang *et al.*, 2004), maturation (Perera *et al.*, 2008), and release (Kuhn *et al.*, 2002). More information about E protein conformation is to be provided in a latter section regarding the DENV life cycle in mammalian cells (section 1.1.4.5).

1.1.3.4 NS1 protein

The NS1 protein is a ~48 kDa glycoprotein, containing twelve invariant Cys, six intramolecular SS bonds, and two conserved N-linked glycans (at residues 130 and 207). NS1 is secreted as a hexamer (Somnuke *et al.*, 2011). The N-linked glycan at residue 130 (complex sugar chain) is essential for the stabilisation of NS1 hexamer secretion, whereas the N-linked glycan at residue 207 (high mannose chain) is critical for extracellular protein stability (Somnuke *et al.*, 2011).

NS1 is expressed directly on the surface of infected cells via either glycosylphosphatidyl inositol (GPI) linkage or lipid raft association (Jacobs *et al.*, 2000; Noisakran *et al.*, 2008a). Furthermore, during the early stages of DENV infection, NS1 is highly secreted into the sera of patients. Soluble NS1 can also integrate back into the plasma membrane of cells by interacting with specific sulphated glycosaminoglycans (Avirutnan *et al.*, 2007). Thus, NS1 has been used as an effective marker to diagnose DENV infection not only via detecting the plasma concentration of NS1 antigen, but also through measuring the NS1 antigen in tissues (Lima Mda *et al.*, 2011).

1.1.3.5 NS3 protein

The NS3 protein, which is 67 kDa in size, is the second-largest protein in DENV. Residues between 618 and 623 of the NS3 protein have the most conserved aa sequence among the DENV strains. NS3 acts as a serine protease, an RNA helicase, and an RNA triphosphatase (RTPase)/RNA nucleoside triphosphatase (NTPase). In addition, it also participates in viral replication, the interaction with DENV NS5, and apoptosis in DENV-infected cells (Calmon *et al.*, 2009).

The NS3 protease domain, locating at the N-terminus (residues 1–180), has a chymotrypsin-like fold consisting of two β-barrels, each formed of six β-strands. Between the two β-barrels is a catalytic triad composed of histidine (His) 51, aspartic acid (Asp) 75, and serine (Ser) 135 (Erbel *et al.*, 2006). The protease activity of NS3 requires a fragment of 40 residues from the NS2B protein as a cofactor, which is connected to NS3 through a non-cleavable and flexible non-peptide glycine $(Gly)_4$-Ser-Gly_4 linker. The remaining hydrophobic region of NS2b anchors the protease complex to the cellular membrane (Gouvea *et al.*, 2007). The NS3 protease domain cleaves the viral polyprotein at several sites after viral RNA translation (Erbel *et al.*, 2006), and is linked to the helicase domain by a conserved interdomain linker, influencing the activity of helicase (Wu *et al.*, 2005).

The helicase domain (residues 180–618), with seven structural motifs,

locates at the C terminus of NS3. It has three sub-domains, among which subdomain I (residues 181–326) and subdomain II (residues 327–481) both contain a six-stranded parallel β-sheet, surrounded by four helices. Meanwhile, subdomain III (residues 482–618) contains four parallel helices, flanked by three other shorter helices and two solvent-exposable antiparallel β–strands (Luo *et al.*, 2008).

1.1.3.6 NS5 protein

NS5 is the largest protein in DENV, with ~900 residues, and is 104 kDa in size. It is also the most conserved protein of DENV, with 67% sequence similarity among the four DENV serotypes. NS5 acts as a methyltransferase (MTase, residues 1–296) at the N-terminus and as an RNA-dependent RNA polymerase (RdRp, residues 320–900) at the C-terminus (Perera and Kuhn, 2008). The NS5 protein, which has N^7 and 2'-*O* methyltransferase activities, is required for the formation of the 5' type I Cap (m^7GpppAmG) of DENV genome RNA. NS5 also catalyses 2'-*O* methylation of internal adenosine of viral RNA (Dong *et al.*, 2012). The RdRp domain of NS5, composed of a basic right hand conformation, interacts with nucleotides using two metal ions coordinated through structurally-conserved Asp. The residues 320–405 of NS5 encode the nuclear localisation signal region, in which residues 320–368 are strictly conserved (Yap *et al.*, 2007).

1.1.3.7 Other non-structural proteins

DENV also encodes four small hydrophobic proteins: NS2a, NS2b, NS4a, and NS4b. NS2a is a 22-kDa protein, which directly participates in the formation of the replication complex during viral replication. As discussed in previous sections, NS2b plays a role as the cofactor for the proteolytic activity of the NS3 protease. The activity of the NS2b/NS3 protease complex of DENV relies on the association between the ER membrane and NS2b, with the central region (residues 67–80) of the latter being responsible for this association (Gouvea *et al.*, 2007). Another non-structural protein, NS4a (16 kDa), helps to target or anchor the replication complex (Hilgard and Stockert, 2000). NS4b (27 kDa), on the other hand, is involved in viral replication through its interaction with NS3 (Cabrera-Hernandez and Smith, 2005).

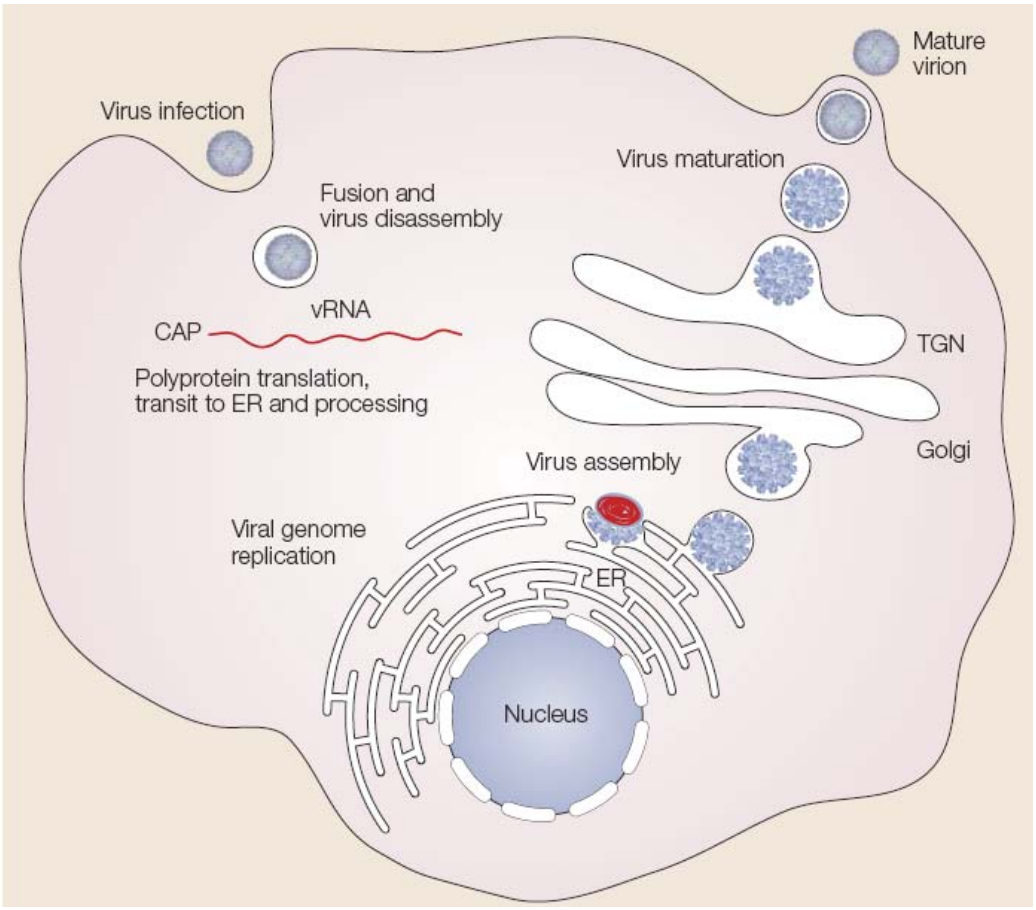

Figure 1-4 Life cycle of DENV in host cells.

DENV invades host cells by binding to attachment factors/cellular receptors. Then, the virions are internalised to the cells through endocytosis. After the disassembly of these virions, the viral RNA is released into the cytoplasm. Viral polyprotein is translated and processed. Viral RNA replicates and is assembled into the capsid as a nucleocapsid while being transported through the ER. An immature DENV is formed through the trans-Golgi network (TGN). After the cleavage of pr from the M protein in TGN, a mature DENV is released (Adapted from Mukhopadhyay *et al*., 2005; Box 1).

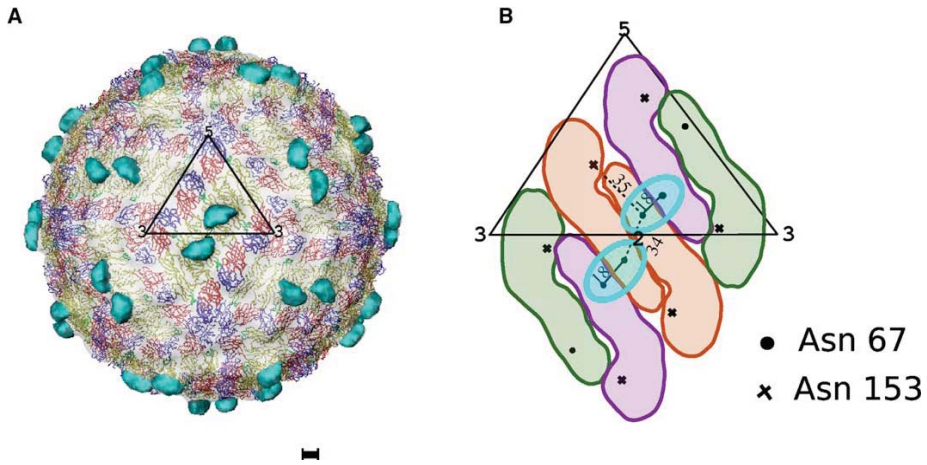

Figure 1-5 Interaction between DENV E protein and DC-SIGN carbohydrate recognition domain (CRD).

(A) On the surface of a mature DENV particle, 90 homodimers of E protein lie in 30 rafts and form a herringbone pattern. E proteins are indicated with domain I in red, domain II in yellow, and domain III in blue. The interacting CRD from DC-SIGN is in cyan. The icosahedral asymmetric unit is in black. The scale bar represents 5 nm. (B) In each raft of E proteins, there are three E protein homodimers. The N-linked glycosylation sites on these six E protein molecules are indicated as Asn67 (•) and Asn153 (×). The two cyan circles indicate the CRD binding site on Asn67 sites. The icosahedral dimer is in red and the other two neighbouring general E protein dimers are in purple and green, respectively. The icosahedral asymmetric unit is in black. (Adapted from Pokidysheva *et al*., 2006; Figure 2).

1.1.4 DENV life cycle in mammalian cells

There are ten major steps of dengue viral life cycle: attachment, entry, fusion, disassembly, polyprotein translation, processing, viral genome replication, assembly, maturation, and release (Clyde *et al.*, 2006). The following sections provide descriptions for each of these ten steps.

1.1.4.1 Attachment and entry

A DENV E protein interacts with attach molecules/cellular receptors on the surface of the target cells as a point of initiation. Having bound to attach molecules/cellular receptors, DENV particles are delivered to pre-existing clathrin-coated pits by diffusion along the cell surface, and are transported to early endosomes. These virions are then internalised by the specific receptor-mediated endocytosis (van der Schaar *et al.*, 2008).

1.1.4.1.1 DENV receptors

During DENV infection, the appearance of DENV antigens in various organs and cell types indicates that the host receptors are broadly distributed. So far, host receptors identified include heparan sulphate, heat shock proteins, mannose receptors (MR), and DC-SIGN (Cabrera-Hernandez and Smith, 2005; Hilgard and Stockert, 2000; Miller *et al.*, 2008).

Heparan sulphate is expressed in almost all mammalian cells. It consists of alternating hexuronic acid/D-glucosamine disaccharides that contain different degrees and patterns of sulphation, presenting as a linear chain with diversity in length and with complexity in structure. Elimination or reduction of heparin sulphate can partially reduce the binding and internalisation intensity of DENV, indicating that heparin sulphate is responsible for the concentration of virions on the cell surface (Cabrera-Hernandez and Smith, 2005; Hilgard and Stockert, 2000).

In addition, affinity chromatography and the virus overlay protein binding assay (VOPBA) have helped to identify a group of proteins that are able to bind to DENV. A 90-kDa heat shock protein (HSP90) and 70-kDa heat shock protein (HSP70, also known as 78-kDa glucose-regulated protein [GRP78]) are thought to be components of the receptor complex during DENV entry to macrophage and monocyte. As chaperones, HSP90 and HSP70 may also participate in DENV E protein conformational changes upon binding to the viral receptors (Upanan *et al.*, 2008).

Other putative DENV receptors on mammalian cells discovered during the last decade are listed in Table 1-1. Two of those receptors, DC-SIGN and MR, which are expressed on DENV-initiated host cell DCs, are reviewed in the following sections 1.1.4.1.2 and 1.1.4.1.3.

Table 1-1 Putative DENV receptors on mammalian cells discovered in the last decade

Receptor	Virus type	Host type	Assay	Reference
27K, 45K, 67K and 87K proteins	Native DENV2	Monocyte-derived macrophage; U-937	Affinity chromatography; VOPBA; Immunofluorescence; Antibody inhibition assay	(Moreno-Altamirano *et al*., 2002)
37/67-kDa high-affinity laminin receptor	Native DENV1-4	HepG2; Porcine kidney cell line PS Clone D	VOPBA; Immunofluorescence; Northern blot; 2D gel electrophoresis; MALDI-TOF MS; Immunostaining	(Thepparit and Smith, 2004, Tio *et al*., 2005)
CLEC5A	Native DENV1-4	Monocyte-derived macrophage and DC; Murine macrophage-like Raw264.7 cells; HEK 293T; Recombinant human CLEC5A	Immunofluorescence assay; Immunoprecipitation and immunoblotting; ELISA; Gene expression knockdown; *In-vivo* test; Surface analyses; Glycan microarray; Docking studies	(Chen *et al*., 2008)
DC-SIGN	Native DENV1-4, DENV1 recombinant prM and E protein	Monocyte-derived macrophage; Monocyte-derived DCs and LCs; THP-1	Immunofluorescence assays; Flow Cytometry; Immunohistochemistry	(Tassaneetrithep *et al*., 2003, Navarro-Sanchez *et al*., 2003, Lozach *et al*., 2005)
GRP78	Native DENV2	HepG2	VOPBA; Immunofluorescence; MS fingerprinting; Affinity chromatography; Gene expression knockdown	(Jindadamrongwech *et al*., 2004, Upanan *et al*., 2008, Alhoot *et al*., 2012)
HSP90 and HSP70	Native DENV2; DENV4 Recombinant E protein	U937 cells Monocyte-derived macrophage	VOPBA; Affinity chromatography; His tag pull-down assay; Indirect immunofluorescence assay	(Reyes-Del Valle *et al*., 2005)
L-SIGN	Native DENV1-4	THP-1	Flow Cytometry; Immunohistochemistry	(Tassaneetrithep *et al*., 2003)
Mannose receptor	Native DENV1-4	human MR and DC-SIGN expressing NIH3T3 cell line; Monocyte-derived Mϕ and DC	Glycan analysis; Blot overlay assays; ELISA	(Miller *et al*., 2008)
Phosphatidylserine Receptors	Native DENV1-4	HEK293T; CHO745 cells; Cos-7; A549; Vero; Huh7 5.1	cDNA Library Screening; ELISA; Immunofluorescence; Gene expression knockdown; Flow Cytometry; Inhibition of Infection Assay	(Meertens *et al*., 2012)
Syndecan-2	Native DENV2	K562	Gene expression knockdown Flow Cytometry	(Okamoto *et al*., 2012)

1.1.4.1.2 DC-SIGN and its interaction between DENV

DC-SIGN, a C-type lectin, serves in cell adhesion and also as a phagocytic pathogen-recognition receptor (PRR). It has been proven to be the binding target of various pathogens, such as hepatitis C virus (HCV) and HIV (Lozach *et al.*, 2003; Su *et al.*, 2004). DC-SIGN is composed of four parts, including a cytoplasmic domain, a transmembrane domain, an extracellular neck domain, which contains eight tandem 23 aa residues, and a carbohydrate recognition domain (CRD). It is present, as a tetramer, on the surface of antigen presenting cells (APCs). In the tetramer, DC-SIGN molecules are attached to one another by neck domain repeats, but their CRDs remain monomeric. CRD has the typical C-type lectin fold, a mixed α/β structure with two primary antiparallel β sheets. Several loops are gathered on one side of the CRD, shaping the oligosaccharide-binding site that is close to neither the N termini nor the C termini (Pokidysheva *et al.*, 2006). The C terminus of the CRD of DC-SIGN can bind to high mannose glycans in an environment with Ca^{2+} (Jessie *et al.*, 2004; Mitchell *et al.*, 2001b).

DC-SIGN is essential for DENV infections through its interaction with carbohydrate moieties on the E protein. On the surface of a mature DENV, each icosahedral asymmetric unit contains three covalently-identical E glycoprotein molecules (Kuhn *et al.*, 2002). The CRD from DC-SIGN can bind to two of the three E proteins, leaving the remaining E protein non-associated as a space for other subsequent receptors. One of the CRD binding sites is Asn67 in the E molecule, which belongs to the dimer, and the

other is Asn67 in the adjacent molecule owned by the other E protein dimer. The third Asn67 remains unoccupied, as well as all the Asn153 sites (Figure 1-5) (Pokidysheva *et al.*, 2006).

A DC-SIGN expression renders poorly-susceptible cells infected by DENV (Lozach *et al.*, 2005). Moreover, soluble DC-SIGN and antibodies against DC-SIGN inhibit DENV infection (Lozach *et al.*, 2005). However, the DENV E protein does not undergo any significant conformational changes during binding to DC-SIGN CRD (Pokidysheva *et al.*, 2006). More importantly, the internalisation function of DC-SIGN is not necessary for DENV infectivity (Lozach *et al.*, 2005).

These evidences indicate that DC-SIGN may serve as an attachment receptor to concentrate virions on cell membranes, rather than mediating internalisation (Pokidysheva *et al.*, 2006).

1.1.4.1.3 Mannose receptor and its interaction between DENV

MR has similar sugar specificity to that of DC-SIGN. It belongs to the C-type lectin superfamily as DC-SIGN does. Each MR molecule contains three components: a Cys-rich (CR) domain, which obtains lectin activity and attaches to sulphate sugars, a fibronectin type-II (FNII) domain mediating binding to collagen; and eight CRDs (Martinez-Pomares *et al.*, 2006). The

fourth CRD (CRD4) from the top of the CRD domain controls most of the recognition towards the terminal glycan residues in mannose, fucrose, and N-acetyl glucosamine in a Ca^{2+}-dependent manner, while the CRD in DC-SIGN recognises high-mannose oligosaccharides and fucosylated glycans. Under a low endosomal pH condition, MR undergoes a great conformational change: the CR domain folds back to bind to the CRD4 (Boskovic *et al.*, 2006). MR can bind to bacteria, fungi, and viruses. As an endocytosis mediator, approximately 85% of MR is constitutively internalised from the cell surface through clathrin-mediated endocytosis, and is then recycled back from the endosomal system to the cytoplasm membrane. A tyrosine (Tyr)-based motif locating in the cytoplasmic tail is responsible for intracellular targeting during recycling (Taylor *et al.*, 2005).

The process by which DENV binds to MR is also mediated by the interaction between receptor CRD and viral E glycoprotein. The expression of MR enables DENV binding to non-susceptible cells. Anti-MR antibodies or MR ligands can extensively, although incompletely, block DENV infection and production in permissive host macrophage. Furthermore, given the fact that MR participates in macropinocytosis, pinocytosis, receptor-mediated endocytosis and phagocytosis, MR is believed to be the receptor for DENV internalisation (Miller *et al.*, 2008).

Since it is believed that multiple receptors are involved in DENV binding and

entry, the relationship between these receptors has also been investigated. Using antibody specific to DC-SIGN and antibody specific to MR together can inhibit DENV infection more efficiently than using antibodies to either of the receptors alone. Although the DENV infection inhibition rate achieved 90% in double receptor-blocking assay on monocyte-derived DC, complete inhibition failed, indicating that other receptors or entry pathways exist for DCs during DENV infection. Thus, further investigation is required (Alen *et al.*, 2011; Miller *et al.*, 2008).

1.1.4.2 DENV fusion and disassembly

As introduced in section 1.1.4.1, DENV binds to a primary receptor and is delivered into endosomes, in which the fusion peptide of the E protein is exposed at its distal end and inserts itself into the outer bilayer of cell membrane, inducing conformational rearrangement of the viral particle. This process enables trimerisation of the E protein (Kuhn *et al.*, 2002; Nayak *et al.*, 2009). A low-pH environment within the endosomes induces further structural rearrangements of the E protein. The transmembrane domains that previously anchored in the viral membrane are pulled closer to the fusion peptide, forming a hairpin structure. The hairpin structure then activates the fusion between the viral membrane and the host membrane (Figure 1-6) (Modis *et al.*, 2004). DENV utilises bis(monoacylglycero)phosphate, a lipid specific to late endosomes, as a co-factor for its endosomal acidification-dependent fusion machinery (Zaitseva *et al.*, 2010).

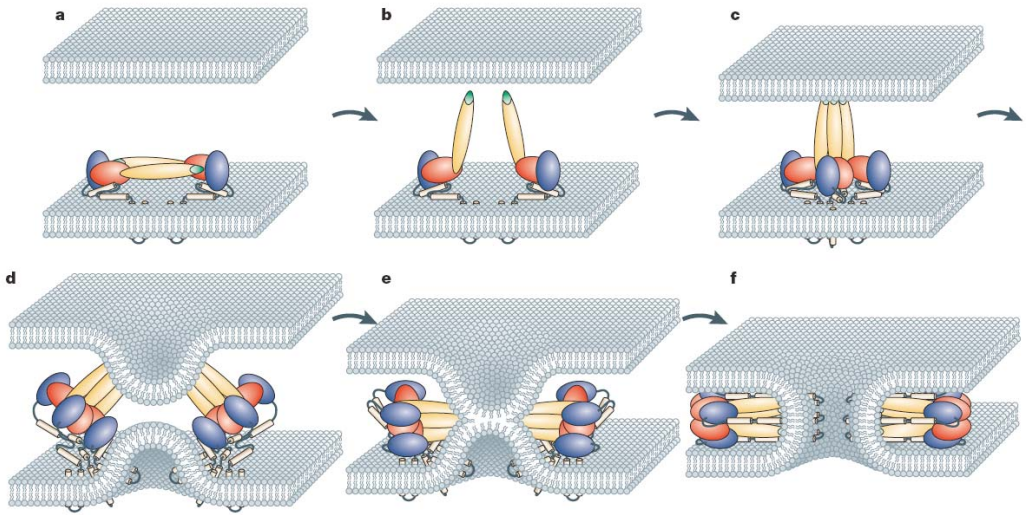

Figure 1-6 Procedure of DENV membrane fusion.

The figure is adopted from Mukhopadhyay *et al.*, 2005; Figure 7B. Domain I: red; domain II: yellow; domain III: blue; fusion peptide: green. At the beginning, the fusion peptide hides in the E protein dimer (a). Under low pH circumstances, the hinge region between domain I and domain II changes, allowing the latter to swing towards the host cell membrane (b). The E proteins rearrange. The fusion peptide inserts into the outer layer of the host membrane, causing the E protein to form a trimer (c). Domain III folds towards domain II, carrying the viral membrane towards the fusion peptide and the host membrane (d). The fusion between the two membranes takes place (e) and they finally fuse with each other forming the transmembrane regions (f).

1.1.4.3 Polyprotein translation and processing

After internalisation, the ~10,700 kb viral RNA is directly translated into a polyprotein, which contains three structural proteins (C, prM, E) and seven non-structural proteins (NS1-5) (Rice, 2007). The translation obeys the cap-dependent initiation mechanism (Chiu *et al.*, 2005). DENV 5' type I 7-methylguanosine cap, produced by MTase activity of NS5, is recognised and bound to the eukaryotic translation initiation factor 4E (eIF4E) (Dong *et al.*, 2007; Villas-Boas *et al.*, 2009). Two other factors, namely the scaffolding protein eIF4G and the helicase eIF4A, are recruited by eIF4E, forming a complex that binds to 43S ribosomal pre-initiation complex. The latter then associates with the 60S subunit, turning into the 80S ribosomal complex that is competent for elongation. Poly(A)-binding protein (PABP) binds to the DENV 3'UTR, enhancing the translation (Polacek *et al.*, 2009). Additionally, DENV heightens the protein translation by a circularisation mechanism similar to other mRNAs (Alvarez *et al.*, 2005). DENV is also capable of translation via a non-canonical mechanism that enables DENV translation under adverse cellular conditions, which inhibit cellular cap-dependent translation (Edgil *et al.*, 2006). The subsequent DENV translation occurs in tight association with ER-derived membranes (Clyde *et al.*, 2006). The virus-encoded serine protease NS3/NS2B is responsible for cleaving the junctions between NS proteins. Host signalase, on the other hand, is responsible for the cleavage of the structural proteins (Figure 1-3, A) (Perera and Kuhn, 2008).

1.1.4.4 DENV genome replication

Viral replication starts with the synthesis of a negative-sense RNA, which requires genome cyclisation mediated by the complementary 5'/3'CS and 5'/3'UAR sequences (Figure 1-2) (Paranjape and Harris, 2010). The negative-sense RNA serves as a template for the production of additional positive-sense RNA via a replicative intermediate complex (RI). Viral replication progresses on the RI asymmetrically and semi-conservatively, causing the accumulation of positive-sense strand RNA during viral replication (Rice, 2007).

Conserved sequences and structures of DENV, such as 5'SLA, 5' SLB, and 3'SL, are important for viral RNA synthesis (Figure 1-2). Deletion of these regions significantly reduces the replication level of DENV RNA (Paranjape and Harris, 2010). DENV viral replication also involves the viral glycoprotein NS1, the helicase-protease NS3, the hydrophobic proteins NS2A and NS4A, RdRp-MTase NS5, as well as some host factors (Alvarez *et al.*, 2005; Paranjape and Harris, 2010). The dynamic interaction between cis-RNA elements and the subcellular localisation of virus-derived replication components allow for the orchestration of DENV genomic RNA synthesis, further translation of viral proteins, and viral packaging (Paranjape and Harris, 2010).

1.1.4.5 Assembly, maturation, and release

C protein and newly synthesised positive-sense RNA are packed together as a nucleocapsid, which is assembled into prM-E glycoproteins to form the non-infectious immature viral particles. Immature viral particles are subsequently budded into the lumen of ER and are transported into the trans-Golgi network (TGN) via a secretory pathway (Perera and Kuhn, 2008). N-linked glycans and glycan trimers are added to prM and the E protein in TGN. Sixty trimers of prM-E heterodimers separate and then re-associate as 90 E homodimers that lie flat on the viral surface. The conformational change in prM is essential to expose the cleavage site of the cellular protease furin. Then, when the pH of TGN is approximately 5.7, furin mediates the cleavage of prM. In order to protect the membrane from fusion, the cleavage product pr remains associated until the virion is released into the extracellular environment by exocytosis (Qi *et al.*, 2008; Yu *et al.*, 2008).

1.2 Clinical significance of DENV infection

1.2.1 Diagnosis of DENV infection

1.2.1.1 Clinical manifestations

DENV infection is a systemic and dynamic disease. According to the guidelines from WHO, the course of DENV illness can be classified into three phases: febrile, critical, and recovery (Figure 1-7) (World Health Organisation, 2009).

During the febrile phase, patients get a high-grade fever, known as dengue fever (DF), which lasts for two to seven days. The fever is usually accompanied by facial flushing, skin erythema, generalised body ache, myalgia, arthralgia and headache, and sometimes by sore throat, injected pharynx, conjunctival injection, anorexia, nausea, vomiting, and mild haemorrhagic symptoms (Halstead, 2008). Nonetheless, these symptoms are not typically distinguishable between febrile and non- febrile DENV, and between severe DENV infection and non-severe DENV infection. Thus, other clinical parameters are necessary. A progressive decrease in the total white cell count in whole blood is a significant sign for DENV infection (World Health Organisation, 2009).

Between the third and seventh day of the illness, if the body temperature drops with an increase in capillary permeability and haematocrit level, the critical phase begins. The clinically significant plasma leakage may last for 24 to 48 h, during which the severity of plasma leakage can be evaluated by means of the lifted haematocrit level. The illness at this stage is defined as DHF. Once a critical volume of plasma has been lost during the leakage, a process known as DSS takes place, suggested by lower pulse pressure (≤ 20 mm Hg) or poor capillary perfusion in both children and adults. Subsequent organ hypoperfusion causes progressive organ impairment, metabolic acidosis, and disseminated intravascular coagulation. In severe shock, serious haemorrhage occurs, followed by a further decrease in haematocrit (Halstead, 2008; World Health Organisation, 2009).

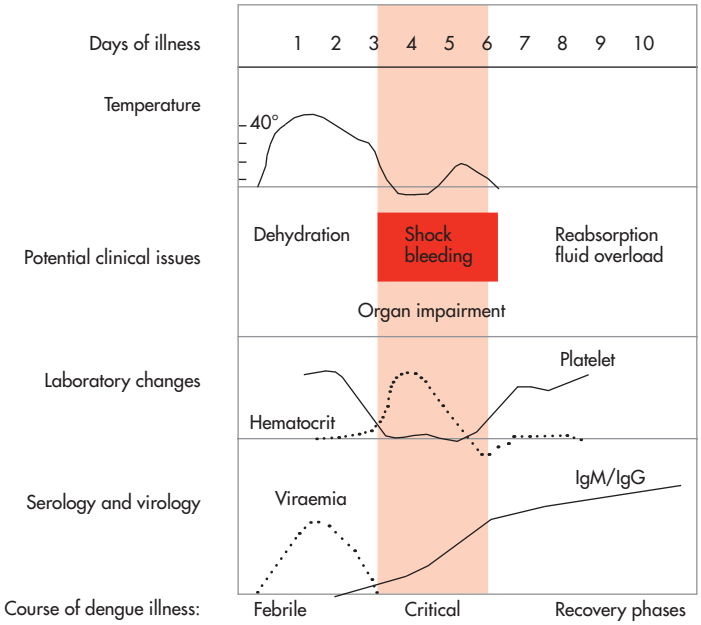

Figure 1-7 The time course of DENV illness.

Along with the days of illness, there are three phases of the DENV illness: febrile, critical and recovery. In each phase, different clinical manifestations can be observed, providing varying diagnostic targets. (Adapted from World Health Organisation, 2009, page 25, Figure 2.1).

In case these patients survive the critical phase, a gradual reabsorption of extravascular compartment fluid occurs during the next 48–72 h. Patients during this recovery phase experience the following: 1) their appetite returns, 2) their gastrointestinal symptoms abate; 3) their haemodynamic status stabilises; and 4) their diuresis ensues. Generalised pruritus, bradycardia, and electrocardiographic changes are also prevalent during this stage. White blood cell count begins to rise, followed by the recovery of platelets (World Health Organisation, 2009).

During DENV infection, infants and children are at high risk of developing severe diseases. In addition, it is easier for shock and bleeding to be developed among infants. DENV diseases in adults appear to be different from those in infants and children. Compared to children under the same epidemic situation, adults may have higher rates of bleeding manifestations, haematemesis, and malaena but less overt shock (Halstead, 2008).

During DF, DHF, and DSS, rare complications may happen, which include hepatomegaly and liver dysfunction (Lin *et al.*, 2008), disseminated intravascular coagulation (Rao *et al.*, 2005), encephalopathy (Cam *et al.*, 2001), myocarditis (Wiwanitkit, 2006), acute renal failure (Lee *et al.*, 2009), haemolytic uraemic syndrome (Lima *et al.*, 2007), optic neuritis and uveitis (Gupta *et al.*, 2009).

1.2.1.2 Laboratory diagnostic methodologies

During DENV infection, diagnoses based on clinical symptoms are neither reliable nor sufficient. An effective and precise diagnosis is important for case confirmation and for precaution with regard to severe complications. Accurate diagnostic results can serve as outbreak surveillance, pathogenesis study, as well as vaccine development (World Health Organisation, 2009). Laboratory diagnosis usually focuses on the detection of the virus, viral nucleic acids, antigens, antibodies, or the combined detection of these factors. Four to five days after the infectious biting of the mosquito, a DENV virion can be detected in serum, plasma, circulating blood cells, as well as in some tissues. Thus, at the early stage of infection, virion isolation and viral nucleic acid/viral antigen detection can be used to diagnose the disease. At the later stage of acute infection, a serological test is appropriate for diagnosis (Peeling *et al.*, 2010). Different DENV infection diagnostic methods are listed and compared in Table 1-2.

Although multiple diagnostic methods are available, none of these methods are rapid, efficient, affordable, and robust at the same time (Peeling *et al.*, 2010).

Table 1-2 Laboratory diagnostic methods for DENV infection

Diagnostic methods	Specimen required	Time point to collect specimen *	Facilities required	Time required	Key references
Virion isolation	Whole blood, serum, tissue	1-5 days	Cell culture facilities; BSL-2/BSL-3 laboratories; Fluorescence microscope; molecular biology equipment	1-2 weeks	(Harris *et al.*, 1998)
Nucleic acid detection	Whole blood, serum, plasma, tissue	1-5 days	BSL-2 laboratory; equipment for molecular biology	1-2 days	(Harris *et al.*, 1998; Lanciotti *et al.*, 1992)
Antigen detection	Serum, tissue	1–6 days	ELISA facilities; Facilities for histology	1-2 days	(Bessoff *et al.*, 2008; Tripathi *et al.*, 2007)
IgM detection	Whole blood, serum, plasma	After 5 days	ELISA facilities	1–2 days	(Branch and Levett, 1999; Bundo and Igarashi, 1985)
IgG detection	Whole blood, serum, plasma	1-5 days,	ELISA facilities; BSL-2 laboratory;	> 7 days	(Miagostovich *et al.*, 1999; Vaughn *et al.*, 1999)

* Time point after the appearance of symptoms.

1.2.2 Control, prevention and treatment of DENV infection

1.2.2.1 Vector control

Vector control and interruption of human–vector contact are the first line of DENV infection control. *Aedes aegypti*, which is the main transmission vector of DENV, is the target of vector control. Control activities are conducted in the habitats of both immature and mature mosquitoes, as well as in places in which human-vector contract occurs (World Health Organisation, 2009). According to WHO Strategy Development and Monitoring for Parasitic Diseases and Vector Control Team, habitats of mosquito aquatic stages are eliminated by frequently emptying and cleaning water containers. Vector inhibitions are also achieved by using insecticides/biological control agents against both the developing wigglers and adult mosquitoes (World Health Organisation, 2004). Besides, biological controllers, such as *larvivorous fish* and copepods, are capable of controlling *Aedes aegypti* (Kay *et al.*, 2002; Nam *et al.*, 2000). Recently, *Wolbachia pipientis*, which is an intracellular inherited bacterium, successfully shorten the life-span of *Aedes aegypti* by activating the innate immune system of the mosquito. Additionally, *Wolbachia pipientis* can be competitive by sharing the limited cellular resources that are required for DENV replication in mosquito (McMeniman *et al.*, 2009; Moreira *et al.*, 2009). Even though the community-based vector control strategies are able to reduce classical *Aedes* larval indices, there is no convincing evidence which shows that the control strategies contribute to the prevention of DENV transmission (Heintze *et al.*, 2007). Thus, a novel, efficient, and economical vector control strategy is desirable. A mosquitocidal vaccine is used in the humans and based on the principle that immune effectors in human blood

can remain active in the mosquito after the human blood has been ingested. Hence, the mosquitocidal vaccine could be an alternative method to control DENV transmission (Billingsley *et al.*, 2008).

1.2.2.2 Vaccine development

Because of the failure of vector control, tetravalent DENV vaccine development is one of the most important issues in public health studies (Guzman *et al.*, 2010). Studies have indicated that neutralising antibodies are the major contributors to protective immunity. Therefore, an ideal DENV vaccine should be able to trigger life-long robust neutralising antibodies against all of the four serotypes of DENV in naïve and previously-immune individuals. Current DENV vaccine candidates include live attenuated viruses, inactivated viruses, subunit vaccines, DNA vaccines, cloned engineered viruses, and chimeric viruses (Normile, 2007). Depending on a model calibrated by Chao *et al.* (2012), a vaccine could be an efficient tool for controlling DENV. According to this model, a competent and cost-effective vaccination strategy should prioritise giving the inoculation to children. Adults should also receive the vaccination when the elimination of local dengue transmission is required (Chao *et al.*, 2012). Recently, a randomised, controlled phase 2b trial of a recombinant, live-attenuated, CYD tetravalent DENV vaccine taken in Thai schoolchildren showed that this vaccine played a protective role against DENV1, DENV3, and DENV4, but not against DENV2. Although this CYD tetravalent DENV vaccine project was a milestone in DENV vaccine development, the lack of efficacy towards

DENV2 indicates the urgent need for knowledge about DENV pathogenesis (Sabchareon *et al.*, 2012).

1.2.2.3 Drug development

The development of a DENV-specific therapeutic agent, which is able to shorten the duration and attenuate the severity of the diseases, and to reduce the occurrence of the major complications, is as important as the development of DENV vaccines itself (Simmons *et al.*, 2012). The identification of anti-DENV agents usually focuses on inhibiting critical steps of the DENV life-cycle. The drug action points could be on both viral factors and host factors (Sampath and Padmanabhan, 2009). For *in-vivo* drug tests, immunocompromised mice models or ADE models are recruited for anti-DENV drug development (Zompi and Harris, 2012). Due to the disadvantages and cost issues associated with these animal models, investigators tend to use *in-vitro* models to screen and test the anti-DENV agents initially. Nowadays, there are three *in-vitro* systems which have been widely used for high throughput-screening the anti-DENV agents: the fire-fly luciferase gene expressing replicon system, the pseudo-infectious particles (PIPS) system, and a *Renilla* luciferase gene expressing replicon system. All of these systems involve the use of engineered viral replicons and permissive host cell lines (Perera *et al.*, 2008). Thus, the establishment of *in-vitro* models which truly reflect the natural pathogenesis of DENV infection is critical for DENV drug development.

DENV attachment and entry events provide potential drug targets, including DENV E proteins and attachment molecules (Perera *et al.*, 2008). Various carbohydrate-binding agents are able to bind to the DENV E protein, subsequently preventing viral attachment (Alen *et al.*, 2011). Viral entry in a later stage can also be inhibited. The pocket at the hinge between domain I and domain II of the E protein (see section 1.1.3.3) has been proven to be a valid target site for anti-DENV therapy. A group of compounds were found to inhibit DENV viral fusion via the computational high-throughput screening and cell biology analysis. They bound to the pocket of the E protein, competing with the known ligand *N*-octyl-β-D-glucoside (Schmidt *et al.*, 2012; Zhou *et al.*, 2008). On the other hand, attachment molecules of DENV can also be therapy targets. For example, antibodies against the 37/67 kDa laminin receptor can probably serve as a therapeutic option for DENV infection (Omar *et al.*, 2011). Moreover, the DENV replication stage is another drug development target. Deoxynojirimycin (DNJ) and its *N*-alkylated derivatives restrain host glucosidases, which are critical for DENV E glycoprotein folding and oligomerisation. According to *in-vitro* and *in-vivo* experiments, DNJ is expected to be a potential drug for the inhibition of DENV assembly (Miller *et al.*, 2012; Whitby *et al.*, 2005; Yu *et al.*, 2012). Viral factors such as DENV NS5 and DENV NS3 were also taken as drug action points in order to block viral replication (Deng *et al.*, 2012; Rothan *et al.*, 2012; Takhampunya *et al.*, 2006). These reported anti-DENV molecular strategies still require further investigations. Even though some of the anti-DENV agents are now undergoing randomised controlled clinical trials, it will still take a long time for anti-DENV drugs to become available on the market

(Sampath and Padmanabhan, 2009; Tricou *et al.*, 2010; Whitehorn *et al.*, 2012).

1.3 Pathogenesis of DENV infection

1.3.1 DENV Tropism

Cell and tissue tropism of DENV may influence the outcome of the disease. It is difficult to identify the primary target cells of DENV infection (Jessie *et al.*, 2004). *In-vitro* findings and *ex-vivo* autopsy investigations detecting viral NS proteins and negative-strand viral RNA indicate that the immune system, the liver, and the endothelial cell linings of blood vessels contribute to the pathogenesis of DHF/DSS (Martina *et al.*, 2009).

Having been bitten by a mosquito, DENV is inoculated into the bloodstream together with the mosquito's saliva. DENV virions spread to both the epidermis and dermis, infecting the Langerhan cells and keratinocytes that reside in the epidermis (Limon-Flores *et al.*, 2005; Wu *et al.*, 2000). Infection then spreads to immature myeloid DCs. Those infected DCs are activated and subsequently migrate from the infection site to the draining lymph nodes. Activated DCs produce interferon alpha and beta (IFN-α/β) and tumour necrosis factor alpha (TNF-α) (Libraty *et al.*, 2001; Marovich *et al.*, 2001). During the migration of DCs, monocyte and macrophage are also recruited as target cells of DENV (Durbin *et al.*, 2008; Kou *et al.*, 2008; Moreno-Altamirano *et al.*, 2002). DENV is amplified and distributed through the

lymphatic system and thoracic duct, including splenic and liver macrophages (Blackley *et al.*, 2007; de Macedo *et al.*, 2006), as well as bone marrow stromal cells (Rothwell *et al.*, 1996). The tropism and replication efficiency of DENV in DCs, monocytes, macrophages, endothelial cells, bone marrow stromal cells, and liver cells determines the viral level in blood and affects the severity of disease development. After inoculation, DENV can be detected in the reticuloendothelial system and several organs, including skin, lymphoid tissue, kidney, lung and plasma (Martina *et al.*, 2009).

DENV is found in hepatocytes and Kupffer cells. Apoptosis of these cells is induced by DENV, causing the occurrence of DENV-associated hepatocyte necrosis, microvesicular steatosis, and councilman bodies (Fabre *et al.*, 2001; Paes *et al.*, 2005). Involvement of the liver during DENV infection may relate to spontaneous bleeding (Seneviratne *et al.*, 2006; Wichmann *et al.*, 2007).

It has been find that viral receptors determine the target sites of viral replication and pathogenesis of viral infection (Schneider-Schaulies, 2000). The interaction between virus and receptor is not only necessary in starting the infection, but also capable of mediating signaling transductions for the secretion of cytokines (Schneider-Schaulies, 2000). Thus, in order to spread viral particles from initial infection site to different target organs and cells, viruses may use varied and multiple receptors (Schneider-Schaulies, 2000)

(Table 1-1).

During a heterologous DENV infection, antibody-dependent enhancement (ADE) is involved in the development of disease (Halstead, 1970). It is hypothesised that Fcγ receptor, which recognises the constant region of IgG, mediates the internalisation of DENV-antibody complex and disturbs the antiviral immune response (Ubol and Halstead, 2010).

Vascular damage and vascular dysfunction play important roles in the pathogenesis of DFS/DSS (Cardier *et al.*, 2006). Compared to mononuclear cells, endothelial cells of the vascular system do not have any Fcγ receptors to facilitate internalisation of virus-antibody complexes. The occurrence of viral RNA in endothelial cells could probably be a consequence of pinocytosis (Jessie *et al.*, 2004). DENV antigen NS1 preferentially binds to endothelial cells located in the lung and the liver (Avirutnan *et al.*, 2007). Endothelial cells in different parts of the vascular-bed system can generate different coagulation responses upon DENV infection, leading to discrete vascular leakage syndrome characteristic in both DHF and DSS (Cardier *et al.*, 2005; Martina *et al.*, 2009).

1.3.2 Humoral immune response

DENV infection and dissemination are controlled by human humoral immune responses. Infection with one DENV serotype enables the immune system to be protected from that specific serotype from that point on. Meanwhile, infection with another DENV serotype (hetero-infection) may only lead to short-term heterotypic immune protection, possibly attributed to cross-reactive viral E protein-specific antibodies. The anti-DENV antibodies mainly target the DENV prM protein, E protein, and NS1 protein. Other NS proteins, for example the NS3 and NS5 proteins, are also targets of antibodies, although their responses are not as strong (Valdes *et al.*, 2000). However, hetero-infection causes severe DENV complications (Whitehorn and Simmons, 2011). This phenomenon is supposed to have been the consequence of cross-reactive antibodies, known as ADE (Halstead, 1970).

IgG1 and IgG4, the major antibody subgroups in DENV infection, are able to efficiently fix and activate the classical complement system by activating C1q binding (Hjelm *et al.*, 2006; Koraka *et al.*, 2001). The DENV NS1-antibody complex, together with other cytokines such as TNF-α and IFN-α, may activate the complement cascade to produce C3a and C5a, both of which contribute to vascular permeability (Avirutnan *et al.*, 2006; Kurosu *et al.*, 2007). On the other hand, the C5b-C9 complex also correlates to DHF/DSS development, triggering other factors involved in intravascular coagulation (Avirutnan *et al.*, 2006; Markiewski *et al.*, 2007).

1.3.3 The cellular immune response

Cellular immunity is another defence mechanism during DENV infection. During primary DENV infection, after mosquito bite, DENV particles are injected into human skin and bloodstream. Virions are firstly captured by APCs. Afterwards, DENV-specific $CD4^+$ T cells and $CD8^+$ T cells are activated by APCs through the antigen presentation process.

DENV-specific T cells are triggered upon stimulation from viral epitopes. Scientists have identified $CD4^+$ T cell and $CD8^+$ T cell epitopes on viral structural proteins, such as two regions (residues 47-55 and residues 83-92) of the DENV4 C protein (Gagnon *et al.*, 1996). Among the five viral NS proteins, NS3 is demonstrated to be the most common target of T cells, as it is multifunctional and the most conserved antigen (see section 1.1.3.5) (Imrie *et al.*, 2007). Upon reorganisation of DENV NS proteins, activated cytotoxic T cells (CTL) can lyse the infected cells (Gagnon *et al.*, 1999).

Apart from T cells, natural killer (NK) cells also play a critical role in viral clearance during primary DENV infection (Shresta *et al.*, 2004). Human blood NK cells are cytotoxic against infected cells by two pathways: direct cytolysis and antibody-dependent cell-mediated cytotoxicity (Kurane *et al.*, 1986). The contact between NK cells and DENV relies on various cytokines and chemokines produced by DCs, and this contact leads to subsequent immunity events, such as DC-induced NK cell proliferation, NK-mediated

shattering of DCs, and NK-dependent DC maturation (Della Chiesa *et al.*, 2005).

The interaction between DCs, T cells, endothelial cells, and DENV, together with elevated levels of CXCR3-reactive chemokine production, correlates with the severity of DENV. In acute infection, CXCR3 is highly expressed on DENV-infected T cells and decreased upon the recovery phase. The contact between CXCR3-expressing lymphocytes and DENV-infected monocytes or DENV-infected DCs triggers the production of a CXCR3-reactive chemokine, for instance CXCL10. CXCR3-reactive chemokines can recruit more activated/memory T cells and NK cells into the anti-DENV defence (Dejnirattisai *et al.*, 2008). Details regarding the interaction between DENV and DCs, as well as the specific function of DCs during DENV infection, are to be reviewed in section 1.4.4.

During secondary DENV infection with heterologous serotype, highly cross-active $CD8^+$ T cells triggered during primary infection are preferentially activated with high avidity for the invading virus (Imrie *et al.*, 2007). These high-avidity cross-reactive $CD8^+$ T cells produce high levels of pro-inflammatory and anti-inflammatory cytokines, including IFN-γ, TNF-α, and interleukin (IL)-13, but low levels of IL-10. On the other hand, low-avidity cross-reactive $CD8^+$ T cells that produce high levels of pro-inflammatory cytokines may be preferentially developed over naïve T cells with high avidity

for the current invading viral serotype. The profile of responding T cells in secondary infection is thus different from that in primary infection (Mongkolsapaya *et al.*, 2006). This phenomenon is known as “original antigenic sin”. Such a process may restrain or hold-up viral eradication, causing higher viral loads and increasing immunopathology (Mongkolsapaya *et al.*, 2003).

1.3.4 Models for DENV pathogenesis research

1.3.4.1 *In-vivo* models

Since most animal models are not permissive to DENV infection, DENV pathogenesis research has been hampered by the lack of suitable animal models. Although some non-human primates are susceptible to DENV infection, they are only able to develop low-level viraemia and fail to show obvious signs of diseases (Bente and Rico-Hesse, 2006). In light of this, a number of immunocompetent models and immunocompromised models have been used to study DENV pathogenesis (Table 1-3).

One of the major issues of immunocompetent models is that they may restrict the DENV replication level. This restriction makes it difficult to discover other factors that cause viral replication failure (St John *et al.*, 2013). On the other hand, the immunocompromised models are able to provide nearly unrestricted viral replication and uniform diseases severity, which makes these models more suitable for anti-DENV drug development (St John

et al., 2013). However, the differences between the human immune system and mice immune system obstruct the investigation of key pathological events, such as vascular bleeding (Mestas and Hughes, 2004). Also, the absence of major immune pathways, IFN-related pathways for example, may cause the resistant mouse cells to be permissive to DENV, generating incompetent results (St John *et al.*, 2013).

Nonetheless, both immunocompetent and immunocompromised models require much higher doses (>10^8 PFU) than that as a result of a natural mosquito bite (~10^4 PFU). Moreover, when using the intracranial route of inoculation, DENV replication does not typically appear in extraneural sites, or in cells involved in innate immunity (DCs, for example). This does not represent the natural route of human DENV infection (Mathew and Rothman, 2008). Peripheral DENV replication in mice can be achieved by intravenous (i.v.) and sub-cutaneous (s.c.) infection of AG129 mice. However, this model is not suitable for the study of humoral memory responses after primary DENV infection due to its short life-span (Zompi and Harris, 2012).

1.3.4.2 *In-vitro* cell models

Apart from the use of mosquito cell lines such as the C6/36 cell line (*Aedes albopictus*) and AP61 cell line (*Aedes pseudoscutellaris*) for studying DENV-mosquito interaction (Chen *et al.*, 2011; Thaisomboonsuk *et al.*, 2005), a wide range of animal cells and human cells are also used for DENV research

(Table 1-4).

Amongst these cell lines, Vero, LLC-MK2 and BHK are commonly used due to the fact that they are well-characterised and easy to maintain, in addition to having a well-studied background (Govorkova *et al.*, 1996). These animal cell lines are mainly used for plaque assays (Armstrong *et al.*, 2011; Kurosu *et al.*, 2010; Moi *et al.*, 2011). Furthermore, these cells lines are also used for drug evaluation and vaccine production (Chan and Tambyah, 2012; Rothan *et al.*, 2012).

Despite the robustness of Vero, LLC-MK2, and BHK cells, they are not the natural target cell types of DENV and may not be suitable for studying DENV pathogenesis in host (Bente and Rico-Hesse, 2006). As a result, a variety of primary cultures and permanent cell lines derived from cells and tissues that are natural DENV targets have been used to study the host-virus interaction. These include DCs, monocytes, macrophage, lymphocytes and endothelial cells (Bente and Rico-Hesse, 2006). Some of the widely used human cell lines used in DENV pathogenesis research are shown in Table 1-3.

Recently, a human challenged model was developed. This model involved subjects that were previously vaccinated with a live-attenuated tetravalent DENV vaccine. Blood mononuclear cells extracted from these subjects were

then challenged by other attenuated strains. Cellular immune responses in these challenged cells were studied (Gunther *et al.*, 2011).

As stated by Clark *et al.* (2012), it is very important for researchers to choose the appropriate host cells for studying DENV pathology *in-vitro*. When DENV is propagated in alternative cell lines or organisms, the virus will undergo mutation in order to adapt to the environment. As a result, *in-vitro* characteristics produced by the virus are irrelevant to those produced *in-vivo* (Clark *et al.*, 2012).

In detail, the over-adapted viral characteristics that are caused by using inappropriate cell models appear in the following aspects:

1) Adapted DENV life-cycle events

When appropriate viral receptors are absent, viruses are able to develop new strategies to entry host cells. Viruses may search for molecules, which have low-binding affinity and are abundantly expressed. The binding between viruses and these molecules cause virion clustering. Having been incubated in high concentrations for a long time, these weak interactions can lead to internalisation (Clark *et al.*, 2012). For example, a DENV vaccine with high affinity to bind to heparan sulphate, which has been mentioned in section 1.1.4.1.1, is demonstrated to be attenuated in macaques in vaccine preclinical trials (Anez *et al.*, 2009).

Table 1-3 Comparison of commonly used *in-vivo* models for DENV pathogenesis study

Name of the model	Features	Examples of Applications	References
AG129 mice	Deficient in the IFN-α/β receptor and IFN-γ receptor	Viral virulence study. Cross-reactive B cells and T cells study	(Watanabe *et al.*, 2012; Zompi *et al.*, 2012)
A/J mice	Immunocompetent inbred	NK cells and B cell responses study. Thrombocytopenia manifestation study.	(Huang *et al.*, 2000a; Shresta *et al.*, 2004)
BALB/C mice	Plasmacytomas and monoclonal antibodies production	Epitopes identification. Neurological manifestations study.	(Tian *et al.*, 2012; Velandia-Romero *et al.*, 2012)
C57BL/6 mice	Deficient in the IFN-α/β receptors	Pathogenic mechanism of liver injury study. Neurological syndromes study.	(de Miranda *et al.*, 2012; Sung *et al.*, 2012)
NOD/SCID/IL2RγKO mice	Deficient in innate and adaptive immune response; deficient in haemolytic complement response; better engraftment of a variety of human cells and tissues	Cross-reactive T cell study.	(Jaiswal *et al.*, 2009; Mota and Rico-Hesse, 2009)
Rhesus macaques	Haemorrhage and coagulopathy inducible.	TLR3- and TLR7/8-mediated innate signalling. Blood components study.	(Onlamoon *et al.*, 2010; Sariol *et al.*, 2011)

Table 1-4 Animal and human cell models widely used in DENV pathogenesis researches

Cell models	Derivation	Examples of Applications	References
293T	Human epithelial cell line	• DENV-stimulated cytokine production • Pathological function of DENV NS1	(Bosch *et al.*, 2002; Noisakran *et al.*, 2008b)
BHK	Baby hamster kidney-derived fibroblast	• DENV-induced apoptosis study • Pathological function of NS1 protein	(Chen *et al.*, 2011; Nasirudeen *et al.*, 2008; Somnuke *et al.*, 2011)
CHO	Chinese hamster ovarian epithelial cell	• DENV receptor study	(Huerta *et al.*, 2008)
COS-7	African green monkey kidney-derived fibroblast	• DENV immune complex infectivity study • Antibody-dependent enhancement of DENV	(Moi *et al.*, 2010; Rodrigo *et al.*, 2006)
ECV304	Human urinary bladder carcinoma	• DENV-stimulated cytokine production • DENV-induced apoptosis	(Avirutnan *et al.*, 1998; Bosch *et al.*, 2002)
H1299	Human non-small cell lung cancer	• DENV-induced apoptosis study	(Nasirudeen and Liu, 2009; Nasirudeen *et al.*, 2008)
HUH-7	Human liver carcinoma	• DENV-induced apoptosis study • Pathological function of DENV C protein	(Nasirudeen *et al.*, 2008; Wang *et al.*, 2002)
HUVEC	Human umbilical vein endothelial cell	• DENV-stimulated cytokine production • Vascular leakage	(Dewi *et al.*, 2008; Huang *et al.*, 2000b)
HeLa	Human cervix adenocarcinoma	• Pathological function of DENV C protein • DENV-induced apoptosis	(Catteau *et al.*, 2003; Wang *et al.*, 2002)
HL-60	Human promyeloblast acute promyelocytic leukaemia	• DENV receptor study	(Bielefeldt-Ohmann, 1998)

(To be continued)

(Continued)

Cell models	Derivation	Examples of Applications	References
HepG2	Human hepatocellular carcinoma	•DENV-induced apoptosis •DENV receptor study	(Jindadamrongwech *et al.*, 2004; Thongtan *et al.*, 2004)
K-562	Human lymphoblast with chronic myelogenous leukaemia	•Antibody-dependent enhancement	(Chan *et al.*, 2012; Goncalvez *et al.*, 2007; Mazzon *et al.*, 2009)
LLC-MK2	Rhesus Kidney derived epithelial cell	•DENV entry mechanism study	(Thaisomboonsuk *et al.*, 2005; Wichit *et al.*, 2011)
Neuro 2a	Murine neuroblastoma cell	•DENV-induced apoptosis study	(Despres *et al.*, 1996; Despres *et al.*, 1998)
P815	Murine mastcytoma line	•DENV-triggered CTLs study	(Masaki *et al.*, 2009; Spaulding *et al.*, 1999)
THP-1	Human peripheral blood monocyte with acute monocytic leukaemia	•Antibody-dependent enhancement •Virulence study	(Chan *et al.*, 2011; Chareonsirisuthigul *et al.*, 2007; Ubol *et al.*, 2008)
U937	Human monocyte with histiocytic lymphoma	•Antibody-dependent enhancement •Heat shock effect	(Chavez-Salinas *et al.*, 2008; Kontny *et al.*, 1988; Puerta-Guardo *et al.*, 2010)
Vero	African green monkey Kidney derived epithelial cell	•DENV receptor study •DENV-induced autophagy study •DENV-induced apoptosis study	(Gangodkar *et al.*, 2010; Martinez-Barragan and del Angel, 2001; Nasirudeen *et al.*, 2008)

2) Adapted DENV virulence

Passaging DENV2 50 times in primary dog kidney cells produced attenuated DENV strains with features such as temperature sensitivity, small plaque size, loss of neurovirulence, and decreased incidences of viraemia in infected monkey. These changes of virulence may be due to the nucleotide mutations in coding regions and UTR (Halstead and Marchette, 2003; Kelly *et al.*, 2011).

Therefore, it is very important to choose the most appropriate cell models for the *in-vitro* study of DENV pathogenesis.

1.4 Background of Dendritic cells (DCs)

DCs are the major connector between innate immunity and adaptive immunity, and are able to capture antigens that appear in the periphery and present these antigens to lymphocytes. Thus, DCs play an extremely significant role in defence against infectious diseases (Belz *et al.*, 2009).

Although a diversity of human cells, such as liver cells and endothelial cells, have been used as subjects for studying DENV-host interactions, they are the consequent targets of DENV infection. On the other hand, DCs are one of the initiate target cells of DENV infection (Libraty *et al.*, 2001; Marovich *et al.*, 2001). It is more important to investigate the initiate hosts of DENV

infection, because the knowledge of DENV infection process can benefit the design of prophylaxis against the DENV infection. Therefore, in this study, DC has been used as a model to study DENV and host interaction for expanding the knowledge of the DENV pathogenesis.

1.4.1 Origin of DC

There are two distinct pathways for the development of immune cells from the hematopoietic stem cells, namely lymphoid lineage and myeloid lineage. Stem cells from the former give rise to progenitor cells of T lymphocytes, B lymphocytes, natural killer T (NKT) cells, and NK cells, etc. In contrast, those from the latter differentiate into distinct progenitor cells, which can further develop into monocytes, neutrophils, a proportion of macrophages, mast cells, erythrocytes, and common DC precursors in the bone marrow.

Common DC precursors generate plasmacytoid DCs and pre-classical DCs; the latter group then leaves the bone marrow, entering the blood circulation and lymphoid tissue to participate in immune activities (Geissmann *et al.*, 2010).

DCs generated from early progenitors have short life-spans, lasting for only two to four weeks (Merad and Manz, 2009). Alternatively, LCs, which differentiate from local stem cells, can migrate to the skin for the period of

late embryonic stage and have a short life span upon leaving the epidermis (Chorro *et al.*, 2009).

1.4.2 Subsets of DC

DCs represent a heterogeneous population of cells. They can be divided into two major sub-groups: 1) non-lymphoid tissue migratory and lymphoid tissue-resident DCs (known as myeloid DCs in the human body); and 2) plasmacytoid DCs (Merad and Manz, 2009). Information regarding general DC subsets in the human body is summarised in Table 1-5.

1.4.2.1 Myeloid DCs

There are three subsets of myeloid DCs in human skin that have been previously studied: LCs, dermal $CD14^+$ DCs, and dermal $CD1a^+$ DCs. LCs preferentially activate $CD8^+$ T lymphocytes, regulating cellular immunity. Dermal $CD14^+$ DCs preferentially regulate humoral immunity through inducing antibodies responses. The biological function of dermal $CD1a^+$ DCs still remains unclear (Ueno *et al.*, 2010).

In the blood circulation, a subpopulation of myeloid DCs can differentiate into macrophages, which express butyrate esterase and CD14 upon stimulation by macrophage colony-stimulating factor (M-CSF). Thus, these myeloid DCs may be related to monocyte-derived DCs in terms of their cellular origin (Ito

et al., 2005).

1.4.2.2 Plasmacytoid DCs

Human plasmacytoid DCs circulate in the blood, and are also located in lymphoid tissues and peripheral tissues. Upon activation by various viruses and non-viral stimuli, plasmacytoid DCs express type I IFN stronger and quicker than other APCs. The interaction between plasmacytoid DCs and pathogens can intensely influence surrounding APCs and lymphocytes (McKenna *et al.*, 2005). According to the expression levels of CD2, plasmacytoid DCs in human bodies include two subsets: $CD2^{high}$ plasmacytoid and $CD2^{low}$ plasmacytoid cells. Compared to $CD2^{low}$ plasmacytoid DCs, the $CD2^{high}$ plasmacytoid DCs distinctively produce lysozyme and IL-12p40, and are more effective at inducing allogeneic T lymphocyte proliferation (Ueno *et al.*, 2010).

1.4.2.3 Monocyte-derived DC

Monocytes represent a heterogeneous mononuclear phagocyte population circulating in the human blood. A human monocyte can be unequivocally defined by its expression of CD14. $CD14^{high}$ monocytes constitute the majority of the population, while $CD14^{low}$ monocytes form an infrequent subset. After microbial infection, monocytes migrate to inflammatory sites and differentiate into DC-like cells (Randolph *et al.*, 2008). *In-vitro* studies showed that different cytokine-combinations can induce differentiation of

monocytes into DCs with identified phenotypes. For example, GM-CSF plus IL-4 (secreted by mast cells) can activate monocyte differentiation into IL-4-DCs (as MoDCs in this study). Meanwhile, type I IFN (secreted by plasmacytoid DCs) activates monocyte-derived IFN-DCs, and IL-15 (secreted by keratinocytes) stimulates monocyte-derived IL-15-DCs (Ueno *et al.*, 2010). These monocyte-derived DCs are different in their immune responses. For example, IL-15-DCs are more effective at activating antigen-specific CTL compared to IL-4-DCs (Dubsky *et al.*, 2007). These observations indicate distinct immune responses and pathological features of different monocyte-derived DCs (Ueno *et al.*, 2010).

1.4.3 Immunological function of DCs during viral infection

1.4.3.1 Antigen capture and activation of DCs

Antigens that are encountered by DCs can be classified into two groups: endogenous antigens (self-synthesised) and exogenous antigens (which originate from bacteria and viruses) (Belz *et al.*, 2009). DCs recognise highly conserved microbial molecular motifs of exogenous antigens by PRR, including toll-like receptors (TLRs) and C-type lectin receptors (CLR) (Rossi and Young, 2005).

Table 1-5 DC subsets in the human body

DC subsets	Surface markers	Location	TLR distribution	Cytokine production profile
LCs	Langerin$^+$E-cadherin$^+$ CD11b$^+$ DCIR$^+$	Epidermis	TLR1, TLR2, TLR3, TLR6, TLR10	IL-8, IL-15
Dermal CD14$^+$ DCs	DC-SIGN$^+$DEC205$^+$LOX-1$^+$CLEC-6$^+$Dectin-1$^+$DCIR$^+$	Dermis	TLR2, TLR4, TLR5, TLR6, TLR8, TLR10	IL-1β, IL-6, IL-8, IL-10, IL-12, GM-CSF, TGF-β
Dermal CD1a$^+$ DCs	CD14$^-$CD207$^-$CD1a$^+$ CD1c$^+$	Dermis	NA	IL-8, IL-15
CD141$^+$ myeloid DCs	CD1c$^+$ CD16$^+$ CD141$^+$CLEC9A$^+$XCR1$^+$	Blood, lymph nodes, bone marrow, tonsil	TLR3	CXCL1, IL-12p70 and IFN-β
CD11c$^+$ myeloid DC	HLA-DR$^+$CD40$^+$CD86$^+$CD83$^+$DC-SIGN$^-$ Lin$^-$	Blood, second lymphoid organs, peripheral tissues	TLR1, TLR2, TLR3	TNF-α, IFN-α and IL-12.
Plasmacytoid DCs	Lin$^-$HLA-DR$^+$ CD123^{high}CLEC4C$^+$ ILT-7$^+$	Blood and lymphoid organs	TLR1, TLR6, TLR7, TLR9, TLR10	Type I IFN, IP-10, TNF, and IL-6

NA: information is not available. This table is drew according to the observations and discussion from Klechevsky *et al*. and Collin *et al*. (Collin *et al.*, 2011; Klechevsky *et al*., 2009).

The expression profile of TLRs in different DC subsets is listed in Table 1-5. Some of the TLRs are involved in the interactions between pathogen components and TLRs include: peptidoglycan-TLR2, viral dsRNA-TLR3, viral glycoproteins-TLR4, viral ssRNA-TLR7, and unmethylated bacterial CpG DNA motif-TLR9 (Akira and Takeda, 2004).

TLR activation stimulates the expression of CD83, constimulatory molecules, and C-C chemokine receptor type 7 (CCR7) in DCs. These cytokines then activate the DCs to migrate to T lymphocyte-abundant draining lymph nodes. Additionally, TLR activation not only drives plasmacytoid DCs to secrete large amounts of IFN-α, but also drives myeloid DCs to produce IL-6, IL-10, IL-12 and TNF-α (Rossi and Young, 2005).

CLRs are membrane-bound molecules expressed by resident or non-activated DCs. CLRs are able to bind to the carbohydrate moieties of glycoproteins from viruses for processing and presentation on major histocompatibility complex (MHC) molecules. CLRs such as MR, DEC-205 (CD205), DC-SIGN, BDCA-2, and dectin-1 are found on the surface of immature myeloid DCs, while Langerin (CD207) is found on LCs (van Kooyk, 2008). Besides antigen recognition and capture, CLRs are involved in T-lymphocyte presentation (Engering *et al.*, 2002). They are also associated with TLRs to induce inflammatory cytokine productions from DCs (Gantner *et al.*, 2003).

Following viral recognition, DCs internalise viral pathogens and immune complexes via phagocytosis, pinocytosis, and endocytosis (Rossi and Young, 2005).

Having encountered viral antigens, immature DCs undergo a maturation process. During this process, DCs secrete cytokines, elevate the expression of co-stimulatory molecules and lessen their antigen capture. Meanwhile, these DCs are able to migrate to lymphoid tissues where the immune information can be conveyed to T lymphocytes, B lymphocytes, NK cells, and NKT cells (Rossi and Young, 2005).

1.4.3.2 Viral antigen presentation

Antigen-bearing DCs are able to present peptide-antigens to lymphocytes via MHC class I molecules (Ackerman *et al.*, 2003) and MHC class II molecules (Villadangos *et al.*, 2005).

The presentation of extracellular components as endogenous antigens, including antigens from tumour cells, viral infected cells, or intracellular pathogens via MHC class I molecules is called cross-presentation. Phagocytosed antigens are firstly transported out from the phagosome into the cytoplasm. In the cytoplasm, endogenous antigens are degraded into peptides by the enzymes inside the proteasome. These peptides will be

translocated back into the ER-fused phagosomes to form the MHC class I-peptide complexes. The complexes are subsequently transported through the Golgi apparatus secretory pathway, arriving at the cytoplasm surface to be presented to T cells (Ackerman *et al.*, 2003; Guermonprez *et al.*, 2003).

The antigenic peptide-binding site of MHC class II $\alpha\beta$ dimers is capable of binding a wide range of peptides with variable sequences and lengths. Before MHC class II $\alpha\beta$ dimers reach the endosomal sites where the antigenic peptides are formed, the peptide-binding site is protected via associations with invariant chain Ii in the ER. When appropriate antigenic ligands for the class II molecules are generated, the Ii subunit will be destroyed in order to clear the binding pocket of class II $\alpha\beta$ dimers for the antigens (Villadangos and Ploegh, 2000). Afterwards, the MHC II–peptide complexes are generated and quickly appear on the surface of DCs for recognition by T cells (Villadangos *et al.*, 2005).

During the antigen presentation process with T lymphocytes, one DC can usually activate 100-3,000 T lymphocytes (Banchereau and Steinman, 1998). Activated T lymphocytes assist DCs with terminal maturation, which further enhances lymphocytes proliferation and differentiation. Activated T lymphocytes consequently reach the injured tissues, where these T lymphocytes eliminate microbes and microbe-infected cells (Ueno *et al.*, 2010).

Activated B lymphocytes, on the other hand, migrate to different tissues and mature as plasma cells, which produce neutralising antibodies against microbes (Ueno *et al.*, 2010).

1.4.4 Interaction between DCs and DENV

1.4.4.1 DC models in DENV research

As previously reviewed in section 1.3, DCs are one of the initial target cells of DENV infection. For more than 10 years, several DC models have been used to investigate the interaction between DCs and DENV, including:

- *in-vitro* human IMMoDCs (Boonnak *et al.*, 2008; Nightingale *et al.*, 2008),
- *ex-vivo* human plasmacytoid DCs/myeloid DCs/epidermal DCs (Limon-Flores *et al.*, 2005; Sun *et al.*, 2009),
- *in-vivo* human plasmacytoid DCs/myeloid DCs/skin DCs (De Carvalho Bittencourt *et al.*, 2012; Marovich *et al.*, 2001),
- human erythroleukaemic K562 cells (Goncalvez *et al.*, 2007; Mazzon *et al.*, 2009),
- human monocytic cell line THP-1 (Padwad *et al.*, 2010; Ubol *et al.*, 2008),
- human promyelocytic leukaemia cell line HL-60 (Diamond *et al.*, 2000).

Due to the importance of DCs in DENV infection, various *in-vitro* DC models

have also been applied in DENV-vaccine or anti-DENV therapy development. For instance, K562 cells were used in DENV-vaccine evaluations (Palmer *et al.*, 2007), while *in-vitro* human MoDC were utilised in both vaccine and anti-DENV agent screening studies (Sanchez *et al.*, 2006; Subramanya *et al.*, 2010).

1.4.4.2 DC responses in DENV pathogenesis

It has been reported that DENV interacts with DC-SIGN and MR in order to invade DCs (Lozach *et al.*, 2005; Miller *et al.*, 2008; Tassaneetrithep *et al.*, 2003). After internalisation, DENV particles could be visualised in cystic vesicles, vacuoles, and the ER of infected DCs (Ho *et al*., 2001). Previous studies have shown that DENV-infected IMMoDCs secrete high level TNF-α, IFN-α, programmed cell death 1 ligand 2 (PD-L2), MHC II molecules, as well as soluble gelatinolytic matrix metalloproteinase (MMP)-9 and MMP-2 in a viral dose-dependent manner (Ho *et al.*, 2001; Libraty *et al.*, 2001; Luplertlop *et al.*, 2006; Nightingale *et al.*, 2008). DENV2 infection in DCs activates STAT1 and STAT3 through both IFN-α-dependent and IFN-α-independent mechanisms. DENV2 acts against IFN-α, but not IFN-γ, antiviral responses by inhibiting Tyk2-STAT signalling in the DCs (Ho *et al.*, 2005).

TNF-α and IFN-α secreted by DENV-infected DCs trigger the activation and maturation of bystander DCs, increasing the expression of cell surface co-stimulatory molecules and inducing migration, while secreted MMP-9 and

MMP-2 are involved in enhancing endothelial permeability (Dejnirattisai *et al.*, 2008; Luplertlop *et al.*, 2006).

However, compared to bystander DCs, infected DCs produce less CXCL10, PD-L1, CD80, CD86, IL-12 p70, and MHC I molecules (Libraty *et al.*, 2001; Nightingale *et al.*, 2008). Additionally, infected DCs are apoptotic but not activated or matured (Palmer *et al.*, 2005).

DENV-infected DCs activate DENV-specific T lymphocytes. The activated T lymphocytes, or the CD40 ligand that is expressed by activated T lymphocytes, can overcome the inhibition of maturation in DENV-infected DCs. This indicates a possible T lymphocyte-dependent mechanism for the immune-mediated enhancement of the severity of DENV-related diseases (Dejnirattisai *et al.*, 2008; Sun *et al.*, 2006).

DENV2 replicates at a higher level in growth factor-treated $Lin1^{-}CD11c^{+}CD14^{-}CD123^{+}$ *ex-vivo* myeloid cells. An increased production of inflammatory cytokine was also observed *in-vitro*. In addition, the numbers of myeloid DCs are significantly lower in most of the DENV-infected patients. On the other hand, DENV2 replicates at a lower level in cytokine-treated $Lin1^{-}CD11c^{-}CD123^{high}$ *ex-vivo* plasmacytoid DCs. A quicker and stronger cytokine production *in-vitro* was observed in these plasmacytoid DCs, and

the number of plasmacytoid DCs was significantly lower only in high and intermediate viraemia DENV patients. These observations suggest that plasmacytoid DCs and myeloid DCs play different but significant roles during DENV infection (De Carvalho Bittencourt *et al.*, 2012; Sun *et al.*, 2009).

During secondary infection, DENV enters DCs through ADE, which requires FcγRIIa. However, studies revealed that FcγRIIa is inversely correlated with the surface expression of DC-SIGN. Therefore, FcγRIIa-bearing mature DCs are capable of increasing DENV viral RNA replication levels by more than 100-fold compared to immature DCs that highly express DC-SIGN (Boonnak *et al.*, 2008). Besides, DENV infection in mature DCs is further enhanced by the CD40 ligand, which is produced by activated memory T cells, indicating the importance of DC-T cell interaction during secondary infection (Sun *et al.*, 2006).

Lately it has been realised that host genetic polymorphism plays a role in DENV-DC interaction during secondary infection. In secondary infection, infected-DCs dominantly produce IFN-β, while infected-macrophages mainly secrete IFN-α and infected-monocytes produce IL-10. Single nucleotide polymorphism (SNP) is believed to contribute to these complicated responses (Boonnak *et al.*, 2011).

1.4.4.3 Obstacles and gaps in investigating DENV-DC interactions

There are several issues about DENV-DC interactions that still remain controversial. As mentioned in 1.1.4.1, the entry mechanism of DENV to DCs is still not known in detail. It is believed that, besides DC-SIGN and MR, there are other unknown factors/receptors also involved in DENV entry into DCs (Miller *et al.*, 2008). Additionally, the modified immune responses triggered by DENV in DCs need to be investigated in depth. For example, what causes the different DENV replication levels in different DC subsets (Sun *et al.*, 2009)? What induces the cytokine response to shift from Th1 (TNF-α, IFN-γ, IL-2) to Th2 (IL-4, IL-6, and IL-10) in DHF (Chaturvedi, 2009)? What is the role of each specific DC subset during DENV infection?

Furthermore, the establishment of an appropriate *in-vitro* model for the study of DC-DENV interaction is another issue. Having been reviewed in 1.3.4.2, an appropriate *in-vitro* model should reflect both the natural viral load and natural viral pathogenesis reaction. Although for nearly 20 years human MoDCs have been applied in numerous DC experiments, variations between blood donors have yielded conflicting experimental observations (Barnes *et al.*, 2008). Susceptibility of primary DC cultures to viral infection could be varied due to gene variations in populations, as reviewed in section 1.4.4.2. Several differences between MoDCs and *ex-vivo* DCs have been noted. MoDCs exhibited a higher capacity to capture antigen but a lower degree of internalisation compared to *ex-vivo* isolated $CD11c^+$ DCs (Andersson *et al.*, 2012). Moreover, blood $CD11c^+$ did not express DC-SIGN and activated

fewer proliferative mixed leukocyte responses (MLR) than MoDCs (Osugi *et al.*, 2002). Thus, in the human body, blood myeloid DCs may use other attachment molecules/receptors, rather than DC-SIGN, to recognise DENV. Also, they use an alternative mechanism to internalise the DENV virion and trigger MLR towards DENV. Additionally, as reviewed before, different cytokine combinations can give rise to different MoDCs with distinct immune characteristics. These observations raise concern around the use of MoDCs to study DENV pathogenesis.

On the other hand, DCs generated from HL-60, K562 and THP-1 failed to fully present the DC-specific phenotype, such as the expression of MHC class II and co-stimulatory molecules, the antigen up-take/antigen presentation ability, and adhesion/migration abilities (Santegoets *et al.*, 2008b; van Helden *et al.*, 2008). Using these DC lines alone in DENV investigations may lead to misunderstandings or irrelevant observations.

To conclude, the choice of an appropriate cell model that is naturally infected by DENV and also displays typical properties of DC is one of the most significant concerns in the investigation of DC-DENV interactions.

1.5 Background of MUTZ-3 cell line

MUTZ-3 cells originated from the peripheral blood of a 29-year-old male patient with acute myelomonocytic leukaemia (AML) FAB M4. Karyotyping

proved that a rare but recurrent AML-associated translocation (12;22)(p13;q11-q12) was carried by the MUTZ-3 chromosome (Hu *et al*., 1996).

MUTZ-3 cells showed monocytic features morphologically and immunophenotypically, expressing monocytic markers, such as CD14, monocyte-specific esterase, myeloperoxidase, and tartrate-resistant acid phosphatase enzymes (Hu *et al*., 1996). Compared to peripheral blood monocytes, MUTZ-3 cells generated similar reactions upon IL-4 and lipopolysaccharide stimulation, making this an *in-vitro* monocytic cell model (Quentmeier *et al.*, 1996).

MUTZ-3 cells can differentiate into immature and mature myeloid DCs or LCs in response to different doses and combinations of cytokines (Masterson *et al.*, 2002). Compared to other DC lines such as THP-1 and K562, MUTZ-3-derived DCs (MDCs) are closer to *ex-vivo* DCs in morphological, phenotypic, and immunological characteristics, such as T cell priming and antigen capturing (Larsson *et al.*, 2006).

Transcriptional profiling studies showed that, as an *in-vitro* DC model, MDCs resembled $CD1c^+$ and $CD141^+$ tonsillar myeloid DCs. Besides, MDCs, together with MoDCs and CD34-derived DCs, can differentially represent

specific characteristics of primary DCs. For instance, several immune-related transcripts were expressed by MDCs, indicating the possibility of applying MDCs in immune research; the gene of one C-type lectin receptor was uniquely expressed by MDCs, suggesting the suitability of using MDCs for receptor studies (Lundberg *et al.*, 2013).

MDCs exhibit the functional properties crucial for the *in-vivo* generation of cytotoxic T lymphocyte-mediated immunity and thus, currently represent the most valuable, sustainable model system for myeloid DC differentiation (van de Ven *et al.*, 2006; van de Ven *et al.*, 2008), for immunotherapeutic T cell activation (Chang *et al.*, 2005; Santegoets *et al.*, 2008a; Santegoets *et al.*, 2006), and for DC vaccination studies (Hoefnagel *et al.*, 2011).

In addition to having been commonly used in evaluations of sensitising compounds (Johansson *et al.*, 2013; Python *et al.*, 2009), MUTZ-3-derived LCs (MLCs) have also been applied in investigating virus-host interactions. Using this MLC model, it was proven that the Langerin inhibition enhanced the transmission of HIV between MLCs and T cells. Carbohydrate microbicides against HIV infection were also evaluated using this MLC model (de Jong *et al.*, 2010). Additionally, in varicella-zoster virus infection study, MLCs were demonstrated to be permissive to this virus, and the infected MLCs did not undergo apoptosis, therefore playing a role in virus spread (Huch *et al.*, 2010).

Recently, the MUTZ-3 cell line has drawn the attention of DENV researchers (Thomas *et al.*, 2009b). Nonetheless, MDCs have not been used to study DENV pathogenesis. It is desired to apply MDCs as an *in-vitro* DC model to study DENV infection.

1.6 Aims of the study

The aim of this study was to establish a novel *in-vitro* DC model to investigate the interaction between DCs and DENV2. Because: 1) current *in-vitro* DC models fail to fully represent the features of *in-vivo* DCs; 2) the primary DC culture has its own drawbacks; 3) the knowledge of the interaction between DENV and DC is extremely important, many aspects of which are still remained sealed. The development of the novel model can be benefit to the investigation of DENV pathogenesis, providing an option as a tool for studying DENV and DC interaction.

2 Objectives of the Study

The study had three main objectives:

1. A novel *in-vitro* DC model using MUTZ-3 cell-derived immature DCs (IMDC) was established. The phenotype, morphology and anti-viral gene expression profile of IMDCs were then examined.

2. The permissiveness of IMDCs to DENV2 replication was also studied.

3. In parallel with IMMoDCs, IMDCs were applied to study anti-DENV pathways. Both native DENV2 virions and DENV2 replicons were used for this purpose. Firstly, the gene expression profile after DENV2 RNA replication was studied using a reverse transcription-polymerase chain reaction (RT-PCR) array. Afterwards, a group of genes selected from the RT-PCR array due to their high fold-changes after DENV2 RNA replication were further investigated.

4. Depending on established IMDCs, DENV2 entry mechanism to DCs was investigated. The interaction between two known DENV receptors, DC-SIGN and MR, was also studied.

3 Materials and Methods

3.1 Cell culture and differentiation

3.1.1 Culture and generation of MUTZ-3-derived immature dendritic cells

The human myeloid leukaemia cell line MUTZ-3 (DSMZ, Braunschweig, Germany) was maintained at 5-8 × 10^5 cells/millilitre (ml) in 24-well tissue culture plates (Nunc, NY, USA). MUTZ-3 cells and other cells used in this study were counted by haemocytometer and cell viability was determined by the Trypan blue exclusion test. To each well, 1 ml of MUTZ-3-competent medium (Appendix I) was added. The medium was changed every 2-3 days. IMDC was generated according to the procedures described by others previously (Masterson *et al.*, 2002). Briefly, 5 × 10^5 cells/ml MUTZ-3 cells were cultured in MUTZ-3-competent medium with high-dose GM-CSF (100 nanogram (ng)/ml, GENTAUR, Kampenhout, Belgium), IL-4 (10 ng/ml, Sigma-Aldrich, MO, USA) and TNF-α (2.5 ng/ml, Sigma-Aldrich) for 6-7 days.

3.1.2 Generation of monocyte-derived dendritic cells

Buffy coat obtained from healthy donors was provided anonymously by the Hong Kong Red Cross Blood Transfusion Service, with approval from the Human Subject Ethics Sub-committee of the Hong Kong Polytechnic University. Human peripheral blood mononuclear cells (PBMCs) were

isolated using Ficoll-Paque PLUS (GE Healthcare, Sweden) from the buffy coats. Human $CD14^+$ monocytes were negatively selected from PBMCs using Dynabeads Untouched Human Monocytes Kit (Invitrogen Corporation, CA, USA). Monocytes were then seeded in a 24-well plate at 5×10^5 cells/ml. To each well, 1 ml of primary DC-competent medium was added. Primary DC-competent medium was RPMI 1640 (GIBCO) with 10% FBS (GIBCO), 100 U/ml penicillin and 100 μg/ml streptomycin (GIBCO), in the presence of GM-CSF (100 ng/ml, GENTAUR) and IL-4 (10 ng/ml, Sigma-Aldrich). After 6-7 days, immature monocyte-derived dendritic cells (IMMoDCs) were obtained.

3.1.3 Generation of leukaemia cell line-derived dendritic cells

Human acute monocytic leukaemia cell line THP-1 (American Type Culture Collection [ATCC], VA, USA, TIB-202), human chronic myelogenous leukaemia cell line K562 (ATCC, USA, CCL-243), and human acute promyelocytic leukaemia cell line HL-60 (ATCC, CCL-240) were maintained at 5×10^5 cells/ml in RPMI 1640 medium (GIBCO) supplemented with 10% FBS (GIBCO), 100 U/ml penicillin and 100 μg/ml streptomycin (GIBCO). For the generation of immature THP-1-derived DCs (IMTDCs), THP-1 was cultured at a density of 2×10^5 cells/ml in six-well plates in the presence of GM-CSF (40 ng/ml, GENTAUR) and IL-4 (40 ng/ml, Sigma-Aldrich) for five days. For the generation of immature K562-drived DCs (IMKDCs), K562 was cultured at a density of 2×10^5 cells/ml in six-well plates with 10 ng/ml

phorbol 12-myristate 13-acetate (PMA) (Sigma-Aldrich) in the medium for seven days. In order to generate immature HL-60-derived DCs (IMHDCs), HL-60 was seeded at a density of 3×10^5 cells/ml in a six-well plate in the RPMI medium supplemented with calcium Ionophore A23187 (180 ng/ml, Sigma-Aldrich) for one week. All media were changed every 2-3 days.

3.2 DENV2 infection of immature DCs

For experiments that conducted in Hong Kong, native DENV2 was handled in class II biosafety cabinet in the biosafety level III laboratory of Queen Mary Hospital, Hong Kong. For experiments that were done in Taiwan, native DENV2 was conducted in class II biosafety cabinet in the biosafety level II laboratory of Department of Public Health and Parasitology, Chang Gung University, Taiwan.

3.2.1 DENV2 propagation

DENV2 (New Guinea C strain) was propagated in *Aedes albopictus* clone C6/36 cells as described elsewhere (Chen *et al.*, 2011). Briefly, C6/36 cells were cultured in 10-cm petri dishes (Nunc) with minimal essential medium (MEM, GIBCO) supplemented with 10% FBS (GIBCO), 2% non-essential amino acids (GIBCO), 2 g/ml 4-(2-hydroxyethyl)-1-piperazineethanesulfonic acid (HEPES) (Sigma-Aldrich), and 0.4% of an antibiotic-antimycotic (GIBCO). C6/36 cells were incubated at 28°C without CO_2 supply. Virus suspension or fresh medium only (as mock control) at a volume of 1 ml were

added to the monolayer of C6/36 with ~70% confluence. The culture dish was then incubated at 28°C for 1 hour (h) with gentle shaking, allowing virus absorption. Nine millilitres of fresh medium was then added to the C6/36 monolayer. Cells were then incubated at 28°C for three or four days. The culture medium was collected, followed by centrifugation at 3000 × *g* for 10 minutes (min). Supernatant that contained virions was harvested and stored as 1-ml aliquots in -80°C until use.

3.2.2 DENV2 titration

DENV2 was titrated in baby hamster kidney (BHK-21) cells using the plaque assay as described by *Chen et al.* (2011). BHK-21 cells were cultured in 6-well plates (Nunc) as monolayers with 80% confluence. Two hundred microlitres of serially-diluted virus suspensions were added to BHK-21 monolayers in each well of a 6-well plate. Cells were kept at 37°C for 1 h with gentle shaking. After that, virus suspensions were removed. Cell monolayers were overlaid with 4 ml of 1.1% methyl cellulose medium (Appendix I). Having been incubated at 37°C for 4 days, cells in each well were fixed in 3 ml 10% formalin at room temperature for 30 min, followed by staining in 1 ml 1% crystal violet for 15 min. The virus titre was calculated and expressed as plaque-forming units (PFUs) per millilitre.

3.2.3 DENV2 infection of derived dendritic cells

During DENV2 infection, approximately 1×10^7 IMDC cells/IMMoDC cells or 1×10^6 IMTDC cells/IMKDC cells/IMHDC cells were harvested and washed twice with phosphate-buffered saline (PBS, pH 7.4). DENV2 suspension (with multiplicity of infection [MOI] = 1) or MEM medium with 10% FBS (mock control) was added to the cells. The cells were then incubated at 37°C with gentle agitation every 15 min. After incubation for 1 h, viral suspension was removed by centrifugation at 1000 × *g* for 10 min. Cells were seeded at a density of 5×10^5 cells/ml and kept at 37°C before performing the subsequent procedures.

3.2.4 DENV2 second-round infection in BHK-21

Medium was collected from DENV2-infected IMDCs or IMMoDCs together with the mock controls 48 h after infection. One millilitre of the collected medium was then mixed with 2 ml fresh medium (MEM medium with 10% FBS). The mixtures were inoculated onto BHK-21 monolayers. After incubation for two days, total RNA was extracted (see section 3.6.1) from the second-round infected BHK-21 cells and mock controls. DENV2 was detected by real-time RT-PCR (see section 3.6.2) using the specific primer pair of D2V2F and D2V2R (Appendix II). 18S rRNA of BHK-21 was used as an internal control and amplified using primer pair of BHK18sF and BHK18sR (Appendix II). Real-time RT-PCR products were confirmed by agarose electrophoresis.

3.2.5 DENV2-binding blocking assay

For receptor-blocking assay, approximately 1×10^6 IMDC or IMMoDC cells were firstly incubated with anti-DC-SIGN & DC-SIGNR monoclonal antibody (R&D, MN, USA), and/or anti-MR monoclonal antibody (Abcam, MA, USA), and/or anti-inter-alpha-trypsin inhibitor heavy chain 2 (ITIH2) C-terminal polyclonal antibody (Abcam) (Appendix III) with the concentrations of 10 μg/ml. The cells with antibodies were kept on ice for 1 h. For endocytosis-inhibition, 1×10^6 cells were incubated with chlorpromazine (CPZ) (Sigma-Aldrich) at a concentration of 10 micromoles (μM) or 15 μM at 37°C for half an hour. After incubation with antibodies or CPZ, 1×10^6 cells were infected with native DENV2, as described in section 3.2.3. Cells were then seeded at a density of 5×10^5 cells/ml and incubated at 37°C until the next experiments.

3.3 DENV2 replicon generation and transfection into IMDCs and IMMoDCs

3.3.1 Construction of DENV2 replicons

DENV2 (Tonga/74) subgenomic replicon p2C102 was a generous gift from Professor Wei-Kung Wang of the University of Hawaii (previously from National Taiwan University). p2C102 was generated from the full-length DENV2 (Tonga/74) cDNA clone p2 by deleting most of the structural regions (Lai *et al.*, 2008). p2C102 contains i) genes encoding the N-terminal 102 residues of C protein which has the authentic cleavage site recognised by viral protease, ii) genes encoding the C-terminal 26 residues of E protein that

also encode the signal sequence of NS1, and iii) all the non-structural proteins coding regions. p2C102 plasmid was maintained by transforming into *E. coli* BD1528 (*E. coli* Genetic Stock Centre, Yale University, USA). Before *in-vitro* transcription of the DENV2 replicon, plasmid p2C102 was extracted from the *E. coli* host. p2C102 construction was confirmed by *AvaI* (Fermentas, Ontario, Canada) single digestion and *KpnI/AscI* (Fermentas) double digestion at 37°C for 1 h. Digested fragments were examined by agarose electrophoresis (USB Corporation).

3.3.2 *In-vitro* transcription of DENV2 replicon

High Yield Capped RNA Transcription Kit (Applied Biosystems, San Francisco, USA) was used for *in-vitro* transcription of the DENV2 replicon from p2C102. Briefly, 1 microgram (μg) p2C102 was linearised using 2 units (U) of *KpnI* (Fermentas) at 37°C for 1 h. The reaction was terminated by adding 1/20 volume of 0.5 M EDTA, 1/10 volume of 3 molar (M) sodium acetate and 2 volumes of absolute ethanol. The content was mixed thoroughly and chilled at -20°C for 30 min. The DNA was then concentrated by centrifugation at 18,000 × *g* for 15 min. Subsequently, DNA was resuspended in RNase free water with a concentration of 0.5 μg/microlitre (μl). The linearised p2C102 was added to the transcription reaction mixture prepared according to the Manufacturer's instructions. In order to optimise the yield, 2 μl of additional GTP (20 millimolar [mM]) was added. The final reaction mixture was incubated at 37°C for 2 h. At the end of the transcription

reaction, TURBO DNase (ABI) was added to eliminate template DNA. After transcription, an RNA product with a size of around 8.8 kb was purified using 30 μl lithium chloride precipitation solution (ABI) (7.5 M), and then kept at -80ºC until being used.

3.3.3 *In-vitro* transfection of DENV2 replicon into IMDCs or IMMoDCs

IMMoDCs or IMDCs with a cell count of 8×10^5 cells were suspended in 500 μl medium (RPMI 1640 for IMMoDC, MEM-α for IMDC, without FBS and antibiotics) and added into each well of a 24-well plate. To each well, an aliquot of Lipofectamine 2000 (Invitrogen) and transcribed RNA product of DENV2 replicon mix was added. The mixture was prepared by mixing 1 μl Lipofectamine with 0.8 μg RNA (ratio 1:1.25) in 100 μl RPMI 1640 or MEM-α medium without FBS and antibiotics. The Lipofectamine-RNA mixture was incubated at room temperature for 20 min before being added to the cells. Cells with Lipofectamine only were set up as the mock controls. Cells were then incubated at 37ºC for 6 h. After that, medium was replaced by MUTZ-3-competent medium or primary DC-competent medium supplemented with low concentration growth factors, as described in sections 3.1.1 and 3.1.2. Cells were incubated again at 37ºC for up to 48 h.

3.4 Microscopic examinations

3.4.1 Phase contrast microscopy

Cells cultured in the 24-well plate were examined by Leica DMI 4000B (Leica Microsystems GmbH, Wetzlar, Germany) with Leica application suite software (Leica).

3.4.2 Transmission electron microscopy (TEM) examination

DENV2-infected cells were fixed in 4% glutaraldehyde in 0.1 M phosphate buffer (Appendix I) at 4°C for 2 h followed by washing three times with 0.1 M phosphate buffer. Cells were then post-fixed with 1% osmium oxide in 0.1 M phosphate buffer (Appendix I) for 1 h at 4°C. After washing three times with 0.1 M phosphate buffer, cells were dehydrated in an alcohol series (30%--50%--70%--80%--90%--95%--100%) for 15 min in each concentration at room temperature. Then cells were embedded in Spurr's resin (Appendix I) in 100% alcohol in a series of concentrations (50%--66%--75%--100%) for 1 h at each concentration. The embedded cells were incubated in pure Spurr's resin for 24-72 h at 70°C. Ultrathin sections (0.85-μm thick) were cut with Leica REICHERT Ultracut S (Leica), which were then stained with 1% toluidine blue O (Appendix I). Ultrathin sections were then cut 60-nm to 90-nm thick using a diamond knife, and stained with aqueous uranyl acetate for 30 min and with 0.4% lead citrate (Appendix I) for another 5 min. The ultrathin sections were examined using the JEOL JEM 1230 electron microscope system (JEOL Ltd, Tokyo, Japan) at 100 kV.

3.4.3 Confocal microscope examination

Glass coverslips (Matsunami, Tokyo, Japan) in 24-well plates (Nunc) were incubated with Poly-L-lysine (Sigma-Aldrich) at a concentration of 50 μg/ml at 37°C overnight. Coverslips were then washed three times with PBS. Subsequently, 5×10^5 cells were added onto the coverslips in each well of the 24-well plate, incubated at 37°C for 2 h. After incubation, unattached cells were washed away by PBS. DENV2 suspensions or MEM medium with 10% FBS (mock control) was added to attached cells with MOI = 1. Cells were incubated at 4°C for 1 h, allowing virus binding. Unattached virions were removed by washing three times with PBS at 4°C, five minutes for each. Cells were then fixed by 4% paraformaldehyde in PBS at 4°C for 10 min and then at room temperature for 20 min. After fixation, cells were blocked with 3% BSA in PBS for 1 h at room temperature.

Cells were stained with mouse anti-DENV E monoclonal antibody 4G2 (Millipore, MA, USA) as 1:200 in 1% BSA-PBS at 37°C for 1 h. Then rabbit anti-mouse secondary antibody conjugated with R-Phycoerythrin (R-PE) (Invitrogen) as 1:200 in 1% BSA-PBS was added to cells, and incubated at 37°C for 1 h. Next, cells were stained with anti-MR-PECy5 (BioLegend, CA, USA) as 1:20 in 1% BSA-PBS and anti-DC-SIGN-FITC (BD, NJ, USA) in 1 as 1:200 in 1% BSA-PBS at 37°C for 1 h. Three PBS washings were required after staining to eliminate unattached antibodies.

For the co-capping assays, one group of IMDCs were stained with anti-DC-SIGN-FITC firstly at 37°C for 30 min. Non-cross-linked antibodies were washed away by PBS and cells were fixed by 4% paraformaldehyde in PBS at room temperature for 20 min. Then, cells were incubated with anti-MR-PECy5 antibody at 37°C for another 30 min. For the other group of IMDCs, cells were stained in reverse order of antibodies.

One drop of ProLong Gold Anti-fade reagent (Invitrogen) was added to the stained cells. Cells were then incubated at room temperature for 12 h in the dark. After incubation, the edges of the coverslip were completely sealed with nail polish. Cells were then exam by LSM 510 META NLO (Carl Zeiss AG, Oberkochen, Germany).

3.5 Cell surface marker studies by flow cytometric assays

3.5.1 Surface marker expression of naïve IMDCs and naïve IMMoDCs

Expressions of specific surface markers on cells were determined by flow cytometry on FC500 (Beckman Coulter, CA, USA). Mouse anti-human Mab used in this assay included anti-CD83-FITC, anti-CD80-R-PE, anti-CD1a-R-PE, anti-CD14-PE-TR (Invitrogen), anti-MR-PECy5 (BioLegend), and anti-DC-SIGN-FITC (BD), as listed in Appendix III. Propidium iodide (PI) (Invitrogen) was used to determine the viability of cells. In order to perform multi-colour staining, the cells were divided into four groups (Figure 3-1, A). Three groups were used for four-colour staining, which contained anti-MR-

Cy5 (detected by filter 4), anti-DC-SIGN-FITC (detected by filter 1), PI (detected by filter 2 or filter 3), and PE or PE-TR-labelled antibodies that can be detected by the additional filter on FC500. The remaining group was used for three-colour staining, which contained anti-CD83-FITC, anti-MR-Cy5 and PI. Having been washed in PBS, 3-5 $\times$ 10^5 cells were collected. The cells were resuspended in 100 μl PBS, which were then subjected to three- or four-colour staining. Colour compensation was accomplished by AbC Anti-Mouse Beads (Invitrogen). The compensation beads were single-stained with the corresponding antibodies and then examined on the flow cytometer using the same parameters as the cell samples. Based on the flow cytometry data of compensation beads, the compensation matrixes were calculated and generated by FLOWJO software (Tree Star, OR, USA). The compensation matrixes were subsequently applied to cell sample data by FLOWJO. Non-specific binding was monitored using isotypic controls. Non-stained cells were used as negative controls.

3.5.2 Surface marker expression of infected/transfected IMDCs and infected/transfected IMMoDCs

Two-colour staining was used to monitor surface marker expression changes after DENV2 replication. 48 h after native DENV2 infection or DENV2 replicon transfection, cells were harvested and washed by PBS. After that, cells were fixed by 4% paraformaldehyde in PBS for 20 min, followed by washing in PBS three times. Cells were then permeabilised by 0.2% Triton-X-100 in PBS for 10 min, followed by three PBS washes. In order to exclude

non-specific binding, cells were incubated with 3% BSA-PBS for 15 min. After washing in PBS for three times, cells were incubated with mouse anti-DENV2 NS1 Mab (Abcam) or mouse anti-E Mab 4G2 (Millipore) (Appendix III) at 37°C for 1 h, followed by three PBS washes. Anti-mouse secondary antibody conjugated with R-PE (Invitrogen) or anti-mouse secondary antibody conjugated with FITC (Invitrogen) (Appendix III) was added to cells and incubated at 37°C for 1 h. Non-binding antibodies were washed away by PBS. Afterwards, antibodies for surface markers described in section 3.5.1. were added to the cells according to the grouping shown in Figure 3-1 B. Cells were incubated at 37°C for 1 h, followed by washing three times with PBS. The cells were subjected to flow cytometry on FC500 system (Beckman Coulter). Twenty thousand cells were countered for data collection of every sample. Colour compensation was performed as described in section 3.5.1.

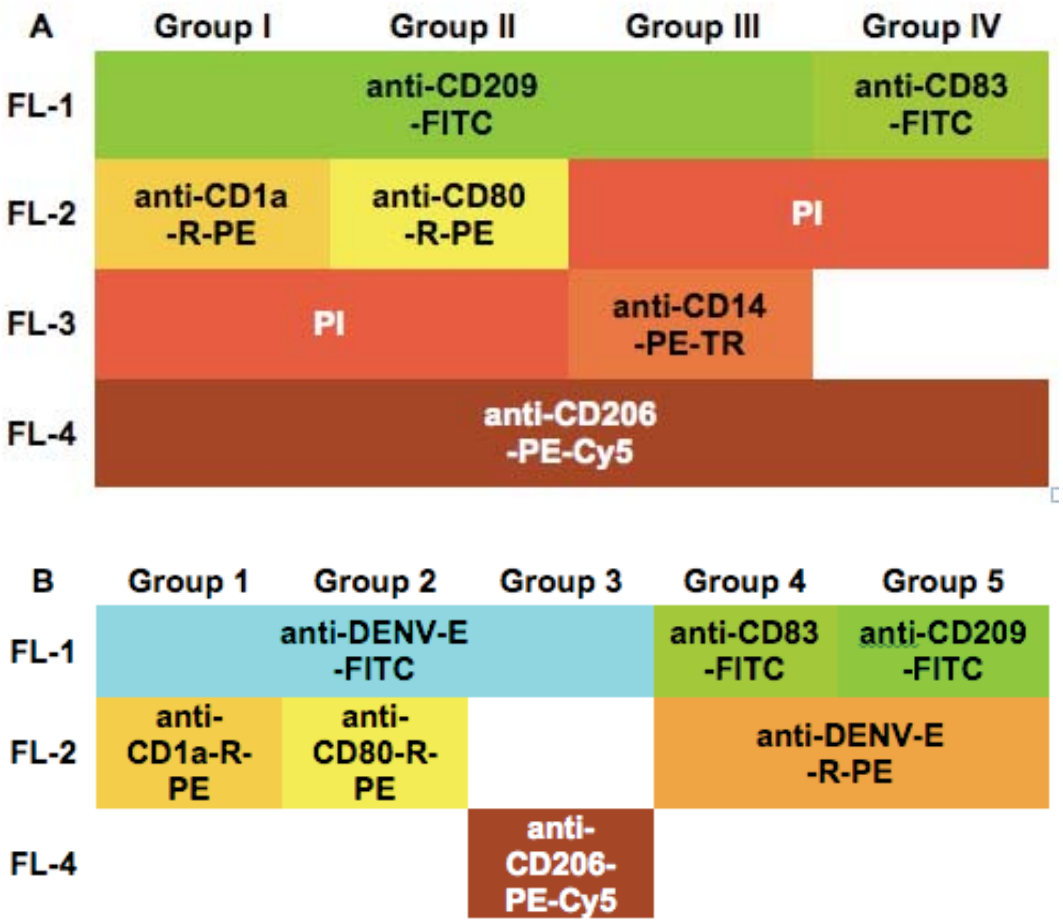

Figure 3-1 Groupings of antibodies for flow cytometric assays.

A: Groupings of antibodies for detecting surface marker expressions on naïve IMDCs and naïve IMMoDCs. B: Groupings of antibodies for examination of surface marker expressions on IMDCs and IMMoDCs after native DENV2 infection. FL: filter of flow cytometry FC500.

3.6 Real time RT-PCR

3.6.1 RNA extraction

3.6.1.1 Total RNA extraction from cells

Total RNA was extracted 48 h after transfection or infection. Approximately 1 × 10^7 transfected/infected cells and the mock control cells were harvested and washed twice in PBS. Total RNA was extracted using the PureLink RNA Mini Kit (Invitrogen). Briefly, 1 × 10^7 cells were resuspended in Lysis Buffer containing 1% 2-mercaptoethanol. Homogenisation of cells was done by passing the lysates 10 times through the 21-gauge needles attached to RNase-free syringes. One volume of 70% ethanol was added to each volume of the cell homogenates, followed by thoroughly mixing the content. Samples were then transferred to the Spin Cartridges and were bound to the membranes by pulse centrifugation at 12000 × *g*. Afterwards, 350 μl Wash Buffer I was added to the membranes, followed by quick spinning down. On-column DNase treatment was achieved by adding 80 μl PureLink DNase mixture onto the surface of the membranes. PureLink DNase mixture contained 8 μl 10 × DNase I Reaction Buffer, 10 μl DNase (3 U/μl), and 62 μl RNase-Free Water (all from Invitrogen). The columns were kept at room temperature for 15 min. Subsequently, membranes were washed once by 350 μl Wash Buffer I, and twice by 500 μl Wash Buffer II with ethanol. RNA was finally eluted by 20 μl RNase-Free Water. The quality of the extracted RNA samples was determined by Agilent 2100 bioanalyser using the RNA 6000 Nano total RNA assay (Genome Research Centre, The University of

Hong Kong, Hong Kong). Extracted RNA samples with RNA Integrity Number (RIN) above 9.0 were used for subsequent analysis.

3.6.1.2 Viral RNA extraction from cell culture medium

Five hundred microlitres of cell culture medium was harvested from each sample and centrifuged at 1000 × *g* in order to remove the cell debris. After centrifugation, 420 μl supernatant was subjected to QIAamp Viral RNA Mini Kit (Qiagen) following the manufacturer's instruction. Briefly, 1680 μl AVL buffer containing 16.8 μg carrier RNA was mixed well with the 420 μl supernatant and incubated at room temperature for 10 min. Following the incubation, 1680 μl absolute ethanol was added to the mixture and mixed well by pulse-vortexing. The mixtures were then transferred to QIAamp spin columns and bound to the membrane by centrifuging at 6000 × *g* for 1 min. The membrane of each column was washed by 500 μl Buffer AW1 and centrifuged at 6000 × *g* for 1 min. Afterwards, 500 μl Buffer AW2 was added to each column. The columns were then centrifuged at 20000 × *g* for 1 min. Viral RNA was finally eluted via adding 30 μl Buffer AWE to the membranes, incubating at room temperature for 1 min, and then centrifuging at 6000 × *g* for 1 min.

3.6.2 Two-step real-time RT-PCR using SYBR Green I

3.6.2.1 Reverse transcription of DENV2 RNA

cDNA was amplified from total RNA. Briefly, the 20 μl reaction mixture contained 1 × first strand buffer (Invitrogen), 200 U M-MLV reverse transcriptase (Invitrogen), 40 U RNase OUT (Invitrogen), 0.01 M DDT (Invitrogen), 3 μg random hexamer (Invitrogen), 0.5 mM dNTPs (GE healthcare) and 1 μl of RNA template. RNA template, random hexamer and dNTPs were heated at 70°C for 5 min, followed by immediate incubation on ice. The remaining components were then added and incubated at 37°C for 50 min. The reverse transcriptase was finally inactivated by heating at 70°C for 15 min. cDNA was stored at 4°C until required.

3.6.2.2 Relative-quantitative real-time PCR

Relative-quantitative real-time PCR was performed by the 7500 Real-Time PCR System (ABI) with QuantiFast SYBR Green PCR kit (Qiagen, Hilden, Germany). The 25 μl mixture contained 12.5 μl 2 × QuantiFast SYBR Green PCR Master Mix, 1 μM forward primer, 1 μM reverse primer, and 100 ng cDNA template. Primers used for real-time PCR are listed in Appendix II. The real-time cycler conditions were initiated at 95°C for 5 min, followed by 40 cycles of PCR reaction of 10 seconds (sec) at 95°C and 30 sec at 60°C. The fluorescent signal was collected at 60°C for each PCR cycle. The melting curve analysis protocol was set as 95°C for 15 sec, 60°C for 20 sec, and 95°C for 15 sec. For each sample, the signal of the target gene was

normalised using the signals of the housekeeping genes ribosomal protein L13a (RPL13A) and glyceraldehyde 3-phosphate dehydrogenase (GAPDH). Relative gene expression levels of samples were calculated using the comparative ∆threshold cycle (Ct) method. The calculation was performed by the 7500 Software using the following formulas (ABI):

- The difference in threshold cycles for target gene and housekeeping gene:
$$\Delta Ct = Ct_{target} - Ct_{housekeeping}$$
- The difference in threshold cycles for test group and calibrator:
$$\Delta\Delta Ct = \Delta Ct_{test} - \Delta Ct_{calibrator}$$
- The amount of target gene, normalized to a housekeeping genes and relative to a calibrator:
$$2^{-\Delta\Delta Ct}$$

Calibrator: sample used as basis for comparative result

3.6.2.3 Absolute-quantitative real-time PCR

Purified DENV2 RNA with a known concentration was serially-diluted to 1/10, 1/100 and 1/1000 of the concentration in RNase-free water. Afterwards, the diluted RNA samples were subjected to RT-PCR. cDNA generated from RT-PCR was then quantitated via real-time PCR using the SYBR Green PCR kit (Qiagen). The Ct values of viral RNA amplifications were proportional to logarithm (log) of the amount of viral RNA in the samples. Standard curve was plotted according to the real-time PCR Ct values obtained from serially diluted RNA templates (Appendix IV).

For the quantitation of viral RNA in culture supernatants, RNA templates with exact same amount were firstly reverse-transcribed into cDNA. Then, the exact same amount of generated cDNA was subjected to real-time PCR using the same conditions as the standard. After real-time PCR, the viral RNA concentrations of target samples were determined using the standard curve, and were then transformed as viral copy number using the following formula (ABI):

$$\text{number of viral copies} = \frac{\text{amount} \times 6.022 \times 10^{23}}{(\text{length} \times 320.5) + 159.0}$$

3.6.3 TaqMan assay for detecting negative sense RNA of DENV2 replicon

Extracted total RNA, which was subjected to TaqMan assay, was divided into two groups. For one group, 1 μg RNA was reverse transcribed into genomic cDNA using random hexamers (Invitrogen). For another group, DENV2 negative sense RNA was detected and amplified by the sense primer DV2_NegS_RT5 (Appendix II). The reverse transcription procedures were the same as those described in section 3.6.2.1.

Specific primers and FAM-labelled probe for DENV2 3' untranslated regions (UTR) were designed (DV-2_F, DV-2_R, DV-2_M FAM, Appendix II) to detect DENV2 replication by the TaqMan assay (ABI). Human β-actin

included as an endogenous control was detected by TaqMan assay using primers and a VIC-labelled probe (ABI). Each 50 μl TaqMan assay reaction mixture contained 25 μl 2 × TaqMan Universal PCR Master Mix (ABI), 2.5 μl DENV2 custom primers and probe, 2.5 μl human β-actin primers and probe, 5 μl DENV2 cDNA and 5 μl genomic cDNA. The TaqMan assay was performed on the 7500 Real-Time PCR System (ABI) using thermal cycling conditions recommended by the Manufacturer. Briefly, the reaction was incubated at 50°C for 2 min, followed by 95°C for 10 min, 40-cycle of PCR reactions at 95°C for 15 sec and at 60°C for 1 min.

3.6.4 RT-PCR array and data analysis

RNA extracted from transfected IMDCs or IMMoDCs was reverse-transcribed using the RT² First Strand Kit (SABiosciences, MD, USA). Briefly, 5 μg of RNA was mixed with 2 μl 5 × Genomic DNA Elimination Buffer. The mixture was kept at 42°C for 5 min, followed by incubating on ice immediately for 1 min. The mixture was then added to RT cocktail, which contained 4 μl 5 × RT buffer, 1 μl Primer and External control Mix, 2 μl RT enzyme Mix, and 3 μl RNase-Free water. The whole mixture was incubated at 42°C for 15 min, then at 95°C for 5 min. A total of 91 μl of RNase-Free water was added to each 20-μl cDNA synthesis reaction. The synthesised and diluted cDNA was then subjected to the Human Interferon (IFN) α, β Response PCR Array and Human JAK/STAT Signalling Pathway PCR Array (SABiosciences). Real-time PCR was performed on the LightCycler 480 Real-Time PCR System

(Roche Applied Science, Upper Bavaria, Germany). The real-time cycler conditions were set as 10 min at 95°C, followed by 45-cycles of PCR reaction at 95°C for 15 sec, and 60°C for 1 min. SYBR Green fluorescence for every well was detected and recorded during each annealing step at 60°C. The ramp rate was adjusted to 1°C /sec.

PCR array results were evaluated by analysis software provided by the Manufacturer (SABiosciences). Three different batches of IMDC prepared in three separate occasions or IMMoDC generated from three different healthy donors were used as biological replicates. Selected genes which showed significant fold-changes in expression were confirmed by real-time RT-PCR using specific primers (Appendix II), as explained in section 3.6.2.

3.7 Protein extractions and analysis

3.7.1 Total protein extraction

Approximately 1×10^7 DENV2-infected cells were collected and washed with PBS three times. Cells were then lysed by RIPA buffer (Appendix I). The cell lysates were kept on ice for 1-2 h and then centrifuged at 18,000 × *g* at 4ºC for 15 min. The supernatants containing the extracted total proteins were collected and kept at -80ºC until use. Protein concentrations were determined by the Bradford Method.

3.7.2 Transmembrane protein extraction

Transmembrane proteins were extracted from cells by the ProteoExtract Transmembrane Protein Extraction Kit (Novagen, Merck EMD, Darmstadt, Germany) following the Manufacturer's instruction. Briefly, 1×10^7 cells were collected and washed three times by PBS. Cells were then resuspended in 1 ml Extraction Buffer 1 supplemented with 10 μl Protease Inhibitor Cocktail Set III. The lysates were incubated on ice for 10 min with gentle agitation.

Following incubation, the lysates were centrifuged at 1000 × *g* for 5 min at 4°C. Pellets were resuspended in an extraction mixture composed of 0.1 ml Extraction Buffer 2, 0.1 ml TM-PEK Reagent B and 5 μl Protease Inhibitor Cocktail Set III. The mixtures were then kept in room temperature for 1 h with gentle agitation and then centrifuged at 16,000 × *g* for 15 min at 4°C. Transmembrane proteins that were enriched in supernatants were collected and stored at -80°C until next required. Protein concentrations were examined by Bradford Method.

3.7.3 Virus-transmembrane protein complex immunoprecipitation (Co-IP)

Sixty microgram transmembrane proteins were added to DENV2 suspensions (4×10^6 PFU) and incubated at room temperature with continuous shaking for 2 h. DENV2 suspension only was set as the mock

control. Subsequently, 1/100 volume of mouse anti-DENV E Mab 4G2 (Millipore) or rabbit anti-DENV2 prM-E Pab (*Lo et al.*, unpublished) was added to the virus-protein mixtures and kept at 4°C with gentle continuous shaking overnight. 20 μl pre-washed protein G sepharose bead slurry (GE Healthcare) was added to the reaction mixtures, followed by incubation at 4°C with gentle shaking. Non-cross linked molecules were removed by pulse centrifugation at 8000 × *g*. Sepharose beads were separated from virus-protein complexes by incubation at 100°C for 5 min in 60 μl 6 × SDS-PAGE loading buffer (Appendix I), followed by pulse centrifugation at 8000 × *g*. The precipitated proteins were kept at -80°C.

3.7.4 Sodium dodecyl sulphate polyacrylamide gel electrophoresis (SDS-PAGE)

The in-house sodium dodecyl sulphate (SDS) polyacrylamide gels were used to separate target proteins from protein mixtures under reducing conditions. Each SDS-polyacrylamide gel was set in the gel casting module (1.0 mm) Mini-PROTEAN system (Bio-Rad) with 4 ml of 10% separating gel (pH 8.8), overlaid with 2 ml of 5% stacking gel (pH 6.8) (Appendix I). Protein samples were mixed well with 6 × SDS sample loading buffer (Appendix I), then incubated at 100°C for 5 min. Protein samples were then loaded into each well of the SDS-polyacrylamide gels. Novex sharp standard (Invitrogen) with a known molecular weight ranging from 3.5-260 kDa was run in parallel as a standard. Protein samples were separated at room temperature in the Mini-

PROTEAN tetra cell (Bio-Rad) with 1 × electrophoresis buffer (Appendix I) at 200 volts (V) for 1 h.

For protein separation in non-reducing conditions, NuPAGE Novex 4-12% Bis-Tris Gel (1.0 mm) (Invitrogen) was used. Proteins were mixed with 6 × non-reducing SDS sample loading buffer without β-Mercaptoethanol (Appendix I). Then proteins and protein standard were loaded to each well of the gels. Electrophoresis was performed at room temperature by using XCell SureLock Mini-Cell (Invitrogen) in 1 × MOPS SDS Running Buffer (Invitrogen) at 200 V for 55 min.

3.7.5 Western blotting

After SDS-PAGE, the separated proteins were electroblotted from the SDS-PAGE onto polyvinylidene difluoride (PVDF) membranes (GE Healthcare) in 1 × transfer buffer (Appendix I) at 4°C, using Mini-PROTEAN tetra cell (Bio-Rad) at 100 V for 1 h. The membranes were blocked in 5% non-fat milk (Anchor, New Zealand) in TBST (Appendix I) at room temperature for 1 h, and then incubated overnight at 4ºC with primary antibodies in 5% non-fat milk in TBST or 1% BSA-TBST. Primary antibodies used in this study are listed in Appendix III.

After being washed three times in TBST at room temperature, the membranes were incubated at room temperature for 1 h with secondary antibodies solved in 5% non-fat milk-TBST (Appendix III). Visual signals were developed using BM Chemiluminescence Western Blotting Substrate (POD) (Roche Applied Science). Membranes were incubated in detection solution for 1 min, which was freshly mixed by 1 ml of luminescence substrate solution A with 10 μl of starting solution B. Amersham Hyperfilm ECL (GE Healthcare) was exposed for 5 min in an x-ray film cassette. The visible images were developed by developer solution and fixer solution (Fuji, Tokyo, Japan) and the films were left to dry naturally.

Western blot images were quantified by ImageJ software (National Institutes of Health, MD, USA). Each unit of the blot signal of target protein was presented as net intensity multiply by band area, nomalised to that of Na^+K^+ATPase.

3.7.6 Dot blot

One millilitre culture medium was harvested from cell culture plates. Cell debris was removed by centrifugation at 1000 × *g* for 5 min. Afterwards, 100 μl supernatant from each sample was added to PVDF membrane and immobilised onto the membrane by SRC 96D Dot-Blotter manifold (Schleicher & Schuell BioScience, Dassel, Germany). The membrane was then blocked in non-fat milk and stained with primary and secondary

antibodies, as described in section 3.7.5. The signals from the dots were developed and detected as mentioned in section 3.7.5.

3.7.7 Silver Staining

All steps of silver staining were performed at room temperature with gentle shaking. After SDS-PAGE, gels were fixed in fix solution (Appendix I) overnight. After fixation, gels were incubated in 30% methanol for 15 min, followed by three washings with double-distilled water (ddH_2O). Gels were then sensitised by 0.8 mM sodium thiosulphate ($Na_2S_2O_3$) solved in ddH_2O for 2 min, followed by three washings with ddH_2O. The consequent steps were kept in the dark. Gels were then subjected to silvering in 0.2% (w/v) silver nitrate ($AgNO_3$) in ddH_2O for 25 min, followed by three washes with ddH_2O. Gels were placed in a clean staining tray with developer solution (Appendix I). Gels were incubated until bands were visible. When staining was sufficient, the develop reaction was terminated by changing the solution for 0.042 M disodium ethylenediamine tetraacetate (Na_2EDTA) in ddH_2O. Gels were washed by ddH_2O before protein identification.

3.7.8 Protein identification by MALDI-TOF mass spectrometry

Silver-stained bands were excised from gels. Sections were destained by 1% potassium ferricyanide and 1.6% sodium thiosulfate (Sigma-Aldrich). Proteins were then reduced by 25 mM ammonium bicarbonate (NH_4HCO_3) containing

10 mM dithiothreitol (DTT) (Biosynth, Switzerland) at 60ºC for 30 min and alkylated with 55 mM iodoacetamide (Amersham Biosciences, UK) at room temperature for 30 min. Following reduction and alkylation, the proteins were digested by trypsin (Promega, Madison, WI, USA) (20 mg/ml) at 37ºC overnight. Then, the tryptic peptides were acidified with 0.5% trichloroacetic acid and loaded onto an MTP AnchorChip 600/384 TF (Bruker-Daltonik, MA, USA). Samples were analysed on an Ultraflex MALDI-TOF mass spectrometer (Bruker-Daltonik). Monoisotopic peptide masses were assigned and searched for matches using the MASCOT search engine (http://www.matrixscience.com) (Matrix Science, London, UK).

3.8 Surface plasmon resonance

3.8.1 Surface plasmon resonance instruments

The binding reactions between DENV2 virions and receptors/binding molecules were analysed via Surface plasmon resonance (SPR) technology, using Autolab Model SPRINGLE (Metrohm Autolab, Utrecht, The Netherlands) with an open cuvette system. The optical functioning was based on Kretchmannm configuration and a flexible software package was used to control the functioning of the instrument. Gold-coated BK7 type microscopic glass plates (Eco-Chemie, Utrecht, The Netherlands) were used as sensor chips. All experiments were carried out at 25ºC. All injections were of 50 μl. PBS with pH 7.2 was used to flow over the sensor surface briefly between injections.

3.8.2 Precipitation and UV-inactivation of DENV2

DENV2, which was propagated in C6/36, was concentrated using PEG-it Virus Precipitation Solution (System Biosciences, CA, USA). Briefly, one volume of cold (4ºC) PEG-it Virus Precipitation Solution was mixed well with every four volumes of DENV2-containing supernatant. The supernatant-PEG-it mixture was incubated at 4ºC overnight with gentle shaking. After incubation, the mixture was centrifuged at 1500 × g for 30 min at 4ºC. Afterwards, the supernatant was removed by aspiration. The DENV2 particles appeared as beige pallet and were resuspended in one-tenth of the original volume of cold PBS.

The concentrated DENV2 was inactivated by exposure under an ultraviolet lamp (wavelength, 254 nm) at a distance of 10 centimeters for 3 h at room temperature. The inactivation was confirmed by inoculating the treated-DENV2 to C6/36.

3.8.3 The modification and activation of gold sensor chips

The SPR sensor chips, cleaned by the Piranha solution (Appendix I) were left immersed overnight in 1 mM 11-mercaptoundecanoic acid (11-MUA) (Sigma-Aldrich) (Appendix I). The self-assembled monolayer (SAM) therefore formed upon the sensor chips. The SAM-modified gold sensor chips were washed with ethanol three times, and then washed with ddH2O three times.

Thereafter, the sensor chips were attached to the prism of the SPR instrument using a matching oil with refractive index as 1.515. The baseline angle was adjusted as -1500 millidegrees (m°) using acetic buffer (Appendix I). The baseline was then stablised via washing the sensor chips with acetic buffer, 0.1 M HCl, and 0.1 M NaOH cyclically until every solution showed the same SPR angle every time when it was injected on the surface.

The SAM-modified gold sensor chips were then activated via introducing the activation solution as a mixture of N-hydroxysuccinimide (NHS) (Sigma-Aldrich) and Dimethylaminopropyl-N'Ethylcarbodiimide N-3-hydrochloride (EDC) (Sigma-Aldrich) (Appendix I) for 5 min. After activation of the sensor chip, UV-inactivated DENV2 in acetic buffer containing 10 mg/ml BSA was injected onto the sensor chip and incubated for 15 min. Afterwards, the sensor chip surface was blocked by 1 M aqueous ethanolamine solution (Appendix I) for 5 min.

3.8.4 Detection of the interaction between DENV2 and receptors/binding molecules

Human recombinant MR (R&D), human ITI protein (BIOPUR AG) were dissolved in PBS at five pH conditions (5.5, 6.0, 6.5, 7.0, 7.5) with concentrations as 500 nM, 250 nM, and 125 nM, respectively. An incubation time as approximately 20 min was satisfactory to get a stable SPR signal. Blank PBS buffers were used as dissociation buffer. The surface-bound

molecules were removed by 10 mM HCl. After 5 min regeneration, the surface of the sensor chip was available for the next injection.

3.8.5 SPR data analysis

All SPR data were analysed by Kinetic Evaluation software (Metrohm Autolab). The association and dissociation fit the monophasic model as the following reaction equation (Metrohm Autolab):

$$A + B \underset{k_d}{\overset{k_a}{\rightleftharpoons}} AB$$

The binding affinities between receptor/binding molecule and DENV2 were presented as dissociation constants, calculated as the following equation (Metrohm Autolab):

$$K_D = \frac{k_d}{k_a} = \frac{[A][B]}{[AB]}$$

3.9 Statistical analysis

All quantitative data were analysed and graphed by the Prism 5.0 (Graphpad Software, CA, USA). Differences among groups were evaluated by t-test or ANOVA according to the specific assay. Details of the statistic analysis were explained in the Chapter 4.

4 Results

4.1 IMDCs as a permissive *in-vitro* model of DENV2

4.1.1 Cytokine-induced differentiation of MUTZ-3 cells and human monocytes

MUTZ-3 cells and human $CD14^+$ monocytes were induced with cytokine cocktails (GM-CSF, IL-4, +/- TNF-α) in the medium. Seven days after induction, cultured MUTZ-3 cells differentiated from round (Figure 4-1 A) and suspending cells (Figure 4-1 C) into slightly adherent cells with blunt dendrites (Figure 4-1 B). Meanwhile, cell clusters were observed in the induced IMDC culture (Figure 4-1 D). Additionally, Compared to immature DCs generated from cytokine-triggered THP-1 (Figure 4-1 H), K562 (Figure 4-1 J), and HL-60 (Figure 4-1 L), IMDC was morphologically more close to IMMoDC (Figure 4-1 F).

When assessed by flow cytometry, MUTZ-3, IMDCs, and monocytes displayed more than 90% viability after PI staining, while that of IMMoDCs was lower, at approximately 60-80% (data not shown). Both monocytes and MUTZ-3 cells were $CD1a^-CD80^-DC\text{-}SIGN^-CD14^+$ (Figure 4-2). Approximately 80% and 99% of monocytes and MUTZ-3 cells were MR^+, respectively. After differentiation, DC-SIGN and MR were co-expressed in 42.3% and 55.6% of IMDC and IMMoDC populations, respectively (Figure 4-2). In addition, CD1a and CD80 were expressed on IMDCs and IMMoDCs, which were MR^+DC-

SIGN^{+}, while the monocyte marker CD14 disappeared in both populations (Figure 4-2). Furthermore, as in the immature status, both IMDCs and IMMoDCs were CD83^{-} (data not shown). These data indicated that after differentiation, IMDCs displayed similar phenotypes and morphologies to IMMoDCs.

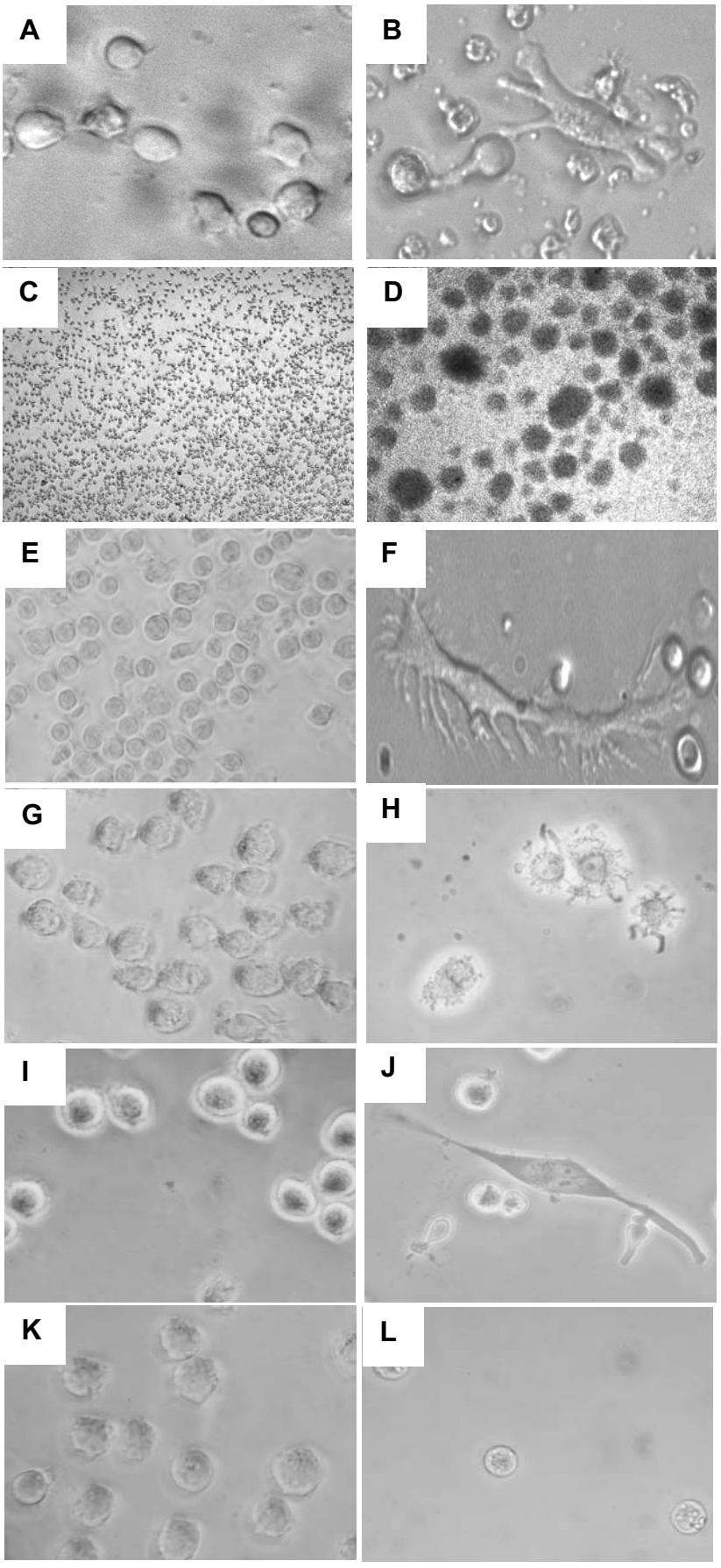
A
B
C
D
E
F
G
H
I
J
K
L

Figure 4-1 Morphology of DCs generated from leukaemia cells and human monocytes.

MUTZ-3 cells were round and blast-like (A,), growing as single cells like THP-1 (G), K562 (I), and HL-60 (K) and sometimes in small clumps in suspension (C), while monocytes were round and in suspension (E). After differentiation, IMDC showed cell clusters in suspension (D). Dendrites were seen in some IMDC cells (B) and in IMMoDCs (F), IMTDC (H), and IMKDC (J), but not on IMHDC (L). Total magnification for image C and image D was 50 ×, while that for other images was 400 ×.

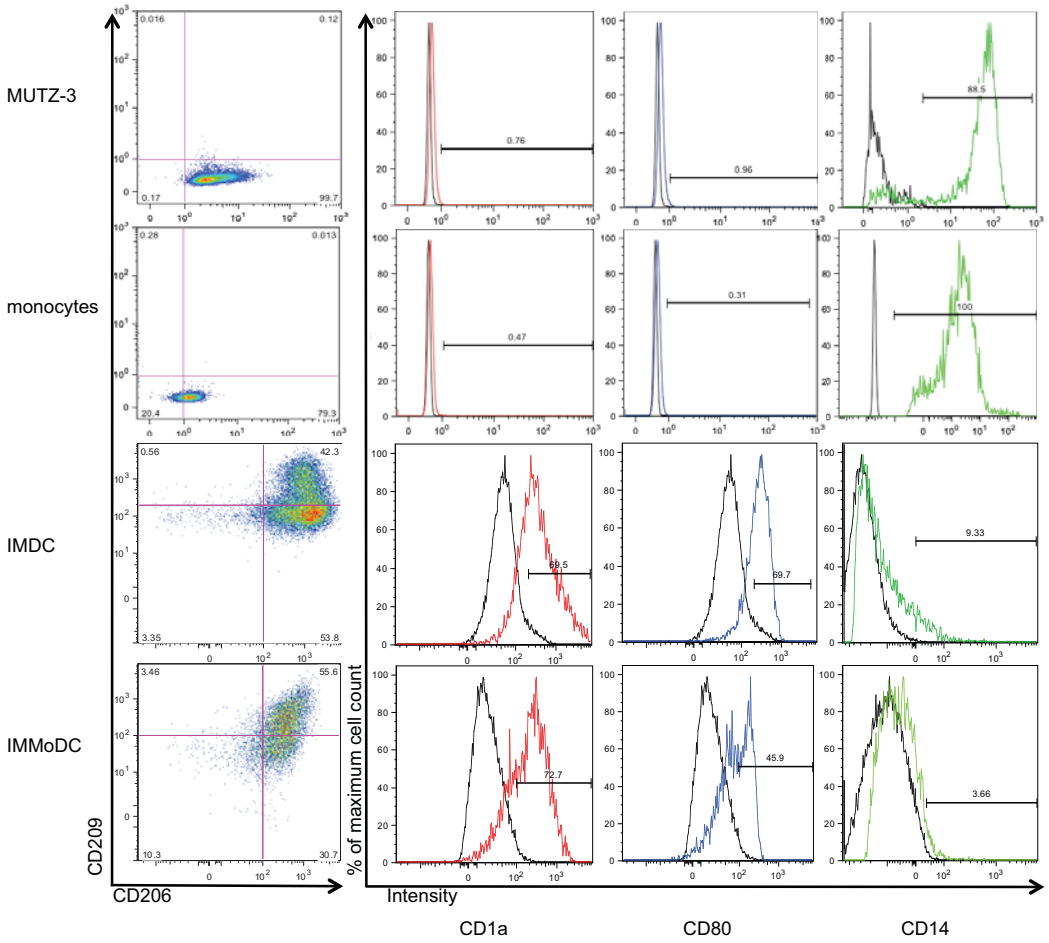

Figure 4-2 Surface markers expression profiles of monocyte and MUTZ-3 before/after differentiation.

For each sample, PI^- population representing viable cells were firstly gated for further analysis. Monocytes and MUTZ-3 cells were $CD14^+CD1a^-CD80^-$ DC-$SIGN^-$. After differentiation, 43.3% of IMDC and 55.6% of IMMoDC populations were DC-$SIGN^+MR^+$. The double positive populations were gated and the expression levels of CD1a, CD80 and CD14 were analysed. The experiment shown was one representative of three. Black line: non-stained control. Red line: CD1a staining. Blue line: CD80 staining. Green line: CD14 staining.

4.1.2 Replication levels of native DENV2 and DENV2 replicons in IMDCs and IMMoDCs

Having proven that IMDCs obtained immature DC-like features like IMMoDCs, whether DENV2 replication was permitted inside IMDCs and IMMoDCs was investigated. Results of the TaqMan assay indicated that negative-sense DENV2 RNA was produced inside IMDCs and IMMoDCs after infection (Figure 4-3 B). Although both types of cells were permissive to native DENV2 replication, it was found that the level of viral replication in IMDCs was significantly lower than that in IMMoDCs (Figure 4-3 B). Interestingly, the replication levels of native DENV2 in IMTDCs and IMKDCs were as same as that in IMMoDCs, while IMHDCs showed a significant higher replication level of native DENV2 compared to the others (Figure 4-3 C). Therefore, DENV2 replication level in IMDCs was the lowest among that in DCs generated from other leukaemia cells.

In order to understand the underlying reasons for the lower viral replication levels in IMDCs, the influences from viral receptors were studied. The viral receptor expressions on both types of cells were compared. As expected, expression of MR and DC-SIGN increased after IL-4 induction (Larsson *et al.*, 2006), and similar percentages of IMDCs and IMMoDCs co-expressed MR and DC-SIGN (Figure 4-2). In addition, when DENV2 subgenomic replicon was transfected into IMDCs and IMMoDCs, the replication level in IMMoDCs was 30 times higher than that in IMDCs (Figure 4-3 A). Since DENV2 replicon transfection was independent of viral receptors on the host

cell surface, it was possible that low DENV2 replication was caused by intracellular anti-viral responses.

For the purpose of investigating different DENV2 replication levels in IMDCs and IMMoDCs, a time-course experiment was conducted using real time RT-PCR (Figure 4-4). In IMDCs, DENV2 replication remained low until 24 h post-infection (100-fold compared to the mock sample). During 24 h to 48 h post-infection, DENV2 replication levels significantly increased to more than 300-fold compared to the mock control. The viral replication time-course showed a different pattern in infected IMMoDCs. Viral replication in IMMoDCs started with a rather high level (approximately 1100-fold compared to the mock group). Although the replication dropped slightly at 12 h post-infection (around 800-fold relative to the mock group), it remained at high levels through 24 h post-infection (1500-fold compared to the mock group) to 48 h post-infection (1600-fold in comparison to the mock sample). There were no significant differences between the replication levels of different time points in IMMoDCs. For all of the tested time points, viral replication levels in IMMoDCs were noticeably higher than in IMDCs (Figure 4-4).

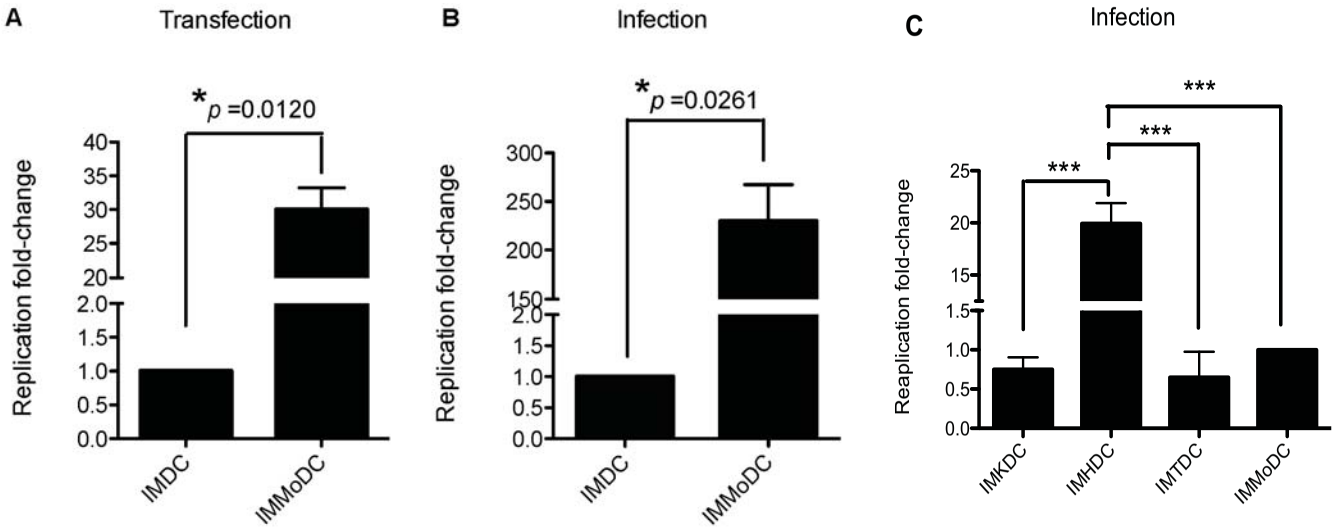

Figure 4-3 Comparison of DENV2 replication in IMDC, IMMoDC, and DCs generated from other leukaemia cells.

Both DENV2 replicon (A) and native DENV2 virus (B) replicated inside IMDCs and IMMoDCs. The replicon and native virus replication levels in IMMoDCs were much higher than in IMDCs (*prevalence [p]*<0.05, with specific *p* values indicated). Native DENV2 virus also replicated in DCs generated from K562, HL-60, and THP-1 (C). Y-axis represented DENV2 RNA replication level fold-changes. The data show mean ± SEM of results from three independent experiments. Statistical significances of A and B was analysed by t-test (A, B) and one-way ANOVA followed by Tukey's HSD post hoc test (C). * $p<0.05$, *** $p<0.001$

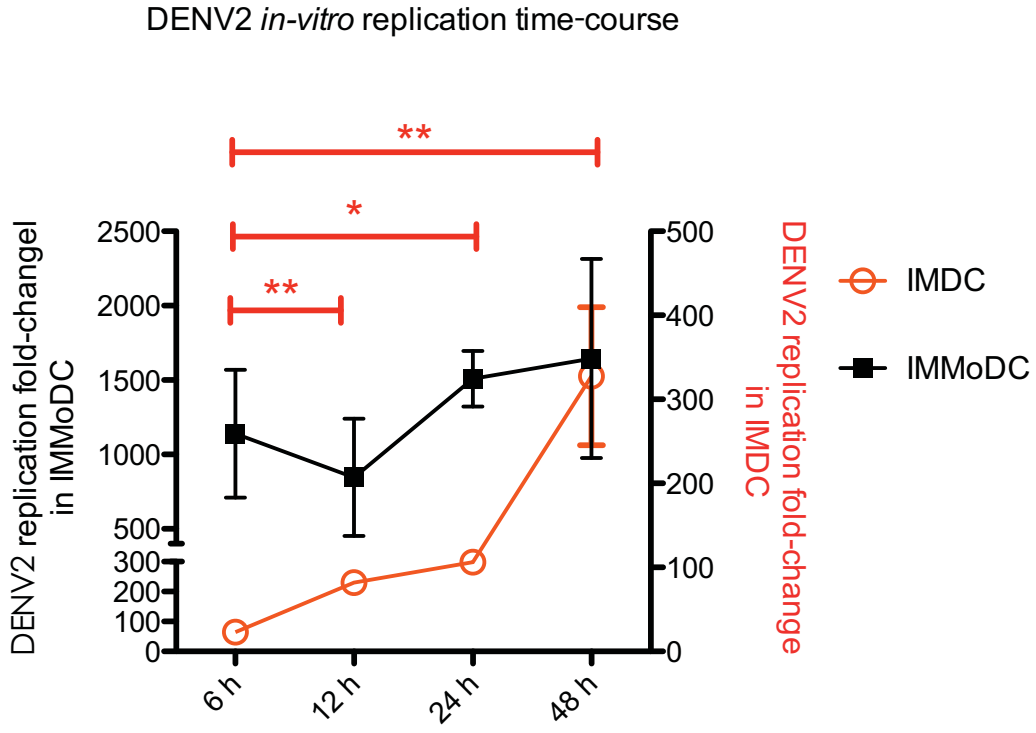

Figure 4-4 DENV2 replication time-course in IMDC and IMMoDC.

Total RNA was extracted from cells infected with DENV2 at 6 h, 12 h, 24 h, and 48 h post-infection, respectively. The extracted RNA was subjected to RT-PCR in order to examine the viral RNA replication level. Red circle: DENV2-infected IMDCs; black square: DENV2-infected IMMoDCs. Left y-axis: DENV2 replication fold-change in IMMoDCs relative to mock controls; right y-axis: DENV2 replication fold-change in IMDCs compared to mock controls. The results are expressed as mean ± SEM of data from three independent experiments. Two-way ANOVA was used to analyse the data. The effect between cell types was significant ($F = 95.82$, p value = 0.0006). * $p<0.05$, ** $p<0.01$

4.1.3 Effect of DENV2 RNA replication on the expression of surface markers on IMDCs and IMMoDCs

Afterwards, the effects of DENV2 RNA replication on the expression of DENV receptors DC-SIGN and MR, maturation marker CD83, the antigen-presenting protein CD1a, and the co-stimulatory molecule CD80 in both types of cells were compared after both DENV2 infection and replicon transfection. The viral replication showed no effect on cell viability as assessed via PI staining (data not shown). However, due to the heavy staining background of the viral E protein and the NS1 protein in the flow cytometric analysis, it was not able to gate and examine the surface marker expression of the DENV2-infected cells. Therefore, the surface marker expression of the whole IMDC and IMMoDC populations were examined. Nonetheless, in IMDCs and IMMoDCs there was no discernible difference in the expression of CD1a, CD80, CD83, MR, and DC-SIGN after DENV2 infection (Figure 4-5). For gene expression levels, IMDCs showed no notable change in the expression of these markers after DENV2 challenge (Figure 4-6) except for CD83, for which the expression level was 3-fold up-regulated, but without statistical significance ($p>0.05$). On the other hand, IMMoDCs had significant up-regulation in gene expression of MR (+17.6 folds, $p<0.01$), while expression of CD1a was down-regulated (-7.2 folds, $p<0.01$), as well as DC-SIGN (-6.6 folds, $p<0.05$). CD80, on the other hand, was up-regulated in IMMoDCs after DENV2 replicon transfection (+6.2-fold, $p<0.05$). These gene expression changes were not reflected by the protein expression levels using flow cytometry (Figure 4-5).

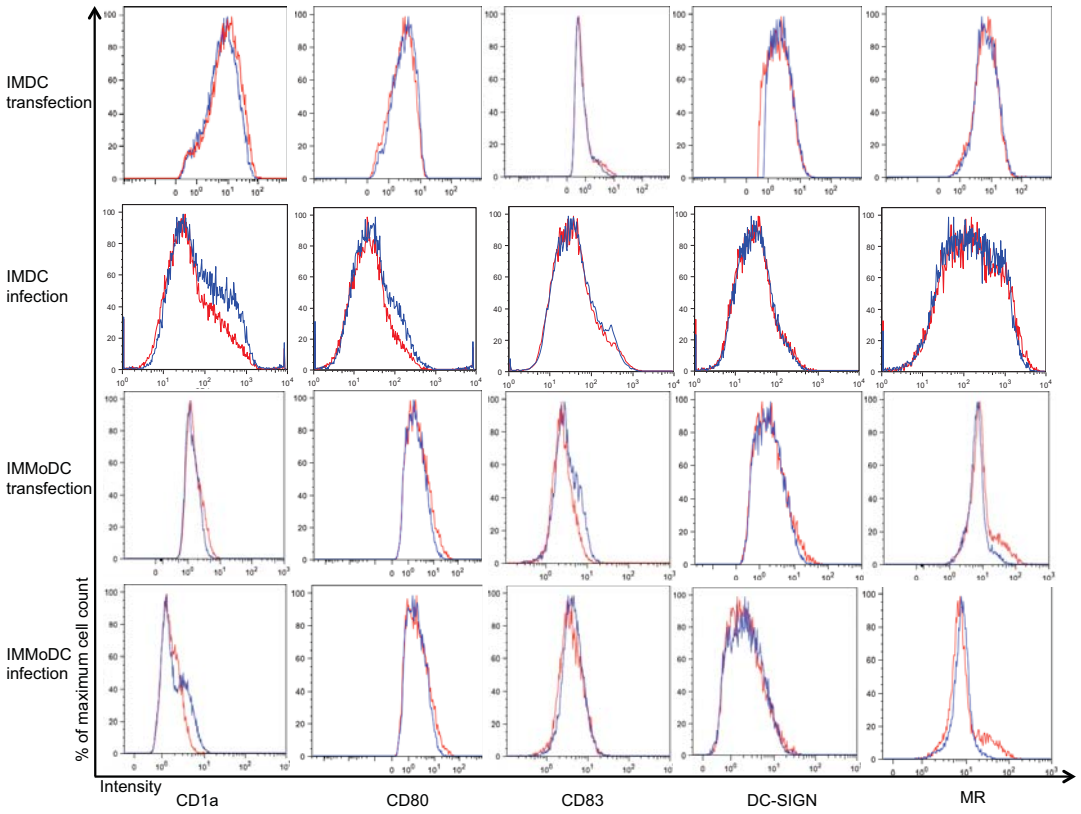

Figure 4-5 IMDC and IMMoDC surface marker expression profiles after DENV2 transfection and infection.

Cells were stained with conjugated antibodies to examine the surface marker expression changes 48 h post-transfection or post-infection. Neither transfection nor infection of DENV2 induced significant changes in surface marker expressions in IMDCs and IMMoDCs. The experiment shown was one representative of three. Blue line: cells after DENV2 transfection or infection; red line: mock controls.

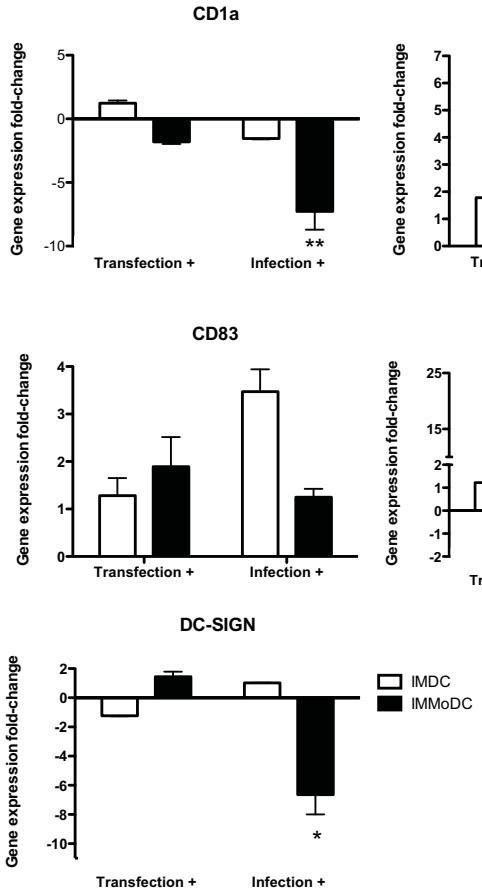

Figure 4-6 Expression of DC surface markers was detected by real-time PCR.

Signals from the target genes were normalised with the corresponding signal from non-transfected or uninfected samples. There was no significant change in surface marker gene expression in IMDCs after transfection or infection (open column). In IMMoDCs, CD80 was significantly up-regulated after transfection, while MR was up-regulated and CD1a together with DC-SIGN were significantly down-regulated after infection (solid column). The results are expressed as mean ± SEM of data from three independent experiments. Data were analysed by one-way ANOVA followed by Tukey's HSD post hoc test. * $p<0.05$, ** $p<0.01$

4.1.4 Production of infectious DENV2 in IMDCs and IMMoDCs

Results of the Western blotting analyses showed that DENV2 E protein and NS1 proteins were synthesised inside DENV2-infected IMDCs, and DENV2-infected IMMoDCs as well (Figure 4-7).

Moreover, the occurrence of DENV2 NS1 protein, which is an important antigen of DENV infection (Lima Mda *et al.*, 2011), as well as the occurrence of DENV2 E protein, were studied in the culture medium of infected IMDCs and infected IMMoDCs at different time points after viral infection (Figure 4-8). Compared to mock controls, DENV2 E protein began to be detectable in the culture medium of infected IMMoDCs at 24 h post-infection, and the signal became stronger at 48 h post-infection. Meanwhile, NS1 could only be observed from the sample of 48 h post-infected IMMoDCs. The same detection patterns of DENV E protein and NS1 protein were observed in samples from infected IMDCs. However, the immunoblotting signals in infected IMDCs were poorer in comparison to those in infected IMMoDCs (Figure 4-8).

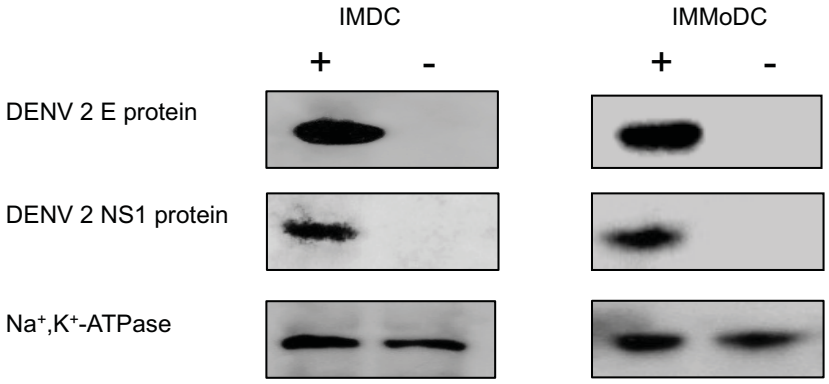

Figure 4-7 DENV2 protein synthesis in IMDCs and IMMoDCs.

Western blotting analysis of DENV2 viral antigens in total protein extracted from IMDCs and IMMoDCs after 48 h of infection. Na^+,K^+-ATPase was used as an internal control. +: infected samples; -: mock controls.

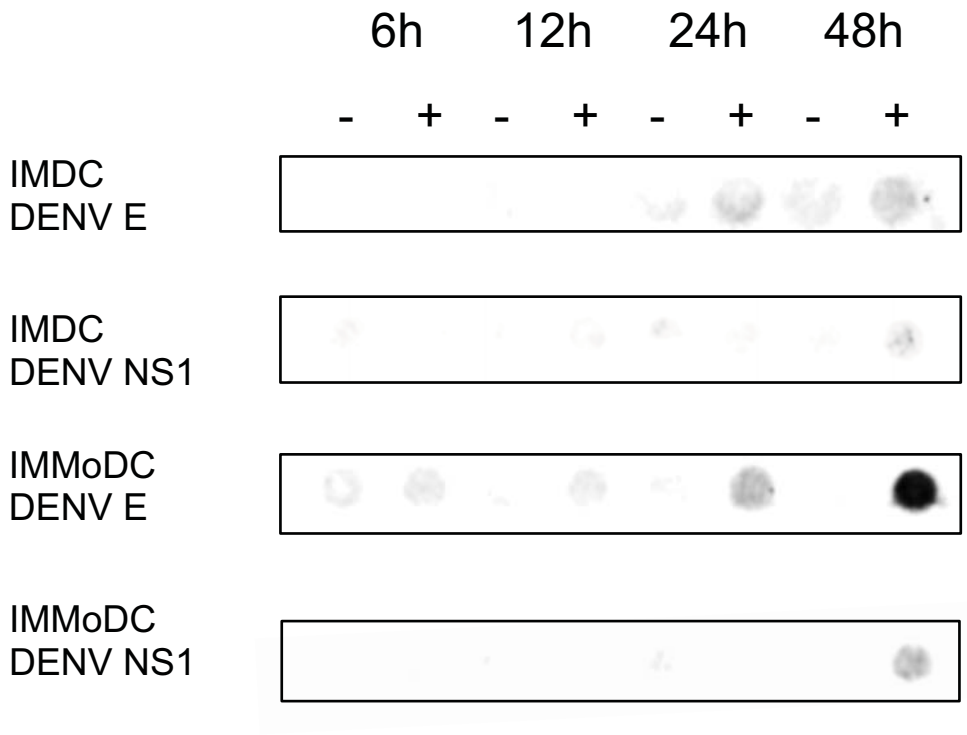

Figure 4-8 Detection of DENV2 proteins in the culture medium of IMDCs and IMMoDCs after infection.

Culture media was collected from DENV2-infected IMDCs and IMMoDCs at different time-points were dotted to PVDF. The PVDF membrane was stained with specific antibodies against DENV E protein and NS1 protein. Compared to the uninfected controls, DENV2 E protein was detectable in the supernatant of IMMoDCs and IMDCs at 24 h post-infection, while DENV2 NS1 protein was detectable in the supernatant of infected IMMoDCs and IMDCs 48 h after infection. +: infected samples; -: uninfected controls.

Besides, the presence of DENV2 RNA in culture medium of infected IMDCs and IMMoDCs was also investigated using real time RT-PCR (Figure 4-9). DENV2 copy number increased significantly in a time-dependent manner in the culture media of infected IMMoDCs. The DENV2 copy number started with 7.9 $\log_{10}$ copies at 6 h post-infection, and significantly increased at 12 h post-infection (14.0 $\log_{10}$ copies), then rose to 16.7 $\log_{10}$ copies after 24 h infection and reached 18.7 $\log_{10}$ copies after 48 h infection. The viral copy numbers reached the peak at 48 h post-infection. The viral copy numbers in the culture media of infected IMDCs were 9.8 $\log_{10}$ copies at 6 h post-infection, and increased to 14.3 $\log_{10}$ copies at 12 h post-infection. Then the viral copy number decreased a little to 12.9 $\log_{10}$ copies at 24 h post-infection. At 48 h post-infection, the viral copy numbers was 14.0 $\log_{10}$ copies in the infected IMDCs medium.

Having detected viral RNA and proteins released into the culture medium from infected IMDCs/IMMoDCs, the production of DENV2 particles within IMDCs and IMMoDCs 24 h post-infection was examined under TEM (Figure 4-10). Viral particles with diameters about 40-50 nm were observed in the ER and Golgi apparatuses of the infected IMMoDCs (Figures 4-10 A and B). However, only a few vacuoles (with diameters about 0.3 μm) carrying virion-like particles (with diameters about 50-60 nm) were observed in the infected IMDCs (Figure 4-10 C). Nothing related to DENV2 particles was seen in the IMDC mock group (Figure 4-10 D).

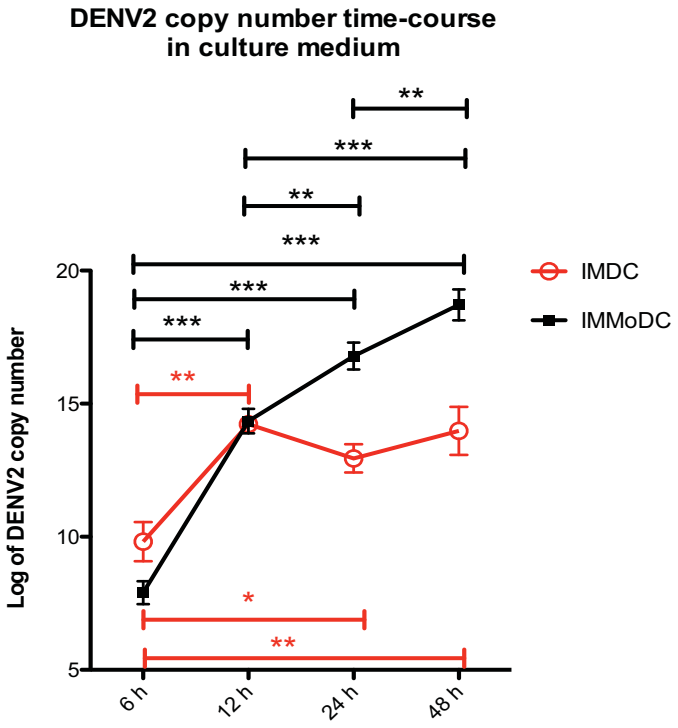

Figure 4-9 Detection of DENV2 RNA in the culture medium of IMDCs and IMMoDCs after infection.

Culture media were harvested from infected IMDCs and infected IMMoDCs at 6 h, 12 h, 24 h, and 48 h post-infection, respectively. Viral RNA was extracted from the collected culture media samples. Real-time RT-PCR was used to detect the viral copy number in the culture media. The y-axis represents the logarithmic DENV2 copy number. Red circle: culture medium of DENV2-infected IMDC; black block: culture medium of DENV2-infected IMMoDC. The results are presented as mean ± SEM of data from three independent experiments. Data were analysed by two-way ANOVA. The effect of cell types was significant (F = 7.78, *p* value = 0.0494). Time also had significant affect on the results (F = 110.71, *p* value<0.0001). * $p<0.05$, ** $p<0.01$, *** $p<0.001$

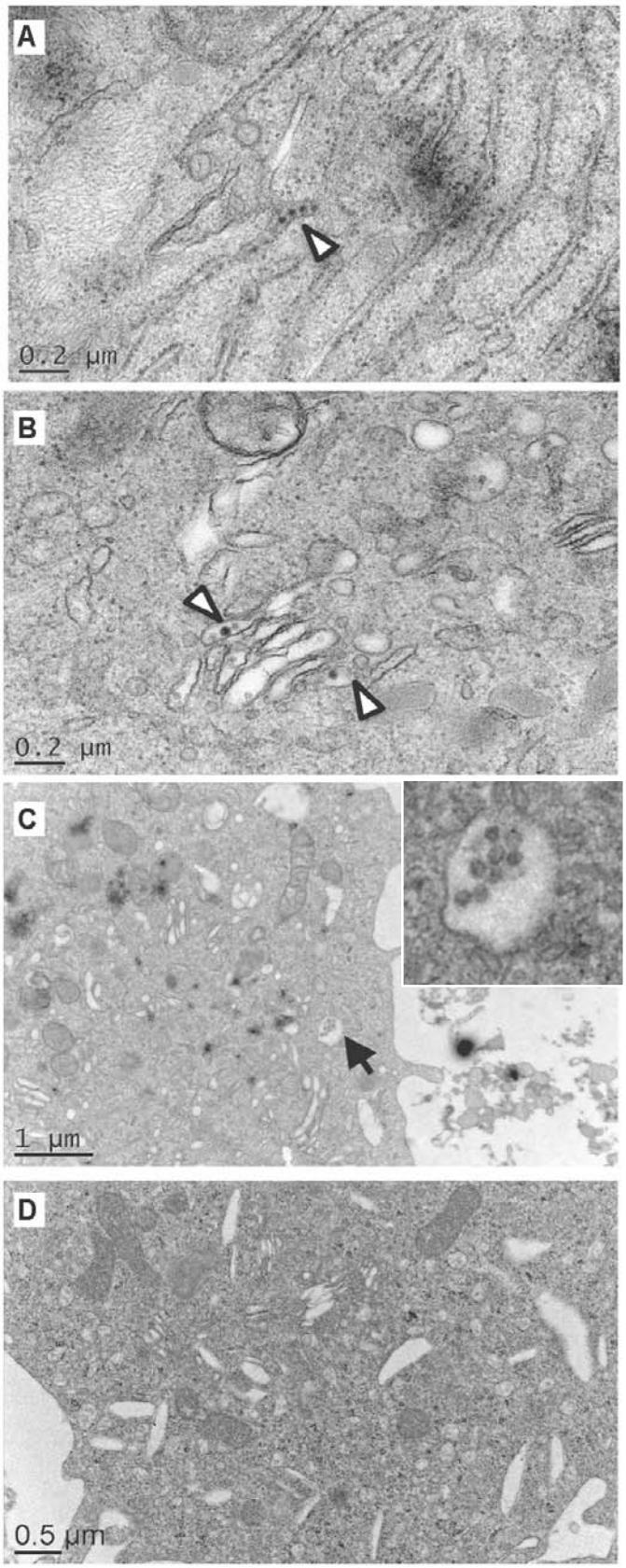
A
0.2 µm
B
0.2 µm
C
1 µm
D
0.5 µm

Figure 4-10 Electron microscopy of IMDCs and IMMoDCs infected by DENV2.

IMDCs and IMMoDCs were infected by DENV2 with MOI=1 for 24 h. In DENV2-infected IMMoDCs, DENV2 virions were observed in intracellular compartments, the morphology of which is compatible to endoplasmic reticulum (A) and Golgi apparatuses (B) (indicated by white arrowheads). In DENV2-infected IMDCs, only a vacuole carrying particles was seen, as shown in this micrograph of TEM (C) (indicated by black arrow and enlarged as expanded view of the box in panel). There were no similar observations in the IMDCs mock control (D).

Then, a DENV2 recovery assay was conducted to detect whether these observed particles were infectious. Culture medium of the DENV2-infected IMDCs or infected IMMoDCs was used to infect BHK-21 cells. Results of the RT-PCR assay suggested that the BHK-21 cells were infected by DENV2, which also showed that IMDCs and IMMoDCs were capable of producing infectious DENV2 virions (Figure 4-11).

Taken together, the results showed that both IMDCs and IMMoDCs supported DENV2 viral replication and intact viral particle production.

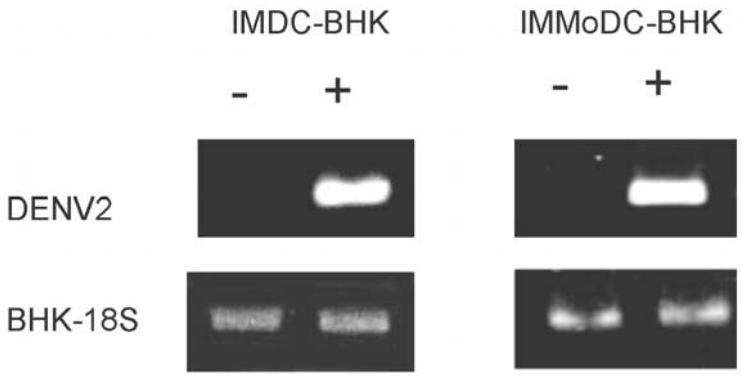

Figure 4-11 Infectious DENV2 particles production by infected-IMDCs and IMMoDCs.

BHK was incubated with culture medium from DENV2-infected IMDCs/IMMoDCs. After 48 h, total RNA was extracted from treated BHK and mock controls. DENV2 production was detected by RT-PCR. +: infected samples; -: mock controls.

4.2 Anti-DENV2 immune responses in immature DCs

4.2.1 Effect of DENV2 RNA replication on antiviral gene expression in IMDCs and IMMoDCs

In order to study the effect of DENV2 RNA replication on host antiviral mechanisms, gene expression of the antiviral pathway induced by the DENV2 replication in IMDCs and IMMoDCs after 48 h incubation was examined (Table 4-1). According to the RT-PCR array results of the DENV2-transfected IMMoDCs, expression levels of 21 genes were statistically different from those of the mock control. Additionally, expression levels of 16 genes were significantly up-regulated in IMMoDCs after DENV2 infection.

Among the fourteen genes activated in both transfected IMMoDCs and infected IMMoDCs, five genes associated with intrinsic IFN resistance were considerably up-regulated. These included genes coding IFIT family members (IFIT1, +287.88-fold, $p<0.05$ after transfection; +190.28-fold, $p<0.05$ in infection; IFIT3, +52.93-fold, $p<0.05$ in transfection; +53.77-fold, $p<0.05$ after infection); IFITM family members (IFITM1, +394.17-fold, $p<0.05$ after transfection; +10.35-fold, $p<0.01$ after infection; IFITM2, +12.55-fold, $p<0.01$ after transfection; +2.26-fold, $p<0.05$ after infection); ISG15 (+32.51-fold, $p<0.05$ after transfection; +34.19-fold, $p<0.05$ after infection). Besides, there were three IFN-inducible genes that were highly up-regulated after transfection and infection but without significant *p* value in the latter, including ISG20 (+41.43-fold, $p<0.05$ after transfection; +12.48-fold, $p=0.055$ after infection), IFI6 (+32.73-fold changes, $p<0.05$ after transfection; +26.76-fold,

p=0.062 after infection); IFI27 (+529.81-fold, *p*<0.01 in transfected IMMoDCs; +274.12-fold, *p*=0.128 in infected IMMoDCs). Other genes involved in innate antiviral responses were also up-regulated by DENV2 replicon and DENV2 native virion in IMMoDCs. These included IFN-regulatory factor 7 (IRF7) (+5.32-fold, *p*<0.01 after transfection; +6.67-fold, *p*<0.05 after infection), signal transducers and activators of transcription protein 1 (STAT1) (+4.82-fold, *p*<0.05 after transfection; +3.99-fold, *p*<0.01 after infection), 2',5'-oligoadenylate synthetase family (OAS1, +5.72-fold, *p*<0.05 after transfection, +7.19-fold, *p*<0.01 after infection; OAS2, +26.53-fold, *p*<0.01 after transfection; +7.72-fold, *p*<0.05 after infection) and IFN-induced GTP-binding proteins (MX1, +39.65-fold, *p*<0.05 after transfection; +22.19-fold, *p*<0.05 after infection; MX2, +18.58-fold, *p*<0.01 after transfection; +11.81-fold, *p*<0.05 after infection). Despite the substantial changes in gene expression of the antiviral pathways in the DENV2-transfected and DENV2-infected IMMoDCs, there was no significant change in gene expression in the transfected IMDCs or infected IMDC samples (Table 4-1).

Table 4-1 Genes that were up-regulated by DENV2 replication in two types of cells.

GenBank ID	Gene name	Description	DENV2 replicon transfection				Native DENV2 infection			
			IMMoDC		IMDC		IMMoDC		IMDC	
			F[#]	*p*[§]	F[#]	*p*[§]	F[#]	*p*[§]	F[#]	*p*[§]
NM_004335	BST2	Bone marrow stromal cell antigen 2	3.42	0.057	1.47	0.18	4.34	0.049*	1.52	0.42
NM_002038	IFI6	IFN, alpha-inducible protein 6	32.73	0.035*	1.15	0.73	26.76	0.062	3.53	0.23
NM_005532	IFI27	IFN, alpha-inducible protein 27	529.81	0.003 **	1.41	0.51	274.12	0.128	3.85	0.35
NM_022168	IFIH1	IFN induced with helicase C	5.03	0.016*	-1.03	0.70	7.77	0.009**	2.06	0.31
NM_001548	IFIT1	IFN-induced protein with tetratricopeptide repeats 1	287.88	0.045*	1.18	0.46	190.28	0.019*	1.92	0.22
NM_001549	IFIT3	IFN-induced protein with tetratricopeptide repeats 3	52.93	0.043*	1.00	0.89	53.77	0.032*	1.86	0.27
NM_003641	IFITM1	IFN induced transmembrane protein 1 (9-27)	394.17	0.039*	1.08	0.66	10.35	0.001**	2.55	0.17
NM_006435	IFITM2	IFN induced transmembrane protein 2 (1-8D)	12.55	0.005 **	1.13	0.59	2.26	0.047*	1.52	0.42
NM_002199	IRF2	IFN regulatory factor 2	1.66	0.028*	-1.02	0.95	1.41	0.243	1.74	0.45
NM_002201	ISG20	IFN stimulated exonuclease gene 20kDa	41.43	0.018*	1.28	0.74	12.48	0.055	2.62	0.36
NM_005101	ISG15	ISG15 ubiquitin-like modifier	32.51	0.031*	1.23	0.47	34.19	0.049*	2.42	0.30
NM_002463	MX2	Myxovirus (influenza virus) resistance 2 (mouse)	18.58	0.006**	1.07	0.74	11.81	0.019*	2.18	0.18
NM_001565	CXCL10	Chemokine (C-X-C motif) ligand 10	21.65	0.008**	1.01	0.86	71.28	0.277	11.66	0.36

(To be continued)

(Continued)

GenBank ID	Gene name	Description	DENV2 replicon transfection				Native DENV2 infection			
			IMMoDC		IMDC		IMMoDC		IMDC	
			F#	p§	F#	p§	F#	p§	F#	p§
NM_002759	EIF2AK2	Eukaryotic translation initiation factor 2-alpha kinase 2	4.30	0.001**	-1.06	0.91	5.76	0.016*	1.49	0.25
NM_002198	IRF1	IFN regulatory factor 1	1.86	0.042*	1.25	0.99	1.68	0.167	3.27	0.39
NM_001572	IRF7	IFN regulatory factor 7	5.32	0.001 **	-1.09	0.81	6.67	0.011*	2.54	0.07
NM_006084	IRF9	IFN regulatory factor 9	2.81	0.004 **	1.35	0.29	1.42	0.171	1.96	0.36
NM_002462	MX1	Myxovirus (influenza virus) resistance 1, IFN-inducible protein p78 (mouse)	39.65	0.014*	1.23	0.68	22.19	0.022*	1.84	0.37
NM_004688	NMI	N-myc (and STAT) interactor	2.61	0.010 **	1.04	0.82	3.73	0.001**	1.44	0.47
NM_002534	OAS1	2',5'-oligoadenylate synthetase 1,40/46kDa	5.72	0.047*	1.06	0.76	7.19	0.010**	2.31	0.27
NM_002535	OAS2	2'-5'-oligoadenylate synthetase 2, 69/71kDa	26.53	0.005 **	1.12	0.81	7.72	0.024*	1.98	0.28
NM_007315	STAT1	Signal transducer and activator of transcription 1, 91kDa	4.82	0.018*	-1.11	0.87	3.99	0.008**	2.57	0.18
NM_005419	STAT2	Signal transducer and activator of transcription 2, 113kDa	2.43	0.119	1.14	0.80	3.84	0.033*	1.52	0.31

The results show the mean results from three independent experiments. Data were calculated by T-test.

F: gene expression fold-change of transfected samples vs. mock controls; § *p: p*-value

** $p<0.01$; *$p<0.05$

4.2.2 Effect of DENV2 RNA replication on selected IFN-inducible molecules

The results of the eight genes associated with intrinsic IFN resistance and with exceptionally high expression levels (>10-fold increase) in transfected and/or infected IMMoDCs were further confirmed using RT-PCR (Figure 4-12). These genes were IFI6, IFI27, IFIT1, IFIT3, IFITM1, IFITM2, ISG15, and ISG20. IFIT2 was also included in this experiment. As expected, both DENV2 replicon and native virus increased the expression levels of all nine genes in IMMoDCs, with IFI27 and IFIT1 being the most up-regulated. On the contrary, neither transfection nor infection was able to induce significant expressions of these genes in IMDCs (Figure 4-12).

Having observed that IFIT1 and IFI27 were dramatically induced by DENV2 replication in IMMoDCs, the protein expression levels of IFIT family and of IFI27 were examined by Western blot (Figure 4-13). Protein expressions of IFIT1 (Figure 4-13, A) and IFIT3 (Figure 4-13, C) were detected in the DENV2-infected IMMoDCs. In contrast, IFIT2 (Figure 4-13, B) and IFI27 (Figure 4-13, D) protein expressions were detected in the naïve IMMoDCs, but the expressions of these two proteins in IMMoDC remained the same after DENV2 infection.

Interestingly, expressions of IFI27 and the three IFIT proteins were detected in naïve IMDCs. After DENV2 infection in IMDCs, protein levels of IFI27,

IFIT1, and IFIT2 were slightly up-regulated, while IFIT3 protein expression was decreased. However, all these changes were not statistically significant.

These results suggested that the major IFN-induced antiviral pathway was activated by DENV2 replication in IMMoDCs. However, the occurrence of IFIT proteins in naïve IMDCs inspired the following experiments to investigate the IFN-related antiviral pathways in naïve IMDCs.

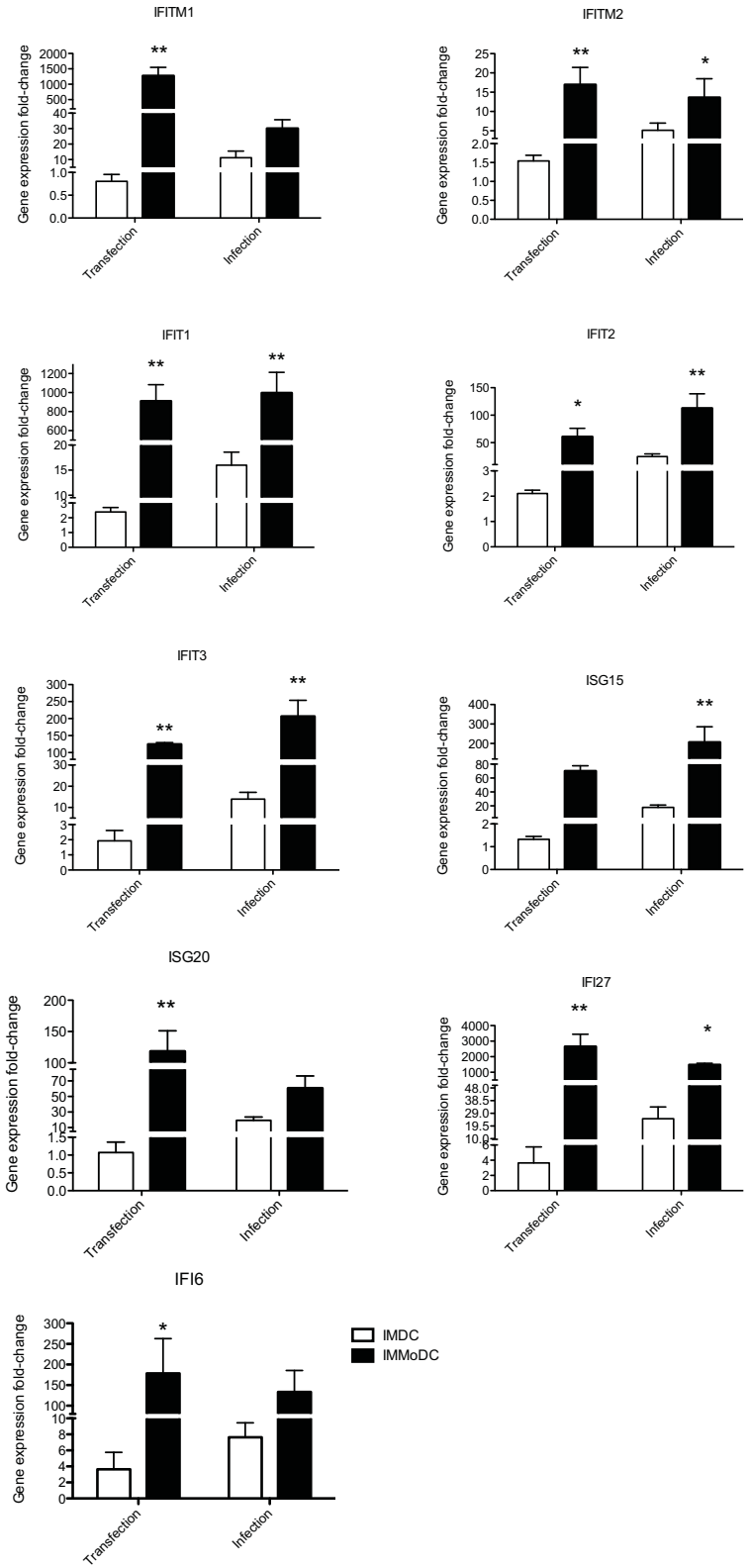
IFITM1
IFITM2
IFIT1
IFIT2
IFIT3
ISG15
ISG20
IFI27
IFI6
Gene expression fold-change
Transfection
Infection
IMDC
IMMoDC

Figure 4-12 Expression of IFN-inducible genes in IMDCs and IMMoDCs after DENV2 transfection and infection.

Expression levels of nine genes belonging to the IFN-inducible genes were confirmed by real-time RT-PCR. No statistical significant change in gene expression was detected in IMDCs after DENV2 infection or transfection (open columns). On the contrary, gene expression increased significantly in IMMoDCs after DENV2 transfection and infection (solid columns). The results are expressed as mean ± SEM of data from three independent experiments. Data were analysed by one-way ANOVA followed by Tukey's HSD post hoc test. * $p<0.05$, ** $p<0.01$

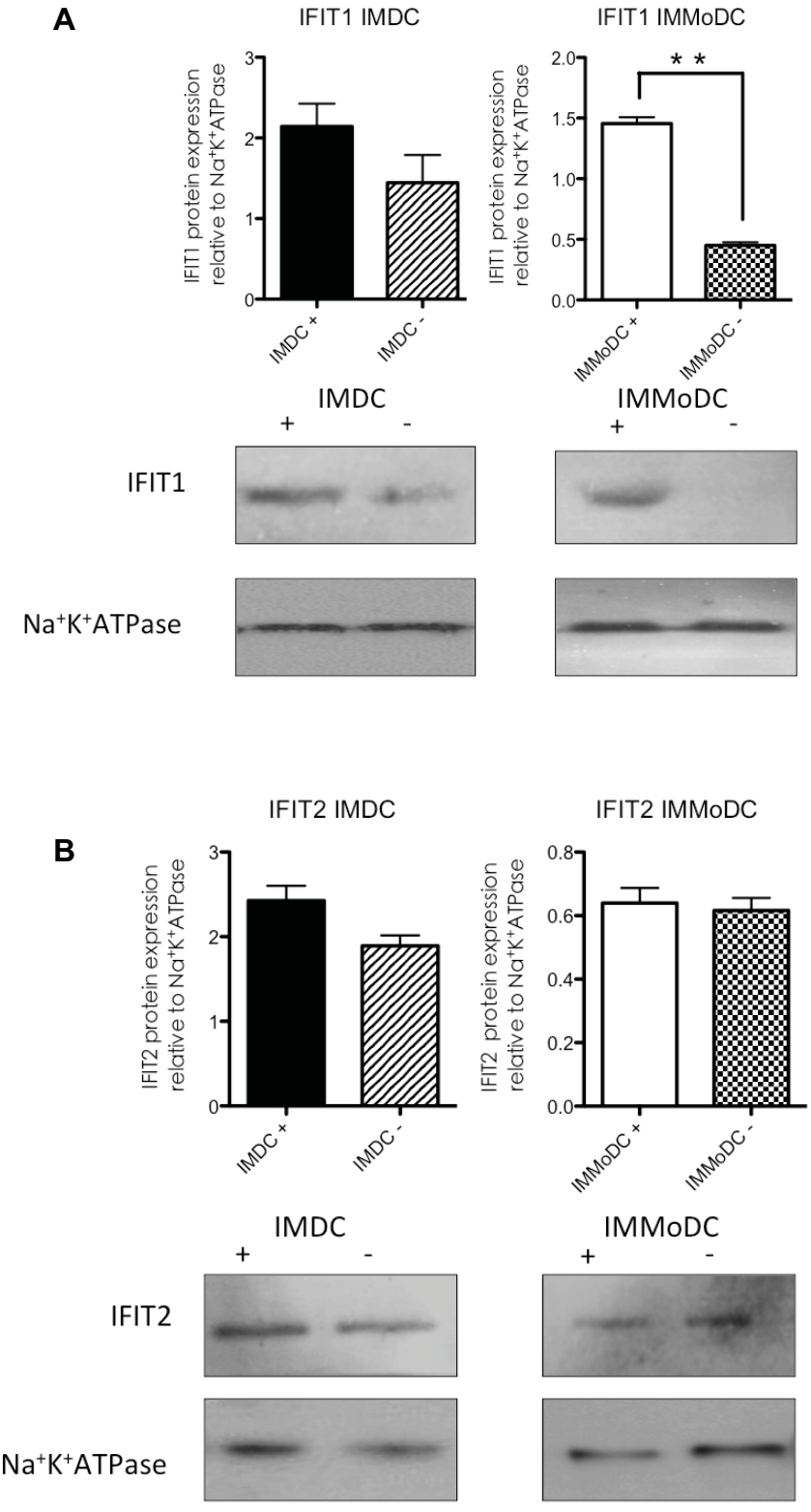
A
IFIT1 IMDC
IFIT1 protein expression relative to Na+K+ATPase
3
2
1
0
IMDC+
IMDC-
IFIT1 IMMoDC
IFIT1 protein expression relative to Na+K+ATPase
2.0
1.5
1.0
0.5
0.0
* *
IMMoDC+
IMMoDC-
IMDC
+
-
IMMoDC
+
-
IFIT1
Na+K+ATPase
B
IFIT2 IMDC
IFIT2 protein expression relative to Na+K+ATPase
3
2
1
0
IMDC+
IMDC-
IFIT2 IMMoDC
IFIT2 protein expression relative to Na+K+ATPase
0.8
0.6
0.4
0.2
0.0
IMMoDC+
IMMoDC-
IMDC
+
-
IMMoDC
+
-
IFIT2
Na+K+ATPase

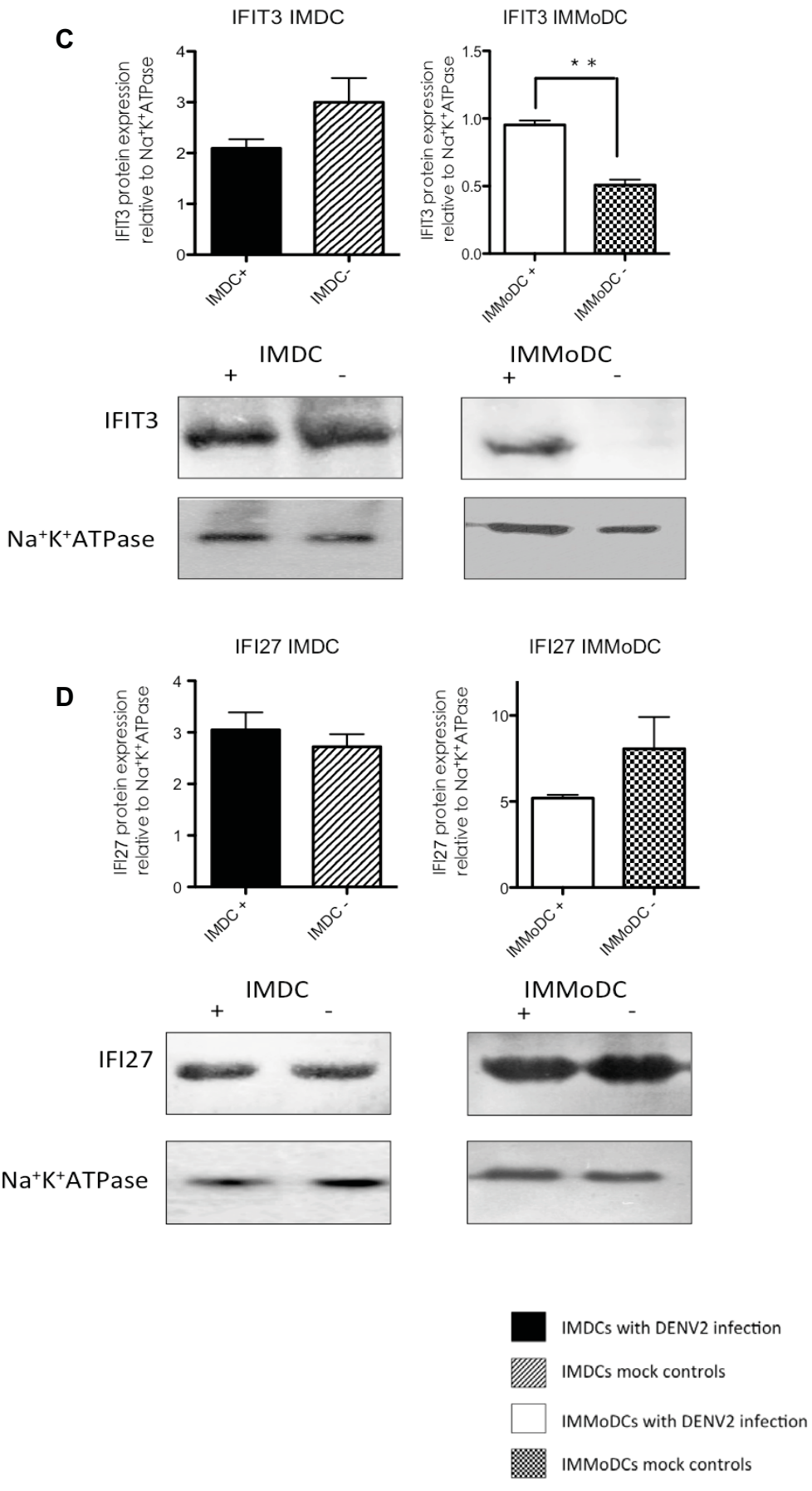
C
IFIT3 IMDC
IFIT3 protein expression relative to Na+K+ATPase
IMDC+
IMDC-
IFIT3 IMMoDC
* *
IMMoDC+
IMMoDC-
IMDC
IMMoDC
IFIT3
Na+K+ATPase
D
IFI27 IMDC
IFI27 protein expression relative to Na+K+ATPase
IFI27 IMMoDC
IFI27
IMDCs with DENV2 infection
IMDCs mock controls
IMMoDCs with DENV2 infection
IMMoDCs mock controls

Figure 4-13 Protein expressions of IFN-inducible proteins before/after DENV2 infection in IMDCs and IMMoDCs.

Protein expressions of IFIT1 (A), IFIT2 (B), IFIT3 (C), and IFI27 (D) with/without DENV infection in IMDCs and IMMoDCs were examined via Western blot. Cells were infected by DENV2 native virus with MOI=1. Total protein was extracted from infected cells or the mock controls after 48 h. Na^+,K^+-ATPase was recruited as an internal control. Image-results represent one of three independent experiments. Western blot results were quantified by ImageJ software. Solid columns: IMDCs with DENV2 infection. Columns with upward diagonals: IMDCs mock controls. Open columns: IMMoDCs with DENV2 infection. Columns with checkerboards: IMMoDCs mock controls. +: native DENV2 infected samples. -: mock controls. ** $p<0.01$

4.2.3 Comparison of gene expression between naïve IMDCs and naïve IMMoDCs

In order to further study the IFN-related antiviral pathways in naïve IMDCs, the differences in signal transduction pathways involved in anti-DENV immune responses (human IFN α/β response, human JAK/STAT signalling pathway) between the naïve IMDCs and naïve IMMoDCs were determined. Unexpectedly, it was found that the basal expression levels of 21 genes were significantly higher and one gene was significantly lower in the naïve IMDCs compared to that in the naïve IMMoDCs (Table 4-2). Genes that were dramatically activated in the naïve IMDCs included IFN-induced transmembrane proteins (IFITM1) (+1879.33-fold, $p<0.01$) and IFN-inducible protein 27 (IFI27) (+307.83-fold, $p<0.05$). Changes in the expression levels of some genes appeared less tremendous but still significant, including IFN-induced protein with tetratricopeptide repeats 1 (IFIT1) (+136.18-fold, $p<0.01$), chemokine (C-X-C motif) ligand 10 (CXCL10) (+115.04-fold, $p<0.01$), as well as IFITM2 (+85.19-fold, $p<0.01$) (Table 4-2). Genes that were poorly expressed in naïve IMDCs included IFN-inducible guanylate binding protein 1 (GBP1) (-24.34-fold change, $p<0.01$).

Table 4-2 Anti-viral genes differently expressed between naïve IMDCs and naïve IMMoDCs

GenBank ID	Gene name	Description	2^-ΔCt		Naïve IMDCs vs. naïve IMMoDCs		
			Naïve IMDCs	Naïve IMMoDCs	Fold-change	*p*-value	
NM_000395	CSF2RB	Colony stimulating factor 2 receptor, beta, low-affinity (granulocyte-macrophage)	2.0E-02	6.6E-03	3.43	0.02	*
NM_001565	CXCL10	Chemokine (C-X-C motif) ligand 10	4.4E-03	3.8E-05	115.04	0.007	**
NM_001992	F2R	Coagulation factor II (thrombin) receptor	1.6E-03	4.5E-05	34.49	0.002	**
NM_000566	FCGR1A	Fc fragment of IgG, high affinity Ia, receptor (CD64)	2.8E-03	1.3E-04	21.63	0.006	**
NM_002053	GBP1	Guanylate binding protein 1, interferon-inducible, 67kDa	1.1E-03	2.7E-02	-24.34	0.001	**
NM_005531	IFI16	Interferon, gamma-inducible protein 16	7.3E-02	9.2E-03	7.94	0.02	*
NM_005532	IFI27	Interferon, alpha-inducible protein 27	3.1E-01	1.0E-03	307.83	0.044	*
NM_002038	IFI6	Interferon, alpha-inducible protein 6	2.4E+00	1.1E-01	22.2	0.041	*
NM_022168	IFIH1	Interferon induced with helicase C domain 1	6.1E-02	1.9E-02	3.28	0.004	**
NM_001548	IFIT1	Interferon-induced protein with tetratricopeptide repeats 1	7.7E-02	5.6E-04	136.18	0.001	**
NM_001549	IFIT3	Interferon-induced protein with tetratricopeptide repeats 3	1.8E-01	6.2E-03	28.43	0.031	*
NM_003641	IFITM1	Interferon induced transmembrane protein 1 (9-27)	2.8E-01	1.5E-04	1879.33	0.001	**
NM_006435	IFITM2	Interferon induced transmembrane protein 2 (1-8D)	6.8E-01	8.0E-03	85.19	0.002	**
NM_005101	ISG15	ISG15 ubiquitin-like modifier	2.9E-01	1.1E-02	27	0.002	**
NM_002463	MX2	Myxovirus (influenza virus) resistance 2 (mouse)	8.2E-02	4.3E-03	19.24	0.011	*
NM_002744	PRKCZ	Protein kinase C, zeta	1.6E-02	1.9E-03	8.07	0.021	*
NM_004219	PTTG1	Pituitary tumour-transforming 1	1.4E-02	1.8E-03	7.9	0.03	*
NM_002838	PTPRC	Protein tyrosine phosphatase, receptor type, C	1.9E-01	4.7E-02	3.97	0.001	**

(To be continued)

(Continued)

GenBank ID	Gene name	Description	2^-ΔCt		Naïve IMDC vs. naïve IMMoDC		
			Naïve IMDC	Naïve IMMODC	Fold-change	*p*-value	
NM_004219	PTTG1	Pituitary tumour-transforming 1	1.4E-02	1.8E-03	7.9	0.03	*
NM_018191	RCBTB1	Regulator of chromosome condensation (RCC1) and BTB (POZ) domain containing protein 1	3.2E-02	1.0E-02	3.04	0.044	*
NM_005902	SMAD3	SMAD family member 3	3.5E-03	4.2E-04	8.33	0.024	*
NM_003877	SOCS2	Suppressor of cytokine signalling 2	5.7E-04	3.2E-05	17.73	0.006	**

**$p<0.01$; *$p<0.05$

Confirmatory RT-PCR was done for the eight IFN-inducible genes (IFIT1, IFIT3, IFITM1, IFITM2, ISG15, IFIH1, IFI6, and IFI27), CXCL10, and MX2 in the naïve IMDCs and the naïve IMMoDCs. These genes were selected because they were significantly up-regulated after DENV2 RNA replication in the IMMoDCs (Table 4-1) and highly expressed in the naïve IMDCs (Table 4-2). Besides, IFIT2 was also assayed in the confirmatory RT-PCR. IFIT2 was not included in RT-PCR array but it forms an antiviral-complex together with IFIT1 and IFIT3 (Ablasser and Hornung, 2011). The results were presented as gene expression levels in the naïve IMDCs relative to those in the naïve IMMoDCs, calculated as fold-changes (Table 4-3).

The expression fold-changes of these 11 genes in the naïve IMTDCs, the naïve IMHDCs, and the naïve IMKDCs relative to the naïve IMMoDCs were also determined (Table 4-3).

In agreement with the RT-PCR array data (Table 4-2), even though basal expression levels of these genes were detectable in naïve IMMoDCs, IFI27 (+363.96-fold, $p<0.05$), IFITM1 (+39.88-fold, $p<0.05$), IFITM2 (+8.08-fold, $p<0.05$), ISG15 (+37.16-fold, $p<0.05$), MX2 (+4.34-fold, $p<0.05$), and IFIT1 (+155.53-fold, $p<0.05$), as well as IFIT3 (+91.35-fold, $p<0.05$), had significant higher expression levels in the naïve IMDCs (Table 4-3). IFIT2 was also spontaneously expressed in the naïve IMDCs relative to the naïve IMMoDCs (+13.03-fold, $p<0.05$) (Table 4-3). Unexpectedly, the expression level of

CXCL10 in the naïve IMDCs was lower than that in the naïve IMMoDCs (-29.63-fold, $p<0.05$).

Interestingly, as showed in Table 4-3, the expression levels of selected genes were significantly lower in the naïve DCs generated from the leukaemia cells. In the naïve IMKDCs, eight out of eleven selected genes were poorly expressed relative to that in the naïve IMMoDCs, including CXCL10 (-11.25-fold, $p<0.05$), IFIT1 (-3.49-fold, $p<0.001$), IFIT2 (-3.78-fold, $p<0.01$), IFIT3 (-6.29-fold, $p<0.01$), IFITM1 (-5.54-fold, $p<0.01$), IFITM2 (-2.74-fold, $p<0.05$), ISG15 (-1.84-fold, $p<0.05$), and MX2 (-2.71-fold, $p<0.05$). There were 10 genes down-regulated in the naïve IMTDCs compared to the naïve IMMoDCs (CXCL10 [-99.2-fold, $p<0.05$], IFI27 [-2.28-fold, $p<0.05$], IFI6 [-4.97-fold, $p<0.05$], IFIH1 [-6.23-fold, $p<0.01$], IFIT1 [-18.60-fold, $p<0.05$], IFIT2 [-5.29-fold, $p<0.05$], IFIT3 [-14.51-fold, $p<0.05$], IFITM1 [-4.42-fold, $p<0.05$], IFITM2 [-1.74-fold, $p<0.01$], MX2 [-5.59-fold, $p<0.05$]). Additionally, in the naïve IMHDCs, IFI6 (-5.84-fold, $p<0.05$), IFIH1 (-5.05-fold, $p<0.05$), IFIT1 (-20.39-fold, $p<0.05$), IFIT2 (-7.50-fold, $p<0.05$), IFIT3 (-6.10-fold, $p<0.05$), MX2 (-3.05-fold, $p<0.05$) were down-regulated, while IFITM1 (+2.90-fold, $p<0.05$) were up-regulated (Table 4-3).

Table 4-3 Comparison of the expression levels of selected genes in naïve DCs generated from leukaemia cells and naïve IMMoDCs

Gene name	IMKDC		IMTDC		IMHDC		IMDC	
	Fold-change	*p*-value	Fold-change	*p*-value	Fold-change	*p*-value	Fold-change	*p*-value
CXCL10	-11.25	0.028*	-99.20	0.027*	-27.32	0.064	-29.63	0.025*
IFI27	-47.95	0.098	-2.28	0.031*	-7.04	0.052	363.96	0.049*
IFI6	-16.94	0.064	-4.97	0.029*	-5.84	0.0388*	6.18	0.069
IFIH1	-6.13	0.063	-6.23	0.005**	-5.05	0.021*	0.66	0.899
IFIT1	-3.49	0.001***	-18.60	0.011*	-20.39	0.031*	155.53	0.031*
IFIT2	-3.78	0.005**	-5.29	0.042*	-7.50	0.032*	13.03	0.023*
IFIT3	-6.29	0.007**	-14.51	0.034*	-6.10	0.020*	91.35	0.017*
IFITM1	-5.54	0.010**	-4.42	0.032*	2.90	0.041*	39.88	0.050*
IFITM2	-2.74	0.022*	-1.74	0.004**	-1.90	0.549	8.08	0.017*
ISG15	-1.84	0.015*	-0.03	0.457	0.44	0.539	37.16	0.033*
MX2	-2.71	0.024*	-5.59	0.026*	-3.05	0.014*	4.34	0.041*

4.2.4 DENV2 infection induced autophagy in IMDCs and IMMoDCs

The low replication level of DENV2 in IMDCs may be due to the spontaneous activation of IFN-inducible anti-viral pathways, but it was still necessary to determine whether other pathways were involved in anti-DENV responses in IMDCs. Moreover, the vacuoles carrying virus like particles, which were observed in DENV2 infected IMDCs, could be autophagosomes. Therefore, DENV2 infection-induced autophagy was also examined by detecting microtubule-associated protein light chain 3 (LC3) (Figure 4-14). Endogenous LC3 displayed two bands during SDS-PAGE: LC3I, with molecular mass as 16 kDa is cytosolic, while LC3II with molecular mass as 14 kDa is conjugated with phosphatidylethanolamine (PE), presented on autophagosomes (Mizushima and Yoshimori, 2007).

The conversion of LC3I to LC3II was observed in 48 h post-infected IMDCs. It was clear that after DENV2 infection, the amount of LC3II was increased in IMDCs, indicating the accumulation of autophagosomes. The observation made in DENV2 infected IMMoDCs had a different pattern. Forty-eight hours after DENV2 infection, both LC3I and LC3II were up-regulated in IMMoDCs compared to in mock controls. However, the ratio of LC3II/internal control was obviously increased in infected IMMoDCs compared to the mock control, suggesting the activation of autophagy in infected IMMoDCs.

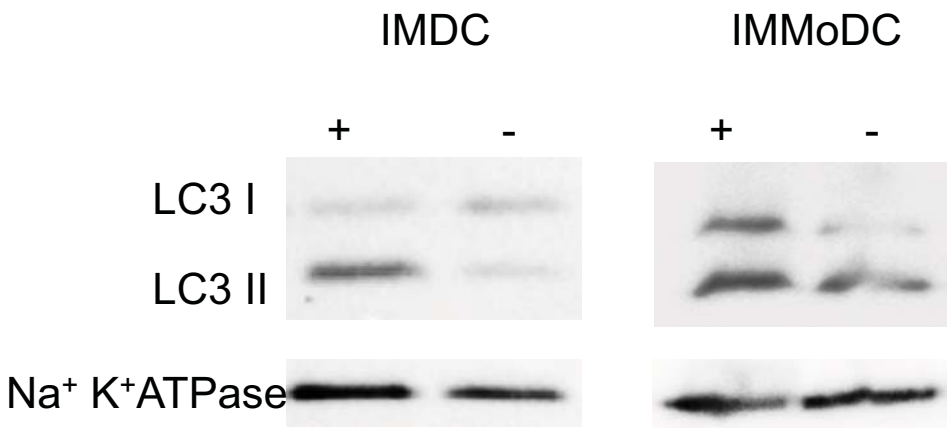

Figure 4-14 DENV2 infection induced autophagic signal changes in IMDCs and IMMoDCs.

Proteins were extracted from 48 h post-infected IMDCs and IMMoDCs, together with mock controls. The LC3II/LC3I ratio was increased in infected IMDCs. In infected IMMoDCs, expression of LC3I and LC3II, as well as the ratio of LC3II/Na^+,K^+-ATPase, was up-regulated. Na^+,K^+-ATPase was used as the internal control. +: native DENV2 infected samples. -: mock controls.

4.3 Mechanism of DENV2 entry into immature DCs

4.3.1 Expression characters of DENV receptors on IMDCs and IMMoDCs

In agreement with the results of flow cytometry, DC-SIGN and MR were expressed on the surface of IMDCs and IMMoDCs according to confocal microscopy results (Figure 4-15 A and B; Figure 4-16 A and B). Furthermore, having been stained by anti-DC-SIGN and anti-MR antibodies at the same time, a proportion of IMDCs and IMMoDCs were found to be DC-SIGN$^+$MR$^+$ (Figure 4-15 E and Figure 4-16 C). While DC-SIGN were stained evenly equally on the cell surfaces, that of MR displayed dotted pattern. Moreover, on some of the DC-SIGN$^+$MR$^+$ cells, the anti-DC-SIGN and the anti-MR antibodies presented overlapped-fluorescent signals (Figure 4-15 E and Figure 4-16 C). This observation was not due to florescent spill-over, because the florescent patterns did not duplicate each other. In order to examine whether this overlap was caused by co-capping, IMDCs were firstly stained with anti-DC-SIGN or anti-MR. Non-cross-linked antibodies were washed away and cells were fixed. Thereafter, cells were stained with the other antibody. The results showed that, when the IMDCs were stained with anti-MR antibody prior to anti-DC-SIGN antibody (Figure 4-15 C), the MR expression pattern tended to be dotted as observed in double-staining (Figure 4-15 E). However, when IMDCs were stained with anti-DC-SIGN first, the MR distribution pattern was more even (Figure 4-15 D). The observation here indicated a possible co-localisation of these two receptors.

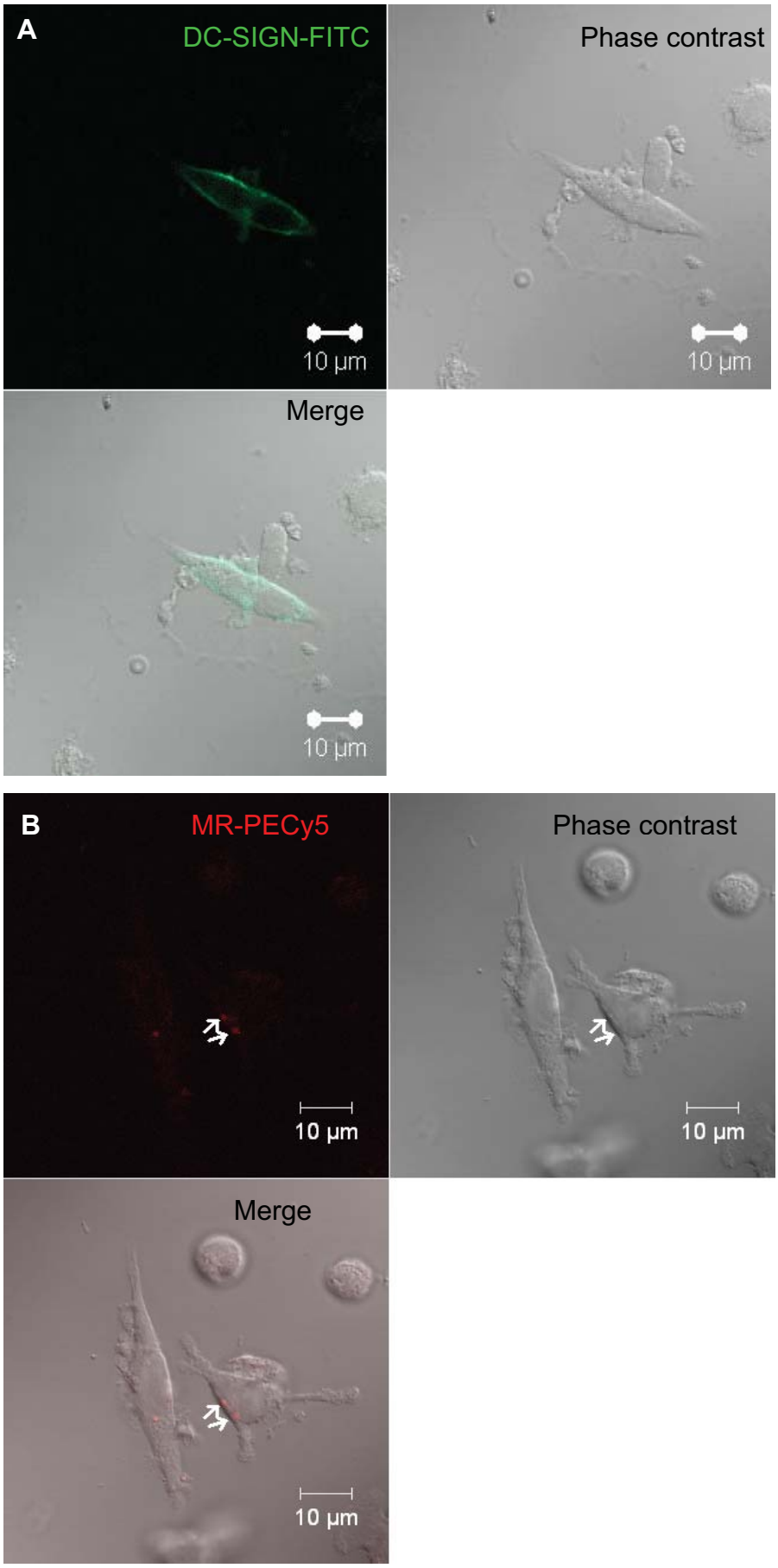

(To be continued)

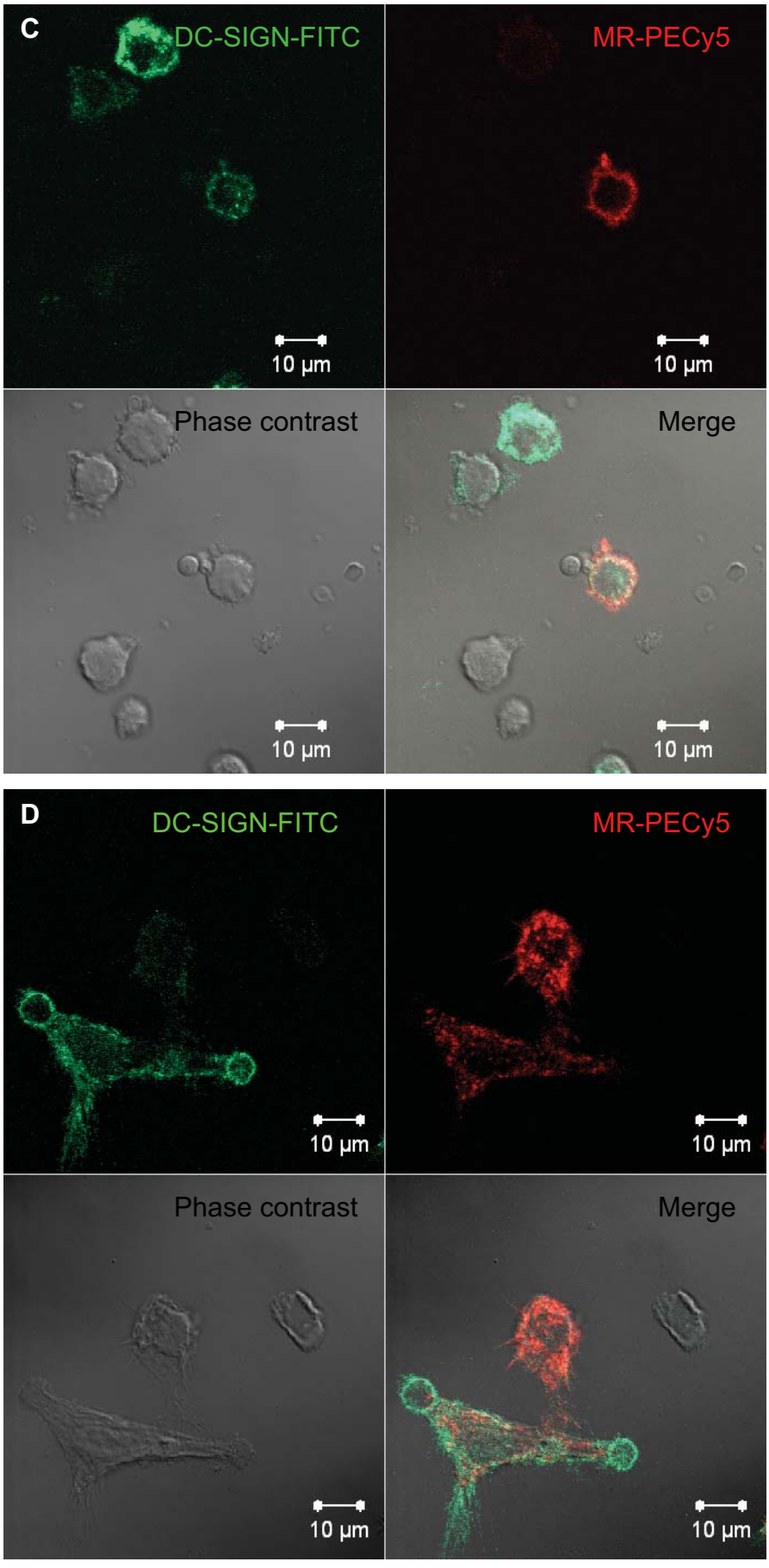

(To be continued)

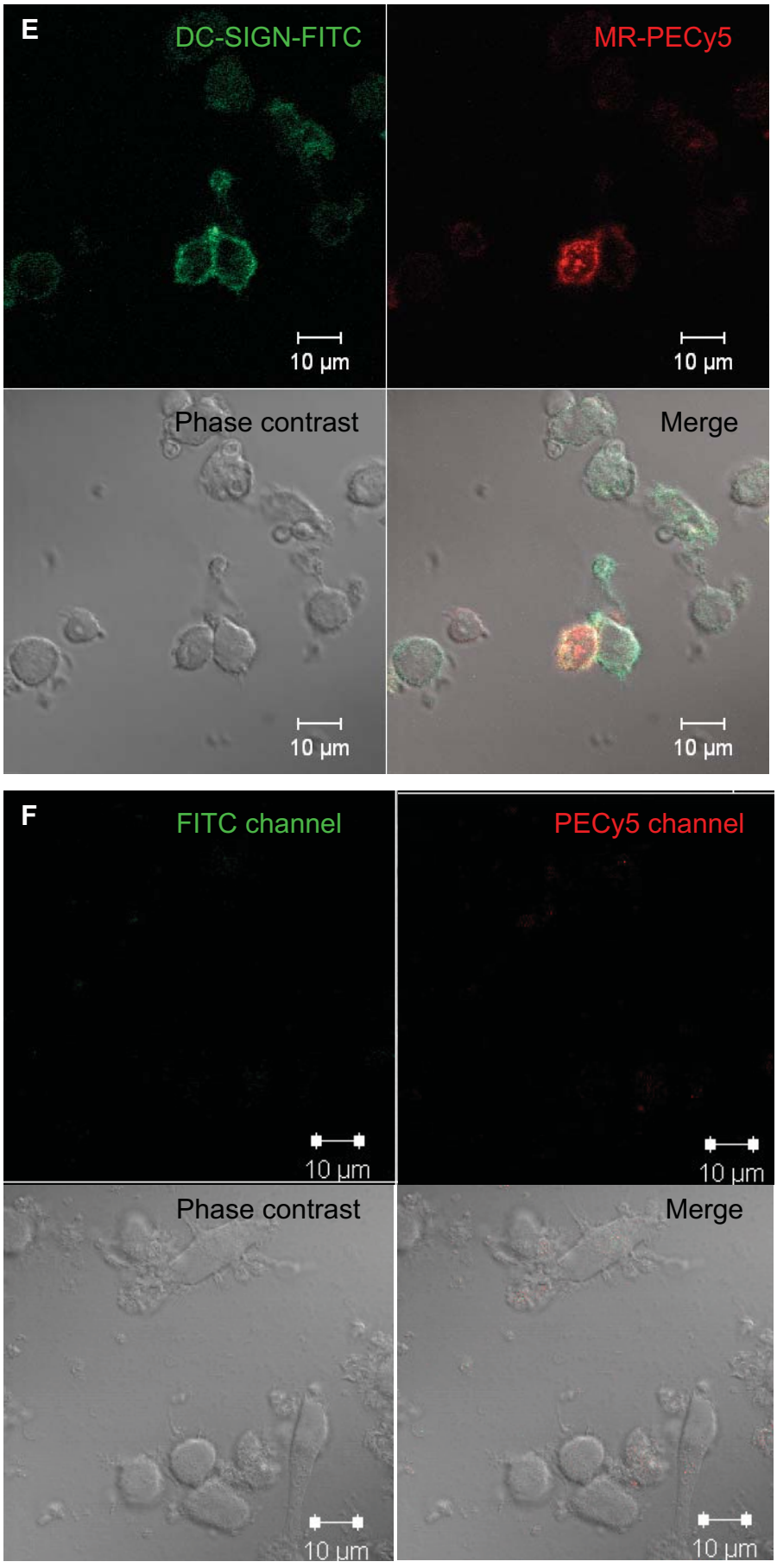
E
DC-SIGN-FITC
MR-PECy5
10 µm
10 µm
Phase contrast
Merge
10 µm
10 µm
F
FITC channel
PECy5 channel
10 µm
10 µm
Phase contrast
Merge
10 µm
10 µm

Figure 4-15 The expression of DC-SIGN and MR on IMDC surface.

IMDCs were stained with anti-DC-SIGN (A) or anti-MR (B) separately. The expression of DC-SIGN was equal on the cell surface, while the expression of MR was dotted. Then, IMDCs were stained with anti-DC-SIGN firstly for 30 min before adding anti-MR (C), or in the opposite order (D). For double-staining, anti-DC-SIGN and anti-MR antibodies were added to the cells at the same time point (E). Non-stained sample was recruited to adjust the self-fluorescence of the cells (F). Green: anti-DC-SIGN-FITC. Red: anti-MR-PE-Cy5.

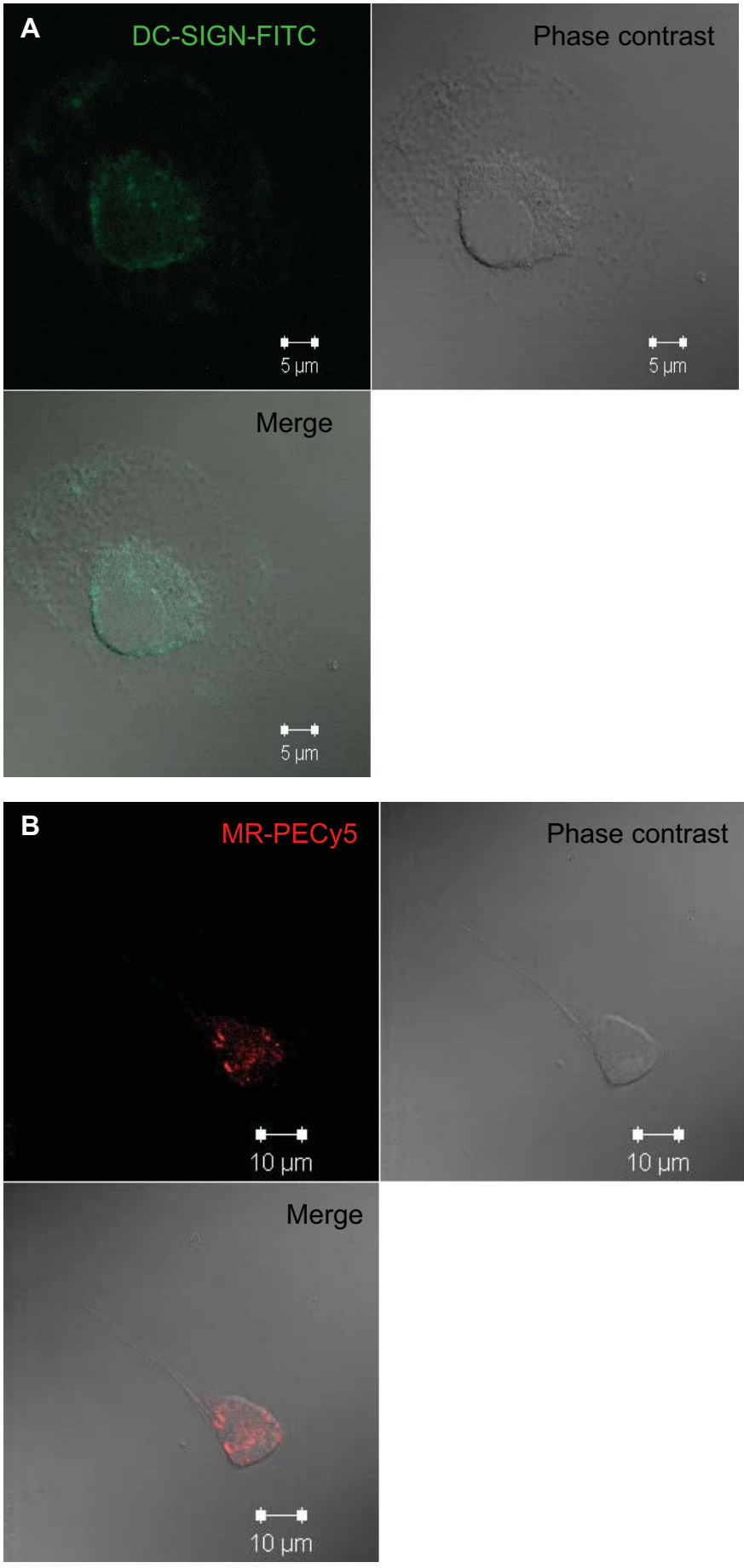

(To be continued)

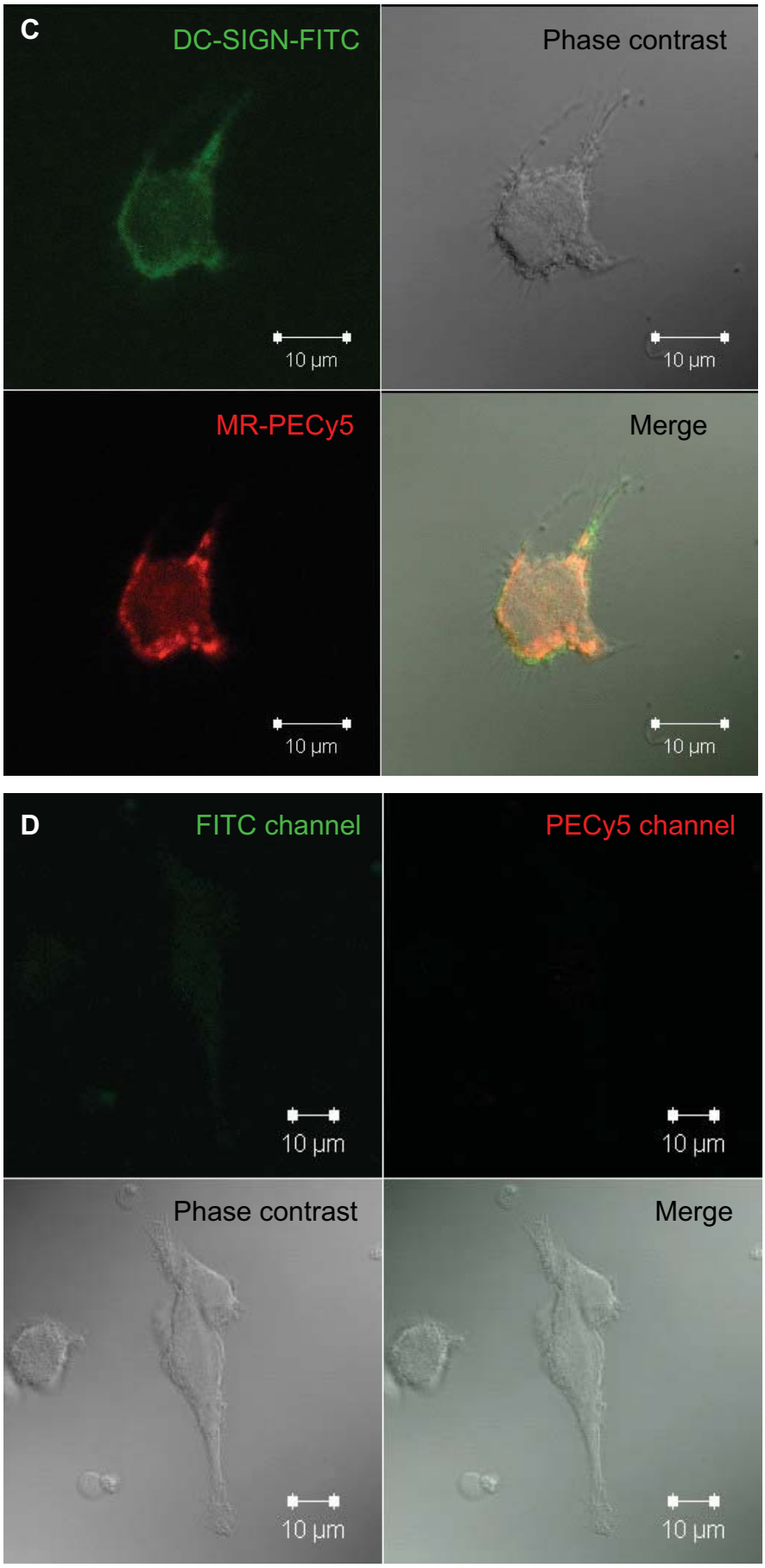
C
DC-SIGN-FITC
Phase contrast
MR-PECy5
Merge
10 µm
D
FITC channel
PECy5 channel
Phase contrast
Merge
10 µm

Figure 4-16 Expression of DC-SIGN and MR on IMMoDCs.

IMMoDCs were stained with anti-DC-SIGN antibody (A) or anti-MR antibody (B) individually. IMMoDCs were also double-stained with both of the antibodies simultaneously (C). Background signals from the cells were adjusted by non-stained sample (F). Green: anti-DC-SIGN-FITC. Red: anti-MR-PE-Cy5.

4.3.2 Native DENV2 attachment on IMDCs and IMMoDCs

When the temperature was kept at 4°C, native DENV2 particles were capable of binding to the surfaces of IMDCs without internalisation (Figure 4-17 A). Having been stained with the anti-DC-SIGN antibody or anti-MR antibody, the DENV2 attached-IMDCs showed that the DENV2 binding sites were associated with the expression of DC-SIGN (Figure 4-17 B) or MR (Figure 4-17 C). After staining the DENV2 attached-IMDC with both anti-DC-SIGN and anti-MR antibodies simultaneously, it was interesting to observe that the DENV2-attached IMDCs were DC-SIGN^{+}MR^{+}. The DENV2 binding sites were co-localised with the expression sites of both DC-SIGN and MR (Figure 4-17 D, as indicated by white arrows). However, the expression of DC-SIGN and/or MR did not guarantee the attachment of DENV2 (Figure 4-17 D, as indicated by yellow arrows).

The same phenomenon was also observed in DENV2-attached IMMoDC (Figure 4-18 A, with white arrows indicating the DENV2 binding sites, and with yellow arrows indicating the DC-SIGN^{+} or MR^{+} expression sites that without DENV2 binding). This observation suggested that although native DENV2 was able to attach to IMDCs and IMMoDCs via interacting with DC-SIGN and MR, there could be other molecules that play significant roles during DENV2 entry, associating with DC-SIGN and/or MR.

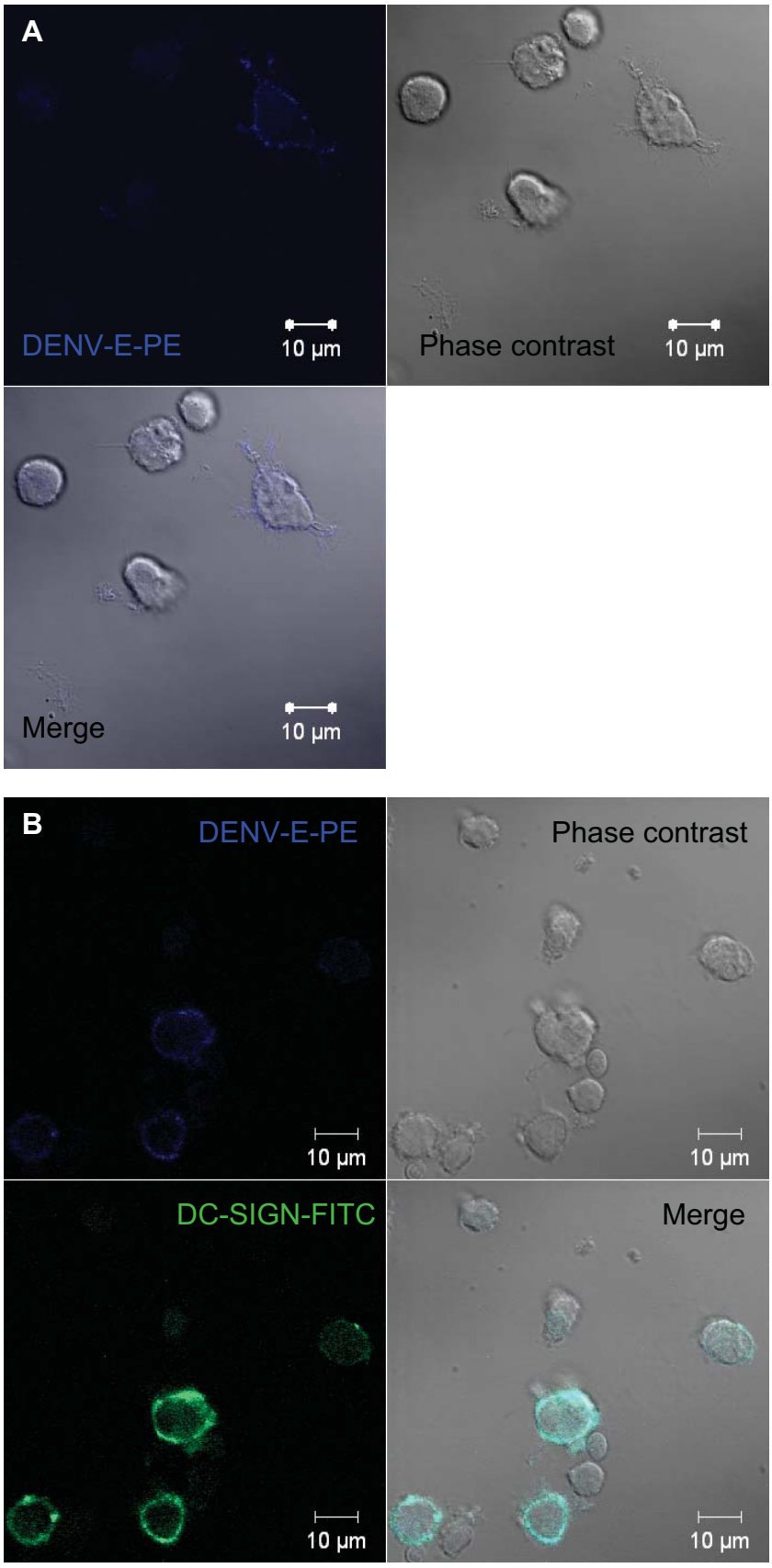

(To be continued)

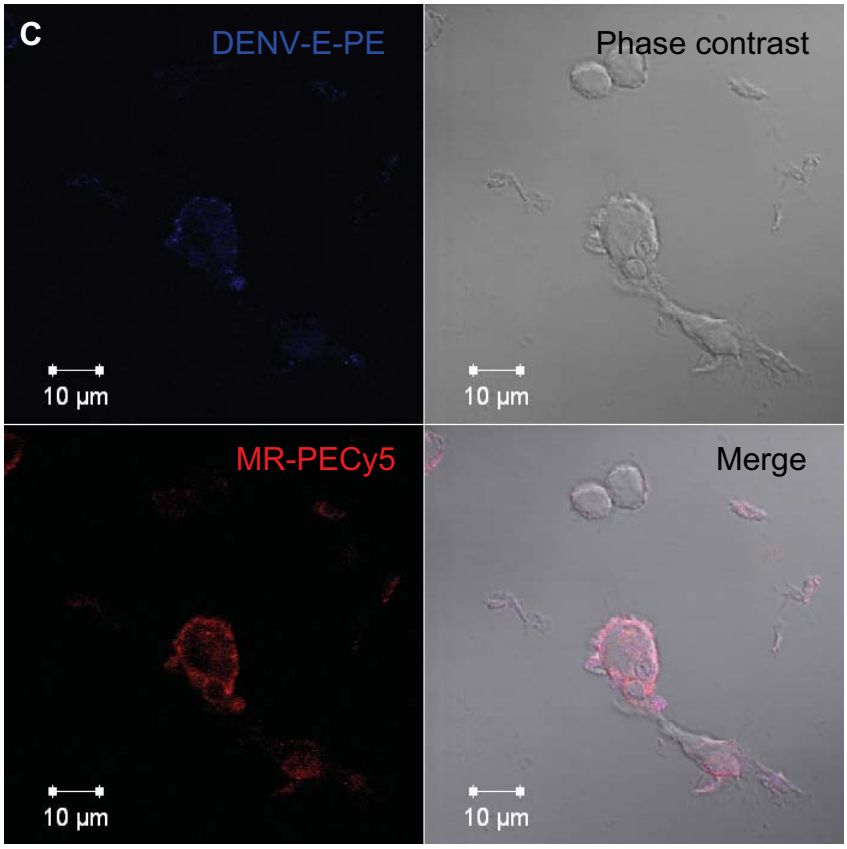

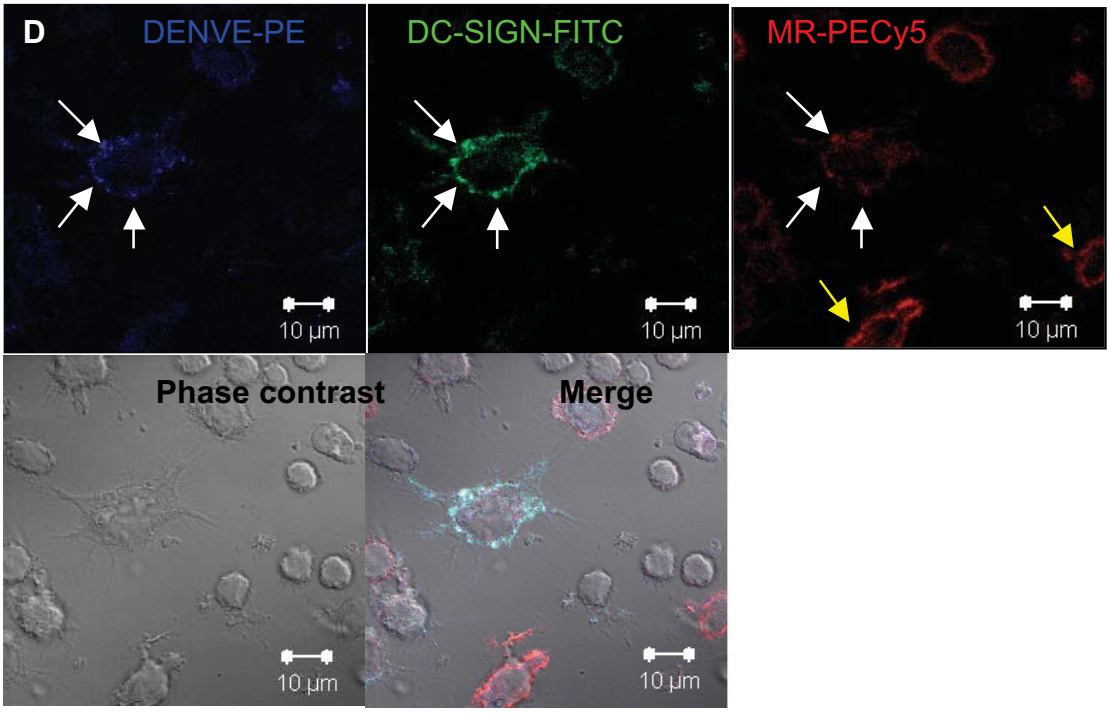

(To be continued)

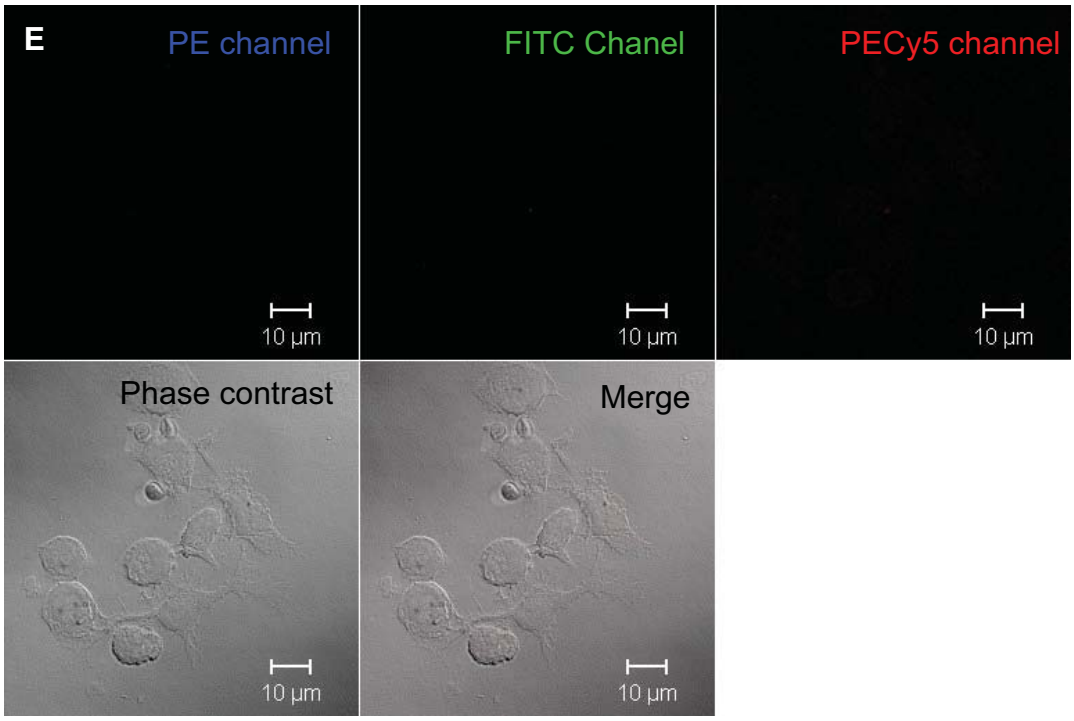

Figure 4-17 DENV2 binding sites on IMDCs.

Having been incubated with native DENV2 at 4°C for one hour, IMDCs were stained with anti-DENV-E antibody only (A), or anti-DENV-E antibody in addition to anti-DC-SIGN antibody (B), or anti-DENV-E antibody plus anti-MR antibody (C), or anti-DENV-E antibody with antibodies for both receptors (D). Mock-infected and non-stained cells were used to adjust the non-specific signals (E). Green: anti-DC-SIGN-FITC. Red: anti-MR-PE-Cy5. White arrows: DENV2 binding site co-localised with DC-SIGN and MR expression sites. Yellow arrows: DC-SIGN or MR expression sites without DENV2 attachment.

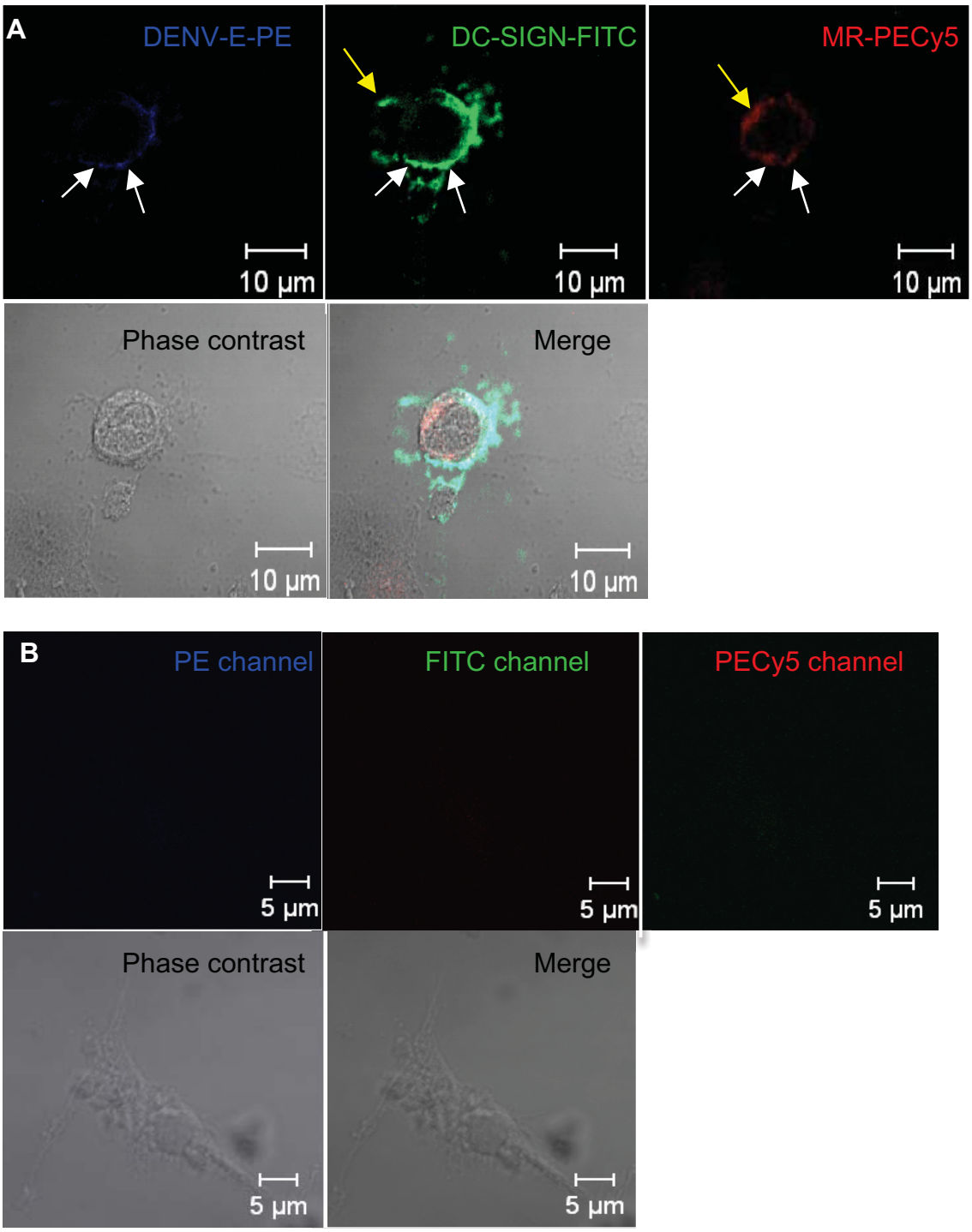
A
DENV-E-PE
DC-SIGN-FITC
MR-PECy5
10 µm
10 µm
10 µm
Phase contrast
Merge
10 µm
10 µm
B
PE channel
FITC channel
PECy5 channel
5 µm
5 µm
5 µm
Phase contrast
Merge
5 µm
5 µm

Figure 4-18 DENV2 binding sites on IMMoDC.

A: Cells were incubated with DENV2 and then stained with anti-DENV-E, anti-DC-SIGN and anti-MR antibodies. B: mock-infected and non-stain control. Green: anti-DC-SIGN-FITC. Red: anti-MR-PE-Cy5. White arrows: DENV2 binding site co-localised with DC-SIGN and MR expression sites. Yellow arrows: DC-SIGN or MR expression sites without DENV2 attachment. DC-SIGN and MR co-expression was also observed on IMMoDC. DENV2 particles that attached to IMMoDCs were visible.

4.3.3 Inhibition of DENV2 attachment on IMDCs and IMMoDCs

On the purpose of investigating the entry mechanism of DENV2 on immature DCs, a series of inhibitory assays were conducted on IMDCs and IMMoDCs.

Firstly, endocytosis inhibitor CPZ was used to block the internalisation of DENV2 on IMDCs and IMMoDCs. CPZ, belonging to cationic amphiphilic class of drugs, can induce the relocation of clathrin AP-2 subunit, preventing coated pit assembly at the cell surface (Wang *et al.*, 1993). CPZ was previously used to block the clathrin-mediated endocytosis of DENV on *Aedes albopictus* mosquito cells (Acosta *et al.*, 2008). In this experiment, the cells without CPZ pre-treatment but had DENV2 infection were positive controls. The viral replication level within cells reflected the inhibition of DENV2 entry. Pre-incubation with CPZ before DENV2 infection could efficiently inhibit DENV2 entry to IMDCs and IMMoDCs in a dose-dependent manner. A CPZ concentration of 15 μM was sufficient to inhibit DENV2 entry to both IMDCs and IMMoDCs to approximately 80% with a significant *p* value. Especially in IMMoDCs, 10 μM CPZ was enough to significantly inhibit DENV2 entry (Figure 4-19). Thus, it was demonstrated that DENV2 utilised receptor-mediated endocytosis via clathrin-coated pits on IMDC, and on IMMoDCs as well.

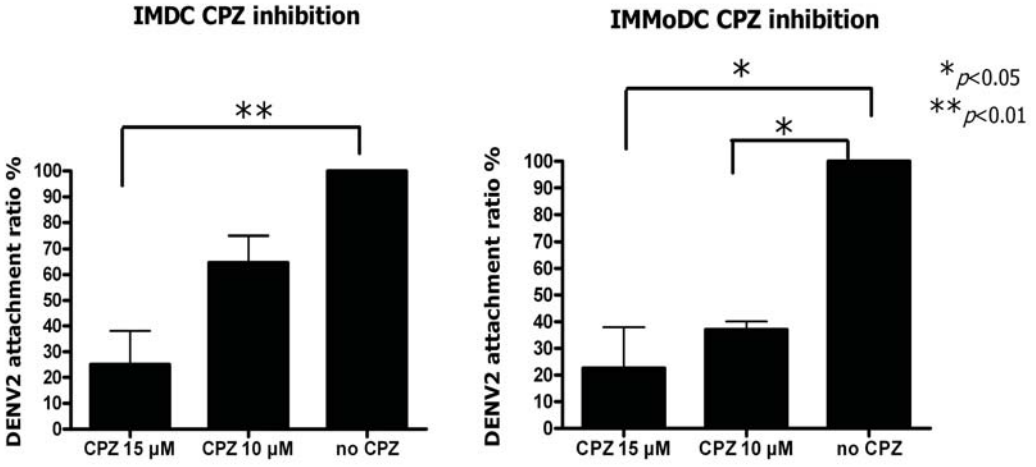

Figure 4-19 DENV2 attachment and internalisation were inhibited by the endocytosis inhibitor CPZ on both IMDCs and IMMoDCs.

Cells were incubated with DMSO dissolved CPZ before adding DENV2. Viral attachment was determined by measuring viral RNA replication level using RT-PCR. Cells without CPZ treatment were positive controls. Pre-incubation of CPZ can inhibit DENV2 attachment to both IMDCs (left) and IMMoDCs (right) in a dose-dependent manner. Results were analysed with one-way ANOVA followed by Tukey's HSD post hoc test and presented as mean ± SEM from three independent experiments. *p<0.05, **p<0.01.

Subsequently, the DC-SIGN and MR double-blocked assay was conducted in order to study the interaction between these two receptors during DENV2 entry (Figure 4-20). In IMDCs, although pre-incubation with anti-DC-SIGN or anti-MR antibodies alone were not able to significantly inhibit DENV2 entry, pre-incubation of IMDC with both anti-DC-SIGN and anti-MR efficiently decreased the attachment of DENV2 (Figure 4-20). However, the blocking efficiency was only approximately 60%, and was not improved when the antibody amount was increased (data not shown).

In IMMoDCs, anti-DC-SIGN antibody inhibited DENV2 entry, with an effect that was statistically significant. The combination of anti-DC-SIGN and anti-MR antibodies effectively blocked DENV2 entry to IMMoDCs, even though the blockage was not complete. Additionally, there was no significant difference between inhibiting efficacy of anti-DC-SIGN blocking and that of double-blocking (Figure 4-20). Thus, the role that MR played in IMMoDCs during DENV2 entry was not as certain as that in IMDCs. Also, the incomplete inhibition indicated that there could be other molecules on the surfaces of IMDCs and IMMoDCs involved in DENV2 entry.

IMDC DC-SIGN and MR blocking assay

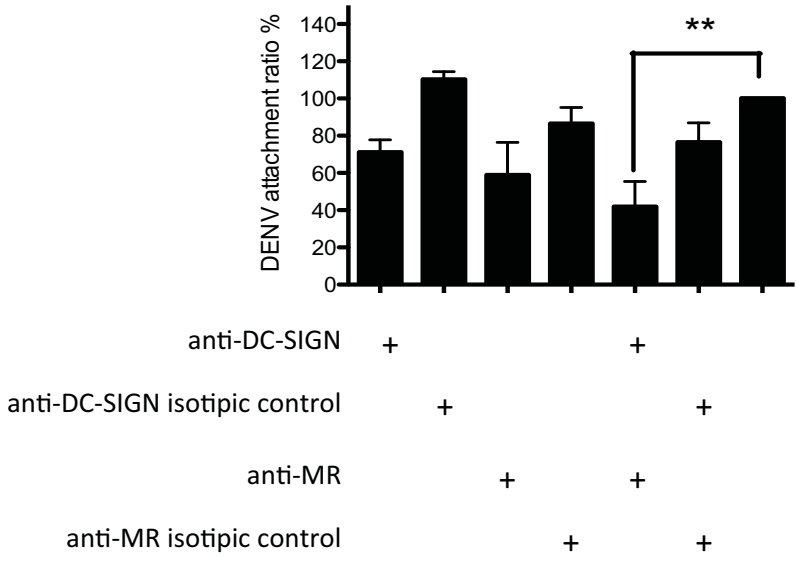

IMMoDC DC-SIGN and MR blocking assay

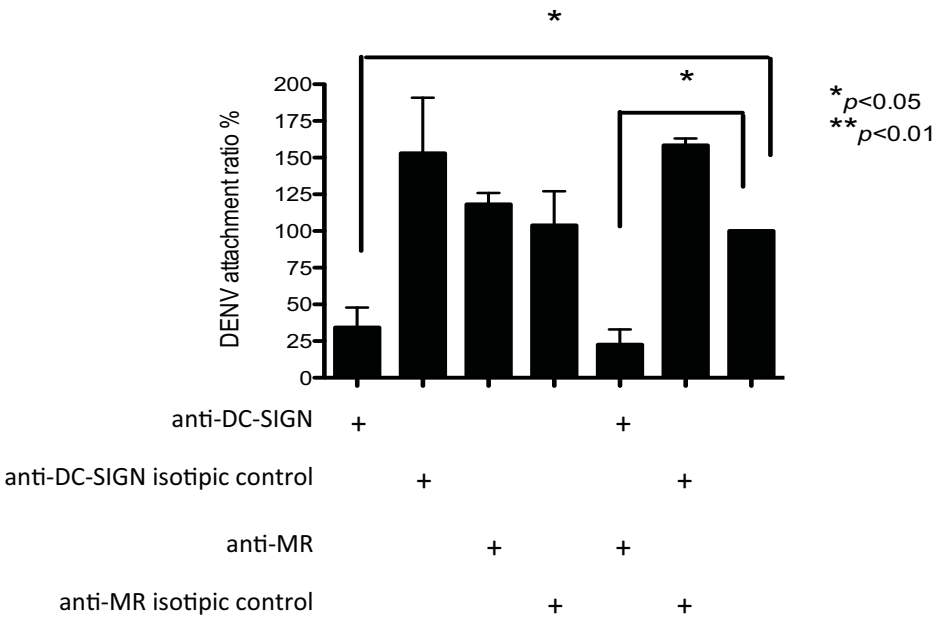

Figure 4-20 DC-SIGN and MR double-block assay on IMDCs and IMMoDCs to inhibit DENV2 entry.

Specific antibodies were added to IMDCs or IMMoDCs before DENV2 infection. Compared to isotypic controls, anti-DC-SIGN or anti-MR antibodies alone failed to inhibit DENV2 entry efficiently in IMDCs. The anti-DC-SIGN antibody only can inhibit DENV2 infection in IMMoDCs. Double-blocking of these two receptors significantly inhibited DENV2 entry to IMDC to more than 50% and to IMMoDCs to more than 75%. iso: isotypic control. Results were shown as mean ± SEM from three independent experiments. Results were analysed with one-way ANOVA followed by Tukey's HSD post hoc test. *p<0.05, **p<0.01.

4.3.4 Involvement of inter-alpha-trypsin inhibitor heavy chain 2 (ITIH2) during DENV2 entry to IMDCs and IMMoDCs

Having observed that endocytosis-inhibitor CPZ failed to completely block DENV2 entry to both IMDCs and IMMoDCs, which was the same for the double-blocking of DC-SIGN and MR, it was wondered whether there was any other molecule/mechanism involved in DENV2 entry to immature DCs. Thus, a Co-IP assay was performed to explore the possible attachment molecule on IMDC/IMMoDC cytoplasm membranes. It was quite interesting to discover that, compared to negative controls, DENV2-IMDC Co-IP group, as well as DENV2-IMMoDC Co-IP group, presented extra and strong bands on the silver-stained gels between 100 and 130 kDa (Figure 4-21, indicated by red arrows). It was indicated that native DENV2 particles were able to pull down a protein with a molecular weight close to 130 kDa from the total transmembrane proteins extracted from IMDCs or IMMoDCs. This molecule was analysed for protein identification via tandem mass spectrometry. The protein identity of this molecule was subsequently found to be ITIH2. Compared to controls, DENV2 E protein monomers with a molecular weight around 50 kDa, together with DENV2 E protein dimers that appeared around 110 kDa, were also observed on the silver-stained gels. Besides, in the DENV2-IMDC Co-IP and DENV2-IMMoDC Co-IP groups, extra bands with different molecular weights also appeared (around 70 kDa, 130-180 kDa, and above 300 kDa). However, those bands were too blurred to be analysed.

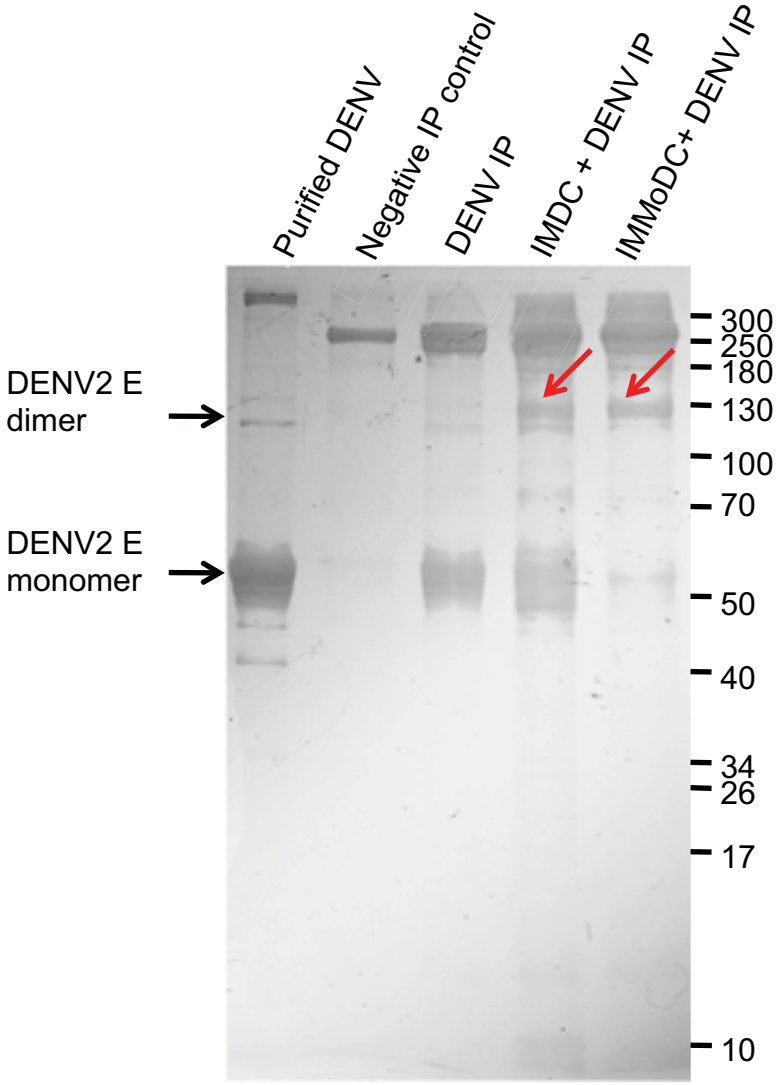

Figure 4-21 Analysis of IMDC and IMMoDC membrane proteins that were co-immunoprecipitated with DENV2 particles.

Proteins collected from the Co-IP assay were analysed by SDS-PAGE and silver staining of polyacrylamide gels. Bands corresponding to the approximate molecular weight of DENV2 E monomers and DENV2 E dimers were indicated by black arrows. Red arrows indicate extra bands that were pulled down by DENV2 with a molecular weight around 130 kDa, which were cut from the gel and subsequently analysed by mass spectrometry.

Since ITIH2 is not a transmembrane protein (Anderson *et al.*, 2004), the detection of ITIH2 from the extracted total transmembrane protein samples was unexpected. Thus, the occurrences of ITIH2 on the surfaces of IMDC and IMMoDC were detected by flow cytometry after exterior staining (Figure 4-22). Although not abundant, the presence of ITIH2 was detectable on IMDC and IMMoDC surfaces. However, whether these ITIH2 molecules were autogenously expressed by the cells or integrated into the cytoplasmic membrane from the external environment needs further investigation.

In order to further investigate the role that ITIH2 played in DENV2 entry, an ITIH2-blocking assay was conducted (Figure 4-23). Inhibiting ITIH2 only with a specific antibody failed to block DENV2 entry to neither IMDCs nor IMMoDCs. However, when combined with an anti-DC-SIGN antibody, the anti-ITIH2 antibody can block DENV2 entry into IMMoDCs by more than 80%. The combination of the anti-MR antibody and anti-ITIH2 antibody resulted in approximately 50% inhibition of DENV2 entry into IMMoDCs. When combining these three antibodies together, the inhibitory rate on IMMoDCs was more than 90% with a significant *p* value.

For IMDCs, the combination of these three antibodies could significantly inhibit DENV2 entry by 80%. More interestingly, anti-DC-SIGN antibody and anti-ITIH2 antibody together significantly increased DENV2 entry into IMDCs by more than 50%.

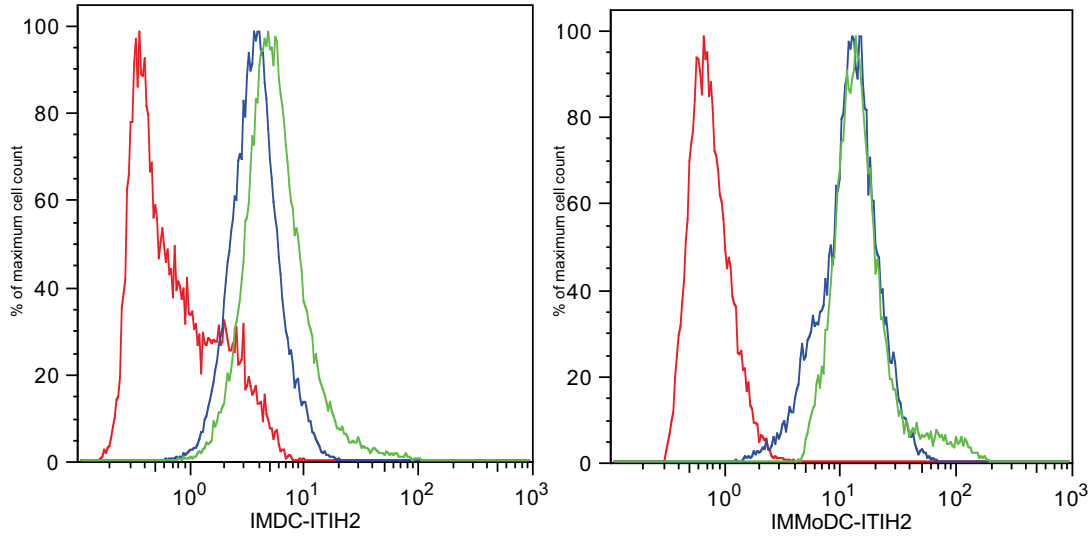

2nd antibody control group X mean= 4.24
ITIH2 staining group X mean = 7.43

2nd antibody control group X mean = 14.2
ITIH2 staining group X mean = 20.4

Figure 4-22 Surface detection of ITIH2 on IMDCs and IMMoDCs.

Red: non-stained controls. Blue: secondary antibody only controls. Green: ITIH2 staining groups. In both IMDCs and IMMoDCs, the ITIH2 staining group presented higher X mean values compared to secondary antibody only control groups, with noticeable peak-shifts. It is thus indicated that presence of ITIH2 was detectable on IMDC and IMMoDC surfaces with a specific antibody.

IMDC ITIH2 blocking assay

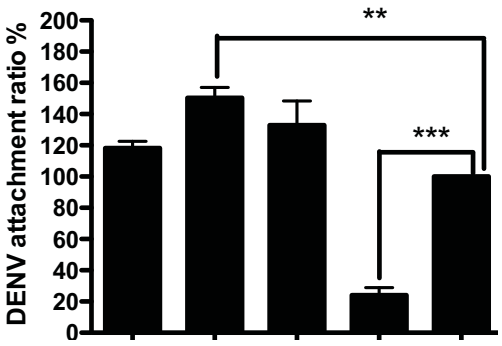

anti-ITIH2	+	+	+	+
anti-DC-SIGN		+		+
anti-MR			+	+

IMMoDC ITIH2 blocking assay

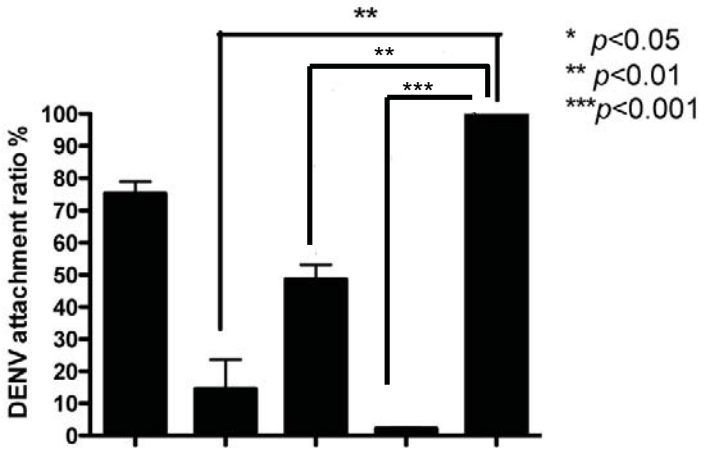

anti-ITIH2	+	+	+	+
anti-DC-SIGN		+		+
anti-MR			+	+

Figure 4-23 Anti-ITIH2 antibody, together with anti-DC-SIGN antibody and anti-MR antibody inhibited DENV2 attachment to IMDCs and IMMoDCs.

Cells were incubated with anti-ITIH2 antibody, and/or anti-DC-SIGN, and/or anti-MR antibody prior to DENV2 infection. In IMMoDCs, anti-ITIH2 antibody, together with anti-DC-SIGN antibody and/or anti-MR antibody significantly blocked DENV2 attachment, while anti-ITIH2 antibody alone failed to do so. In IMDCs, only the antibody-combination of anti-ITIH2+anti-DC-SIGN+anti-MR significantly inhibited the DENV2 attachment to 80%. In contrast, anti-ITIH2 antibody+anti-DC-SIGN antibody efficiently increased DENV2 attachment on IMDC. Data were analysed with one-way ANOVA followed by Tukey's HSD post hoc test and are shown as mean ± SEM from three independent experiments.

Table 4-4 Comparison of dissociation constants of MR and ITI to DENV2 particles

	pH 5.5	pH 6.0	pH 6.5	pH 7.0	pH 7.5
MR (K_D)	1.06 μM	276 nM	248 nM	514 nM	3.58 μM
ITI (K_D)	308 nM	121 nM	63.4 nM	4.16 nM	102 nM

Binding affinities of human recombinant MR and human ITIH2 to DENV2 virions were detected by SPR, presented as dissociation constant K_D (Table 4-4). Because the purification of human ITIH2 protein from plasma was difficult, human ITI complex consisted of ITI heavy chains and ITI light chains was used in this assay. MR was able to bind to DENV2 virions with higher affinity in mild acidic environment (6.0-6.5). Compared to MR, human ITI showed higher binding affinities under five tested pH conditions, in which the neutral pH condition (7.0) showed the lowest K_D, indicating the binding between ITI protein and DENV2 required a moderate environment.

The previous results of the RT-PCR arrays showed that DENV2 replication had no significant influence on ITIH2 mRNA expression in IMDCs and IMMoDCs (data not shown). The effects of DENV2 infection or transfection on the expression of ITIH2 and related factors were determined by real time RT-PCR (Figure 4-24). Bikunin was the light chain of ITI complex, related to the maturation of the ITIH2 protein (Martin-Vandelet *et al.*, 1999), while tumour necrosis-stimulated gene 6 (TSG-6) was involved in the function of ITIH2 (Mukhopadhyay *et al.*, 2004). There was approximately eight-fold up-regulation of TSG-6 mRNA expression in DENV2-infected IMMoDCs. However, the mRNA levels of bikunin were not altered by DENV2 transfection or infection in IMDCs and in IMMoDCs. The RNA expression level of ITIH2 was not detectable in IMDCs and IMMoDCs after using different primer-pairs (data not shown).

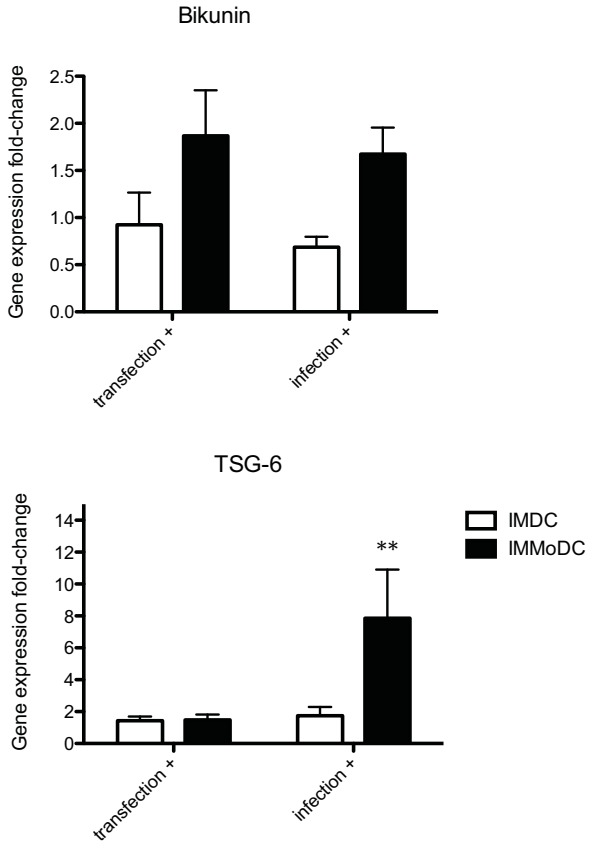

Figure 4-24 Gene expression of ITIH2 light chain bikunin and co-factor TSG-6 in IMDCs and IMMoDCs after transfection and infection.

The mRNA level of bikunin did not change in IMDCs nor IMMoDCs after DENV2 transfection/infection. DENV2 infection induced significant up-regulation of TSG-6 mRNA expression in IMMoDCs, but had no effect on that of IMDCs. Solid column: IMMoDCs. Open column: IMDCs. Data were analysed with one-way ANOVA followed by Tukey's HSD post hoc test and presented as mean ± SEM from three independent experiments. The expression level of TSG-6 in infected IMMoDC was significantly increased than that in mock control. (** $p<0.01$).

5 Discussions

5.1 IMDC as an *in-vitro* model to DENV2 infection

The major objective of this project was to establish an *in-vitro* model to study DENV2 and host DC interactions. Although human PBMC-derived immature DCs (IMMoDCs) have been widely utilised to study DC function *in-vitro*, the use of IMMoDCs may give rise to inconsistent results due to donor-to-donor variations. Thus, appropriate *in-vitro* models are essential for investigating the biology of DC (Santegoets *et al.*, 2008b; van Helden *et al.*, 2008). MUTZ-3-differentiated immature DCs (IMDCs) were described as an appropriate DC model and were used to generate Langerhan cells to study virus-host interactions (de Jong *et al.*, 2010; Masterson *et al.*, 2002). In this study, an *in-vitro* model involving IMDCs was established. The IMDC model was compared with IMMoDCs for morphology, DC-related surface marker expression, the ability to support DENV2 replication, DC antiviral responses during DENV2 replication, and the DENV2 entry mechanism. This study was the first to assess DENV2-DC interaction using IMDC in comparison with IMMoDCs. The major findings will be discussed in this chapter.

5.1.1 The differentiation of MUTZ-3 into DC-like cells

Upon induction by the cytokine cocktail, both MUTZ-3 cells and human monocytes differentiated into IMDCs and IMMoDCs. Both types of differentiated cells acquired typical DC morphology. Meanwhile, except HL-

60 cells, K562 cells and THP-1 cells also produced altered morphologies upon stimulation. However, the morphologies that IMKDCs and IMTDCs obtained were different from the one of IMMoDCs. Approximately half of the induced IMDC and IMMoDC cell populations were $MR^+DC\text{-}SIGN^+$, and the majority of these double-positive populations exhibited classic DC surface phenotype as $CD1a^+$ or $CD80^+$. The high viability of MUTZ-3, IMDCs, and monocytes (over 90%) indicated that the culture conditions were promising. However, the lower and inconsistent viability of IMMoDCs suggested the vulnerability and variability of the DC primary culture. Furthermore, while the DC mature marker CD83 was not expressed on IMDCs, this marker was sometimes detected on the surface of IMMoDCs even without further induction (such as virus, LPS, or cytokine) (data not shown). This observation further demonstrated that the characteristics of IMMoDCs were blood donor-dependent.

5.1.2 Less permissiveness of IMDCs to DENV2 replication and production

It was demonstrated that IMDCs were not only permissive to DENV2 attachment and replication, but also to the production of intact viral particles. However, when compared with IMMoDCs, the level of DENV2 replication in IMDCs was much lower. Although as DCs differentiated from leukaemia cells, IMKDCs and IMTDCs showed same DENV2 viral load as IMMoDCs did. DENV2 displayed even higher replication level in IMHDCs than in IMMoDCs. DENV viral load plays a significant role in the development of DHF and DSS,

because it is critical in activating immune responses that lead to haemorrhage and plasma leakage (Lei *et al.*, 2001). Therefore, it was important to investigate the mechanism accounting for the low viral load in DENV-infected IMDCs.

These different viral loads might not be associated with the availability of DENV receptors, since a similar percentage of IMDC and IMMoDC populations co-expressed MR and DC-SIGN. Furthermore, when the DENV2 replicon was transfected into IMDCs and IMMoDCs, viral replication was also less effective in the IMDCs. Since the replicon transfection process was independent on receptors, it was therefore suspected that other factors inside the IMDCs suppress the viral replication.

Investigation of DENV2 replication at different time points after infection in IMDCs and in IMMoDCs provided more information. After entering into IMDCs, DENV2 replication remained low in the first 24 h post-infection, and increased two times in the 48 h post-infection. This indicated that, although DENV2 was able to replicate in IMDCs, the environment inside of IMDCs did not support effective DENV2 replication, but the adverse intracellular condition could be overcome by the virus 24 h after infection. In the culture medium of infected IMDCs, viral copy numbers also increased along with the post-infection time. Additionally, viral proteins appeared at the late stage of the incubation in the culture medium of infected IMDCs. These observations

suggested that, although the production was not vigorous, infectious DENV2 virions could be produced from IMDCs. Additionally, it was very interesting to notice that although the viral load increased along with the incubation time, the release of viral particles from the infected IMDCs was not increased after 12 h post-infection, suggesting a possible antiviral response in the IMDCs that might inhibit viral assembly and/or viral budding. And this inhibition took 12 h to effect.

On the other hand, DENV2 RNA replication in IMMoDCs remained at high levels throughout the whole incubation period, without a dramatic increase along with incubation time. Moreover, elevation in the amount of released DENV2 virions was observed when incubation time was extended. Thus, the IMMoDCs were obviously more permissive for DENV2 replication and production compared with IMDCs.

Additionally, viral morphology in IMDCs was different from that in IMMoDCs. While virions were clearly detected in the ER and Golgi apparatuses of infected IMMoDCs, only a vacuole-like organelle, which contained virus like particles, was seen in infected IMDCs. It was previously suggested that when the cellular environment is harsh to viral replication, viruses would develop alternative morphology as a strategy to escape from the cellular immune suppression (Clark *et al.*, 2012). The presence of atypical morphologies could be due to the harsh intracellular environment. However, in this study, the appearance of viruses with alternative morphology was based on direct

EM examination; more reliable confirmatory experiments are required to determine whether the particles observed in IMDC were DENV virions. Immuno-electron microscopy, which combines immunostaining and electron microscopy, may help to determine the observed particles in IMDCs. However, as discussed above, the viral alternative morphology is used for escaping the immune system, such as antibody recognition; therefore, whether the immune-electron microscopy is suitable for virus alternative morphology observation requires to be determined.

On the other hand, the vacuole-like organelle observed in infected IMDCs could be autophagosome due to its characteristic double-membrane and size. To clarify this point, autophagy marker was detected in infected IMDCs and IMMoDCs afterwards and the results are to be discussed in section 5.1.4.

Besides, initial viral dosage may also affect the level of viral replication in DCs. In the current study, cells were exposed to native DENV2 with MOI=1. During assay optimisation, using MOI=10 did not show any significant difference compared to applying MOI=1. Additionally, the attempt to use a higher MOI in this study was hampered by the difficulty in preparing high-dosage virus suspension and concentrating virus particles by ultra-centrifugation. On the other hand, as reviewed in section 1.3.4.1, the viral dosage that occurs via mosquito biting is as low as 10^4 PFU, and as one of the initiate target cells, DC, whose absolute count in blood is around 10 ×

10^6 cells/L blood (Fearnley *et al.*, 1999), may not receive very high MOI during a real infection. Regardless, it is necessary to use higher MOI in future studies to investigate the influence of DENV dosage on viral replication levels in IMDCs.

5.1.3 Influence of DENV2 replication on IFN-inducible genes in DCs

Although IMDCs were morphologically and phenotypically similar to IMMoDCs, the replication level of DENV2 subgenomic replicon and DENV2 were quite lower in IMDCs than in IMMoDCs. Furthermore, while a panel of antiviral genes were strongly activated by DENV2 replicon in IMMoDCs, unexpectedly, it was found out that a group of IFN-inducible genes were activated in the naïve IMDCs, including IFIT1, IFIT3, IFI6, IFITM1, ISG15, and IFI27. These genes can impair different steps of DENV life-cycle. Thus, it was suspected that the spontaneously activated intracellular antiviral responses in IMDCs might be accountable for the low DENV2 replication level.

ISG15 is an ubiquitin-like molecule that has an important function in antiviral responses against various viruses, including DENV (Dai *et al.*, 2011). The antiviral function of ISG15 is probably achieved via: 1) regulating several stages of viral budding that require ubiquitin machinery and endosomal sorting complex required for transport pathway; 2) targeting viral proteins for ISGylation, which is a process that mature ISG15 mediates its covalent

conjugation to the target proteins via its C-terminal LRLRGG motif; and 3) impacting host proteins by disrupting ubiquitination (Lenschow, 2010). This can explain why ISG15 was significantly increased in the infected IMMoDCs rather than in transfected IMMoDCs, since there was no viral budding in the latter (Figure 4-13, and Table 4-1).

IFITM1 belongs to the subfamily IFN-inducible transmembrane genes, initially inhibits DENV clathrin-mediated endocytosis *in-vitro* (Brass *et al.*, 2009; Jiang *et al.*, 2010). Another family member IFITM2 also inhibits molecular events of virus life cycle before viral RNA translation. Besides, IFITM2 has pro-apoptosis function, which is independent on p53 (Siegrist *et al.*, 2011). In this study, replicons were directly delivered into cells by liposome-based reagents. Whether this process is endocytosis-dependent or not remains unknown (Akita *et al.*, 2004; McLaggan *et al.*, 2006). The transfection process could stimulate IFITM genes directly, which probably explained why DENV2 transfection induced IFITM1 and IFITM2 more strongly in IMMoDCs than DENV infection did (Figure 4-13, Table 4-1). Furthermore, IFITM1, together with IFITM2 and IFITM3, hampered antibody-dependent enhancement of DENV in human K562 cells (Chan *et al.*, 2012).

IFI27 is a putative hydrophobic protein of 122 amino acids containing a conserved 80 amino-acid motif (Parker and Porter, 2004). The protein product is encoded by the *ifi27* gene located in band q32 of human

chromosome 14 (Rasmussen *et al.*, 1993). The putative antiviral action of IFI27 may not involve direct interaction with the virus. Alternatively, as an inner mitochondrial membrane protein, IFI27 participates in apoptosis by altering mitochondrial integrity (Cheriyath *et al.*, 2011). IFI27 is induced by IFN-α rather than IFN-γ, but the induction level varies from cell to cell (Gjermandsen *et al.*, 2000). The inducibility is affected by interferon-inducible elements: ISRE, IRF1/IRF2 and STAT located at the promoter region of *ifi27* (Martensen *et al.*, 2001). Human cytomegalovirus infection induced the IFI27 expression *in-vitro,* while DENV1 greatly induced this gene expression in *Rhesus Macaques* (Sariol *et al.*, 2007; Zhu *et al.*, 1998).

IFIT1 is an interferon-inducible protein with 10 tandem arrayed tetratricopeptide repeat motifs (TPR), which is involved in protein-protein interaction and protein complex assembly (Guo *et al.*, 2000). IFIT1 forms a complex with IFIT2 and IFIT3; the complex exerts antiviral action by recognising the 5' triphosphorylation structural of viral RNA (Pichlmair *et al.*, 2011). The proposed antiviral mechanism of the IFIT family is to sense the viral genome RNA or 2′-*O* methylation-lacking mRNA (Daffis *et al.*, 2010). DENV has a type I cap with 2′-*O* methylation at its 5' terminal, as well as the DENV2 replicon used in this study (Dong *et al.*, 2012; Lai *et al.*, 2008). Hence, it is questionable whether the elevated expression of IFIT1 can antagonise DENV replication via the classical mechanism. Apart from sensing the viral mRNA 5' triphosphorylation, IFIT1 can also inhibit viral replication by direct interaction with viral proteins (Terenzi *et al.*, 2008).

Furthermore, IFIT1 proteins can suppress viral replication indirectly by the inhibition of host protein translation via binding to eukaryotic initiation factor-3 (EIF-3) (Hui *et al.*, 2005), or by inducing apoptosis via binding to eukaryotic elongation factor-1A (eEF1A) (Li *et al.*, 2010). Another family member, IFIT2, also induced apoptosis via damaging mitochondrial pathways in a process that was negatively regulated by IFIT3 (Fensterl and Sen, 2011).

In addition to IFIT3, another mitochondrial-localised protein, IFI6 (G1P3), was also significantly up-regulated in transfected IMMoDCs. IFI6 plays a role in anti-apoptosis. A previous study showed that IFI6 assisted IFN-induced antiviral activity during HCV replicon replication (Cheriyath *et al.*, 2011). This protein molecule might also play the same role during DENV2 infection in DCs.

The simultaneous stimulation of both pro-apoptosis (IFI27, IFIT1, IFIT2) and anti-apoptosis factors (IFI6, IFIT3) in IFN-antiviral responses could be the consequence of immune balance. On one hand, induction of apoptosis in virus-infected cells at early stage can efficiently reduce viral production. On the other hand, at the late stage of viral infection, virus particles accumulate inside the cells and induce apoptosis for the effective release of virions to neighbouring cells. Delaying apoptosis of the infected-cells at a late stage reduces the spread of viruses to neighbouring cells (Teodoro and Branton, 1997).

In this study, we detected an up-regulation of the IFI27 gene, especially in the DENV2 replicon-transfected IMMoDCs. Interestingly, in contrast to the observations in transcriptional level, DENV2 infection slightly decreased IFI27 protein expression in IMMoDCs (Figure 4-14). The gene expression levels of three family members of IFIT were up-regulated upon DENV2 replication in IMMoDCs (Figure 4-13, Table 4-1), while the protein expression levels of IFIT1 and IFIT3 were obviously induced after DENV2 infection in IMMoDC (Figure 4-14), indicating an overall activation of the IFIT signalling pathway. These observations suggested that pro-apoptosis pathways and anti-apoptosis remained competitive to each other in infected IMMoDCs.

As noticed here, the transcriptional measurements did not perfectly correlate with the protein expressions in IMDCs and IMMoDCs. Causes of this weak correlation could be complicated post-transcriptional processes and regulatory mechanisms. When mRNA is held in the nucleus, the amount of such mRNA could be over-estimated relative to protein expression level (Gry *et al.*, 2009).

The reason for spontaneous activation of IFN-inducible genes in naïve IMDCs (Table 4-2, Table 4-3) needs to be discussed. In fact, activation of IFN-inducible genes has been detected in bone marrow, peripheral blood cells and tumour tissues from cancer patients (Einav *et al.*, 2005; Yang *et al.*, 2005).

One possible cause for the activation of IFN-inducible genes is mutation. In MUTZ-3-derived IMDCs, two critical regions in chromosome 7 encoding three zinc finger proteins were deleted (De Weer *et al.*, 2010); these zinc finger proteins participate in the stimulation of IFN-inducible genes, including IFITs, OASs, IRFs, ISG15 and ISG20 (Xu *et al.*, 2009). Whether the chromosomal deletions in MUTZ-3 contributed to the continuous activation of IFN-related pathways and to the reduced DENV2 permissiveness warrants further investigation.

In addition to this study, other investigators have also compared the transcription profiles between IMDCs and IMMoDCs (Larsson *et al.*, 2006; Rasaiyaah *et al.*, 2009). However, in contrast to the observations here, Larsson *et al.* found that IMDCs had generally similar transcription profile as IMMoDC, while Rasaiyaah *et al.* reported that genes for certain immunological mediators were under-expressed in IMDCs (Larsson *et al.*, 2006; Rasaiyaah *et al.*, 2009). The different culture methods that were used between different laboratories could be one reason for these controversial findings. On the other hand, technical noises and limitations of these studies, such as cross-hybridisation of microarray analysis and affinity/specificity of antibodies in immunoblotting, may also cause the conflicted observations.

Despite the activation of IFN antiviral pathways, there was an active replication of DENV2 in IMMoDCs; this could be due to a time lag between

viral replication and the activation of antiviral mechanisms. Previous studies showed that both IFITM and IFIT proteins were up-regulated 48 h after IFN stimulation (Brass *et al.*, 2009; Fink *et al.*, 2007). Therefore, the basal level of these IFN-inducible proteins in IMMoDCs may not be sufficient to inhibit DENV2.

The replication levels of DENV2 in other generated DCs, on the other hand, were rather higher than that in IMDCs. At the same time, antiviral genes that continuously expressed in the naïve IMDCs were suppressed in the naïve DC-like cells differentiated from HL-60, K562, and THP-1. These results further indicated a possible correlation between viral load and the expression level of these antiviral genes.

5.1.4 DENV2 infection-induced autophagy in IMDCs and IMMoDCs

Autophagy is a process by which cytoplasmic materials are sequestered in double-membrane vesicles and subsequently delivered to lysosomes for degradation when cells receive signals such as starvation or infection (Kundu and Thompson, 2008). These signals interact with the mammalian target of rapamycin (mTOR) to initiate the formation of the autophagosome, which requires various autophagy-related (ATG) proteins, two ubiquitin-like systems Atg12-Atg5 and LC3-PE, and the lipid kinase signalling complex phosphoinositide 3-kinase (PI3K)/Beclin-1. The mature autophagosomes fuse with lysosomes, becoming autolysosome. The contents of the

autolysosomes, which are degraded by lysosomal acid hydrolases, can return to the cytoplasm through the autolysosomal membrane (Tanida, 2011). Autophagy has a significant function in the maintenance of cellular homeostasis, and the prevention of cell death under pressure conditions as well (Mizushima, 2007).

During viral infection, autophagy, which can be activated via IFN-γ by phosphorylation of eIF2α and the activation of double-stranded RNA-activated protein kinase (PKR), can serve a pro-viral or anti-viral role (Kudchodkar and Levine, 2009). For example, in HIV infection, while the viral proteins can regulate autophagy in order to amplify virion production, they are also capable of disrupting autophagy in bystander cells, inducing $CD4^+$ T cell death and HIV pathogenesis (Killian, 2012).

In this study, it was demonstrated that DENV2 infected-IMDCs had decreased amounts of LC3I, while the amount of LC3II increased. This suggested the accumulation of internal autophagosomes. The LC3 conversion pattern in DENV2 infected-IMMoDCs is different from that of infected IMDCs. Compared to the mock control, both LC3I and LC3II were up-regulated in infected IMMoDCs at 48 h post-infection, with the ratio of LC3II/internal control being increased as well. An-increased amount of endogenous LC3II can be due to the lipidation of LC3I to form LC3II during autophagy, inhibition of the fusion between autophagosomes and lysosomes,

and blocking of lysosomal degradation (Tanida *et al.*, 2005). Also, the increase of LC3I can be due to the overexpression of Atg4B, which cleaves the carboxyl termini of LC3 (Tanida *et al.*, 2004). Thus, the observation from infected IMMoDCs suggested a complicated autophagic-network upon DENV2 infection.

One problem of LC3II detection is that this molecule is more sensitive to detection during immunoblotting than LC3I (Mizushima and Yoshimori, 2007). Therefore, in order to precisely monitor the process of autophagy in DENV2-infected IMDCs and IMMoDCs, there are several aspects that require attention. Detecting LC3 expression at different time-points is necessary to illustrate the autophagy flux of infected IMDCs and infected IMMoDCs. Furthermore, to compare the amount of LC3II in the presence and absence of lysosomal protease inhibitor can help to measure the amount of LC3II that is delivered to lysosomes (Mizushima and Yoshimori, 2007). Another autophagy indicator, p62, which can bind to LC3 and serve as a selective substrate of autophagy (Pankiv *et al.*, 2007), should be included in the detection as well. These experiments are necessary for future work.

In agreement with our findings in infected IMMoDCs, DENV2 replication was able to activate the autophagy machinery with autophagosome formation and up-regulate viral replication in Huh7 cells (Lee *et al.*, 2008). Moreover, the inducer of autophagy can effectively increase DENV2 viral load and production. On the contrary, adding the inhibitor of autophagy 3-

Methyladenine and knocking down of the autophagy-related genes down-regulated the DENV replication levels in infected cells (Lee *et al.*, 2008).

A proportion of DENV NS1 protein was proven to be co-localised with autophagosomes and the ribosomal protein L28. Furthermore, the endosomal marker M6P-R co-localised with autophagosomes, suggesting that autophagosomes fuse with endosomes to form amphisomes, which linked DENV entry and replication (Panyasrivanit *et al.*, 2009). However, inhibiting the fusion between autophagosomes and amphisomes with lysosomes generated contrasting effects on viral yield in DENV2-infected HepG2 and DENV3-infected HepG2, suggesting different translation and replication strategies between DENV serotypes and the involvement of virus-encoded factors in host autophagy (Khakpoor *et al.*, 2009; Panyasrivanit *et al.*, 2009).

In addition to viral-type specificity, it was indicated that DENV-autophagy interaction was cell type-dependent and tightly related to virus pathogenesis. Although autophagy was observed in DENV-infected monocytic cells, the induction of autophagy in monocytic cells significantly decreased viral yield (Panyasrivanit *et al.*, 2011). As observed in this study, DENV2-infected IMDCs presented typical autophagic markers, but with a lower viral yield, while a non-typical autophagic pattern appeared in infected IMMoDCs, with a rather higher viral load, suggesting different anti-viral responses from these

two types of cells.

5.1.5 Other factors involved in the lower-level replication of DENV2 in IMDCs

5.1.5.1 Host genetic polymorphism

Variation of promoter sequences in DC-SIGN was found to be strongly associated with the severity of dengue infection (Sakuntabhai *et al.*, 2005). A similar observation was obtained in a study of HIV infection (Liu *et al.*, 2004a). Besides genes of DENV receptors, cytokine gene polymorphisms also contribute to the development of DENV-related diseases. As reported by Perez *et al*, the TNF-α (-308) A allele together with the IL-10 (-1082/-819/-592) ACC/ATA haplotype were correlated with DHF, while TNF-α (-308) GG and TGF-β1 (c25) GG genotypes prevented the development of the disease (Perez *et al.*, 2010). Variations also appear in IFI27 and IFITM1 coding regions, especially abundant in cancer cells (Parker and Porter, 2004; Siegrist *et al.*, 2011; Smidt *et al.*, 2003). These host genetic polymorphisms may lead to different DENV2 replication levels in IMDCs and IMMoDCs.

5.1.5.2 DENV serotypes and DENV strains

The low replication level of DENV2 in IMDCs in the current study may also be due to the choices of DENV serotypes and strains.

Entry of DENV into host cells is serotype-specific (Thepparit and Smith, 2004). Furthermore, different DENV serotypes have varying affinities in different cell lines (Barr *et al*., 2012). According to immunostaining and PCR detection, DENV1 and DENV4 were found to infect a wider range of cells, while DENV2 showed a quite narrow infectivity range (Barr *et al*., 2012). As a result, only if the replication levels of DENV1, DENV3, and DENV4 in IMDCs are investigated, can the permissiveness of IMDC to DENV be concluded.

The majority of *in-vitro* investigations, including this study, have used high-passaged laboratory-adapted standard DENV strains, in that these strains are able to induce susceptibility in a broad range of cells, growing to high titres and showing more plaques during titration. Results generated with high-passage DENV strains may differ from those with low-passage clinical isolation strains (Bente and Rico-Hesse, 2006). Therefore, clinically-isolated DENV strains need to be included in the investigation of permissiveness of IMDCs to DENV.

5.1.6 Factors that lead to different antiviral responses in transfected cells and infected cells

In this study, it was noticed that the DENV2 subgenomic replicon could not completely reproduce the reactions that native DENV2 triggered in IMDCs and IMMoDCs. Because the DENV2 replicon was purified as single-stranded positive-sense RNA containing no structural protein coding regions, it was

delivered into the host cells artificially. There were no viral binding or internalisation processes, not to mention the virion assembly and budding, which could trigger cellular activation and antiviral defences. In addition, the process that delivers the replicon into cells via liposome-based reagents may also trigger cellular responses.

It was believed that efficient innate immune reactions came from pathogen recognition via PRRs on DCs (Geijtenbeek and Gringhuis, 2009). Meanwhile, DC-SIGN and MR belong to the C-type lectin receptors as subfamily of PRRs (Geijtenbeek and Gringhuis, 2009). Upon viral binding onto DC-SIGN, the serine/threonine protein kinase RAF1 will be stimulated, which induces the phosphorylation of the nuclear factor kappa-light-chain-enhancer of activated B cells (NF-κB), and thereby activates downstream immune responses (den Dunnen *et al.*, 2009; Geijtenbeek and Gringhuis, 2009). In contrast, although MR lacks the cytoplasmic signalling motifs, specific antibodies binding to MR activated a series of signal transduction events (Taylor *et al.*, 2005). As observed in HIV-infected plasmacytoid DCs, not only the interaction between the viral envelope glycoprotein and the CD4 receptor, but also the endocytosis process was responsible for the plasmacytoid DC activation (Beignon *et al.*, 2005). Therefore, leaving DC-SIGN and MR untouched during transfection in this study might have caused an incomplete antiviral response.

Besides viral binding and endocytosis, there was no viral budding or release in the replicon system. Some signal transduction pathways that related to these two processes, such as heterotrimeric guanine nucleotide-binding regulatory proteins and casein kinase pathways (Hui and Nayak, 2002), were probably absent or poorly activated. Therefore, the global gene expression profiles resulted from the replicon system and the native virus are important, as they provide a direction regarding the signalling transductions that relate to DENV attachment/internalisation and assembly/budding.

5.2 Investigation of entry mechanism of DENV2 on immature DCs

5.2.1 The interaction of DC-SIGN and MR during DENV2 infection

Attaching to the cell surface is the first step of viral infection. The attachment molecules varied from virus to virus, and from cells to cells. Some of these molecules play a role as attachment factors, concentrating virions on the cell surfaces. On the other hand, other molecules serve as real receptors to bind to the virions and lead into endocytic pathways, with antiviral signals being transmitted to the cytoplasm (Smith and Helenius, 2004). As observed in HIV-1 infection, the initial contacts between HIV-1 virions and attachment factors such as DC-SIGN and MR do not trigger conformational changes of the glycoprotein. Once the glycoprotein 120 subunit of the virus envelope protein attaches to the outermost immunoglobulin G domain of CD4, the virion experiences conformational changes, making it possible to bind to co-receptors such as CXCR4 or CCR5. The associations between gp120 and

co-receptors thus activate the fusion-competent conformation of HIV1 (Smith and Helenius, 2004).

As reviewed in section 1.1.4.1.2 and section 1.1.4.1.3, DC-SIGN and MR have been shown to be involved in DENV entry. As PRRs, these two receptors belong to transmembrane CLRs (Figure 5-1). Both MR and DC-SIGN were shown to be critical factors for DENV entry. DC-SIGN facilitates the attachment of DENV particles on the target cell surface; the viral particles will then be internalised by MR-mediated endocytosis (Lozach *et al.*, 2005; Miller *et al.*, 2008). In this study, it was found that less than half of the induced DCs were susceptible to native DENV2 infection and increasing viral dosage to MOI=10 failed to increase the infection rates significantly (data not shown). This concurred with the finding that about half of the induced IMDC and induced IMMoDC populations were $MR^{+}DC\text{-}SIGN^{+}$. On some of the $DC\text{-}SIGN^{+}MR^{+}$ IMMoDCs or $DC\text{-}SIGN^{+}MR^{+}$ IMDCs, the expression site of DC-SIGN and MR appeared to be overlapped (Figure 4-17, Figure 4-18), which could be caused by two reasons: the co-capping effect, and the functional-related association.

Co-capping is a phenomenon that when cell surface receptors are cross-linked by antibodies or multivalent ligands, they form aggregated patches, which then assembly as a cap on the cell surface. This process can generate signals to initiate the activation of the cell (Graziadei *et al.*, 1990). In this

study, antibodies staining and DENV2 binding might have caused the co-capping-like phenomenon on IMMoDCs and IMDCs (Figure 4-17, Figure 4-18). It was realised that anti-DC-SIGN antibody binding prior to MR staining changed the distribution pattern of MR from clusters to evenly distributed on the IMDC surface (Figure 4-17). This observation agreed with the hypothesis that during DENV2 infection, the virion first bound to DC-SIGN, which served as an attachment factor (Clyde *et al.*, 2006). The interaction between DC-SIGN and the DENV2 virion subsequently triggered the relocation of MR, because MR was recruited to the DENV2 invading sites to fulfil its function of virus internalisation of the virions (Miller *et al.*, 2008). Although more evidences are needed, it is suggested that DC-SIGN may somehow influence the activity of MR on IMDCs. Due to the limitation of the resources, the co-capping assay was not performed on IMMoDCs in this study; however, this should be included in the future work.

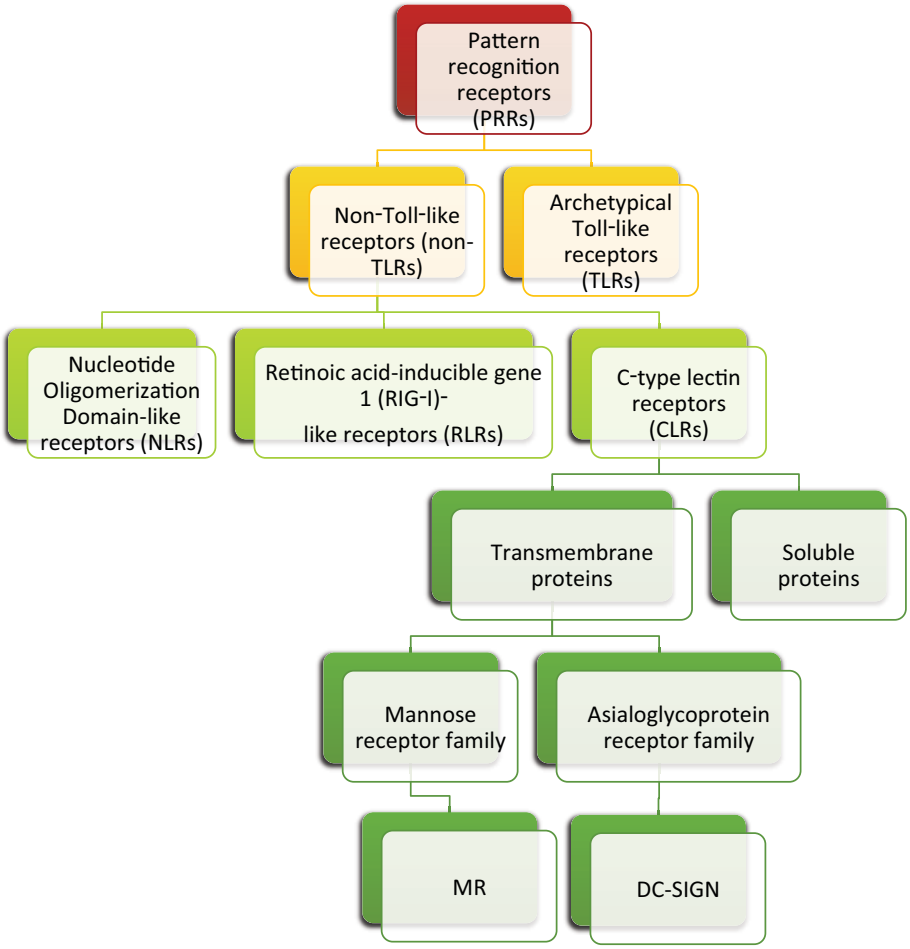

Figure 5-1 The system of DC-SIGN and MR in the human body.

Both DC-SIGN and MR belong to the CLRs subfamily, which represent one subgroup of PRRs. MR has three other family members from the mannose receptor family that are not shown in this graph, including CD205, phospholipases A2 (PLA2), and 180 kDa endocytic receptor (Endo180) (East and Isacke, 2002). DC-SIGN also has three members that belong to the asialoglycoprotein receptor family: Langerin, CLEC10A, and CLEC5A (Geijtenbeek and Gringhuis, 2009).

Table 5-1 Comparison of DC-SIGN and MR in pathogen recognition and signalling.

Name	Expression	Glycan PAMPs	Exogenous pathogenic ligands	Signalling proteins involved	Immunological activity
DC-SIGN (CD209)	Myeloid DCs	High mannose and fucose	• Bacteria: *Mycobacterium tuberculosis, Lactobacilli* spp., etc. • Virus: HIV-1, DENV, SARS coronavirus, etc. • Fungi: *Candida albicans* • Parasite: *Leishmania* spp. • Others: Tick *Ixodes scapularis* saliva protein Salp15, *Schistosoma mansoni* soluble egg antigens, etc.	LSP1, LARG, RHoA, Ras proteins, RAF1, Src kinases and PAKs	• Up-regulate IL-10 production • Activate T cell subsets differentiation • Induct of regulatory T cells • Antigen presentation
L-SIGN (CD299)	Endothelial cells of liver, lymph nodes, and placenta	High mannose	• Bacteria: *M. tuberculosis, Leishmania infantum*, etc. • Virus: HIV-1, Hepatitis C virus, SARS coronavirus, etc.	N/A	Pathogen internalisation
MR (CD206)	Myeloid DCs and macrophages	High mannose, fucose and sulphated sugars	• Bacteria: *M. tuberculosis, Streptococcus pneumonia*, etc. • Virus: HIV-1 and DENV • Fungi: *C. albicans, Cryptococcus neoformans*, etc. • Parasite: *Leishmania* spp.	CDC42, RHoB, PAKs and RoCK1	Pathogen endocytosis and phagocytosis; antigen presentation

This table is drawn based on the information from Geijtenbeek and Gringhuis (2009) and Khoo *et al.* (2008).

Results of the receptor-blocking assay in this study (Figure 4-22) agreed with previous findings by Alen *et al*. (2011), who showed that blocking DC-SIGN and MR with specific antibodies at the same time inhibited DENV2 attachment more efficiently than just blocking either one of them. Although the antibodies used in this assay were different clones (anti-DC-SIGN, clone DC28; anti-MR, clone 15-2) from those used in the study by Alen *et al.* (anti-DC-SIGN, clone 120612; anti-MR, clone 19.2), similar results were obtained. Thus, the inhibition of DENV2 entry was likely due to the specific receptor-blockage on DC-SIGN and MR, rather than non-specific effects of antibodies.

For anti-DC-SIGN antibodies, both clone DC28 and clone 120612 were capable of cross-reacting with liver/lymph node-specific ICAM-3 grabbing non-integrin (L-SIGN), which shares 77% aa identity with DC-SIGN and especially shares 84% aa homology of the CRD with DC-SIGN (Table 5-1). While the tandem-neck-repeat region of DC-SIGN keeps a constant size that is rather conserved, the same area of L-SIGN has significant polymorphism, which may cause the varied ligand-binding affinity of L-SIGN (Khoo *et al.*, 2008). Clone DC28 and clone 120612 inhibited DENV infections in MoDCs more efficiently than other monoclonal antibodies of DC-SIGN did (Miller *et al.*, 2008; Tassaneetrithep *et al.*, 2003). On the other hand, the different blocking efficiency could be due to the difference in antibody affinities. Regardless, the role that L-SIGN plays in DENV2-DC interactions is worth investigating in depth.

As noticed in this study, MR mRNA expression was significantly up-regulated in infected IMMoDCs, while DC-SIGN gene expression was decreased seven-fold upon infection in IMMoDCs (Figure 4-6). Although mRNA amount might not reflect the protein level in cells, it still suggested that there could be some interactions between DC-SIGN and MR upon DENV infection.

As introduced in section 1.1.4.1.1, there are other receptors/attach molecules of DENV on host cells, including the highly sulfated form of the glycosaminoglycan heparan sulphate. Considering the fact that heparan sulphate is expressed on nearly all cell types, while molecules like DC-SIGN and MR only exist on APCs, it agrees with the perspective that cell-free virion used a different strategy to invade initiate target cells compared to that used by cell-spread virions to entry subsequent host cells.

To conclude, it was probable that these two receptors interacted with each other during DENV2 infection.

5.2.2 DENV2 uses clathrin-dependent endocytosis for entry into immature DCs

DENV uses clathrin-coated pit-mediated endocytosis to enter permissive cells (Acosta *et al.*, 2008; van der Schaar *et al.*, 2008). Visualising DENV2 particles and a group of endocytic markers at the same time revealed that

DENV2 virions directly associated to clathrin at less than two minutes post-attachment to the cell surface of African green monkey kidney cells (van der Schaar *et al.*, 2008). Additionally, inhibitors of clathrin-dependent endocytosis, such as CPZ, dramatically inhibited DENV viral protein expression and DENV production in mosquito cells (C6/36) and mammalian cells (HeLa) (Acosta *et al.*, 2008; van der Schaar *et al.*, 2008). Mutation of molecules that are essential for clathrin-dependent endocytosis also impaired DENV infection (Acosta *et al.*, 2008; Suksanpaisan *et al.*, 2009). Silencing the genes for clathrin heavy polypeptide (CLTC), which is required in forming clathrin-coated pits, and Dynamin 2 (DNM2), which is needed for releasing the endocytic vesicles from the plasma membrane, can efficiently reduce DENV2 entry to HepG2 cells and human monocytes (Alhoot *et al.*, 2011, 2012).

However, considering the fact that DENV entry mechanism to mammalian cells is cell-type dependent (Acosta *et al*., 2009), the choice of cell models in these studies generated concern around whether the same mechanism was applied to DENV initiate target cells, such as DC and Mϕ. Therefore, the CPZ inhibition assay was conducted in this study in order to answer this question. Finally, DENV2 was proven to enter IMDCs and IMMoDCs via clathrin-dependent endocytosis, because the endocytosis inhibitor CPZ significantly inhibited viral entry in a dose-dependent manner (Figure 4-21).

Endocytosis entry has many advantages for invading viruses. Virions can be transmitted through the barrier of the cytoskeleton and the well-structured cytoplasm. Viruses thus can enter into endosomal structures directly, and be exposed to compartmental environments that differ from the extracellular environment. The mild acidic environment of the endosome is more suitable for viruses to penetrate and un-coat. One disadvantage of endocytosis for viruses is that viruses could be delivered into lysosome. For this reason, viruses will adjust the threshold pH to one that is more suitable for early endosomes (pH 6-6.5) or for late endosomes (pH 5-6) (Smith and Helenius, 2004).

Meanwhile, other strategies are also employed by DENV to enter target cells. The inhibition of clathrin-mediated endocytosis via negative mutants of essential molecules leads to incomplete reduction of DENV1 entry to HepG2 cells. Adding an inhibitor of macropinocytosis can block the remaining DENV1 entry, indicating an alternative pathway for DENV invasion (Suksanpaisan *et al.*, 2009). More interestingly, DENV2, although it was demonstrated to enter into the human lung carcinoma cell A549 via clathrin-dependent endocytosis, was proven to invade Vero cells via dynamin-dependent endocytosis (Acosta *et al.*, 2009). It is suggested that the route of DENV entry is diverse and dependent on the virus serotypes and cell types.

To understand DENV entry mechanisms will not only enable exploration of the knowledge of viral pathogenesis, but will also provide novel strategies and targets for antiviral agent development. The inhibition of DENV entry represents a hurdle, which prevents viral infection at the initiate stages.

5.2.3 The involvement of ITIH2 in DENV2 entry

According to the previous findings by other investigators and the observations in this study, it was believed that there were other molecules involved in DENV2 entry to immature DCs besides DC-SIGN and MR. Hence, a Co-IP assay was designed to explore the extra attachment molecules of DENV2 (Figure 4-23). After mixing the native DENV2 with the transmembrane protein mix of IMDCs or IMMoDCs, the virion-attachment factor complex was pulled down by sepharose beads-linked anti-DENV-E antibodies. It was clearly shown in the silver-stained polyacrylamide gel that extra bands were generated from the experimental group compared to negative controls. Within these extra bands, the strongest bands that appeared around 120 kDa were subsequently identified to be ITIH2 by MS/MS. This was the first time that ITIH2 had been found to interact with virus particles directly. The remaining sections will discuss the background of ITIH2 and the interaction between this molecule and DENV2.

5.2.4 Sources of ITIH2

ITIH2, with molecular weight of 106 kDa and theoretical PI=6.40, belongs to the family of inter-α-trypsin inhibitor proteins (ITI). Proteins of this family are named by their serine protease inhibition abilities (Bost *et al.*, 1998; de Souza *et al.*, 2006). ITI proteins are mainly detected in body fluids, such as serum (de Souza *et al.*, 2006), lymph fluid (Gronborg *et al.*, 2004), and plasma (Schenk *et al.*, 2008). Additionally, ITI proteins or mRNA are expressed by several human tissues, for example lung (Plymoth *et al.*, 2006), liver (Salier *et al.*, 1987), and kidney (Mizushima *et al.*, 1998).

In addition to the α1-microglobulin (α1m)/bikunin precursor gene (*AMBP*), four genes, namely *H1, H2, H3* and *H4,* are involved in the synthesis of ITI proteins. *H1, H2,* and *H3* encode the precursor of polypeptides, while *H4* encodes ITIH4 directly (Heron *et al.*, 1995). It has been shown that the maturation of ITIH2 from its precursor requires the existence of bikunin. The maturation process takes place together with the formation of the protein-glycosaminoglycan-protein (PGP) cross-link between ITIH2 and bikunin (Martin-Vandelet *et al.*, 1999).

ITI heavy chains are believed to be secretory proteins, because there are no predicted transmembrane segments in the sequence (Anderson *et al.*, 2004). Interestingly, in this study, ITIH2 was found in the insoluble fraction during transmembrane protein extraction, instead of staying with other cytoplasmic

proteins in the soluble fraction. One possible reason could be that the transmembrane solubilisation agents used in this process were able to extract not only the integral membrane proteins but also the peripherally-integrated proteins. ITIH2, which could firmly associate with the extracellular matrix (ECM), was integrated into the cytoplasm membrane, exteriorly detected by a flow cytometer on the cell surfaces (Figure 4-24), and subsequently extracted with other transmembrane proteins.

The results of this study showed that gene expression of bikunin, but not that of ITIH2, was detectable in IMDC and IMMoDC. The source of the ITIH2 detected in this study was an issue. The occurrences of ITIH2 on IMDCs and IMMoDCs were weakly detected on the cytoplasmic membranes in this study (Figure 4-24). However, human ITIH2 is high-degree similar to bovine ITIH2 (Chang *et al.*, 2012). Whether the ITIH2 detected in this study came from cultivated human DCs or bovine serum in the culture medium was uncertain. Culturing cells in serum-free medium may help to identify the origin of ITIH2. Nevertheless, in this study, MUTZ-3 cells cannot survive without a high percentage of serum in the medium. Additionally, monocytes had interacted with autologous plasma before being isolated from buffy coat. Therefore, determination of the origin of ITIH2, which is not feasible in this study, deserves further investigation.

5.2.5 Structure of ITIH2

In order to discuss the possible mechanism by which ITIH2 attaches to DENV2 virions, the structure of ITIH2 is briefly introduced in this section.

The major active form of the ITI protein complex consists of two heavy chains (ITIH1 and ITIH2) and the light chain: bikunin. These three polypeptide chains are covalently linked by a glycosaminoglycan chain (Flahaut *et al.*, 1998).

ITIH2, containing 648 aa residues, is similar to ITIH1 in amino acid sequence, with 40% identity (Diarra-Mehrpour *et al.*, 1992). In the N-terminal region of the protein, ITIH2 carries only one complex-type N-glycan attached to Asn64. ITIH2 also contains two strong glycosylation sites, Asn42-Asn-Ser and Asn391-Ile-Ser. In the C-terminal, there are three or four O-linked carbohydrate chains that consist of the type-1 core structure with one or two N-acetylneuraminic acid (NeuAc) moieties on ITIH2 (Figure 5-2) (Flahaut *et al.*, 1998).

The glycosylation pattern of ITIH2 (single N-glycan plus a cluster of O-glycans) is distinguished from that of other heavy chain members (only two N-glycans) (Flahaut *et al.*, 1998). The unique cluster of O-glycans plays a critical role in ITIH2 functions (Figure 5-2). The ITIH2 O-glycan, which carries

the necessary signal for the specific recognition of the partner-proteins (ITIH1, for instance), influences the metabolism of the ITI complex (Flahaut *et al.*, 1998).

There is a von Willebrand factor type A domain (VWFA) (Pfam code: PF00092) in each ITIH2 molecule. The von Willebrand factor (VWF) is known as a large glycoprotein observed in plasma. The type A domain is the prototype for a protein superfamily. Proteins with VWFA domains are involved in diverse biological activities, interacting with numerous ligands (Luo *et al.*, 2012).

5.2.6 Biological activities of ITIH2

As a complex, the major biological function of ITI is protease inhibition. However, it is bikunin that takes responsibility for the protease inhibition ability of ITI complex. Bikunin can inhibit a wide range of important proteases, including trypsin, plasmin, etc. (Zhuo and Kimata, 2008). Although having been taken seen as the precursor for protease inhibitor bikunin for a long time, the most important function of ITI heavy chains was later found to be as serum-derived hyaluronan (HA)-associated proteins (SHAPs) (Huang *et al.*, 1993).

HA is a polysaccharide that exists in the ECM of epithelial tissues and neural tissues; it is crucial for cell migration, differentiation, and proliferation. As a consequence, HA participates in tissue injury, tissue repair, and wound healing (Jiang *et al.*, 2011). The ITIH proteins (SHAPs) are firmly and covalently linked to HA. ASP at the C-terminal of ITI heavy chains is esterified to the C6-hydroxyl group of an internal N-acetylglucosamine of the HA chain (Zhao *et al.*, 1995). During this process, ITI heavy chains are efficiently transferred to HA oligosaccharides with eight or more monosaccharides. This transfer reaction is mediated by an inflammation-associated protein known as TSG-6 (Mukhopadhyay *et al.*, 2004). TSG-6 is released after the transfer of ITI heavy chains towards HA and is then recycled. The whole transport procedure requires Mg^{2+} or Mn^{2+}, and can be negatively controlled by Co^{2+} (Rugg *et al.*, 2005). As observed in this study, the mRNA level of TSG-6 was increased significantly in DENV2-infected IMMoDCs (Figure 4-26), indicating that more TSG-6 activity was required by the infected IMMoDCs. TSG-6 can be induced by TNF-α (Wisniewski and Vilcek, 1997), which is produced by DENV-infected DCs (Dejnirattisai *et al.*, 2008). Therefore, it is possible that DENV infection induced TSG-6 expression in DCs indirectly via TNF-α in order to recruit the participation of the SHAP-HA complex during DENV infection.

Several organs, such as the liver and kidney, are responsible for HA and ITI protein metabolism. Consequently, damage to these organs causes an imbalance between the synthesis and clearance of these molecules, leading

to altered levels of circulating HA and ITI proteins (Jiang *et al.*, 2011). In DENV infection, serum HA level of dengue-infected patients was significantly higher not only than that in healthy controls, but also than that in hepatitis A virus (HAV)-infected patients. This phenomenon might be due to the fact that DENV attacks liver endothelial cells while HAV causes hepatocyte damage via a direct cytopathic effect (Honsawek *et al.*, 2007). Additionally, during severe DENV diseases, such as DSS, the plasma level of the ITI complex was notably decreased (Koraka *et al.*, 2010). This observation may be as a result of the interaction between the ITI complex and complement activation, and the interaction between the ITI complex and HA. Additionally, the decreased ITI level also indicates liver injury during DENV infection, because the liver is the major synthesis and assembly location of ITI proteins (Koraka *et al.*, 2010).

Besides attaching to HA, another important function of the ITI complex is to inhibit complement activation *in-vitro* and *in-vivo*. Both the ITI light chain and ITI heavy chains are required to accomplish this activity. On one hand, VWFA on the ITI heavy chains can bind to integrin-like sites on complement factors C1, C2, and C4. ITI heavy chains interact with the formation of C1 complex and C3-convertase, thus inhibiting the early stage of the classical complement activate pathway. On the other hand, the ITI light chain can inhibit furin, which can cleave complement. Subsequently, the light chain and heavy chains of the ITI protein work together to impair complement activation (Garantziotis *et al.*, 2007; Okroj *et al.*, 2012). This also explains why ITI

heavy chains are involved in the development of diseases during DENV infection.

5.2.7 Possible mechanism for ITIH2 binding to DENV2

Although ITIH2 was pulled down by the DENV2 virion from transmembrane protein mixtures in this study (Figure 4-22), there are no published data to prove that ITIH2 bind to any virus. Furthermore, according to the Database of Protein Domain Interactions (DOMINE) (Yellaboina *et al.*, 2011), there was no association between the VWFA domain and DENV E protein/DENV C protein. Instead, the VWFA domain can interact with C-type lectin domain (Pfam code: PF00059), which is contained by DC-SIGN (Yellaboina *et al.*, 2011).

In the blocking assay of this study, blocking ITIH2 together with blockage of DC-SIGN and MR inhibited DENV2 binding to IMDC and IMMoDC more efficiently than blocking DC-SIGN and MR only (Figure 4-24). It is further indicated that the DENV2 entry mechanism was multistep and required multiple molecules. Moreover, DC-SIGN played a more critical role in associating with ITIH2 on IMMoDCs compared to MR. In contrast, it was interesting to observe that anti-ITIH2 together with anti-DC-SIGN significantly increased DENV2 attachment to IMDCs instead of blocking it. Thus, it is tempting to hypothesise that the antibodies might trigger the interaction between ITIH2 and DC-SIGN, which assisted DENV2 attachment to IMDCs.

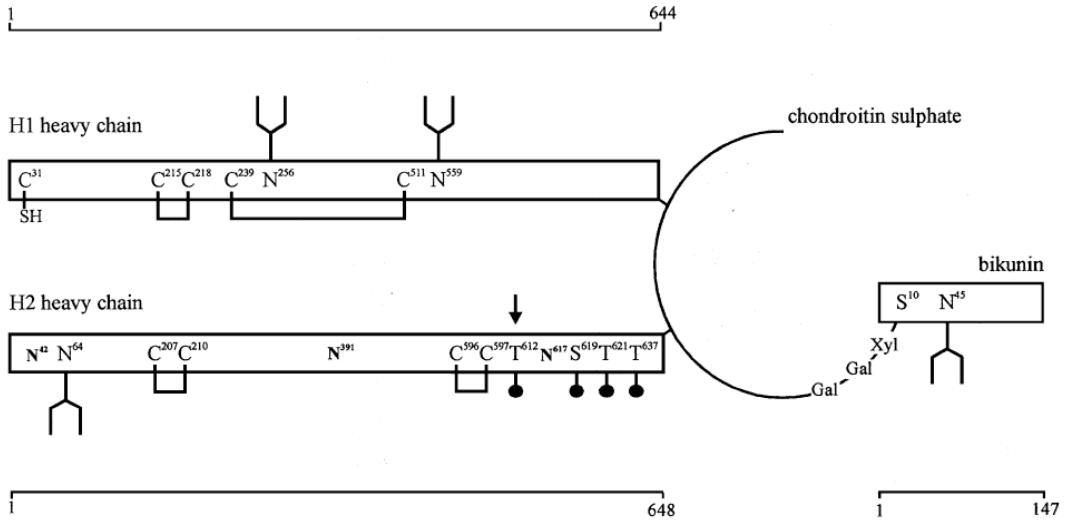

Figure 5-2 Glycosylation structure of human ITI molecule.

This figure was modified from (Flahaut *et al.*, 1998). The human ITI molecule consists of one light chain (147 aa) and two heavy chains (ITIH1, 644 aa; ITIH2, 648 aa) covalently linked by a chondroitin sulphate chain. It is ester bonds between the C-terminal Asp residues of ITIH1 and ITIH2 that linked these two heavy chains to the chondroitin sulphate. The glycosylation pattern of ITIH2 is different from that of ITIH1. ITIH2 has one N-glycan and an O-glycan cluster. (Y): N-glycan carrying either zero, one or two N-acetylneuraminic acid (NeuAc) residue(s) at the non-reducing terminal position. (●): O-linked glycan: NeuAc-Gal-GalNAc. (🡻): the only site partially O-glycosylated. (∏), the SS bridges of heavy chains.

On the other hand, PCR is a very sensitive detection method; a little difference in the initiate template will be amplified exponentially by the chain reaction. As a result, the increased viral replication signal after ITIH2 and DC-SIGN double-blocking could be a false-positive. Therefore, the plaque assay, which is necessary for determining the virus binding efficiency, will be included in the future work.

As demonstrated by the ITIH2 blocking assay and Co-IP assay (Figure 4-22, Figure 4-24), ITIH2 interacted with DENV2 virions during viral attachment, even though the spring of the ITIH2 and the reaction mechanism could not be determined yet.

Additionally, because it was suspected that ITIH2 was involved in DENV2 entry in collaboration with DC-SIGN and MR, the binding affinities of these molecules to DENV2 particles was worth measuring. SPR was used to achieve this goal (Takemoto *et al.*, 1996). It was believed that molecules with lower binding affinity probably serve as attachment factors, while those with higher binding affinity take responsibility for virus entry (Liu *et al.*, 2004b).

According to our investigation, acidic pH condition was more suitable for the binding reaction between MR and DENV2. This observation agreed with the fact that membrane fusion during DENV internalisation and MR-dependent endocytosis were under acidic conditions (Gazi and Martinez-Pomares, 2009;

van der Schaar *et al.*, 2008). This also explained why the Co-IP assay, which was under neutral condition, failed to precipitate MR from the transmembrane protein mixture by DENV2 virions. Unexpectedly, human ITI protein had higher affinity to DENV2 than recombinant human MR did. Furthermore, ITI protein attached to DENV2 virions much stonger under neutral pH condition. It could be supposed that DENV2 virions attach to the heavy chain of ITI protein (with neutral pH) prior to bind to MR (with acidic pH), followed by the MR-dependent endocytosis of DENV2.

The differences of the virus-receptor binding affinities correlate with the viral tropism and disease kinetics (Smelt *et al*., 2001). Therefore, in order to have a deep insight of the interaction between DENV2 and the receptors/attachment molecules, the binding affinities between these molecules and DENV should be examined with different serotypes and strains of DENV.

In the current study, the investigation of the binding affinity between DC-SIGN and DENV2 was hampered by the lack of high quality human recombinant DC-SIGN. This is going to be included in the future work.

Besides, as discussed in section 5.2.6, the biological functions of ITIH2 were usually involved HA. Therefore, it is necessary to include HA and ITIH-HA

complex in the SPR assay, to study their binding affinities and binding conditions when interacting with DENV2 virions.

5.3 Conclusion

In this study, a novel *in-vitro* DC model for studying DENV2 infection was established using MUTZ-3 cell-derived immature DCs. After cytokine stimulation, MUTZ-3 cells generated typical DC-like morphology and a similar phenotype to IMMoDCs. Then, the investigation of DENV2-DC interaction was conducted with two major scopes: the antiviral mechanism and the viral entry mechanism.

As expected, DENV2 was able to attach to, enter into, and replicate in IMDCs as in IMMoDCs. Although alternative morphology of the virions in IMDCs were observed under electron microscope and the replication level of DENV2 in IMDC was lower than that in IMMoDCs, the production of infectious DENV2 virions was demonstrated by a series of experiments, indicating that IMDCs were permissive overall to DENV2 infection. To our knowledge, this study was the first report demonstrating that IMDCs were permissive to DENV2 replication and production.

What was unexpected was that the type I IFN-related antiviral pathway was somehow spontaneously activated in naïve IMDCs, while it was up-regulated

upon DENV2 infection in IMMoDCs. This observation suggested a correlation between the suppression of DENV2 and the spontaneously activated type I IFN-related antiviral pathway in IMDCs. It meant that this IMDC model was suitable for studying the antiviral responses towards DENV2.

DENV2 used clathrin-dependent endocytosis to enter immature DCs. This entry activity involved DC-SIGN and MR, which were not only co-expressed by immature DCs on the cell surface, but also functionally related, as demonstrated in this study. Although both of these receptors were critical for DENV2 entry, double-blocking these two receptors failed to inhibit DENV2 infection one hundred percent. As a result, extra attachment factors were indicated and the Co-IP assay was applied for exploring these additional attachment factors of DENV2. This resulted in the key findings that a novel attachment factor candidate ITIH2 bound to DENV2 and might participate in the viral entry process. Nevertheless, the discovery of this molecule generated several issues and concerns. The origin of ITIH2 had not been decided in this study. Furthermore, the binding mechanism between ITIH2 and DENV2 still remained unclear.

This was the first time that ITIH2 was found to interact with DENV virions. Since ITIH2 was not a transmembrane protein, it might possibly serve as an attachment factor rather than a receptor during DENV2 entry to DCs. Thus, it was hypothesised that DENV2 first attaches to ITIH2 under neutral pH

condition with a high affinity; thereafter, these attachments triggered the involvement of MR, which then accomplished the endocytosis of the viral particles with mild acidic environment.

The key findings of this study indicated that the IMDC model might be less competent for studying DENV replication or for the screening of anti-DENV drugs compared to IMMoDCs. Nonetheless, the IMMoDCs used here were an induced-DC model, as well, representing IL-4-DC (see section 1.4.2.3). IMMoDCs may not absolutely represent *in-vivo* DCs. Thus, although the performances of IMDCs were not consistent with those of IMMoDCs at every studied aspect, it was still a valuable tool that could be further applied to investigate the viral suppression mechanisms and entry mechanisms.

Hopefully, IMDC can also provide some hints to the interaction between leukaemia and DENV infection, as this interaction has just begun to draw attention in clinical studies. However, as discussed, the culture condition might influence the performance of MUTZ-3. Therefore, caution is highly required when using MUTZ-3-derived DCs.

5.4 Future work

5.4.1 Anti-DENV effect of IFIT genes in immature DCs

Genes of the IFIT family, including IFIT1, IFIT2, and IFIT3, were continuously

expressed in naïve IMDCs, in which DENV2 replication was suppressed. Additionally, DENV2 infection triggered the expression of IFIT members in IMMoDCs at both the mRNA and protein level. It was suspected that IFIT genes might contribute to the low replication level of DENV2 in IMDCs. However, as discussed in section 5.1.3, the anti-viral mechanism of IFIT genes involves recognising 2′ O-methylation-lacking mRNA, which is not observed in DENV2. Thus, if IFIT proteins take responsibility for the suppressed DENV replication in IMDCs, an alternative mechanism may be involved.

It has been known that IFIT proteins can interact with host proteins to either inhibit viral translation or induce apoptosis. Whether these anti-viral mechanisms are applicable to DENV infection in immature DCs is worth investigating.

For this purpose, first, over-expression of IFIT proteins in IMMoDCs is needed, as well as the knocking-down of these proteins in IMDCs. DENV2 replication in these IFIT over-expressed or knocked-down immature DCs will be observed. The binding reaction between IFIT complex and DENV2 RNA also needs to be determined. The electrophoretic mobility shift assay (EMSA) can be applied to study the viral RNA-host protein interactions. This technique is based on the principle that the shift speed of RNA-protein complexes is slower than that of free linear RNA fragments in polyacrylamide

or agarose gel electrophoresis (Shcherbakov and Piendl, 2007). If the IFIT complex is proven to bind to DENV2 RNA, the recognition mechanism of IFIT proteins needs to be further studied. On the other hand, if there is no binding reaction between IFIT proteins and DENV2 RNA, IFIT probably utilises other strategies to fulfil its anti-DENV function, for instance interacting with viral proteins or host proteins. Yeast two-hybrid screen of the cDNA libraries from immature DCs and DENV2 is helpful to explore the possible protein-protein interactions. Hopefully, the possible associations between IFIT complex and DENV/DCs proteins may explain why the low permissiveness for DENV2 in IMDCs is ascribed to the activation of IFIT proteins in naïve IMDCs.

5.4.2 DENV2 infection induced autophagy in DCs

Selective autophagy, as mentioned in a previous section, may also be involved in the suppressed DENV replication level in IMDCs. Initially, it is needed to detect the progress of autophagy in infected IMDCs and infected IMMoDCs. Besides LC3 conversion at different time-points, other autophagy indicators such as p62 should be included in the detection. Once the autophagy has been proven to be present in infected IMDCs, the next step is to find out that at which step of DENV life-cycle the autophagy is activated. Adding autophagy inhibitor 3-Methyladenine or autophagy inducer rapamycin at different time points during DENV2 infection may help to elucidate this.

Besides biochemical methods, confocal microscopy is helpful for detecting

the dynamic aspects of autophagy. Moreover, EM technology is still indispensable for analysing the ultrastructure of the autophagosome, which is induced by DENV infection (Eskelinen *et al.*, 2011).

Host lipid droplets were previously proven to play critical roles in DENV assembly and release (Samsa *et al.*, 2009). Furthermore, it was recently discovered that DENV degraded host lipid droplets by inducing autophagy (Heaton and Randall, 2010). Thus, it is very interesting to determine whether host lipid droplets are involved in DENV-induced autophagy in immature DCs.

Additionally, because DENV NS4a was report to induce autophagy and NS4a of West Nile virus (WNV) was found to stimulate unfolded protein response (UPR), which is stimulated by accumulation of unfolded/misfolded proteins in the ER lumen, it is questionable whether UPR indirectly participates in DENV replication control in host cells via autophagy.

5.4.3 The role of ITIH2 during DENV2 entry into DCs

The mechanism of ITIH2 and DENV2 association needs to be investigated in depth. Although the available protein-protein interaction database cannot provide information regarding the ITIH2-DENV interaction, the binding mechanism can be studied via computational modelling using softwares such

as F2dock, which is a rigid-body protein-protein docking software (Bajaj *et al.*, 2011). The *in-silico* approach has been used in investigating the DENV and DC-SIGN interaction, indicating specific binding sites that can be used for the design of anti-DENV agents (Shah *et al*., 2013). Having figured out the reaction sites between ITIH2 and DENV, it is necessary to examine whether mutations of the putative reaction sites on either DENV E protein or ITIH2 can restrain the viral entry. As observed in the current study, the ITIH2 domain had the potential to interact with the domain from DC-SIGN, in addition to double-blocking ITIH2 and DC-SIGN at the same time, which increased viral binding to IMDCs. Consequently, the association between ITIH2 and DC-SIGN during DENV2 entry is believed to be important. The affinities of DC-SIGN and ITI protein binding to DENV virions should be investigated and compared.

HA is known to tightly associate with ITIH2 and relate to DENV diseases development, as a result, knowledge of the activity of HA during DENV infection, especially during viral entry to immature DCs, is valuable. It is believed that the novel-binding molecule found in this study can possibly shed light on the new treatment strategy.

ITIH2 may recruit TSG-6 and HA during its interaction with DENV. Therefore, the other two molecules need further investigation as well. The protein expression level of TSG-6 and HA concentration in IMDCs and IMMoDCs,

both before and after DENV infection, need to be determined. Because ITIH2 is a secreted protein, the concentration-change of ITIH2 in the culture medium of infected IMDCs/IMMoDCs is also necessary to be measured.

5.4.4 Further application of the IMDC model

5.4.4.1 DC-T cell interaction during DENV infection

MDCs have been shown to be capable of priming functional T cells (Chang *et al.*, 2005; Santegoets *et al.*, 2008a; Santegoets *et al.*, 2006). Moreover, as reviewed in sections 1.1.5.3 and 1.4.3.2, after infected DCs present the DENV antigen to T cells, activated T cells are competent to lyse infected cells.

MoDCs have been applied for studying DC-T cell interactions during DENV infection (Dejnirattisai *et al*., 2008; Palmer *et al*., 2005). Compared to DCs that were generated from other leukaemia cell lines, such as THP-1 and K562, MDCs resembled MoDCs better in terms of T cell activation (Larsson *et al.*, 2006; van Helden *et al.*, 2008). Hence, it is essential to evaluate how DENV-infected IMDCs react with co-cultured T cells, for a better understanding of this DC model and the interaction between DENV infection and leukaemia.

References

Ablasser, A., and Hornung, V. (2011). Where, in antiviral defense, does IFIT1 fit? Nat Immunol *12*, 588-590.

Ackerman, A.L., Kyritsis, C., Tampe, R., and Cresswell, P. (2003). Early phagosomes in dendritic cells form a cellular compartment sufficient for cross presentation of exogenous antigens. Proc Natl Acad Sci U S A *100*, 12889-12894.

Acosta, E.G., Castilla, V., and Damonte, E.B. (2008). Functional entry of dengue virus into Aedes albopictus mosquito cells is dependent on clathrinmediated endocytosis. J Gen Virol *89*, 474-484.

Acosta, E.G., Castilla, V., and Damonte, E.B. (2009). Alternative infectious entry pathways for dengue virus serotypes into mammalian cells. Cell Microbiol *11*, 1533-1549.

Akira, S., and Takeda, K. (2004). Toll-like receptor signalling. Nat Rev Immunol *4*, 499-511.

Akita, H., Ito, R., Khalil, I.A., Futaki, S., and Harashima, H. (2004). Quantitative three-dimensional analysis of the intracellular trafficking of plasmid DNA transfected by a nonviral gene delivery system using confocal laser scanning microscopy. Mol Ther *9*, 443-451.

Alen, M.M., De Burghgraeve, T., Kaptein, S.J., Balzarini, J., Neyts, J., and Schols, D. (2011). Broad antiviral activity of carbohydrate-binding agents against the four serotypes of dengue virus in monocyte-derived dendritic cells. PLoS One *6*, e21658.

Alen, M.M., Kaptein, S.J., De Burghgraeve, T., Balzarini, J., Neyts, J., and Schols, D. (2009). Antiviral activity of carbohydrate-binding agents and the role of DC-SIGN in dengue virus infection. Virology *387*, 67-75.

Alhoot, M.A., Wang, S.M., and Sekaran, S.D. (2011). Inhibition of dengue virus entry and multiplication into monocytes using RNA interference. PLoS Negl Trop Dis *5*, e1410.

Alhoot, M.A., Wang, S.M., and Sekaran, S.D. (2012). RNA interference mediated inhibition of dengue virus multiplication and entry in HepG2 cells. PLoS One *7*, e34060.

Alvarez, D.E., Filomatori, C.V., and Gamarnik, A.V. (2008). Functional analysis of dengue virus cyclization sequences located at the 5' and 3'UTRs. Virology *375*, 223-235.

Alvarez, D.E., Lodeiro, M.F., Luduena, S.J., Pietrasanta, L.I., and Gamarnik, A.V. (2005). Long-range RNA-RNA interactions circularize the dengue virus genome. J Virol *79*, 6631-6643.

Anderson, N.L., Polanski, M., Pieper, R., Gatlin, T., Tirumalai, R.S., Conrads, T.P., Veenstra, T.D., Adkins, J.N., Pounds, J.G., Fagan, R.*, et al.* (2004). The human plasma proteome: a nonredundant list developed by combination of four separate sources. Mol Cell Proteomics *3*, 311-326.

Andersson, L.I., Cirkic, E., Hellman, P., and Eriksson, H. (2012). Myeloid blood dendritic cells and monocyte-derived dendritic cells differ in their endocytosing capability. Hum Immunol *73*, 1073-1081.

Anez, G., Men, R., Eckels, K.H., and Lai, C.J. (2009). Passage of dengue virus type 4 vaccine candidates in fetal rhesus lung cells selects heparin-sensitive variants that result in loss of infectivity and immunogenicity in rhesus macaques. J Virol *83*, 10384-10394.

Armstrong, P.M., Andreadis, T.G., Finan, S.L., Shepard, J.J., and Thomas, M.C. (2011). Detection of infectious virus from field-collected mosquitoes by vero cell culture assay. J Vis Exp.

Ashley, R.L., Henkes, L.E., Bouma, G.J., Pru, J.K., and Hansen, T.R. (2010). Deletion of the Isg15 gene results in up-regulation of decidual cell survival genes and down-regulation of adhesion genes: implication for regulation by IL-1beta. Endocrinology *151*, 4527-4536.

Avirutnan, P., Malasit, P., Seliger, B., Bhakdi, S., and Husmann, M. (1998). Dengue virus infection of human endothelial cells leads to chemokine production, complement activation, and apoptosis. J Immunol *161*, 6338-6346.

Avirutnan, P., Punyadee, N., Noisakran, S., Komoltri, C., Thiemmeca, S., Auethavornanan, K., Jairungsri, A., Kanlaya, R., Tangthawornchaikul, N., Puttikhunt, C.*, et al.* (2006). Vascular leakage in severe dengue virus infections: a potential role for the nonstructural viral protein NS1 and complement. J Infect Dis *193*, 1078-1088.

Avirutnan, P., Zhang, L., Punyadee, N., Manuyakorn, A., Puttikhunt, C., Kasinrerk, W., Malasit, P., Atkinson, J.P., and Diamond, M.S. (2007). Secreted NS1 of dengue virus attaches to the surface of cells via interactions with heparan sulfate and chondroitin sulfate E. PLoS Pathog *3*, e183.

Bajaj, C., Chowdhury, R., and Siddavanahalli, V. (2011). F2Dock: fast Fourier protein-protein docking. IEEE/ACM Trans Comput Biol Bioinform *8*, 45-58.

Banchereau, J., and Steinman, R.M. (1998). Dendritic cells and the control of immunity. Nature *392*, 245-252.

Barnes, E., Salio, M., Cerundolo, V., Francesco, L., Pardoll, D., Klenerman, P., and Cox, A. (2008). Monocyte derived dendritic cells retain their

functional capacity in patients following infection with hepatitis C virus. J Viral Hepat *15*, 219-228.

Barr, K.L., Anderson, B.D., Heil, G.L., Friary, J.A., Gray, G.C., and Focks, D.A. (2012). Dengue serotypes 1–4 exhibit unique host specificity in vitro. Virus Adaptation and Treatment *2012:4* , 9.

Beignon, A.S., McKenna, K., Skoberne, M., Manches, O., DaSilva, I., Kavanagh, D.G., Larsson, M., Gorelick, R.J., Lifson, J.D., and Bhardwaj, N. (2005). Endocytosis of HIV-1 activates plasmacytoid dendritic cells via Toll-like receptor-viral RNA interactions. J Clin Invest *115*, 3265-3275.

Belz, G., Mount, A., and Masson, F. (2009). Dendritic cells in viral infections. Handb Exp Pharmacol, 51-77.

Bente, D.A., and Rico-Hesse, R. (2006). Models of dengue virus infection. Drug Discov Today Dis Models *3*, 97-103.

Bessoff, K., Delorey, M., Sun, W., and Hunsperger, E. (2008). Comparison of two commercially available dengue virus (DENV) NS1 capture enzyme-linked immunosorbent assays using a single clinical sample for diagnosis of acute DENV infection. Clin Vaccine Immunol *15*, 1513-1518.

Bielefeldt-Ohmann, H. (1998). Analysis of antibody-independent binding of dengue viruses and dengue virus envelope protein to human myelomonocytic cells and B lymphocytes. Virus Res *57*, 63-79.

Billingsley, P.F., Foy, B., and Rasgon, J.L. (2008). Mosquitocidal vaccines: a neglected addition to malaria and dengue control strategies. Trends Parasitol *24*, 396-400.

Blackley, S., Kou, Z., Chen, H., Quinn, M., Rose, R.C., Schlesinger, J.J., Coppage, M., and Jin, X. (2007). Primary human splenic macrophages, but not T or B cells, are the principal target cells for dengue virus infection in vitro. J Virol *81*, 13325-13334.

Boonnak, K., Dambach, K.M., Donofrio, G.C., Tassaneetrithep, B., and Marovich, M.A. (2011). Cell type specificity and host genetic polymorphisms influence antibody-dependent enhancement of dengue virus infection. J Virol *85*, 1671-1683.

Boonnak, K., Slike, B.M., Burgess, T.H., Mason, R.M., Wu, S.J., Sun, P., Porter, K., Rudiman, I.F., Yuwono, D., Puthavathana, P.*, et al.* (2008). Role of dendritic cells in antibody-dependent enhancement of dengue virus infection. J Virol *82*, 3939-3951.

Bosch, I., Xhaja, K., Estevez, L., Raines, G., Melichar, H., Warke, R.V., Fournier, M.V., Ennis, F.A., and Rothman, A.L. (2002). Increased production of interleukin-8 in primary human monocytes and in human epithelial and endothelial cell lines after dengue virus challenge. J Virol *76*, 5588-5597.

Boskovic, J., Arnold, J.N., Stilion, R., Gordon, S., Sim, R.B., Rivera-Calzada, A., Wienke, D., Isacke, C.M., Martinez-Pomares, L., and Llorca, O. (2006). Structural model for the mannose receptor family uncovered by electron microscopy of Endo180 and the mannose receptor. J Biol Chem *281*, 8780-8787.

Bost, F., Diarra-Mehrpour, M., and Martin, J.P. (1998). Inter-alpha-trypsin inhibitor proteoglycan family - A group of proteins binding and stabilizing the extracellular matrix. Eur J Biochem *252*, 339-346.

Branch, S.L., and Levett, P.N. (1999). Evaluation of four methods for detection of immunoglobulin M antibodies to dengue virus. Clin Diagn Lab Immunol *6*, 555-557.

Brass, A.L., Huang, I.C., Benita, Y., John, S.P., Krishnan, M.N., Feeley, E.M., Ryan, B.J., Weyer, J.L., van der Weyden, L., Fikrig, E.*, et al.* (2009). The IFITM proteins mediate cellular resistance to influenza A H1N1 virus, West Nile virus, and dengue virus. Cell *139*, 1243-1254.

Bryant, J.E., Calvert, A.E., Mesesan, K., Crabtree, M.B., Volpe, K.E., Silengo, S., Kinney, R.M., Huang, C.Y.H., Miller, B.R., and Roehrig, J.T. (2007). Glycosylation of the dengue 2 virus E protein at N67 is critical for virus growth in vitro but not for growth in intrathoracically inoculated Aedes aegypti mosquitoes. Virology *366*, 415-423.

Bundo, K., and Igarashi, A. (1985). Antibody-capture ELISA for detection of immunoglobulin M antibodies in sera from Japanese encephalitis and dengue hemorrhagic fever patients. J Virol Methods *11*, 15-22.

Cabrera-Hernandez, A., and Smith, D.R. (2005). Mammalian Dengue Virus Receptors. Dengue Bulletin *29*, 17.

Calmon, M.F., Rodrigues, R.V., Kaneto, C.M., Moura, R.P., Silva, S.D., Mota, L.D., Pinheiro, D.G., Torres, C., de Carvalho, A.F., Cury, P.M.*, et al.* (2009). Epigenetic silencing of CRABP2 and MX1 in head and neck tumors. Neoplasia *11*, 1329-1339.

Cam, B.V., Fonsmark, L., Hue, N.B., Phuong, N.T., Poulsen, A., and Heegaard, E.D. (2001). Prospective case-control study of encephalopathy in children with dengue hemorrhagic fever. Am J Trop Med Hyg *65*, 848-851.

Cardier, J.E., Marino, E., Romano, E., Taylor, P., Liprandi, F., Bosch, N., and Rothman, A.L. (2005). Proinflammatory factors present in sera from patients with acute dengue infection induce activation and apoptosis of human microvascular endothelial cells: possible role of TNF-alpha in endothelial cell damage in dengue. Cytokine *30*, 359-365.

Cardier, J.E., Rivas, B., Romano, E., Rothman, A.L., Perez-Perez, C., Ochoa, M., Caceres, A.M., Cardier, M., Guevara, N., and Giovannetti, R. (2006). Evidence of vascular damage in dengue disease: demonstration of high levels of soluble cell adhesion molecules and circulating endothelial cells. Endothelium *13*, 335-340.

Catteau, A., Roue, G., Yuste, V.J., Susin, S.A., and Despres, P. (2003). Expression of dengue ApoptoM sequence results in disruption of mitochondrial potential and caspase activation. Biochimie *85*, 789-793.

Chan, C.Y., and Tambyah, P.A. (2012). Preflucel(R): a Vero-cell culture-derived trivalent influenza vaccine. Expert Rev Vaccines *11*, 759-773.

Chan, K.R., Zhang, S.L., Tan, H.C., Chan, Y.K., Chow, A., Lim, A.P., Vasudevan, S.G., Hanson, B.J., and Ooi, E.E. (2011). Ligation of Fc gamma receptor IIB inhibits antibody-dependent enhancement of dengue virus infection. Proc Natl Acad Sci U S A *108*, 12479-12484.

Chan, Y.K., Huang, I.C., and Farzan, M. (2012). IFITM Proteins Restrict Antibody-Dependent Enhancement of Dengue Virus Infection. PLoS One *7*, e34508.

Chang, C.C., Satwani, P., Oberfield, N., Vlad, G., Simpson, L.L., and Cairo, M.S. (2005). Increased induction of allogeneic-specific cord blood CD4+CD25+ regulatory T (Treg) cells: a comparative study of naive and antigenic-specific cord blood Treg cells. Exp Hematol *33*, 1508-1520.

Chang, M.Y., Chan, C.K., Braun, K.R., Green, P.S., O'Brien, K.D., Chait, A., Day, A.J., and Wight, T.N. (2012). Monocyte-to-macrophage differentiation: synthesis and secretion of a complex extracellular matrix. J Biol Chem *287*, 14122-14135.

Chao, D.L., Halstead, S.B., Halloran, M.E., and Longini, I.M., Jr. (2012). Controlling dengue with vaccines in Thailand. PLoS Negl Trop Dis *6*, e1876.

Chareonsirisuthigul, T., Kalayanarooj, S., and Ubol, S. (2007). Dengue virus (DENV) antibody-dependent enhancement of infection upregulates the production of anti-inflammatory cytokines, but suppresses anti-DENV free radical and pro-inflammatory cytokine production, in THP-1 cells. The Journal of general virology *88*, 365-375.

Chaturvedi, U.C. (2009). Shift to Th2 cytokine response in dengue haemorrhagic fever. Indian J Med Res *129*, 1-3.

Chavez-Salinas, S., Ceballos-Olvera, I., Reyes-Del Valle, J., Medina, F., and Del Angel, R.M. (2008). Heat shock effect upon dengue virus replication into U937 cells. Virus research *138*, 111-118.

Chen, W.J., Chen, T.H., Tang, P., Yang, C.F., Kao, L.H., Lo, Y.P., Chuang, C.K., and Shih, Y.T. (2011). Antioxidant defense is one of the mechanisms by which mosquito cells survive dengue 2 viral infection. Virology *410*, 410-417.

Cheriyath, V., Leaman, D.W., and Borden, E.C. (2011). Emerging roles of FAM14 family members (G1P3/ISG 6-16 and ISG12/IFI27) in innate immunity and cancer. J Interferon Cytokine Res *31*, 173-181.

Chiu, W.W., Kinney, R.M., and Dreher, T.W. (2005). Control of translation by the 5'- and 3'-terminal regions of the dengue virus genome. J Virol *79*, 8303-8315.

Chorro, L., Sarde, A., Li, M., Woollard, K.J., Chambon, P., Malissen, B., Kissenpfennig, A., Barbaroux, J.B., Groves, R., and Geissmann, F. (2009). Langerhans cell (LC) proliferation mediates neonatal development, homeostasis, and inflammation-associated expansion of the epidermal LC network. J Exp Med *206*, 3089-3100.

Clark, K.B., Hsiao, H.M., Noisakran, S., Tsai, J.J., and Perng, G.C. (2012). Role of microparticles in dengue virus infection and its impact on medical intervention strategies. Yale J Biol Med *85*, 3-18.

Clyde, K., Kyle, J.L., and Harris, E. (2006). Recent advances in deciphering viral and host determinants of dengue virus replication and pathogenesis. J Virol *80*, 11418-11431.

Collin, M., Bigley, V., Haniffa, M., and Hambleton, S. (2011). Human dendritic cell deficiency: the missing ID? Nat Rev Immunol *11*, 575-583.

Colmone, A., Li, S., and Wang, C.R. (2006). Activating transcription factor/cAMP response element binding protein family member regulated transcription of CD1A. J Immunol *177*, 7024-7032.

D'Amico, A., and Wu, L. (2003). The early progenitors of mouse dendritic cells and plasmacytoid predendritic cells are within the bone marrow hemopoietic precursors expressing Flt3. J Exp Med *198*, 293-303.

Daffis, S., Szretter, K.J., Schriewer, J., Li, J., Youn, S., Errett, J., Lin, T.Y., Schneller, S., Zust, R., Dong, H.*, et al.* (2010). 2'-O methylation of the viral mRNA cap evades host restriction by IFIT family members. Nature *468*, 452-456.

Dai, J., Pan, W., and Wang, P. (2011). ISG15 facilitates cellular antiviral response to dengue and west nile virus infection in vitro. Virol J *8*, 468.

De Carvalho Bittencourt, M., Martial, J., Cabie, A., Thomas, L., and Cesaire, R. (2012). Decreased peripheral dendritic cell numbers in dengue virus infection. J Clin Immunol *32*, 161-172.

de Jong, M.A., de Witte, L., Santegoets, S.J., Fluitsma, D., Taylor, M.E., de Gruijl, T.D., and Geijtenbeek, T.B. (2010). Mutz-3-derived Langerhans cells are a model to study HIV-1 transmission and potential inhibitors. J Leukoc Biol *87*, 637-643.

de Macedo, F.C., Nicol, A.F., Cooper, L.D., Yearsley, M., Pires, A.R., and Nuovo, G.J. (2006). Histologic, viral, and molecular correlates of dengue fever infection of the liver using highly sensitive immunohistochemistry. Diagn Mol Pathol *15*, 223-228.

de Miranda, A.S., Rodrigues, D.H., Amaral, D.C., de Lima Campos, R.D., Cisalpino, D., Vilela, M.C., Lacerda-Queiroz, N., de Souza, K.P., Vago, J.P., Campos, M.A.*, et al.* (2012). Dengue-3 encephalitis promotes anxiety-like behavior in mice. Behav Brain Res *230*, 237-242.

de Souza, G.A., Godoy, L.M., and Mann, M. (2006). Identification of 491 proteins in the tear fluid proteome reveals a large number of proteases and protease inhibitors. Genome Biol *7*, R72.

De Weer, A., Poppe, B., Vergult, S., Van Vlierberghe, P., Petrick, M., De Bock, R., Benoit, Y., Noens, L., De Paepe, A., Van Roy, N.*, et al.* (2010). Identification of two critically deleted regions within chromosome segment 7q35-q36 in EVI1 deregulated myeloid leukemia cell lines. PLoS One *5*, e8676.

Dejnirattisai, W., Duangchinda, T., Lin, C.L., Vasanawathana, S., Jones, M., Jacobs, M., Malasit, P., Xu, X.N., Screaton, G., and Mongkolsapaya, J. (2008). A complex interplay among virus, dendritic cells, T cells, and cytokines in dengue virus infections. J Immunol *181*, 5865-5874.

Della Chiesa, M., Sivori, S., Castriconi, R., Marcenaro, E., and Moretta, A. (2005). Pathogen-induced private conversations between natural killer and dendritic cells. Trends Microbiol *13*, 128-136.

den Dunnen, J., Gringhuis, S.I., and Geijtenbeek, T.B.H. (2009). Innate signaling by the C-type lectin DC-SIGN dictates immune responses. Cancer Immunol Immunother *58*, 1149-1157.

Deng, J., Li, N., Liu, H., Zuo, Z., Liew, O.W., Xu, W., Chen, G., Tong, X., Tang, W., Zhu, J.*, et al.* (2012). Discovery of novel small molecule inhibitors of dengue viral NS2B-NS3 protease using virtual screening and scaffold hopping. J Med Chem *55*, 6278-6293.

Despres, P., Flamand, M., Ceccaldi, P.E., and Deubel, V. (1996). Human isolates of dengue type 1 virus induce apoptosis in mouse neuroblastoma cells. J Virol *70*, 4090-4096.

Despres, P., Frenkiel, M.P., Ceccaldi, P.E., Duarte Dos Santos, C., and Deubel, V. (1998). Apoptosis in the mouse central nervous system in response to infection with mouse-neurovirulent dengue viruses. J Virol *72*, 823-829.

Dewi, B.E., Takasaki, T., and Kurane, I. (2008). Peripheral blood mononuclear cells increase the permeability of dengue virus-infected endothelial cells in association with downregulation of vascular endothelial cadherin. The Journal of general virology *89*, 642-652.

Diamond, M.S., Edgil, D., Roberts, T.G., Lu, B., and Harris, E. (2000). Infection of human cells by dengue virus is modulated by different cell types and viral strains. J Virol *74*, 7814-7823.

Diarra-Mehrpour, M., Bourguignon, J., Bost, F., Sesboue, R., Muschio, F., Sarafan, N., and Martin, J.P. (1992). Human inter-alpha-trypsin inhibitor: full-length cDNA sequence of the heavy chain H1. Biochim Biophys Acta *1132*, 114-118.

Dong, H., Chang, D.C., Hua, M.H., Lim, S.P., Chionh, Y.H., Hia, F., Lee, Y.H., Kukkaro, P., Lok, S.M., Dedon, P.C.*, et al.* (2012). 2'-O methylation of internal adenosine by flavivirus NS5 methyltransferase. PLoS Pathog *8*, e1002642.

Dong, H., Ray, D., Ren, S., Zhang, B., Puig-Basagoiti, F., Takagi, Y., Ho, C.K., Li, H., and Shi, P.Y. (2007). Distinct RNA elements confer specificity to flavivirus RNA cap methylation events. J Virol *81*, 4412-4421.

Du, Z., Fan, M., Kim, J.G., Eckerle, D., Lothstein, L., Wei, L., and Pfeffer, L.M. (2009). Interferon-resistant Daudi cell line with a Stat2 defect is resistant to apoptosis induced by chemotherapeutic agents. J Biol Chem *284*, 27808-27815.

Dubsky, P., Saito, H., Leogier, M., Dantin, C., Connolly, J.E., Banchereau, J., and Palucka, A.K. (2007). IL-15-induced human DC efficiently prime melanoma-specific naive CD8+ T cells to differentiate into CTL. Eur J Immunol *37*, 1678-1690.

Durbin, A.P., Vargas, M.J., Wanionek, K., Hammond, S.N., Gordon, A., Rocha, C., Balmaseda, A., and Harris, E. (2008). Phenotyping of peripheral blood mononuclear cells during acute dengue illness demonstrates infection and increased activation of monocytes in severe cases compared to classic dengue fever. Virology *376*, 429-435.

East, L., and Isacke, C.M. (2002). The mannose receptor family. Biochim Biophys Acta *1572*, 364-386.

Edgil, D., Polacek, C., and Harris, E. (2006). Dengue virus utilizes a novel strategy for translation initiation when cap-dependent translation is inhibited. J Virol *80*, 2976-2986.

Einav, U., Tabach, Y., Getz, G., Yitzhaky, A., Ozbek, U., Amariglio, N., Izraeli, S., Rechavi, G., and Domany, E. (2005). Gene expression analysis reveals a strong signature of an interferon-induced pathway in childhood lymphoblastic leukemia as well as in breast and ovarian cancer. Oncogene *24*, 6367-6375.

Engering, A., Geijtenbeek, T.B., van Vliet, S.J., Wijers, M., van Liempt, E., Demaurex, N., Lanzavecchia, A., Fransen, J., Figdor, C.G., Piguet, V.*, et al.* (2002). The dendritic cell-specific adhesion receptor DC-SIGN internalizes antigen for presentation to T cells. J Immunol *168*, 2118-2126.

Erbel, P., Schiering, N., D'Arcy, A., Renatus, M., Kroemer, M., Lim, S.P., Yin, Z., Keller, T.H., Vasudevan, S.G., and Hommel, U. (2006). Structural basis for the activation of flaviviral NS3 proteases from dengue and West Nile virus. Nat Struct Mol Biol *13*, 372-373.

Eskelinen, E.L., Reggiori, F., Baba, M., Kovacs, A.L., and Seglen, P.O. (2011). Seeing is believing: the impact of electron microscopy on autophagy research. Autophagy *7*, 935-956.

Fabre, A., Couvelard, A., Degott, C., Lagorce-Pages, C., Bruneel, F., Bouvet, E., and Vachon, F. (2001). Dengue virus induced hepatitis with chronic calcific changes. Gut *49*, 864-865.

Fearnley, D.B., Whyte, L.F., Carnoutsos, S.A., Cook, A.H., and Hart, D.N. (1999). Monitoring human blood dendritic cell numbers in normal individuals and in stem cell transplantation. Blood *93*, 728-736.

Fensterl, V., and Sen, G.C. (2011). The ISG56/IFIT1 Gene Family. J Interferon Cytokine Res *31*, 71-78.

Fink, J., Gu, F., Ling, L., Tolfvenstam, T., Olfat, F., Chin, K.C., Aw, P., George, J., Kuznetsov, V.A., Schreiber, M.*, et al.* (2007). Host gene expression profiling of dengue virus infection in cell lines and patients. PLoS Negl Trop Dis *1*, e86.

Flahaut, C., Capon, C., Balduyck, M., Ricart, G., Sautiere, P., and Mizon, J. (1998). Glycosylation pattern of human inter-alpha-inhibitor heavy chains. Biochem J *333 (Pt 3)*, 749-756.

Gagnon, S.J., Ennis, F.A., and Rothman, A.L. (1999). Bystander target cell lysis and cytokine production by dengue virus-specific human CD4(+) cytotoxic T-lymphocyte clones. J Virol *73*, 3623-3629.

Gagnon, S.J., Zeng, W., Kurane, I., and Ennis, F.A. (1996). Identification of two epitopes on the dengue 4 virus capsid protein recognized by a serotype-specific and a panel of serotype-cross-reactive human CD4+ cytotoxic T-lymphocyte clones. J Virol *70*, 141-147.

Gangodkar, S., Jain, P., Dixit, N., Ghosh, K., and Basu, A. (2010). Dengue virus-induced autophagosomes and changes in endomembrane ultrastructure imaged by electron tomography and whole-mount grid-cell culture techniques. J Electron Microsc (Tokyo) *59*, 503-511.

Gantner, B.N., Simmons, R.M., Canavera, S.J., Akira, S., and Underhill, D.M. (2003). Collaborative induction of inflammatory responses by dectin-1 and Toll-like receptor 2. J Exp Med *197*, 1107-1117.

Garantziotis, S., Hollingsworth, J.W., Ghanayem, R.B., Timberlake, S., Zhuo, L., Kimata, K., and Schwartz, D.A. (2007). Inter-alpha-trypsin inhibitor attenuates complement activation and complement-induced lung injury. J Immunol *179*, 4187-4192.

Gazi, U., and Martinez-Pomares, L. (2009). Influence of the mannose receptor in host immune responses. Immunobiology *214*, 554-561.

Geijtenbeek, T.B.H., and Gringhuis, S.I. (2009). Signalling through C-type lectin receptors: shaping immune responses. Nat Rev Immunol *9*, 465-479.

Geissmann, F., Manz, M.G., Jung, S., Sieweke, M.H., Merad, M., and Ley, K. (2010). Development of monocytes, macrophages, and dendritic cells. Science *327*, 656-661.

Gjermandsen, I.M., Justesen, J., and Martensen, P.M. (2000). The interferon-induced gene ISG12 is regulated by various cytokines as the gene 6-16 in human cell lines. Cytokine *12*, 233-238.

Goncalvez, A.P., Engle, R.E., St Claire, M., Purcell, R.H., and Lai, C.J. (2007). Monoclonal antibody-mediated enhancement of dengue virus infection in vitro and in vivo and strategies for prevention. Proc Natl Acad Sci U S A *104*, 9422-9427.

Gouvea, I.E., Izidoro, M.A., Judice, W.A., Cezari, M.H., Caliendo, G., Santagada, V., dos Santos, C.N., Queiroz, M.H., Juliano, M.A., Young, P.R.*, et al.* (2007). Substrate specificity of recombinant dengue 2 virus NS2B-NS3 protease: influence of natural and unnatural basic amino acids on hydrolysis of synthetic fluorescent substrates. Arch Biochem Biophys *457*, 187-196.

Govorkova, E.A., Murti, G., Meignier, B., de Taisne, C., and Webster, R.G. (1996). African green monkey kidney (Vero) cells provide an alternative host cell system for influenza A and B viruses. J Virol *70*, 5519-5524.

Graziadei, L., Riabowol, K., and Bar-Sagi, D. (1990). Co-capping of ras proteins with surface immunoglobulins in B lymphocytes. Nature *347*, 396-400.

Gronborg, M., Bunkenborg, J., Kristiansen, T.Z., Jensen, O.N., Yeo, C.J., Hruban, R.H., Maitra, A., Goggins, M.G., and Pandey, A. (2004). Comprehensive proteomic analysis of human pancreatic juice. J Proteome Res *3*, 1042-1055.

Gry, M., Rimini, R., Stromberg, S., Asplund, A., Ponten, F., Uhlen, M., and Nilsson, P. (2009). Correlations between RNA and protein expression profiles in 23 human cell lines. BMC Genomics *10*, 365.

Gubler, D.J. (1998). Dengue and dengue hemorrhagic fever. Clin Microbiol Rev *11*, 480-496.

Gubler, D.J. (2006). Dengue/dengue haemorrhagic fever: history and current status. Novartis Found Symp *277*, 3-16; discussion 16-22, 71-13, 251-253.

Guermonprez, P., Saveanu, L., Kleijmeer, M., Davoust, J., Van Endert, P., and Amigorena, S. (2003). ER-phagosome fusion defines an MHC class I cross-presentation compartment in dendritic cells. Nature *425*, 397-402.

Gunther, V.J., Putnak, R., Eckels, K.H., Mammen, M.P., Scherer, J.M., Lyons, A., Sztein, M.B., and Sun, W. (2011). A human challenge model for dengue infection reveals a possible protective role for sustained interferon gamma levels during the acute phase of illness. Vaccine *29*, 3895-3904.

Guo, J., Peters, K.L., and Sen, G.C. (2000). Induction of the human protein P56 by interferon, double-stranded RNA, or virus infection. Virology *267*, 209-219.

Gupta, A., Srinivasan, R., Setia, S., Soundravally, R., and Pandian, D.G. (2009). Uveitis following dengue fever. Eye *23*, 873-876.

Guy, B., Chanthavanich, P., Gimenez, S., Sirivichayakul, C., Sabchareon, A., Begue, S., Yoksan, S., Luxemburger, C., and Lang, J. (2004). Evaluation by flow cytometry of antibody-dependent enhancement (ADE) of dengue infection by sera from Thai children immunized with a live-attenuated tetravalent dengue vaccine. Vaccine *22*, 3563-3574.

Guzman, M.G., Halstead, S.B., Artsob, H., Buchy, P., Farrar, J., Gubler, D.J., Hunsperger, E., Kroeger, A., Margolis, H.S., Martinez, E.*, et al.* (2010). Dengue: a continuing global threat. Nat Rev Microbiol *8*, S7-16.

Halstead, S.B. (1970). Observations related to pathogensis of dengue hemorrhagic fever. VI. Hypotheses and discussion. Yale J Biol Med *42*, 350-362.

Halstead, S.B. (2007). Dengue. Lancet *370*, 1644-1652.

Halstead, S.B. (2008). Dengue (London Hackensack, NJ, Imperial College Press).

Halstead, S.B., and Marchette, N.J. (2003). Biologic properties of dengue viruses following serial passage in primary dog kidney cells: studies at the University of Hawaii. Am J Trop Med Hyg *69*, 5-11.

Harris, E., Roberts, T.G., Smith, L., Selle, J., Kramer, L.D., Valle, S., Sandoval, E., and Balmaseda, A. (1998). Typing of dengue viruses in clinical specimens and mosquitoes by single-tube multiplex reverse transcriptase PCR. J Clin Microbiol *36*, 2634-2639.

Heaton, N.S., and Randall, G. (2010). Dengue virus-induced autophagy regulates lipid metabolism. Cell Host Microbe *8*, 422-432.

Heintze, C., Velasco Garrido, M., and Kroeger, A. (2007). What do community-based dengue control programmes achieve? A systematic review of published evaluations. Trans R Soc Trop Med Hyg *101*, 317-325.

Heinz, F.X., and Allison, S.L. (2003). Flavivirus structure and membrane fusion. Adv Virus Res *59*, 63-97.

Henchal, E.A., and Putnak, J.R. (1990). The dengue viruses. Clin Microbiol Rev *3*, 376-396.

Heron, A., Bourguignon, J., Diarra-Mehrpour, M., Dautreaux, B., Martin, J.P., and Sesboue, R. (1995). Involvement of the three inter-alpha-trypsin inhibitor (ITI) heavy chains in each member of the serum ITI family. FEBS Lett *374*, 195-198.

Hilgard, P., and Stockert, R. (2000). Heparan sulfate proteoglycans initiate dengue virus infection of hepatocytes. Hepatology *32*, 1069-1077.

Hjelm, F., Carlsson, F., Getahun, A., and Heyman, B. (2006). Antibody-mediated regulation of the immune response. Scand J Immunol *64*, 177-184.

Ho, L.J., Hung, L.F., Weng, C.Y., Wu, W.L., Chou, P., Lin, Y.L., Chang, D.M., Tai, T.Y., and Lai, J.H. (2005). Dengue virus type 2 antagonizes IFN-alpha but not IFN-gamma antiviral effect via down-regulating Tyk2-STAT signaling in the human dendritic cell. J Immunol *174*, 8163-8172.

Ho, L.J., Wang, J.J., Shaio, M.F., Kao, C.L., Chang, D.M., Han, S.W., and Lai, J.H. (2001). Infection of human dendritic cells by dengue virus causes cell maturation and cytokine production. J Immunol *166*, 1499-1506.

Hoefnagel, M.H., Vermeulen, J.P., Scheper, R.J., and Vandebriel, R.J. (2011). Response of MUTZ-3 dendritic cells to the different components of the Haemophilus influenzae type B conjugate vaccine: towards an in vitro assay for vaccine immunogenicity. Vaccine *29*, 5114-5121.

Honsawek, S., Kongtawelert, P., Pothacharoen, P., Khongphatthanayothin, A., Chongsrisawat, V., and Poovorawan, Y. (2007). Increased levels of serum hyaluronan in patients with dengue infection. J Infect *54*, 225-229.

Hu, Z.B., Ma, W., Zaborski, M., MacLeod, R., Quentmeier, H., and Drexler, H.G. (1996). Establishment and characterization of two novel cytokine-responsive acute myeloid and monocytic leukemia cell lines, MUTZ-2 and MUTZ-3. Leukemia *10*, 1025-1040.

Huang, K.J., Li, S.Y., Chen, S.C., Liu, H.S., Lin, Y.S., Yeh, T.M., Liu, C.C., and Lei, H.Y. (2000a). Manifestation of thrombocytopenia in dengue-2-virus-infected mice. J Gen Virol *81*, 2177-2182.

Huang, L., Yoneda, M., and Kimata, K. (1993). A serum-derived hyaluronan-associated protein (SHAP) is the heavy chain of the inter alpha-trypsin inhibitor. J Biol Chem *268*, 26725-26730.

Huang, Y.H., Lei, H.Y., Liu, H.S., Lin, Y.S., Liu, C.C., and Yeh, T.M. (2000b). Dengue virus infects human endothelial cells and induces IL-6 and IL-8 production. Am J Trop Med Hyg *63*, 71-75.

Huch, J.H., Cunningham, A.L., Arvin, A.M., Nasr, N., Santegoets, S.J., Slobedman, E., Slobedman, B., and Abendroth, A. (2010). Impact of varicella-zoster virus on dendritic cell subsets in human skin during natural infection. J virol *84*, 4060-4072.

Huerta, V., Chinea, G., Fleitas, N., Sarria, M., Sanchez, J., Toledo, P., and Padron, G. (2008). Characterization of the interaction of domain III of the envelope protein of dengue virus with putative receptors from CHO cells. Virus Res *137*, 225-234.

Hui, D.J., Terenzi, F., Merrick, W.C., and Sen, G.C. (2005). Mouse p56 blocks a distinct function of eukaryotic initiation factor 3 in translation initiation. J Biol Chem *280*, 3433-3440.

Hui, E.K., and Nayak, D.P. (2002). Role of G protein and protein kinase signalling in influenza virus budding in MDCK cells. J Gen Virol *83*, 3055-3066.

Imrie, A., Meeks, J., Gurary, A., Sukhbataar, M., Kitsutani, P., Effler, P., and Zhao, Z. (2007). Differential functional avidity of dengue virus-specific T-cell clones for variant peptides representing heterologous and previously encountered serotypes. J Virol *81*, 10081-10091.

Ito, T., Liu, Y.J., and Kadowaki, N. (2005). Functional diversity and plasticity of human dendritic cell subsets. Int J Hematol *81*, 188-196.

Jacobs, M.G., Robinson, P.J., Bletchly, C., Mackenzie, J.M., and Young, P.R. (2000). Dengue virus nonstructural protein 1 is expressed in a glycosyl-phosphatidylinositol-linked form that is capable of signal transduction. FASEB J *14*, 1603-1610.

Jaiswal, S., Pearson, T., Friberg, H., Shultz, L.D., Greiner, D.L., Rothman, A.L., and Mathew, A. (2009). Dengue virus infection and virus-specific HLA-A2 restricted immune responses in humanized NOD-scid IL2rgammanull mice. PLoS One *4*, e7251.

Jessie, K., Fong, M.Y., Devi, S., Lam, S.K., and Wong, K.T. (2004). Localization of dengue virus in naturally infected human tissues, by immunohistochemistry and in situ hybridization. J Infect Dis *189*, 1411-1418.

Jiang, D., Liang, J., and Noble, P.W. (2011). Hyaluronan as an immune regulator in human diseases. Physiol Rev *91*, 221-264.

Jiang, D., Weidner, J.M., Qing, M., Pan, X.B., Guo, H., Xu, C., Zhang, X., Birk, A., Chang, J., Shi, P.Y.*, et al.* (2010). Identification of five interferon-induced cellular proteins that inhibit west nile virus and dengue virus infections. J Virol *84*, 8332-8341.

Jindadamrongwech, S., Thepparit, C., and Smith, D.R. (2004). Identification of GRP 78 (BiP) as a liver cell expressed receptor element for dengue virus serotype 2. Arch Virol *149*, 915-927.

Johansson, H., Albrekt, A.S., Borrebaeck, C.A., and Lindstedt, M. (2013). The GARD assay for assessment of chemical skin sensitizers. Toxicol In Vitro *27*, 1163-1169.

Johnson, J.E., and Speir, J.A. (1997). Quasi-equivalent viruses: a paradigm for protein assemblies. J Mol Biol *269*, 665-675.

Kay, B.H., Nam, V.S., Tien, T.V., Yen, N.T., Phong, T.V., Diep, V.T., Ninh, T.U., Bektas, A., and Aaskov, J.G. (2002). Control of aedes vectors of dengue in three provinces of Vietnam by use of Mesocyclops (Copepoda)

and community-based methods validated by entomologic, clinical, and serological surveillance. Am J Trop Med Hyg *66*, 40-48.

Kelly, E.P., Polo, S., Sun, W., and Falgout, B. (2011). Evolution of attenuating mutations in dengue-2 strain S16803 PDK50 vaccine and comparison of growth kinetics with parent virus. Virus Genes *43*, 18-26.

Khakpoor, A., Panyasrivanit, M., Wikan, N., and Smith, D.R. (2009). A role for autophagolysosomes in dengue virus 3 production in HepG2 cells. J Gen Virol *90*, 1093-1103.

Khoo, U.S., Chan, K.Y., Chan, V.S., and Lin, C.L. (2008). DC-SIGN and L-SIGN: the SIGNs for infection. J Mol Med (Berl) *86*, 861-874.

Killian, M.S. (2012). Dual role of autophagy in HIV-1 replication and pathogenesis. AIDS Res Ther *9*, 16.

Kim, J.Y., Kim, H., Suk, K., and Lee, W.H. (2010). Activation of CD147 with cyclophilin a induces the expression of IFITM1 through ERK and PI3K in THP-1 cells. Mediators Inflamm *2010*, 821940.

Klechevsky, E., Liu, M., Morita, R., Banchereau, R., Thompson-Snipes, L., Palucka, A.K., Ueno, H., and Banchereau, J. (2009). Understanding human myeloid dendritic cell subsets for the rational design of novel vaccines. Hum Immunol *70*, 281-288.

Koga, Y., Matsuzaki, A., Suminoe, A., Hattori, H., and Hara, T. (2004). Neutrophil-derived TNF-related apoptosis-inducing ligand (TRAIL): a novel mechanism of antitumor effect by neutrophils. Cancer Res *64*, 1037-1043.

Kontny, U., Kurane, I., and Ennis, F.A. (1988). Gamma interferon augments Fc gamma receptor-mediated dengue virus infection of human monocytic cells. J Virol *62*, 3928-3933.

Koraka, P., Lim, Y.P., Shin, M.D., Setiati, T.E., Mairuhu, A.T., van Gorp, E.C., Soemantri, A., Osterhaus, A.D., and Martina, B.E. (2010). Plasma levels of inter-alpha inhibitor proteins in children with acute Dengue virus infection. PLoS One *5*, e9967.

Koraka, P., Suharti, C., Setiati, T.E., Mairuhu, A.T., Van Gorp, E., Hack, C.E., Juffrie, M., Sutaryo, J., Van Der Meer, G.M., Groen, J.*, et al.* (2001). Kinetics of dengue virus-specific serum immunoglobulin classes and subclasses correlate with clinical outcome of infection. J Clin Microbiol *39*, 4332-4338.

Kou, Z., Quinn, M., Chen, H., Rodrigo, W.W., Rose, R.C., Schlesinger, J.J., and Jin, X. (2008). Monocytes, but not T or B cells, are the principal target cells for dengue virus (DV) infection among human peripheral blood mononuclear cells. J Med Virol *80*, 134-146.

Krawczyk, M., Seguin-Estevez, Q., Leimgruber, E., Sperisen, P., Schmid, C., Bucher, P., and Reith, W. (2008). Identification of CIITA regulated genetic module dedicated for antigen presentation. PLoS Genet *4*, e1000058.

Kudchodkar, S.B., and Levine, B. (2009). Viruses and autophagy. Rev Med Virol *19*, 359-378.

Kuhn, R.J., Zhang, W., Rossmann, M.G., Pletnev, S.V., Corver, J., Lenches, E., Jones, C.T., Mukhopadhyay, S., Chipman, P.R., Strauss, E.G*., et al.* (2002). Structure of dengue virus: implications for flavivirus organization, maturation, and fusion. Cell *108*, 717-725.

Kundu, M., and Thompson, C.B. (2008). Autophagy: basic principles and relevance to disease. Annu Rev Pathol *3*, 427-455.

Kurane, I., Hebblewaite, D., and Ennis, F.A. (1986). Characterization with monoclonal antibodies of human lymphocytes active in natural killing and antibody-dependent cell-mediated cytotoxicity of dengue virus-infected cells. Immunology *58*, 429-436.

Kurosu, T., Chaichana, P., Yamate, M., Anantapreecha, S., and Ikuta, K. (2007). Secreted complement regulatory protein clusterin interacts with dengue virus nonstructural protein 1. Biochem Biophys Res Commun *362*, 1051-1056.

Kurosu, T., Khamlert, C., Phanthanawiboon, S., Ikuta, K., and Anantapreecha, S. (2010). Highly efficient rescue of dengue virus using a co-culture system with mosquito/mammalian cells. Biochem Biophys Res Commun *394*, 398-404.

Lai, C.Y., Hu, H.P., King, C.C., and Wang, W.K. (2008). Incorporation of dengue virus replicon into virus-like particles by a cell line stably expressing precursor membrane and envelope proteins of dengue virus type 2. J Biomed Sci *15*, 15-27.

Lanciotti, R.S., Calisher, C.H., Gubler, D.J., Chang, G.J., and Vorndam, A.V. (1992). Rapid detection and typing of dengue viruses from clinical samples by using reverse transcriptase-polymerase chain reaction. J Clin Microbiol *30*, 545-551.

Larsson, K., Lindstedt, M., and Borrebaeck, C.A. (2006). Functional and transcriptional profiling of MUTZ-3, a myeloid cell line acting as a model for dendritic cells. Immunology *117*, 156-166.

Lauer, M.E., Glant, T.T., Mikecz, K., DeAngelis, P.L., Haller, F.M., Husni, M.E., Hascall, V.C., and Calabro, A. (2013). Irreversible heavy chain transfer to hyaluronan oligosaccharides by tumor necrosis factor-stimulated gene-6. J Biol Chem *288*, 205-214.

Le Vee, M., Gripon, P., Stieger, B., and Fardel, O. (2008). Down-regulation of organic anion transporter expression in human hepatocytes exposed to the proinflammatory cytokine interleukin 1beta. Drug Metab Dispos *36*, 217-222.

Lee, I.K., Liu, J.W., and Yang, K.D. (2009). Clinical characteristics, risk factors, and outcomes in adults experiencing dengue hemorrhagic fever complicated with acute renal failure. Am J Trop Med Hyg *80*, 651-655.

Lee, Y.R., Lei, H.Y., Liu, M.T., Wang, J.R., Chen, S.H., Jiang-Shieh, Y.F., Lin, Y.S., Yeh, T.M., Liu, C.C., and Liu, H.S. (2008). Autophagic machinery activated by dengue virus enhances virus replication. Virology *374*, 240-248.

Lei, H.Y., Yeh, T.M., Liu, H.S., Lin, Y.S., Chen, S.H., and Liu, C.C. (2001). Immunopathogenesis of dengue virus infection. J Biomed Sci *8*, 377-388.

Lenschow, D.J. (2010). Antiviral Properties of ISG15. Viruses *2*, 2154-2168.

Leparc-Goffart, I., Baragatti, M., Temmam, S., Tuiskunen, A., Moureau, G., Charrel, R., and de Lamballerie, X. (2009). Development and validation of real-time one-step reverse transcription-PCR for the detection and typing of dengue viruses. J Clin Virol *45*, 61-66.

Li, H.T., Su, Y.P., Cheng, T.M., Xu, J.M., Liao, J., Chen, J.C., Ji, C.Y., Ai, G.P., and Wang, J.P. (2010). The interaction between interferon-induced protein with tetratricopeptide repeats-1 and eukaryotic elongation factor-1A. Mol Cell Biochem *337*, 101-110.

Li, L., Lok, S.M., Yu, I.M., Zhang, Y., Kuhn, R.J., Chen, J., and Rossmann, M.G. (2008). The flavivirus precursor membrane-envelope protein complex: structure and maturation. Science *319*, 1830-1834.

Li, W.-m., Huang, H.-r., Gao, F., Liu, Y., Fan, W.-x., Dai, G.-m., Jiang, G.-l., Song, X.-y., Zhao, L.-p., and Fu, Y.-h. (2011). Expression profiling of Mycobacterium tuberculosis Beijing genotype invading THP-1 cell line. Journal of Capital Meical University *32*, 6.

Liang, Y., Liu, H., Liu, B., Bai, Y., Wu, H., Zhou, Q., and Chen, J. (2009). [Detection of IFN Response of Non-Specific Effects on RNAi.]. Zhongguo Fei Ai Za Zhi *12*, 16-22.

Libraty, D.H., Endy, T.P., Houng, H.S., Green, S., Kalayanarooj, S., Suntayakorn, S., Chansiriwongs, W., Vaughn, D.W., Nisalak, A., Ennis, F.A.*, et al.* (2002). Differing influences of virus burden and immune activation on disease severity in secondary dengue-3 virus infections. J Infect Dis *185*, 1213-1221.

Libraty, D.H., Pichyangkul, S., Ajariyakhajorn, C., Endy, T.P., and Ennis, F.A. (2001). Human dendritic cells are activated by dengue virus infection: enhancement by gamma interferon and implications for disease pathogenesis. J Virol *75*, 3501-3508.

Lima, E.Q., Gorayeb, F.S., Zanon, J.R., Nogueira, M.L., Ramalho, H.J., and Burdmann, E.A. (2007). Dengue haemorrhagic fever-induced acute kidney injury without hypotension, haemolysis or rhabdomyolysis. Nephrol Dial Transplant *22*, 3322-3326.

Lima Mda, R., Nogueira, R.M., Schatzmayr, H.G., de Filippis, A.M., Limonta, D., and dos Santos, F.B. (2011). A new approach to dengue fatal cases diagnosis: NS1 antigen capture in tissues. PLoS Negl Trop Dis *5*, e1147.

Limon-Flores, A.Y., Perez-Tapia, M., Estrada-Garcia, I., Vaughan, G., Escobar-Gutierrez, A., Calderon-Amador, J., Herrera-Rodriguez, S.E., Brizuela-Garcia, A., Heras-Chavarria, M., Flores-Langarica, A.*, et al.* (2005). Dengue virus inoculation to human skin explants: an effective approach to assess in situ the early infection and the effects on cutaneous dendritic cells. Int J Exp Pathol *86*, 323-334.

Lin, C.F., Wan, S.W., Chen, M.C., Lin, S.C., Cheng, C.C., Chiu, S.C., Hsiao, Y.L., Lei, H.Y., Liu, H.S., Yeh, T.M.*, et al.* (2008). Liver injury caused by antibodies against dengue virus nonstructural protein 1 in a murine model. Lab Invest *88*, 1079-1089.

Liu, H., Hwangbo, Y., Holte, S., Lee, J., Wang, C., Kaupp, N., Zhu, H., Celum, C., Corey, L., McElrath, M.J.*, et al.* (2004a). Analysis of genetic polymorphisms in CCR5, CCR2, stromal cell-derived factor-1, RANTES, and dendritic cell-specific intercellular adhesion molecule-3-grabbing nonintegrin in seronegative individuals repeatedly exposed to HIV-1. J Infect Dis *190*, 1055-1058.

Liu, Y., Liu, H., Kim, B.O., Gattone, V.H., Li, J., Nath, A., Blum, J., and He, J.J. (2004b). CD4-independent infection of astrocytes by human immunodeficiency virus type 1: requirement for the human mannose receptor. J Virol *78*, 4120-4133.

Lozach, P.Y., Burleigh, L., Staropoli, I., Navarro-Sanchez, E., Harriague, J., Virelizier, J.L., Rey, F.A., Despres, P., Arenzana-Seisdedos, F., and Amara, A. (2005). Dendritic cell-specific intercellular adhesion molecule 3-grabbing non-integrin (DC-SIGN)-mediated enhancement of dengue virus infection is independent of DC-SIGN internalization signals. J Biol Chem *280*, 23698-23708.

Lozach, P.Y., Lortat-Jacob, H., de Lacroix de Lavalette, A., Staropoli, I., Foung, S., Amara, A., Houles, C., Fieschi, F., Schwartz, O., Virelizier, J.L.*, et al.* (2003). DC-SIGN and L-SIGN are high affinity binding receptors for hepatitis C virus glycoprotein E2. J Biol Chem *278*, 20358-20366.

Lundberg, K., Albrekt, A.S., Nelissen, I., Santegoets, S., de Gruijl, T.D., Gibbs, S., and Lindstedt, M. (2013). Transcriptional profiling of human dendritic cell populations and models--unique profiles of in vitro dendritic cells and implications on functionality and applicability. PLoS One *8*, e52875.

Luo, D., Xu, T., Hunke, C., Gruber, G., Vasudevan, S.G., and Lescar, J. (2008). Crystal structure of the NS3 protease-helicase from dengue virus. J Virol *82*, 173-183.

Luo, G.P., Ni, B., Yang, X., and Wu, Y.Z. (2012). von Willebrand factor: more than a regulator of hemostasis and thrombosis. Acta Haematol *128*, 158-169.

Luplertlop, N., Misse, D., Bray, D., Deleuze, V., Gonzalez, J.P., Leardkamolkarn, V., Yssel, H., and Veas, F. (2006). Dengue-virus-infected

dendritic cells trigger vascular leakage through metalloproteinase overproduction. EMBO Rep *7*, 1176-1181.

Malavige, G.N., Fernando, S., Fernando, D.J., and Seneviratne, S.L. (2004). Dengue viral infections. Postgrad Med J *80*, 588-601.

Markiewski, M.M., Nilsson, B., Ekdahl, K.N., Mollnes, T.E., and Lambris, J.D. (2007). Complement and coagulation: strangers or partners in crime? Trends Immunol *28*, 184-192.

Marovich, M., Grouard-Vogel, G., Louder, M., Eller, M., Sun, W., Wu, S.J., Putvatana, R., Murphy, G., Tassaneetrithep, B., Burgess, T.*, et al.* (2001). Human dendritic cells as targets of dengue virus infection. J Investig Dermatol Symp Proc *6*, 219-224.

Martensen, P.M., Sogaard, T.M., Gjermandsen, I.M., Buttenschon, H.N., Rossing, A.B., Bonnevie-Nielsen, V., Rosada, C., Simonsen, J.L., and Justesen, J. (2001). The interferon alpha induced protein ISG12 is localized to the nuclear membrane. Eur J Biochem *268*, 5947-5954.

Martin-Vandelet, N., Paris, S., Bourguignon, J., Sesboue, R., Martin, J.P., and Diarra-Mehrpour, M. (1999). Assembly and secretion of recombinant chains of human inter-alpha-trypsin inhibitor in COS-7 cells. Eur J Biochem *259*, 476-484.

Martina, B.E., Koraka, P., and Osterhaus, A.D. (2009). Dengue virus pathogenesis: an integrated view. Clin Microbiol Rev *22*, 564-581.

Martinez-Barragan, J.J., and del Angel, R.M. (2001). Identification of a putative coreceptor on Vero cells that participates in dengue 4 virus infection. Journal of Virology *75*, 7818-7827.

Martinez-Pomares, L., Wienke, D., Stillion, R., McKenzie, E.J., Arnold, J.N., Harris, J., McGreal, E., Sim, R.B., Isacke, C.M., and Gordon, S. (2006). Carbohydrate-independent recognition of collagens by the macrophage mannose receptor. Eur J Immunol *36*, 1074-1082.

Masaki, H., Fujii, Y., Wakasa-Morimoto, C., Toyosaki-Maeda, T., Irimajiri, K., Tomura, T.T., and Kurane, I. (2009). Induction of specific and flavivirus--Cross-reactive CTLs by immunization with a single dengue virus-derived CTL epitope peptide. Virus Res *144*, 188-194.

Masterson, A.J., Sombroek, C.C., De Gruijl, T.D., Graus, Y.M., van der Vliet, H.J., Lougheed, S.M., van den Eertwegh, A.J., Pinedo, H.M., and Scheper, R.J. (2002). MUTZ-3, a human cell line model for the cytokine-induced differentiation of dendritic cells from CD34+ precursors. Blood *100*, 701-703.

Mathew, A., and Rothman, A.L. (2008). Understanding the contribution of cellular immunity to dengue disease pathogenesis. Immunol Rev *225*, 300-313.

Mazzon, M., Jones, M., Davidson, A., Chain, B., and Jacobs, M. (2009). Dengue virus NS5 inhibits interferon-alpha signaling by blocking signal transducer and activator of transcription 2 phosphorylation. J Infect Dis *200*, 1261-1270.

McKenna, K., Beignon, A.S., and Bhardwaj, N. (2005). Plasmacytoid dendritic cells: linking innate and adaptive immunity. J Virol *79*, 17-27.

McLaggan, D., Adjimatera, N., Sepcic, K., Jaspars, M., MacEwan, D.J., Blagbrough, I.S., and Scott, R.H. (2006). Pore forming polyalkylpyridinium salts from marine sponges versus synthetic lipofection systems: distinct tools for intracellular delivery of cDNA and siRNA. BMC Biotechnol *6*, 6.

McMeniman, C.J., Lane, R.V., Cass, B.N., Fong, A.W., Sidhu, M., Wang, Y.F., and O'Neill, S.L. (2009). Stable introduction of a life-shortening Wolbachia infection into the mosquito Aedes aegypti. Science *323*, 141-144.

Merad, M., and Manz, M.G. (2009). Dendritic cell homeostasis. Blood *113*, 3418-3427.

Mestas, J., and Hughes, C.C. (2004). Of mice and not men: differences between mouse and human immunology. J Immunol *172*, 2731-2738.

Miagostovich, M.P., Nogueira, R.M., dos Santos, F.B., Schatzmayr, H.G., Araujo, E.S., and Vorndam, V. (1999). Evaluation of an IgG enzyme-linked immunosorbent assay for dengue diagnosis. J Clin Virol *14*, 183-189.

Mikulak, J., Teichberg, S., Arora, S., Kumar, D., Yadav, A., Salhan, D., Pullagura, S., Mathieson, P.W., Saleem, M.A., and Singhal, P.C. (2010). DC-specific ICAM-3-grabbing nonintegrin mediates internalization of HIV-1 into human podocytes. Am J Physiol Renal Physiol *299*, F664-673.

Miller, J.L., de Wet, B.J., Martinez-Pomares, L., Radcliffe, C.M., Dwek, R.A., Rudd, P.M., and Gordon, S. (2008). The mannose receptor mediates dengue virus infection of macrophages. PLoS Pathog *4*, e17.

Miller, J.L., Lachica, R., Sayce, A.C., Williams, J.P., Bapat, M., Dwek, R., Beatty, P.R., Harris, E., and Zitzmann, N. (2012). Liposome-Mediated Delivery of Iminosugars Enhances Efficacy against Dengue Virus In Vivo. Antimicrob Agents Chemother *56*, 6379-6386.

Mitchell, D.A., Fadden, A.J., and Drickamer, K. (2001a). A novel mechanism of carbohydrate recognition by the C-type lectins DC-SIGN and DC-SIGNR. Subunit organization and binding to multivalent ligands. J Biol Chem *276*, 28939-28945.

Mitchell, D.A., Fadden, A.J., and Drickamer, K. (2001b). A novel mechanism of carbohydrate recognition by the C-type lectins DC-SIGN and DC-SIGNR. Subunit organization and binding to multivalent ligands. J Biol Chem *276*, 28939-28945.

Mizushima, N. (2007). Autophagy: process and function. Genes Dev *21*, 2861-2873.

Mizushima, N., and Yoshimori, T. (2007). How to interpret LC3 immunoblotting. Autophagy *3*, 542-545.

Mizushima, S., Nii, A., Kato, K., and Uemura, A. (1998). Gene expression of the two heavy chains and one light chain forming the inter-alpha-trypsin-inhibitor in human tissues. Biol Pharm Bull *21*, 167-169.

Modis, Y., Ogata, S., Clements, D., and Harrison, S.C. (2003). A ligand-binding pocket in the dengue virus envelope glycoprotein. Proc Natl Acad Sci U S A *100*, 6986-6991.

Modis, Y., Ogata, S., Clements, D., and Harrison, S.C. (2004). Structure of the dengue virus envelope protein after membrane fusion. Nature *427*, 313-319.

Moi, M.L., Lim, C.K., Tajima, S., Kotaki, A., Saijo, M., Takasaki, T., and Kurane, I. (2011). Dengue virus isolation relying on antibody-dependent enhancement mechanism using FcgammaR-expressing BHK cells and a monoclonal antibody with infection-enhancing capacity. J Clin Virol *52*, 225-230.

Moi, M.L., Lim, C.K., Takasaki, T., and Kurane, I. (2010). Involvement of the Fc gamma receptor IIA cytoplasmic domain in antibody-dependent enhancement of dengue virus infection. J Gen Virol *91*, 103-111.

Mondotte, J.A., Lozach, P.Y., Amara, A., and Gamarnik, A.V. (2007). Essential role of dengue virus envelope protein N glycosylation at asparagine-67 during viral propagation. J Virol *81*, 7136-7148.

Mongkolsapaya, J., Dejnirattisai, W., Xu, X.N., Vasanawathana, S., Tangthawornchaikul, N., Chairunsri, A., Sawasdivorn, S., Duangchinda, T., Dong, T., Rowland-Jones, S.*, et al.* (2003). Original antigenic sin and apoptosis in the pathogenesis of dengue hemorrhagic fever. Nat Med *9*, 921-927.

Mongkolsapaya, J., Duangchinda, T., Dejnirattisai, W., Vasanawathana, S., Avirutnan, P., Jairungsri, A., Khemnu, N., Tangthawornchaikul, N., Chotiyarnwong, P., Sae-Jang, K.*, et al.* (2006). T cell responses in dengue hemorrhagic fever: are cross-reactive T cells suboptimal? J Immunol *176*, 3821-3829.

Moreira, L.A., Iturbe-Ormaetxe, I., Jeffery, J.A., Lu, G., Pyke, A.T., Hedges, L.M., Rocha, B.C., Hall-Mendelin, S., Day, A., Riegler, M.*, et al.* (2009). A Wolbachia symbiont in Aedes aegypti limits infection with dengue, Chikungunya, and Plasmodium. Cell *139*, 1268-1278.

Moreno-Altamirano, M.M., Sanchez-Garcia, F.J., and Munoz, M.L. (2002). Non Fc receptor-mediated infection of human macrophages by dengue virus serotype 2. J Gen Virol *83*, 1123-1130.

Mota, J., and Rico-Hesse, R. (2009). Humanized mice show clinical signs of dengue fever according to infecting virus genotype. J Virol *83*, 8638-8645.

Mukhopadhyay, D., Asari, A., Rugg, M.S., Day, A.J., and Fulop, C. (2004). Specificity of the tumor necrosis factor-induced protein 6-mediated heavy chain transfer from inter-alpha-trypsin inhibitor to hyaluronan: implications for the assembly of the cumulus extracellular matrix. J Biol Chem *279*, 11119-11128.

Mukhopadhyay, S., Kuhn, R.J., and Rossmann, M.G. (2005). A structural perspective of the flavivirus life cycle. Nat Rev Microbiol *3*, 13-22.

Muramatsu, D., Iwai, A., Aoki, S., Uchiyama, H., Kawata, K., Nakayama, Y., Nikawa, Y., Kusano, K., Okabe, M., and Miyazaki, T. (2012). beta-Glucan derived from Aureobasidium pullulans is effective for the prevention of influenza in mice. PLoS One *7*, e41399.

Nair, M.P., Reynolds, J.L., Mahajan, S.D., Schwartz, S.A., Aalinkeel, R., Bindukumar, B., and Sykes, D. (2005). RNAi-directed inhibition of DC-SIGN by dendritic cells: prospects for HIV-1 therapy. AAPS J *7*, E572-578.

Nam, V.S., Yen, N.T., Holynska, M., Reid, J.W., and Kay, B.H. (2000). National progress in dengue vector control in Vietnam: survey for Mesocyclops (Copepoda), Micronecta (Corixidae), and fish as biological control agents. Am J Trop Med Hyg *62*, 5-10.

Nasirudeen, A.M., and Liu, D.X. (2009). Gene expression profiling by microarray analysis reveals an important role for caspase-1 in dengue virus-induced p53-mediated apoptosis. J Med Virol *81*, 1069-1081.

Nasirudeen, A.M., Wang, L., and Liu, D.X. (2008). Induction of p53-dependent and mitochondria-mediated cell death pathway by dengue virus infection of human and animal cells. Microbes Infect *10*, 1124-1132.

Nasirudeen, A.M., Wong, H.H., Thien, P., Xu, S., Lam, K.P., and Liu, D.X. (2011). RIG-I, MDA5 and TLR3 synergistically play an important role in restriction of dengue virus infection. PLoS Negl Trop Dis *5*, e926.

Nayak, V., Dessau, M., Kucera, K., Anthony, K., Ledizet, M., and Modis, Y. (2009). Crystal structure of dengue virus type 1 envelope protein in the postfusion conformation and its implications for membrane fusion. J Virol *83*, 4338-4344.

Nightingale, Z.D., Patkar, C., and Rothman, A.L. (2008). Viral replication and paracrine effects result in distinct, functional responses of dendritic cells following infection with dengue 2 virus. J Leukoc Biol *84*, 1028-1038.

Noisakran, S., Dechtawewat, T., Avirutnan, P., Kinoshita, T., Siripanyaphinyo, U., Puttikhunt, C., Kasinrerk, W., Malasit, P., and Sittisombut, N. (2008a). Association of dengue virus NS1 protein with lipid rafts. J Gen Virol *89*, 2492-2500.

Noisakran, S., Sengsai, S., Thongboonkerd, V., Kanlaya, R., Sinchaikul, S., Chen, S.T., Puttikhunt, C., Kasinrerk, W., Limjindaporn, T., Wongwiwat, W., *et al.* (2008b). Identification of human hnRNP C1/C2 as a dengue virus NS1-interacting protein. Biochem Biophys Res Commun *372*, 67-72.

Normile, D. (2007). Tropical diseases. Hunt for dengue vaccine heats up as the disease burden grows. Science *317*, 1494-1495.

Okroj, M., Holmquist, E., Sjolander, J., Corrales, L., Saxne, T., Wisniewski, H.G., and Blom, A.M. (2012). Heavy Chains of Inter Alpha Inhibitor (IalphaI) Inhibit the Human Complement System at Early Stages of the Cascade. J Biol Chem *287*, 20100-20110.

Omar, A., Jovanovic, K., Da Costa Dias, B., Gonsalves, D., Moodley, K., Caveney, R., Mbazima, V., and Weiss, S.F. (2011). Patented biological approaches for the therapeutic modulation of the 37 kDa/67 kDa laminin receptor. Expert Opin Ther Pat *21*, 35-53.

Onlamoon, N., Noisakran, S., Hsiao, H.M., Duncan, A., Villinger, F., Ansari, A.A., and Perng, G.C. (2010). Dengue virus-induced hemorrhage in a nonhuman primate model. Blood *115*, 1823-1834.

Osugi, Y., Vuckovic, S., and Hart, D.N. (2002). Myeloid blood CD11c(+) dendritic cells and monocyte-derived dendritic cells differ in their ability to stimulate T lymphocytes. Blood *100*, 2858-2866.

Padwad, Y.S., Mishra, K.P., Jain, M., Chanda, S., and Ganju, L. (2010). Dengue virus infection activates cellular chaperone Hsp70 in THP-1 cells: downregulation of Hsp70 by siRNA revealed decreased viral replication. Viral Immunol *23*, 557-565.

Paes, M.V., Pinhao, A.T., Barreto, D.F., Costa, S.M., Oliveira, M.P., Nogueira, A.C., Takiya, C.M., Farias-Filho, J.C., Schatzmayr, H.G., Alves, A.M., *et al.* (2005). Liver injury and viremia in mice infected with dengue-2 virus. Virology *338*, 236-246.

Palmer, D.R., Fernandez, S., Bisbing, J., Peachman, K.K., Rao, M., Barvir, D., Gunther, V., Burgess, T., Kohno, Y., Padmanabhan, R., *et al.* (2007). Restricted replication and lysosomal trafficking of yellow fever 17D vaccine virus in human dendritic cells. J Gen Virol *88*, 148-156.

Palmer, D.R., Sun, P., Celluzzi, C., Bisbing, J., Pang, S., Sun, W., Marovich, M.A., and Burgess, T. (2005). Differential effects of dengue virus on infected and bystander dendritic cells. J Virol *79*, 2432-2439.

Pankiv, S., Clausen, T.H., Lamark, T., Brech, A., Bruun, J.A., Outzen, H., Overvatn, A., Bjorkoy, G., and Johansen, T. (2007). p62/SQSTM1 binds directly to Atg8/LC3 to facilitate degradation of ubiquitinated protein aggregates by autophagy. The Journal of biological chemistry *282*, 24131-24145.

Panyasrivanit, M., Greenwood, M.P., Murphy, D., Isidoro, C., Auewarakul, P., and Smith, D.R. (2011). Induced autophagy reduces virus output in dengue infected monocytic cells. Virology *418*, 74-84.

Panyasrivanit, M., Khakpoor, A., Wikan, N., and Smith, D.R. (2009). Co-localization of constituents of the dengue virus translation and replication machinery with amphisomes. J Gen Virol *90*, 448-456.

Paranjape, S.M., and Harris, E. (2010). Control of dengue virus translation and replication. Curr Top Microbiol Immunol *338*, 15-34.

Parker, N., and Porter, A.C. (2004). Identification of a novel gene family that includes the interferon-inducible human genes 6-16 and ISG12. BMC Genomics *5*, 8.

Peeling, R.W., Artsob, H., Pelegrino, J.L., Buchy, P., Cardosa, M.J., Devi, S., Enria, D.A., Farrar, J., Gubler, D.J., Guzman, M.G.*, et al.* (2010). Evaluation of diagnostic tests: dengue. Nat Rev Microbiol *8*, S30-38.

Perera, R., Khaliq, M., and Kuhn, R.J. (2008). Closing the door on flaviviruses: entry as a target for antiviral drug design. Antiviral Res *80*, 11-22.

Perera, R., and Kuhn, R.J. (2008). Structural proteomics of dengue virus. Curr Opin Microbiol *11*, 369-377.

Perez, A.B., Sierra, B., Garcia, G., Aguirre, E., Babel, N., Alvarez, M., Sanchez, L., Valdes, L., Volk, H.D., and Guzman, M.G. (2010). Tumor necrosis factor-alpha, transforming growth factor-beta1, and interleukin-10 gene polymorphisms: implication in protection or susceptibility to dengue hemorrhagic fever. Hum Immunol *71*, 1135-1140.

Pichlmair, A., Lassnig, C., Eberle, C.A., Gorna, M.W., Baumann, C.L., Burkard, T.R., Burckstummer, T., Stefanovic, A., Krieger, S., Bennett, K.L.*, et al.* (2011). IFIT1 is an antiviral protein that recognizes 5 '-triphosphate RNA. Nat Immunol *12*, 624-U177.

Plymoth, A., Yang, Z., Lofdahl, C.G., Ekberg-Jansson, A., Dahlback, M., Fehniger, T.E., Marko-Varga, G., and Hancock, W.S. (2006). Rapid proteome analysis of bronchoalveolar lavage samples of lifelong smokers and never-smokers by micro-scale liquid chromatography and mass spectrometry. Clin Chem *52*, 671-679.

Pokidysheva, E., Zhang, Y., Battisti, A.J., Bator-Kelly, C.M., Chipman, P.R., Xiao, C., Gregorio, G.G., Hendrickson, W.A., Kuhn, R.J., and Rossmann, M.G. (2006). Cryo-EM reconstruction of dengue virus in complex with the carbohydrate recognition domain of DC-SIGN. Cell *124*, 485-493.

Polacek, C., Friebe, P., and Harris, E. (2009). Poly(A)-binding protein binds to the non-polyadenylated 3' untranslated region of dengue virus and modulates translation efficiency. J Gen Virol *90*, 687-692.

Puerta-Guardo, H., Mosso, C., Medina, F., Liprandi, F., Ludert, J.E., and del Angel, R.M. (2010). Antibody-dependent enhancement of dengue virus infection in U937 cells requires cholesterol-rich membrane microdomains. J Gen Virol *91*, 394-403.

Python, F., Goebel, C., and Aeby, P. (2009). Comparative DNA microarray analysis of human monocyte derived dendritic cells and MUTZ-3 cells exposed to the moderate skin sensitizer cinnamaldehyde. Toxicol Appl Pharmacol *239*, 273-283.

Qi, R.F., Zhang, L., and Chi, C.W. (2008). Biological characteristics of dengue virus and potential targets for drug design. Acta Biochim Biophys Sin (Shanghai) *40*, 91-101.

Quentmeier, H., Duschl, A., Hu, Z.B., Schnarr, B., Zaborski, M., and Drexler, H.G. (1996). MUTZ-3, a monocytic model cell line for interleukin-4 and lipopolysaccharide studies. Immunology *89*, 606-612.

Randolph, G.J., Jakubzick, C., and Qu, C. (2008). Antigen presentation by monocytes and monocyte-derived cells. Curr Opin Immunol *20*, 52-60.

Rao, I.S., Loya, A.C., Ratnakar, K.S., and Srinivasan, V.R. (2005). Lymph node infarction--a rare complication associated with disseminated intra vascular coagulation in a case of dengue fever. BMC Clin Pathol *5*, 11.

Rasaiyaah, J., Noursadeghi, M., Kellam, P., and Chain, B. (2009). Transcriptional and functional defects of dendritic cells derived from the MUTZ-3 leukaemia line. Immunology *127*, 429-441.

Rasmussen, U.B., Wolf, C., Mattei, M.G., Chenard, M.P., Bellocq, J.P., Chambon, P., Rio, M.C., and Basset, P. (1993). Identification of a new interferon-alpha-inducible gene (p27) on human chromosome 14q32 and its expression in breast carcinoma. Cancer Res *53*, 4096-4101.

Rice, B.D.L.H.-J.u.T.C.M. (2007). Flaviviridae: The Viruses and Their Replication, 5 th edn (Philadelphia, Lippincott-Raven Publishers).

Rodrigo, W.W., Jin, X., Blackley, S.D., Rose, R.C., and Schlesinger, J.J. (2006). Differential enhancement of dengue virus immune complex infectivity mediated by signaling-competent and signaling-incompetent human Fcgamma RIA (CD64) or FcgammaRIIA (CD32). J Virol *80*, 10128-10138.

Rodrigues, L.M., Theodoro, T.R., Matos, L.L., Mader, A.M., Milani, C., and Pinhal, M.A. (2011). Heparanase isoform expression and extracellular matrix remodeling in intervertebral disc degenerative disease. Clinics (Sao Paulo) *66*, 903-909.

Roehrig, J.T., Bryant, J.E., Calvert, A.E., Mesesan, K., Crabtree, M.B., Volpe, K.E., Silengo, S., Kinney, R.M., Huang, C.Y., and Miller, B.R. (2007). Glycosylation of the dengue 2 virus E protein at N67 is critical for virus growth in vitro but not for growth in intrathoracically-inoculated Aedes aegypti mosquitoes. Am J Trop Med Hyg *77*, 1-1.

Roehrig, J.T., Volpe, K.E., Squires, J., Hunt, A.R., Davis, B.S., and Chang, G.J. (2004). Contribution of disulfide bridging to epitope expression of the dengue type 2 virus envelope glycoprotein. J Virol *78*, 2648-2652.

Rossi, M., and Young, J.W. (2005). Human dendritic cells: potent antigen-presenting cells at the crossroads of innate and adaptive immunity. J Immunol *175*, 1373-1381.

Rothan, H.A., Han, H.C., Ramasamy, T.S., Othman, S., Rahman, N.A., and Yusof, R. (2012). Inhibition of dengue NS2B-NS3 protease and viral replication in Vero cells by recombinant retrocyclin-1. BMC Infect Dis *12*, 314.

Rothwell, S.W., Putnak, R., and La Russa, V.F. (1996). Dengue-2 virus infection of human bone marrow: characterization of dengue-2 antigen-positive stromal cells. Am J Trop Med Hyg *54*, 503-510.

Rugg, M.S., Willis, A.C., Mukhopadhyay, D., Hascall, V.C., Fries, E., Fulop, C., Milner, C.M., and Day, A.J. (2005). Characterization of complexes formed between TSG-6 and inter-alpha-inhibitor that act as intermediates in the covalent transfer of heavy chains onto hyaluronan. J Biol Chem *280*, 25674-25686.

Sabchareon, A., Wallace, D., Sirivichayakul, C., Limkittikul, K., Chanthavanich, P., Suvannadabba, S., Jiwariyavej, V., Dulyachai, W., Pengsaa, K., Wartel, T.A*., et al.* (2012). Protective efficacy of the recombinant, live-attenuated, CYD tetravalent dengue vaccine in Thai schoolchildren: a randomised, controlled phase 2b trial. Lancet *380*, 1559-1567.

Sakuntabhai, A., Turbpaiboon, C., Casademont, I., Chuansumrit, A., Lowhnoo, T., Kajaste-Rudnitski, A., Kalayanarooj, S.M., Tangnararatchakit, K., Tangthawornchaikul, N., Vasanawathana, S*., et al.* (2005). A variant in the CD209 promoter is associated with severity of dengue disease. Nat Genet *37*, 507-513.

Salier, J.P., Diarra-Mehrpour, M., Sesboue, R., Bourguignon, J., Benarous, R., Ohkubo, I., Kurachi, S., Kurachi, K., and Martin, J.P. (1987). Isolation and characterization of cDNAs encoding the heavy chain of human inter-alpha-trypsin inhibitor (I alpha TI): unambiguous evidence for multipolypeptide chain structure of I alpha TI. Proc Natl Acad Sci U S A *84*, 8272-8276.

Sampath, A., and Padmanabhan, R. (2009). Molecular targets for flavivirus drug discovery. Antiviral Res *81*, 6-15.

Samsa, M.M., Mondotte, J.A., Iglesias, N.G., Assuncao-Miranda, I., Barbosa-Lima, G., Da Poian, A.T., Bozza, P.T., and Gamarnik, A.V. (2009). Dengue virus capsid protein usurps lipid droplets for viral particle formation. PLoS Pathog *5*, e1000632.

Sanchez, V., Hessler, C., DeMonfort, A., Lang, J., and Guy, B. (2006). Comparison by flow cytometry of immune changes induced in human

monocyte-derived dendritic cells upon infection with dengue 2 live-attenuated vaccine or 16681 parental strain. FEMS Immunol Med Microbiol *46*, 113-123.

Santegoets, S.J., Bontkes, H.J., Stam, A.G., Bhoelan, F., Ruizendaal, J.J., van den Eertwegh, A.J., Hooijberg, E., Scheper, R.J., and de Gruijl, T.D. (2008a). Inducing antitumor T cell immunity: comparative functional analysis of interstitial versus Langerhans dendritic cells in a human cell line model. J Immunol *180*, 4540-4549.

Santegoets, S.J., Schreurs, M.W., Masterson, A.J., Liu, Y.P., Goletz, S., Baumeister, H., Kueter, E.W., Lougheed, S.M., van den Eertwegh, A.J., Scheper, R.J.*, et al.* (2006). In vitro priming of tumor-specific cytotoxic T lymphocytes using allogeneic dendritic cells derived from the human MUTZ-3 cell line. Cancer immunology, immunotherapy : CII *55*, 1480-1490.

Santegoets, S.J., van den Eertwegh, A.J., van de Loosdrecht, A.A., Scheper, R.J., and de Gruijl, T.D. (2008b). Human dendritic cell line models for DC differentiation and clinical DC vaccination studies. J Leukoc Biol *84*, 1364-1373.

Sariol, C.A., Martinez, M.I., Rivera, F., Rodriguez, I.V., Pantoja, P., Abel, K., Arana, T., Giavedoni, L., Hodara, V., White, L.J.*, et al.* (2011). Decreased dengue replication and an increased anti-viral humoral response with the use of combined Toll-like receptor 3 and 7/8 agonists in macaques. PLoS One *6*, e19323.

Sariol, C.A., Munoz-Jordan, J.L., Abel, K., Rosado, L.C., Pantoja, P., Giavedoni, L., Rodriguez, I.V., White, L.J., Martinez, M., Arana, T.*, et al.* (2007). Transcriptional activation of interferon-stimulated genes but not of cytokine genes after primary infection of rhesus macaques with dengue virus type 1. Clin Vaccine Immunol *14*, 756-766.

Sayce, A.C., Miller, J.L., and Zitzmann, N. (2010). Targeting a host process as an antiviral approach against dengue virus. Trends Microbiol *18*, 323-330.

Schenk, S., Schoenhals, G.J., de Souza, G., and Mann, M. (2008). A high confidence, manually validated human blood plasma protein reference set. BMC Med Genomics *1*, 41.

Schmidt, A.G., Lee, K., Yang, P.L., and Harrison, S.C. (2012). Small-molecule inhibitors of dengue-virus entry. PLoS Pathog *8*, e1002627.

Seneviratne, S.L., Malavige, G.N., and de Silva, H.J. (2006). Pathogenesis of liver involvement during dengue viral infections. Trans R Soc Trop Med Hyg *100*, 608-614.

Shah, M., Wadood, A., Rahman, Z., and Husnain, T. (2013). Interaction and inhibition of dengue envelope glycoprotein with mammalian receptor DC-sign, an in-silico approach. PLoS One *8*, e59211.

Shatkin, A.J. (1976). Capping of eucaryotic mRNAs. Cell *9*, 645-653.

Shcherbakov, D., and Piendl, W. (2007). A novel view of gel-shifts: analysis of RNA-protein complexes using a two-color fluorescence dye procedure. Electrophoresis *28*, 749-755.

Shresta, S., Kyle, J.L., Robert Beatty, P., and Harris, E. (2004). Early activation of natural killer and B cells in response to primary dengue virus infection in A/J mice. Virology *319*, 262-273.

Siegrist, F., Ebeling, M., and Certa, U. (2011). The small interferon-induced transmembrane genes and proteins. J Interferon Cytokine Res *31*, 183-197.

Simmons, C.P., Wolbers, M., Nguyen, M.N., Whitehorn, J., Shi, P.Y., Young, P., Petric, R., Nguyen, V.V., Farrar, J., and Wills, B. (2012). Therapeutics for dengue: recommendations for design and conduct of early-phase clinical trials. PLoS Negl Trop Dis *6*, e1752.

Smelt, S.C., Borrow, P., Kunz, S., Cao, W., Tishon, A., Lewicki, H., Campbell, K.P., and Oldstone, M.B. (2001). Differences in affinity of binding of lymphocytic choriomeningitis virus strains to the cellular receptor alpha-dystroglycan correlate with viral tropism and disease kinetics. J Virol *75*, 448-457.

Smidt, K.C., Hansen, L.L., Sogaard, T.M., Petersen, L.K., Knudsen, U.B., and Martensen, P.M. (2003). A nine-nucleotide deletion and splice variation in the coding region of the interferon induced ISG12 gene. Biochim Biophys Acta *1638*, 227-234.

Smith, A.E., and Helenius, A. (2004). How viruses enter animal cells. Science *304*, 237-242.

Somnuke, P., Hauhart, R.E., Atkinson, J.P., Diamond, M.S., and Avirutnan, P. (2011). N-linked glycosylation of dengue virus NS1 protein modulates secretion, cell-surface expression, hexamer stability, and interactions with human complement. Virology *413*, 253-264.

Spaulding, A.C., Kurane, I., Ennis, F.A., and Rothman, A.L. (1999). Analysis of murine CD8(+) T-cell clones specific for the Dengue virus NS3 protein: flavivirus cross-reactivity and influence of infecting serotype. J Virol *73*, 398-403.

St John, A.L., Abraham, S.N., and Gubler, D.J. (2013). Barriers to preclinical investigations of anti-dengue immunity and dengue pathogenesis. Nat Rev Microbiol *11*, 420-426.

Su, S.V., Hong, P., Baik, S., Negrete, O.A., Gurney, K.B., and Lee, B. (2004). DC-SIGN binds to HIV-1 glycoprotein 120 in a distinct but overlapping fashion compared with ICAM-2 and ICAM-3. J Biol Chem *279*, 19122-19132.

Subramanya, S., Kim, S.S., Abraham, S., Yao, J., Kumar, M., Kumar, P., Haridas, V., Lee, S.K., Shultz, L.D., Greiner, D.*, et al.* (2010). Targeted delivery of small interfering RNA to human dendritic cells to suppress dengue

virus infection and associated proinflammatory cytokine production. J Virol *84*, 2490-2501.

Suksanpaisan, L., Susantad, T., and Smith, D.R. (2009). Characterization of dengue virus entry into HepG2 cells. J Biomed Sci *16*.

Sun, P., Celluzzi, C.M., Marovich, M., Subramanian, H., Eller, M., Widjaja, S., Palmer, D., Porter, K., Sun, W., and Burgess, T. (2006). CD40 ligand enhances dengue viral infection of dendritic cells: a possible mechanism for T cell-mediated immunopathology. Journal of Immunology *177*, 6497-6503.

Sun, P., Fernandez, S., Marovich, M.A., Palmer, D.R., Celluzzi, C.M., Boonnak, K., Liang, Z., Subramanian, H., Porter, K.R., Sun, W.*, et al.* (2009). Functional characterization of ex vivo blood myeloid and plasmacytoid dendritic cells after infection with dengue virus. Virology *383*, 207-215.

Sung, J.M., Lee, C.K., and Wu-Hsieh, B.A. (2012). Intrahepatic infiltrating NK and CD8 T cells cause liver cell death in different phases of dengue virus infection. PLoS ONE *7*, e46292.

Takemoto, D.K., Skehel, J.J., and Wiley, D.C. (1996). A surface plasmon resonance assay for the binding of influenza virus hemagglutinin to its sialic acid receptor. Virology *217*, 452-458.

Takhampunya, R., Padmanabhan, R., and Ubol, S. (2006). Antiviral action of nitric oxide on dengue virus type 2 replication. J Gen Virol *87*, 3003-3011.

Tanida, I. (2011). Autophagy basics. Microbiol Immunol *55*, 1-11.

Tanida, I., Minematsu-Ikeguchi, N., Ueno, T., and Kominami, E. (2005). Lysosomal turnover, but not a cellular level, of endogenous LC3 is a marker for autophagy. Autophagy *1*, 84-91.

Tanida, I., Ueno, T., and Kominami, E. (2004). LC3 conjugation system in mammalian autophagy. Int J Biochem Cell Biol *36*, 2503-2518.

Tassaneetrithep, B., Burgess, T.H., Granelli-Piperno, A., Trumpfheller, C., Finke, J., Sun, W., Eller, M.A., Pattanapanyasat, K., Sarasombath, S., Birx, D.L.*, et al.* (2003). DC-SIGN (CD209) mediates dengue virus infection of human dendritic cells. J Exp Med *197*, 823-829.

Taylor, P.R., Gordon, S., and Martinez-Pomares, L. (2005). The mannose receptor: linking homeostasis and immunity through sugar recognition. Trends Immunol *26*, 104-110.

Teodoro, J.G., and Branton, P.E. (1997). Regulation of apoptosis by viral gene products. J Virol *71*, 1739-1746.

Terenzi, F., Saikia, P., and Sen, G.C. (2008). Interferon-inducible protein, P56, inhibits HPV DNA replication by binding to the viral protein E1. Embo Journal *27*, 3311-3321.

Thaisomboonsuk, B.K., Clayson, E.T., Pantuwatana, S., Vaughn, D.W., and Endy, T.P. (2005). Characterization of dengue-2 virus binding to surfaces of mammalian and insect cells. Am J Trop Med Hyg *72*, 375-383.

Thepparit, C., and Smith, D.R. (2004). Serotype-specific entry of dengue virus into liver cells: identification of the 37-kilodalton/67-kilodalton high-affinity laminin receptor as a dengue virus serotype 1 receptor. J Virol *78*, 12647-12656.

Thomas, S.J., Hombach, J., and Barrett, A. (2009b). Scientific consultation on cell mediated immunity (CMI) in dengue and dengue vaccine development. Vaccine *27*, 355-368.

Thongtan, T., Panyim, S., and Smith, D.R. (2004). Apoptosis in dengue virus infected liver cell lines HepG2 and Hep3B. J Med Virol *72*, 436-444.

Tian, Y., Chen, W., Yang, Y., Xu, X., Zhang, J., Wang, J., Xiao, L., and Chen, Z. (2012). Identification of B cell epitopes of dengue virus 2 NS3 protein by monoclonal antibody. Appl Microbiol Biotechnol *97*, 1553-1560.

Tricou, V., Minh, N.N., Van, T.P., Lee, S.J., Farrar, J., Wills, B., Tran, H.T., and Simmons, C.P. (2010). A randomized controlled trial of chloroquine for the treatment of dengue in Vietnamese adults. PLoS Negl Trop Dis *4*, e785.

Tripathi, N.K., Shrivastva, A., Pattnaik, P., Parida, M., Dash, P.K., Gupta, N., Jana, A.M., and Rao, P.V. (2007). Production of IgM specific recombinant dengue multiepitope protein for early diagnosis of dengue infection. Biotechnol Prog *23*, 488-493.

Ubol, S., Chareonsirisuthigul, T., Kasisith, J., and Klungthong, C. (2008). Clinical isolates of dengue virus with distinctive susceptibility to nitric oxide radical induce differential gene responses in THP-1 cells. Virology *376*, 290-296.

Ubol, S., and Halstead, S.B. (2010). How innate immune mechanisms contribute to antibody-enhanced viral infections. Clin Vaccine Immunol *17*, 1829-1835.

Ueno, H., Schmitt, N., Klechevsky, E., Pedroza-Gonzalez, A., Matsui, T., Zurawski, G., Oh, S., Fay, J., Pascual, V., Banchereau, J*., et al.* (2010). Harnessing human dendritic cell subsets for medicine. Immunol Rev *234*, 199-212.

Upanan, S., Kuadkitkan, A., and Smith, D.R. (2008). Identification of dengue virus binding proteins using affinity chromatography. J Virol Methods *151*, 325-328.

Valdes, K., Alvarez, M., Pupo, M., Vazquez, S., Rodriguez, R., and Guzman, M.G. (2000). Human Dengue antibodies against structural and nonstructural proteins. Clin Diagn Lab Immunol *7*, 856-857.

van de Ven, R., de Jong, M.C., Reurs, A.W., Schoonderwoerd, A.J., Jansen, G., Hooijberg, J.H., Scheffer, G.L., de Gruijl, T.D., and Scheper, R.J. (2006). Dendritic cells require multidrug resistance protein 1 (ABCC1) transporter activity for differentiation. Journal of Immunology *176*, 5191-5198.

van de Ven, R., Scheffer, G.L., Reurs, A.W., Lindenberg, J.J., Oerlemans, R., Jansen, G., Gillet, J.P., Glasgow, J.N., Pereboev, A., Curiel, D.T.*, et al.* (2008). A role for multidrug resistance protein 4 (MRP4; ABCC4) in human dendritic cell migration. Blood *112*, 2353-2359.

van der Schaar, H.M., Rust, M.J., Chen, C., van der Ende-Metselaar, H., Wilschut, J., Zhuang, X., and Smit, J.M. (2008). Dissecting the cell entry pathway of dengue virus by single-particle tracking in living cells. PLoS Pathog *4*, e1000244.

van Helden, S.F., van Leeuwen, F.N., and Figdor, C.G. (2008). Human and murine model cell lines for dendritic cell biology evaluated. Immunol Lett *117*, 191-197.

van Kooyk, Y. (2008). C-type lectins on dendritic cells: key modulators for the induction of immune responses. Biochem Soc Trans *36*, 1478-1481.

Vaughn, D.W., Nisalak, A., Solomon, T., Kalayanarooj, S., Nguyen, M.D., Kneen, R., Cuzzubbo, A., and Devine, P.L. (1999). Rapid serologic diagnosis of dengue virus infection using a commercial capture ELISA that distinguishes primary and secondary infections. Am J Trop Med Hyg *60*, 693-698.

Velandia-Romero, M.L., Acosta-Losada, O., and Castellanos, J.E. (2012). In vivo infection by a neuroinvasive neurovirulent dengue virus. J Neurovirol *18*, 374-387.

Villadangos, J.A., and Ploegh, H.L. (2000). Proteolysis in MHC class II antigen presentation: who's in charge? Immunity *12*, 233-239.

Villadangos, J.A., Schnorrer, P., and Wilson, N.S. (2005). Control of MHC class II antigen presentation in dendritic cells: a balance between creative and destructive forces. Immunol Rev *207*, 191-205.

Villas-Boas, C.S., Conceicao, T.M., Ramirez, J., Santoro, A.B., Da Poian, A.T., and Montero-Lomeli, M. (2009). Dengue virus-induced regulation of the host cell translational machinery. Braz J Med Biol Res *42*, 1020-1026.

Visuthranukul J, B.U., Lawasut P (2009). Dengue hemorrhagic fever in a peripheral blood stem cell transplant recipient: the first case report. Infect Dis Reports *1*, 5-6.

Wang, L.H., Rothberg, K.G., and Anderson, R.G. (1993). Mis-assembly of clathrin lattices on endosomes reveals a regulatory switch for coated pit formation. J Cell Biol *123*, 1107-1117.

Wang, S.H., Syu, W.J., and Hu, S.T. (2004). Identification of the homotypic interaction domain of the core protein of dengue virus type 2. J Gen Virol *85*, 2307-2314.

Wang, S.H., Syu, W.J., Huang, K.J., Lei, H.Y., Yao, C.W., King, C.C., and Hu, S.T. (2002). Intracellular localization and determination of a nuclear localization signal of the core protein of dengue virus. J Gen Virol *83*, 3093-3102.

Watanabe, S., Tan, K.H., Rathore, A.P., Rozen-Gagnon, K., Shuai, W., Ruedl, C., and Vasudevan, S.G. (2012). The magnitude of dengue virus NS1 protein secretion is strain dependent and does not correlate with severe pathologies in the mouse infection model. J Virol *86*, 5508-5514.

Whitby, K., Pierson, T.C., Geiss, B., Lane, K., Engle, M., Zhou, Y., Doms, R.W., and Diamond, M.S. (2005). Castanospermine, a potent inhibitor of dengue virus infection in vitro and in vivo. J Virol *79*, 8698-8706.

Whitehorn, J., Chau, N.V., Truong, N.T., Tai, L.T., Van Hao, N., Hien, T.T., Wolbers, M., Merson, L., Dung, N.T., Peeling, R.*, et al.* (2012). Lovastatin for adult patients with dengue: protocol for a randomised controlled trial. Trials *13*, 203.

Whitehorn, J., and Simmons, C.P. (2011). The pathogenesis of dengue. Vaccine *29*, 7221-7228.

Wichit, S., Jittmittraphap, A., Hidari, K.I., Thaisomboonsuk, B., Petmitr, S., Ubol, S., Aoki, C., Itonori, S., Morita, K., Suzuki, T.*, et al.* (2011). Dengue virus type 2 recognizes the carbohydrate moiety of neutral glycosphingolipids in mammalian and mosquito cells. Microbiol Immunol *55*, 135-140.

Wichmann, O., Gascon, J., Schunk, M., Puente, S., Siikamaki, H., Gjorup, I., Lopez-Velez, R., Clerinx, J., Peyerl-Hoffmann, G., Sundoy, A.*, et al.* (2007). Severe dengue virus infection in travelers: risk factors and laboratory indicators. J Infect Dis *195*, 1089-1096.

Wisniewski, H.G., and Vilcek, J. (1997). TSG-6: an IL-1/TNF-alpha inducible protein with anti-inflammatory activity. Cytokine Growth Factor Rev *8*, 143-156.

Wiwanitkit, V. (2006). Dengue myocarditis, rare but not fatal manifestation. Int J Cardiol *112*, 122.

World Health Organization. (2004). Global strategic framework for integrated vector management (Geneva, World Health Organization).

World Health Organization. (2009). Dengue guidelines for diagnosis, treatment, prevention and control : new edition (Geneva, World Health Organization).

World Health Organization. (2012). Dengue and severe dengue (Geneva, World Health Organization).

Wu, J., Bera, A.K., Kuhn, R.J., and Smith, J.L. (2005). Structure of the Flavivirus helicase: implications for catalytic activity, protein interactions, and proteolytic processing. J Virol *79*, 10268-10277.

Wu, S.J., Grouard-Vogel, G., Sun, W., Mascola, J.R., Brachtel, E., Putvatana, R., Louder, M.K., Filgueira, L., Marovich, M.A., Wong, H.K.*, et al.* (2000). Human skin Langerhans cells are targets of dengue virus infection. Nat Med *6*, 816-820.

Xu, D., Holko, M., Sadler, A.J., Scott, B., Higashiyama, S., Berkofsky-Fessler, W., McConnell, M.J., Pandolfi, P.P., Licht, J.D., and Williams, B.R. (2009). Promyelocytic leukemia zinc finger protein regulates interferon-mediated innate immunity. Immunity *30*, 802-816.

Xu, Q.Y., Gao, Y., Liu, Y., Yang, W.Z., and Xu, X.Y. (2008). Identification of differential gene expression profiles of radioresistant lung cancer cell line established by fractionated ionizing radiation in vitro. Chin Med J (Engl) *121*, 1830-1837.

Yang, Y., Lee, J.H., Kim, K.Y., Song, H.K., Kim, J.K., Yoon, S.R., Cho, D., Song, K.S., Lee, Y.H., and Choi, I. (2005). The interferon-inducible 9-27 gene modulates the susceptibility to natural killer cells and the invasiveness of gastric cancer cells. Cancer Lett *221*, 191-200.

Yap, T.L., Xu, T., Chen, Y.L., Malet, H., Egloff, M.P., Canard, B., Vasudevan, S.G., and Lescar, J. (2007). Crystal structure of the dengue virus RNA-dependent RNA polymerase catalytic domain at 1.85-Angstrom resolution. J Virol *81*, 4753-4765.

Yellaboina, S., Tasneem, A., Zaykin, D.V., Raghavachari, B., and Jothi, R. (2011). DOMINE: a comprehensive collection of known and predicted domain-domain interactions. Nucleic Acids Res *39*, D730-735.

Yu, I.M., Zhang, W., Holdaway, H.A., Li, L., Kostyuchenko, V.A., Chipman, P.R., Kuhn, R.J., Rossmann, M.G., and Chen, J. (2008). Structure of the immature dengue virus at low pH primes proteolytic maturation. Science *319*, 1834-1837.

Yu, W., Gill, T., Wang, L., Du, Y., Ye, H., Qu, X., Guo, J.T., Cuconati, A., Zhao, K., Block, T.M.*, et al.* (2012). Design, synthesis, and biological evaluation of N-alkylated deoxynojirimycin (DNJ) derivatives for the treatment of dengue virus infection. J Med Chem *55*, 6061-6075.

Zaitseva, E., Yang, S.T., Melikov, K., Pourmal, S., and Chernomordik, L.V. (2010). Dengue virus ensures its fusion in late endosomes using compartment-specific lipids. PLoS Pathog *6*, e1001131.

Zhang, W., Chipman, P.R., Corver, J., Johnson, P.R., Zhang, Y., Mukhopadhyay, S., Baker, T.S., Strauss, J.H., Rossmann, M.G., and Kuhn, R.J. (2003a). Visualization of membrane protein domains by cryo-electron microscopy of dengue virus. Nat Struct Biol *10*, 907-912.

Zhang, Y., Corver, J., Chipman, P.R., Zhang, W., Pletnev, S.V., Sedlak, D., Baker, T.S., Strauss, J.H., Kuhn, R.J., and Rossmann, M.G. (2003b). Structures of immature flavivirus particles. Embo J *22*, 2604-2613.

Zhang, Y., Zhang, W., Ogata, S., Clements, D., Strauss, J.H., Baker, T.S., Kuhn, R.J., and Rossmann, M.G. (2004). Conformational changes of the flavivirus E glycoprotein. Structure *12*, 1607-1618.

Zhao, M., Yoneda, M., Ohashi, Y., Kurono, S., Iwata, H., Ohnuki, Y., and Kimata, K. (1995). Evidence for the covalent binding of SHAP, heavy chains of inter-alpha-trypsin inhibitor, to hyaluronan. J Biol Chem *270*, 26657-26663.

Zhou, Z., Khaliq, M., Suk, J.E., Patkar, C., Li, L., Kuhn, R.J., and Post, C.B. (2008). Antiviral compounds discovered by virtual screening of small-molecule libraries against dengue virus E protein. ACS Chem Biol *3*, 765-775.

Zhu, H., Cong, J.P., Mamtora, G., Gingeras, T., and Shenk, T. (1998). Cellular gene expression altered by human cytomegalovirus: global monitoring with oligonucleotide arrays. Proc Natl Acad Sci U S A *95*, 14470-14475.

Zhuo, L., and Kimata, K. (2008). Structure and function of inter-alpha-trypsin inhibitor heavy chains. Connect Tissue Res *49*, 311-320.

Zompi, S., and Harris, E. (2012). Animal models of dengue virus infection. Viruses *4*, 62-82.

Zompi, S., Santich, B.H., Beatty, P.R., and Harris, E. (2012). Protection from secondary dengue virus infection in a mouse model reveals the role of serotype cross-reactive B and T cells. J Immunol *188*, 404-416.

Appendix I

Formulae of buffers and reagents

Buffers and reagents for Transmission electron microscopy

0.2 M phosphate buffer

A. $NaH_2PO_4.H_2O$	27.6 g
ddH_2O	1000 ml
B. $Na_2HPO_4.2H_2O$	35.6 g
ddH_2O	1000 ml

23 ml A + 77 ml B, adjust pH to 7.3 (as 0.2 M phosphate buffer) then add

100 ml ddH_2O

0.1 M phosphate buffer

Add 100 ml ddH_2O to 100 ml 0.2 M phosphate buffer (see above)

0.4% lead citrate solution

Lead citrate	0.2 g
ddH_2O	50 ml
10 N NaOH	0.5 ml

Adjust pH to 12, filtered

0.5-2% uranyl acetate

Saturated uranyl acetate in 50% absolute ethanol	100 ml
50% Ethanol	100 ml

1% Osmium tetroxide (OsO_4) solution

2% OsO_4 in ddH_2O	100 ml
0.2M phosphate buffer	100 ml

1% toluidine blue O solution

1% toluidine blue O	1 ml
borax ($Na_2B_4O_7$•10H_2O)	20 ml

1.1% Methyl cellulose-medium

Methyl cellulose	11 g
double distilled (dd) H_2O	500 ml
Autoclaved	
BHK culture medium	500 ml

4% glutaraldehyde solution

50% glutaraldehyde	20 ml
0.2 M phosphate buffer	125 ml
ddH_2O	105 ml

Spurr's resin

Vinylcyclohexene dioxide	10 g
Diglycidyl ether of Polypropyleneglycol	6 g
Nonenyl succinic anhydride	26 g
Dimethy aminoethanol	0.4 g

Buffers and reagents for Western blot

5% SDS-PAGE Stacking gel

30% acrylamide /0.8% bis-acrylamide	666 µl
4× Stacking gel buffer (pH 6.8)	1000 µl
25% APS	40µl
TEMED	4 µl
MilliQ water	2290 µl

10% SDS-PAGE Separating gel

30% acrylamide /0.8% bis-acrylamide	2333 µl
4× Separating gel buffer (pH 8.8)	1750 µl
25% APS	70 µl
N, N, N', N'-tetramethylethylenediamine (TEMED)	7 µl
MilliQ water	2840 µl

25% Ammonium persulfate (APS)

APS	2.5 g
ddH_2O	10 ml

Store at -20°C in 1 ml aliquot

30% acrylamide /0.8% bis-acrylamide solution (37.5:1)

acrylamide	60 g
bis-acrylamide	1.6 g
ddH_2O	200 ml

Store at 4°C, avoid from light

4× Separating gel buffer (4× Tris-HCl/SDS, pH 8.8)

Tris	36.34 g
10% SDS	8 ml
ddH_2O	200 ml

6 × Sample loading buffer

Adjust the pH to 8.8 with 1 M HCl

Store at 4°C

10%SDS	3 ml
Glycerol	3.6 ml
β-Mercaptoethanol	0.5 ml
4× staking gel buffer (pH 6.8)	1.25 ml
Bromophenol blue	1 mg
ddH_2O	10 ml

Store at -20°C

6 × non-reducing Sample loading buffer

10%SDS	3 ml
Glycerol	3.6 ml
4× staking gel buffer (pH 6.8)	1.25 ml
Bromophenol blue	1 mg
ddH_2O	10 ml

Store at -20°C

10 × Transfer buffer

Glycine	144 g
Tris	30 g
SDS	3.75 g
ddH_2O	1000 ml

Adjust the pH to 8.3

Dilute as 1 × for use

Add absolute methanol freshly to 1× buffer (1:4, v/v)

10 × Electrophoresis buffer

Tris	30.2 g
Glycine	144 g
SDS	10 g
ddH_2O	1000 ml

Store at 4°C

Dilute as 1 × for use

Stacking gel buffer (4× Tris-HCL/SDS, pH 6.8)

Tris	12.1 g
10% SDS	8 ml
ddH_2O	200 ml

adjust the pH to 6.8 with 1 M HCl

Store at 4°C

Tris-buffered saline Tween-20

Tris-HCl	10 mM
NaCl	150 mM
Solved in ddH_2O, adjust pH to 8.0	
Tween-20	0.05%

MUTZ-3-competent medium

Minimum essential medium-α (MEM-α)(GIBCO)	400 ml
Fetal bovine serum (FBS) (GIBCO)	100 ml
Penicillin (GIBCO)	100 U/ml
Streptomycin (GIBCO)	100 mg/ml
GM-CSF (GENTAUR, Brussels, Belgium)	10 ng/ml

Radio-Immunoprecipitation Assay (RIPA) buffer

Tris-HCl [pH 7.5]	20 mM
NaCl	150 mM
Disodium ethylenediamine tetraacetate (Na_2EDTA)	1 mM
Ethylene glycol tetraacetic acid (EGTA)	1 mM
NP-40	1%
sodium deoxycholate	1%
sodium pyrophosphate	2.5 mM

Freshly supplemented with:

protease inhibitor cocktails (Fermentas)	1/100 volume
200 mM sodium orthovanadate	1/2000 volume

Regents for silver stain

Silver stain fixation solution

Absolute methanol	150 ml
acetic acid	75 ml
ddH_2O	Make up to 300 ml

Silver stain developer solution

Na_2CO_3	0.28 M
formaldehyde	0.085% (v/v)
$Na_2S_2O_3$	0.016 mM
ddH_2O	Make up to 300 ml

Buffers and reagents for SPR

Piranha solution

sulphuric acid	7 ml
Hydrogen peroxide	3 ml

Coating solution

11-Mercaptoundecanoic acid	11 mg
Ethanol	50 ml

10 mM acetate buffer (coupling buffer)

Sodium Acetate – trihydrate	68.4 mg
ddH_2O	50 ml

Adjust the pH to 4.5 with acetic acid

20 mg/ml BSA solution (immobilisation solution)

BSA	200 mg
Acetate buffer	10 ml

1 M Ethanolamine solution (blocking solution)

Ethanolamine	600 µl
ddH_2O	Make up to 10 ml

Adjust the pH to 8.5 with 1 M HCl

100 mM N-Hydroxy Succinimide (NHS) solution

NHS	23 mg
ddH_2O	2 ml

400 mM Dimethylaminopropyl-N'Ethylcarbodiimide N-3-hydrochloride (EDC) solution

EDC	153.4 mg
ddH_2O	2 ml

Activation solution

Mix the 100 mM NHS solution and 400 mM EDC solution as 1:1 (v:v)

Appendix II

Primers used in this study

Primer	Sequences 5'- 3'	Tm (°C)	Product length (bp)	Reference
BHK18s F	TTAAGAGGGACGGCCGGGGG	60.0	354	This study
BHK18s R	GCCGGGTGAGGTTTCCCGTG	60.0		
CXCL10 F	CCAGAATCGAAGGCCATCAA	58.0	51	This study
CXCL10 R	CATTTCCTTGCTAACTGCTTTCAG	58.8		
DV2_NegS_RT5	GTGCAGCCTGTAGCTCCACC	52.8		This study
DV-2_F	CGGGAGGCCACAAACCAT	61.1	59	This study
DV-2_R	TCCTCTAACCGCTAGTCCACTAC	52.2		
DV-2_M FAM	CCATGCGTACAGCTTC			
IFI6 F	TGGAGGCAGGTGAGAATG	56.2	93	This study
IFI6 R	CGACGGCCATGAAGGTC	58.1		

(Continued)

Primer	Sequences 5'- 3'	Tm (°C)	Product length (bp)	Reference
IFITM2 F	ATTCTGCTCATCATCATCCCAG	52.1	218	This study
IFITM2 R	TGATGCAGGACTCGGCTGTG	56.7		
ITIH2 F	TGTTCAGATCCCCAAAGGAG	56.8	70	This study
ITIH2 R	GCTCCTAAATGTCTTGCCGT	58.3		
Bikunin F	TTCCCACGCTGGTACTTTGACGTG	65.3	198	(Kuhn *et al.*, 2002)
Bikunin R	GAGGATCAACACCATCACGAACAGC	64.1		
D2V2 F	TGGACCGACAAAGACAGATTCTT	60.8	198	(Leparc-Goffart *et al.*, 2009)
D2V2 R	CGYCCYTGCAGCATTCCAA	61.5		
CD1a F	CATCTGGATCGCATCCTTTT	50.1	233	(Colmone *et al*., 2006)
CD1a R	ACTGCAATTCATGGGCGTAT	52.1		
CD80 F	GGGAAAGTGTACGCCCTGTA	53.6	216	(Nair *et al.*, 2005)
CD80 R	GCTACTTCTGTGCCCACCAT	54.2		

(Continued)

Primer	Sequences 5'- 3'	Tm (°C)	Product length (bp)	Reference
CD83 F	CAACTCATAAGACTTTGGGATAGG	51.0	133	(Xu *et al.*, 2008)
CD83 R	ATGGGTATAAGTGCAGGTTTGT	51.7		
MR F	CACCATCGAGGAATTGGACT	51.5	62	(Mikulak *et al.*, 2010)
MR R	ACAATTCGTCATTTGGCTCA	50.2		
DC-SIGN F	CCCAGCTCGTCGTAATCAA	51.6	74	(Mikulak *et al.*, 2010)
DC-SIGN R	GAAGCGGTTACTTCTGGAAGAC	53.3		
HLA-C F	CAGAAGTACAAGCGCCAGG	58.5	161	(Krawczyk *et al.*, 2008)
HLA-C R	TAGGCGGACTGGTCATACC	58.2		
IFIT1 F	TCAGGTCAAGGATAGTCTGGAG	52.4	147	(Du *et al.*, 2009)
IFIT1 R	AGGTTGTGTATTCCCACACTGTA	53.3		
IFIT2 F	GGAGGGAGAAAACTCCTTGGA	53.0	100	(Liang *et al.*, 2009)
IFIT2 R	GGCCAGTAGGTTGCACATTGT	55.3		

(Continued)

Primer	Sequences 5'- 3'	Tm (°C)	Product length (bp)	Reference
IFIT3 F	AAAAGCCCAACAACCCAGAAT	52.6	103	(Liang *et al.*, 2009)
IFIT3 R	GCCTGCTTCAAAACATCAGTAGA	53.4		
IFITM1 F	CCAAGGTCCACCGTGATTAAC	53.1	91	(Liang *et al.*, 2009)
IFITM1 R	ACCAGTTCAAGAAGAGGGTGTT	53.5		
ISG20 F	TCTACGACACGTCCACTGACA	55.0	115	(Liang *et al.*, 2009)
ISG20 R	CTGTTCTGGATGCTCTTGTGC	53.8		
IFIH1 F	AGTGTCAGCTGCTTAGATGA	56.3	143	(Muramatsu *et al.*, 2012)
IFIH1 R	ATTTGGTAAGGCCTGAGCTG	57.9		
IFI27 F	TCTGCAGTCACTGGGAGCAA	55.5	64	(Kim *et al.*, 2010)
IFI27 R	CCCAATGGAGCCCAGGAT	52.7		
ISG15 F	TGTCCCTGAGCAGCTCCATG	56.0	120	(Ashley *et al.*, 2010)
ISG15 R	TGTCCTGCAGCGCCACACC	59.9		

(Continued)

Primer	Sequences 5'- 3'	Tm (°C)	Product length (bp)	Reference
MX1 F	CAATCAGCCTGCTGACATTG	57.4	70	(Calmon *et al.*, 2009)
MX1 R	TGTCTCCTGCCTCTGGATG	58.4		
MX2 F	CAGCCACCACCAGGAAACA	60.2	77	(Cabrera-Hernandez and
MX2 R	TTCTGCTCGTACTGGCTGTACAG	62.2		Smith, 2005)
OAS1 F	GTCTTCCTCAGTCCTCTCACCAC	61.9	133	(Mitchell *et al.*, 2001a)
OAS1 R	GAGCCTGGACCTCAAACTTCAC	61.1		
OAS2 F	TGAGAGCAATGGGAAATGGG	57.9	79	(Nasirudeen *et al.*, 2011)
OAS2 R	AGGTATTCCTGGATAAACCAACCC	60.1		
TNFRSF9 F	GTGCTTGTGAATGGGACGAA	58.8	177	(Li *et al.*, 2011)
TNFRSF9 R	GAACAGCAGGAAGAGCAACG	59.5		
TNFSF10 F	TGCAGTCTCTCTGTGTGGCTG	62.3	91	(Koga *et al.*, 2004)
TNFSF10 R	CAAGCAATGCCACTTTTGGA	57.5		

(Continued)

Primer	Sequences 5'- 3'	Tm (°C)	Product length (bp)	Reference
TSG-6 F	ATATGGCTTGAACGAGCAGC	58.7	107	(Martinez-Pomares *et al.*,
TSG-6 R	TGGCCGCCTTCAAATTCACA	60.8		2006)
GAPDH F	TGCACCACCAACTGCTTAGC	55.4	87	(Le Vee *et al.*, 2008)
GAPDH R	GGCATGGACTGTGGTCATGAG	55.2		
RPL13A F	CCTGGAGGAGAAGAGGAAAGAGA	54.5	126	(Rodrigues *et al.*, 2011)
RPL13A R	TTGAGGACCTCTGTGTATTTGTCAA	54.2		

Appendix III

Antibodies used in this study

Host	Reaction specificity	Clonality	Clone	CO^	Brand	Catalog number	Dilution (v/v)
M#	Human mannose receptor	Mab	15-2		Abcam	ab8918	**WB*** 1:100
R#	Human ITIH2-C-terminal	Pab			Abcam	ab91487	**WB** 1:50
M	DENV 2 NS 1	Mab	DN2		Abcam	ab41623	**WB** 1:1000
R	DENV 1+2+3+4	Pab			Abcam		**WB** 1:60
R	Human IFIT1	Pab			Abnova	H00003434-D01P	**WB** 1:500
R	Human IFIT2	Pab			Abnova	H00003433-D01P	**WB** 1:500
R	Human IFIT3	Pab			Abnova	H00003437-D01	**WB** 1:500
R	Human IFI27	Pab			Abnova	H000003429-A01	**WB** 1:500
M	Flavivirus envelope protein	Mab	D1-4G2-4-15		Millipore	MAB10216	**WB** 1:5000 **FC*** 1:200 **CM*** 1:200 **CoIP*** 1:100 **IM*** 1:20
R	Human Na^+ K^+ ATPase	Pab			Cell signaling	3010	**WB** 1:1000
R	Human LC3	Pab			Cell signaling	2775S	**WB:** 1:1000
M	Human DC-SIGN and DC-SIGNR	Mab	DC28		R&D	MAB16211	**WB** 1:2500

(Continued)

Host	Reaction specificity	Clonality	Clone	CO^	Brand	Catalog number	Dilution (v/v)
G#	Rabbit IgG (H+L)			HRP	Invitrogen	G21234	**WB** 1:10000
R	Mouse IgG (H+L)			HRP	Invitrogen	81-6720	**WB** 1:10000
M	Human CD1a	Mab	VIT6B	R-PE	Invitrogen	MHCD1a04	**FC** 1:100
M	Human CD14	Mab	TüK4	PE-TR	Invitrogen	MHCD1417	**FC** 1:100
M	Human CD80	Mab	7-480	R-PE	Invitrogen	CD8004	**FC** 1:100
M	Human CD83	Mab	HB15e	FITC	Invitrogen	MHCD8301	**FC** 1:100
M	Mouse IgG1 Isotype control				Invitrogen	MG100	**FC** 1:100
M	Mouse IgG2a Isotype control				Invitrogen	MG2a00	**FC** 1:100
M	Mouse IgG2b Isotype control				Invitrogen	MG2b00	**FC** 1:100
G	Mouse IgG			R-PE	Invitrogen	M30004-1	**FC** 1:100
R	Mouse IgG			FITC	Invitrogen	616511	**FC** 1:100
M	Human MR	Mab	15-2	PE-Cy5	BioLegend	321108	**FC** 1:20 **CM** 1:5
M	Human DC-SIGN	Mab	DCN46	FITC	BD	551264	**FC** 1:20 **CM** 1:5

^CO: conjugation

***WB**: Western blot; FC: Flow cytometry; CM: Confocal microscopy; CoIP: complex immunopecipitation; IM: immunostaining

M: Mouse; G: Goat; R: Rabbit

Appendix IV

Standard curve of DENV2 RNA replication in TaqMan assay